Cardiac Development

The Posterior Heart Field and Atrioventricular Reentry Tachycardia

Nathan D. Hahurij

Cardiac Development

The Posterior Heart Field and Atrioventricular Reentry Tachycardia

Nathan D. Hahurij

Cardiac Development

The Posterior Heart Field and Atrioventricular Reentry Tachycardia

PROEFSCHRIFT

ter verkrijging van
de graad van Doctor aan de Universiteit Leiden,
op gezag van Rector Magnificus prof. mr. P.F. van der Heijden,
volgens besluit van het College voor Promoties
te verdedigen op woensdag 8 juni 2011
klokke 15.00 uur

door

Nathan Dominggus Hahurij

geboren te Roden
in 1981

PROMOTIECOMMISSIE

Promotores: Prof. Dr. N.A. Blom
                Prof. Dr. A.C. Gittenberger-de Groot

Co-promotor: Dr. M.R.M. Jongbloed

Overige leden: Prof. Dr. M.C. de Ruiter
                Prof. Dr. J.M.M. van Lith
                Prof. Dr. A.A.M. Wilde (*Academisch Medisch Centrum, Amsterdam*)

Voor mijn ouders

CONTENTS

1

General Introduction

Congenital heart disease is the most common birth defect with an estimated incidence of six per 1000 live born children.[1] Several mechanisms may underlie congenital heart malformations, like: genetic mutations, maternal disease, environmental influences or combinations of these events. Therefore, it is not surprising that embryonic and fetal cardiovascular development has already been a major focus of study for years. The increasing knowledge of normal as well as abnormal development provides vital information for better prenatal counselling of parents and future (in-utero) therapeutic interventions in case of congenital heart malformations.

1.1 EMBRYONIC DEVELOPMENT

After conception, the 2-cell staged embryo rapidly goes through subsequent developmental stages. Around the seventh day of development, the 150 micrometer sized embryo invades into the uterine epithelium. In the second week by the so-called gastrulation process the third germ layer of the embryo, the intraembryonic mesoderm, is formed. This process turns the bilaminar disk into a trilaminar embryo with three basic germ layers i.e. the ectoderm, endoderm and mesoderm. Each germ layer will give rise to specific structures of the embryonic body. The ectoderm differentiates to form the central nervous system and the epidermis. The endoderm provides the gastrointestinal and respiratory tract and is responsible for development of many endocrine glands and organs, such as the liver and pancreas. The mesoderm transitionally differentiates into the following four compartments known as: axial, paraxial, intermediate and lateral plate mesoderm. The axial mesoderm gives rise to the notochord, which is responsible for formation of the intervertebral disks. From the paraxial mesoderm the somites will give rise to the axial skeleton, skeletal musculature and the dermis. Furthermore, the branchial arches will develop from this compartment, which will form the facial muscle and cartilage. The intermediate mesoderm develops into the urogenital system comprising the kidneys and gonads. Finally, the lateral plate mesoderm is involved in the formation of the body wall, viscera and the circulatory system including the heart.[2]

1.2 EARLY CARDIAC DEVELOPMENT

In human, the development of the heart starts around day 19 (≈mouse 7.0 days post conception (dpc)) in the lateral plate mesoderm region, which is divided into splanchnic and somatic mesoderm. This region is already characterised by the upregulation of certain genes revealing early cardiac specification i.e. *Nkx2.5 (Drosophilas tinman)*[3,4] and *GATA4*.[5] The splanchnic mesoderm located at both sides of the primitive streak then fuses to form a single horseshoe-

shaped heart primordium[6,7] or primary heart tube with a venous and an arterial pole. In human at day 23 (≈mouse 8.25 dpc) the heart tube will loop to the right under influence of genes like *Nodal*,[8] *Lefty*[29] and *Pitx-2c*[10] involved in left and right specification (Figure 1). At subsequent stages septation, outgrowth and remodelling of the individual heart chambers will eventually lead to a four-chambered mature heart.

1.3 THE "BUILDING BLOCKS" OF THE HEART

Throughout the years extensive discussion has taken place about the exact origin of the cardiomyocytes of the developing heart. Around 1968 Manasek concluded that the coelomic epithelium was the only source of cardiomyocytes based on electron microscopy of developing avian hearts.[11] However, in the same period others suggested that cardiomyocytes also derive from the mesenchyme located in the cardiac jelly and in the regions posterior to the primitive atrium.[12] In 1973 Viragh and Challice found electron microscopic evidence that part of the myocardial wall of the sinus venosus originates from the loose mesenchyme of the septum transversum. They postulated that these mesenchymal cells aggregate along the sinus venosus wall and make contact with the pre-existing cardiac muscle and suggested that similar processes occur at the arterial pole of the heart near the truncus arteriosus.[13]
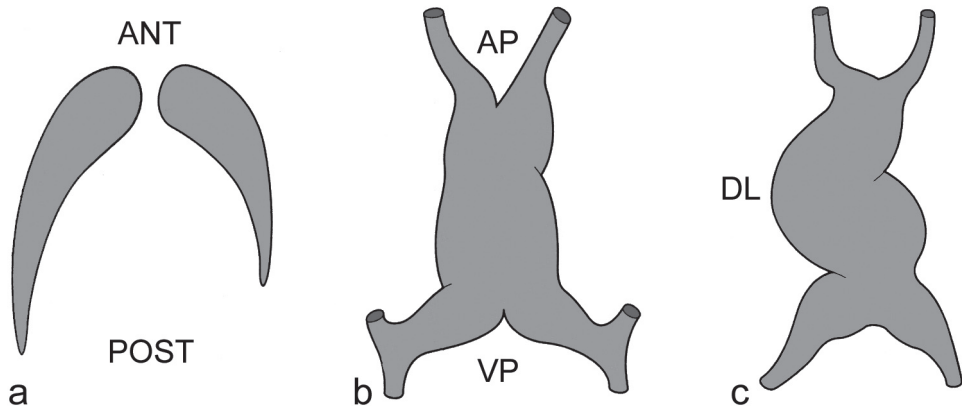
Figure 1. Early cardiogenesis and formation of the heart tube. Schematic representation of the two cardiac mesodermal primordia located in the lateral plate mesoderm (a), which will fuse to form a straight heart tube (b) with a primitive arterial pole (**AP**) and venous pole (**VP**). Subsequently, this heart tube will loop in a dextral manner as depicted in (c). **ANT** indicates anterior; **DL**, dextral-looping; **POST**, posterior. *Figures adapted from Gittenberger-de Groot AC and Poelmann RE.*[229]

1.3.1 First and Second Heart Field

In more recent years with sophisticated research techniques, several studies confirmed that not all cardiomyocytes have the same developmental origin. In lineage tracing studies individual (groups of) cells, derived from the lateral plate mesoderm could be followed during cardiogenesis, which has led to the concept of the so-called heart fields (Figure 2). A heart field can be defined as a discrete embryonic region, which contains cells that contribute to the formation of the heart. However discussion remains whether or not the contribution of a heart field should be considered as a continuum of splanchnic mesoderm. Fact is that the building of the heart occurs in a spatio-temporal fashion. Currently, the splanchnic mesoderm is established to be the first (primary) heart field, from which the cells derive that give rise to the so-called primary heart tube.[14] Several myocardial transcription factors can already be detected in the primary heart field ensuring the ability of these cells to differentiate into cardiomyocytes.[15]

As from 8 dpc in mouse[16] and stage HH14 in chick[17,18] additional cardiomyocytes are incorporated to the arterial and venous pole of the primary heart tube, which are essential for further cardiac development. These cardiomyocytes are derived from a specific area of the splanchnic mesoderm known as the second heart field (SHF) or second lineage. Recent studies on the LIM homeodomain transcription factor Isl1 showed that Isl1 is highly expressed in splanchnic mesodermal cells. Lineage tracing of these Isl1 expressing cells demonstrated that they substantially contribute to the embryonic heart at both the arterial and venous pole, where after Isl1 expression is down-regulated and cardiomyocyte markers become up-regulated. Moreover, *Isl1* mutant embryos showed severe hypoplasia and / or absence of the in- and outflow tract of the developing heart.[19]

1.3.2 Anterior and Secondary Heart Field

Detailed studies in chick[18,20] and mouse[16] concerning the origin and fate of the SHF cardiomyocytes at the arterial pole of the heart resulted in two distinctive areas the so-called anterior and secondary heart field. The anterior heart field is located anterior to the primary heart tube in the pharyngeal mesoderm that extends into the pharyngeal arches. Cardiomyocytes which derive from the anterior heart field contribute to the formation of the entire outflow tract of the heart.[16,20] The secondary heart field is located immediately adjacent and posterior to the outflow tract region behind the heart tube. The contribution of cells from the secondary heart field is only limited to the distal part of the outflow tract and partially overlaps with the cardiomyocytes derived from the anterior heart field (Figure 2).[19]

1.3.3 The Posterior Heart Field

The SHF also contributes cardiomyocytes to the venous pole of the primary heart tube as indicated in the Isl1 tracing studies.[19] Up till now research mainly focused on the addition of

SHF cardiomyocytes at the arterial pole of the heart. In this thesis the mesodermal region responsible for the contribution of cardiomyocytes to the venous pole of the primary heart tube is studied, and will be referred to as the: posterior heart field (PHF; Figure 2).
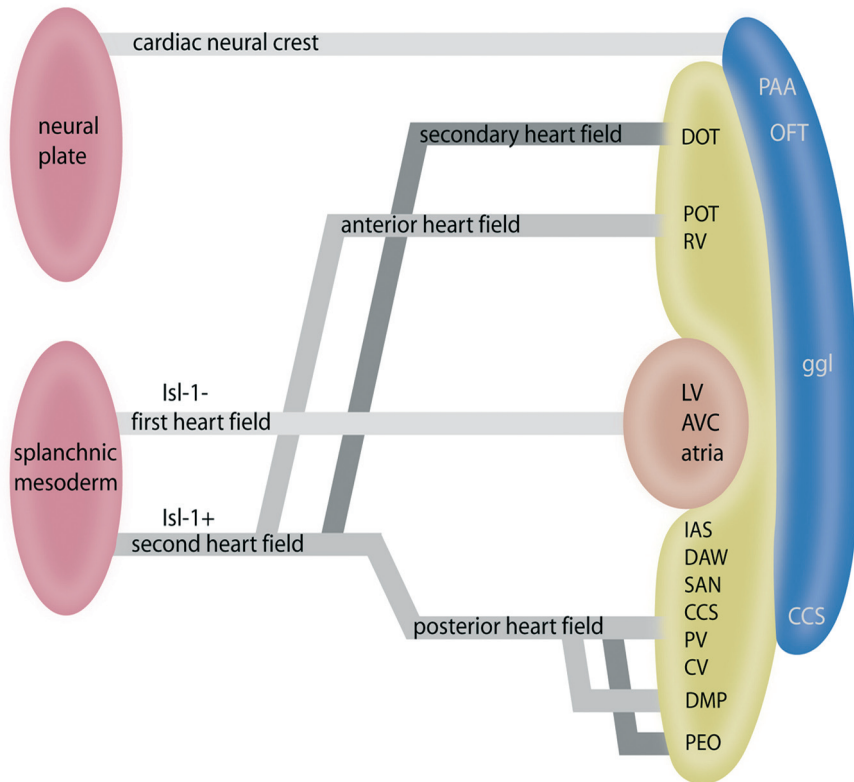
Figure 2. Heart fields in cardiogenesis. This schematic drawing represents the individual contribution of the heart fields during cardiogenesis. The first heart field gives rise to the primary heart tube and solely contains the myocardium that contributes to the future left ventricle (**LV**), atrioventricular canal (**AVC**) and parts of the atria. In contrast to the Isl-1 negative myocardium of the first heart field, the second heart field adds Isl-1 positive cardiomyocytes to the primary heart tube at the arterial as well as the venous pole of the developing heart. The contribution of the second heart field to the arterial pole is divided in two separate areas i.e. the anterior heart field, which adds cardiomyocytes to the right ventricle (**RV**) and proximal part of the outflow tract (**OFT**) and the secondary heart field that mainly contributes to the distal part of the OFT (**DOT**). The contribution of the second heart field to the venous pole is referred to as the posterior heart field. Along development the cardiac neural crest cells migrate from the neural plate at the arterial as well as the venous pole into the heart. **CCS** indicates cardiac conduction system; **CV**, cardinal veins; **DAW**, dorsal atrial wall; **DMP**, dorsal mesenchymal protrusion; **ggL**, cardiac ganglia; **IAS**, inter-atrial septum; **PAA**, pharyngeal arch arteries; **PEO**, pro-epicardial organ; **POT**, proximal part of outflow tract; **PV**, pulmonary vein; **SAN**, sinoatrial node. *Figures adapted and expanded from Gittenberger-de Groot AC and Poelmann RE*.[229]

1.3.4 Epicardium and Epicardium Derived Cells (EPDCs)

The primary heart tube initially is not covered by epicardial cells. These epicardial cells derive during development from a villous structure that occurs near the venous pole of the heart, the pro-epicardial organ (PEO; Figure 3a). Notably, the epicardium covering the arterial pole of the heart seems to have a distinct origin.[21] In mouse embryos of 9.0 - 10.0 dpc the epicardial cells start to migrate from the PEO over the complete outer layer of the developing heart.[22] The adhesion and migration of the epicardial cells seems to be regulated by several factors including: RXRalpha,[23] fibroblast growth factor (FGF),[24] vascular cell adhesion molecule-1 (VCAM-1),[25] Tbx5[26] and alpha4 integrin.[27,28]

After spreading of the epicardium, these cells migrate to the subendcoardial layer. Subsequently, so-called EPDCs are generated by a process known as Epithelial-to-Mesenchymal Transformation (EMT). EPDCs then invade into the myocardium, the subendocardial space and AV cushion tissue, where they contribute in formation of smooth muscle cells, the adventitial layer of the coronary vasculature and in the AV valves (Figure 3a and b).[29] Furthermore, a role for EPDCs has been demonstrated in development of the peripheral conduction system (Purkinje fibers).[22,30]

Thus far, there is no substantiated evidence that EPDC's can differentiate into endothelial cells[31] or myocardium.[32,33]

1.3.5 Neural Crest Cells

Neural crest cells (NCCs) contribute to many organs en tissues during embryonic development. In the early 1980 experiments by Kirby *et al*. demonstrated that a specific region of the dorsal neural tube, between the mid-otic placode and third somite (caudal rhombencephalic segment), provides cells to the developing heart and vessels. Initial experiments showed that these NCCs only contributed to the arterial pole of the heart.[34,35] Later on, more elaborated cell tracing studies confirmed the contribution of NCCs to the arterial pole and also identified an important subpopulation of NCCs migrating to the developing venous pole of the heart (Figure 2).[36]

At the arterial pole NCCs are involved in formation of the pharyngeal arch arteries and remodeling of the outflow tract i.e. formation of the aorticopulmonary septum,[37] the semilunar valves[38] and the myocardialization of the outflow tract septum.[39,40] Furthermore, these cells contribute in the formation of the neurons and ganglia of the cardiac autonomous nerve system.[41] At the venous pole of the heart NCCs are closely involved in development of the base of the atrial septum and an important role of NCCs has been postulated in the anlage of the cardiac conduction system (CCS).[36,42,43] Eventhough, the exact role of NCCs in CCS development remains uncertain, the fact that almost all NCCs located near the developing CCS become apoptotic at a certain time point suggests an inductive role in development.[36,42]
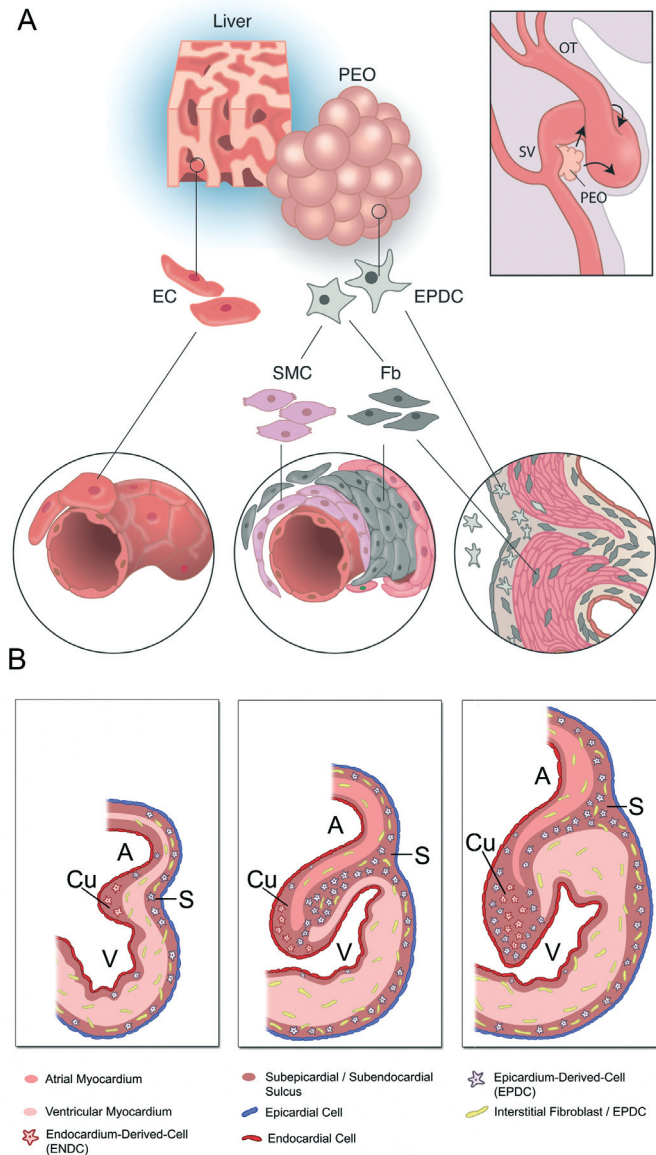
Figure 3. The role of the epicardium and Epicardium Derived Cells (EPDCs) in cardiogenesis. (a) The epicardium derives from the pro-epicardial organ (**PEO**), a cauli-flower like structure, near the sinus venosus (**SV**) of the heart. As from 9.5 dpc in mouse, the epicardial cells start to spread from the PEO to cover the complete heart tube. Subsequently, epithelial-to-mesenchymal (EMT) will occur by which the EPDCs are formed. The EPDCs have an important role in several processes within cardiogenesis, like formation of the myocardial architecture, the coronary arteries and peripheral conduction system (Purkinje fibers). Furthermore, EPDCs have an imperative role in formation of the annulus fibrosus and atrioventricular (**AV**) valve apparatus as schematically depicted in (b). **A** indicates atrium; **Cu**, AV cushion tissue; **EC**, endothelial cell; **Fb**, fibroblast; **OT**, outflow tract; **S**, AV sulcus; **SMC**, smooth muscle cell; **V**, ventricle. *Figure (a): adapted from Winter EM et al.[31] Figure (b): adapted from Kolditz DP et al.[92]*

1.4 THE CARDIAC CONDUCTION SYSTEM (CCS)

The CCS is a specialized network that initiates and closely coordinates the heart beat. Thereby, it facilitates an accurate controlled blood flow from the venous to the arterial pole of the heart, where it subsequently continues into the pulmonary and systemic circulation. The CCS can be divided in different parts, each of them characterized by its specific function in heart beat: The sinoatrial node (SAN), the AV node (AVN) and the His-Purkinje system (HPS; Figure 4). The SAN, located in the lateral wall of the superior caval vein where it enters the right atrium, is the location where the action potential is initiated by a group of spontaneously depolarizing pacemaker cells. From there the action potential stimulates the atrial part of the heart and eventually reaches to the second nodal region, the AVN. Based on its anatomical location and electrophysiological properties the AVN can be considered as "the guardian" of ventricular electrical activation. Anatomically, the half-oval shaped AVN is positioned against the central fibrous body in the so-called triangle of Koch.
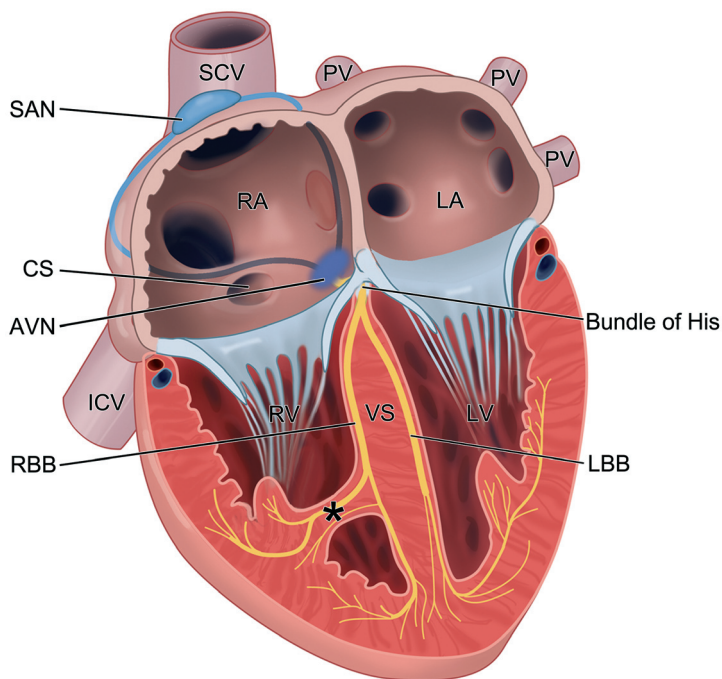
Figure 4. Schematic representation of the cardiac conduction system and impulse propagation through the mature heart. AVN indicates atrioventricular node; **CS**, ostium of coronary sinus; **ICV**, inferior caval vein; **LA**, left atrium; **LBB**, left bundle branch; **LV**, left ventricle; **PV**, pulmonary vein; **RA**, right atrium; **RBB**, right bundle branch; **RV**, right ventricle; **SAN**, sinoatrial node; **SCV**, superior caval vein; **VS**, (inter-) ventricular septum; **asterisk**, the Moderator band / trabecula septo-marginalis; Color codes: Blue lines between SAN and AVN represent the presumptive areas of two of the three internodal tracts. *Figure adapted and expanded from Netter et al.[230]*

This virtual triangular-shaped region is bordered by three structures in the right atrium: the coronary sinus ostium, the tendon of Todaro and the lower side attachment of the septal leaflet of the tricuspid valve.[44] The AVN is continuous with the bundle of His that forms the only myocardial continuity between the atria and ventricles. The remainder of the atria and ventricles are electrophysiologically separated by a layer of non-conducting fibrous tissue, the annulus fibrosus (**1.5.1. *"Annulus fibrosus: The isolating system"***).[45] The AVN controls the rate at which the action potential passes from the atria to the ventricles. In general conduction through the AVN is slow so that it creates a delay between atrial and ventricular systole i.e. contraction. In this manner it enables the atria to empty into the ventricles before the ventricular systole is induced. Furthermore, the AVN encloses a specific subset of cardiac ion channels, which enables the possibility to generate action potentials, i.e. allows it to function as the primary pacemaker in case of hampered SAN function,[46] thus providing an "escape" rhythm (**Chapter 1.4.3-c *"The Atrioventricular node"***). The HPS is a specialized rapid conducting network, which enables a fast and simultaneous contraction of the ventricles. The HPS can be subdivided in several components: (1) the Bundle of His (i.e. common / AV bundle or penetrating bundle), which runs through the isolating annulus fibrosus in an anterior direction ending on the top of the interventricular septum; (2) the bundle branches i.e. the left bundle branch (LBB) and right bundle branch (RBB), which are connected to the bundle of His. Anatomically, these bundle branches run alongside the interventricular septum towards the apex of the heart, the RBB partially via the trabecula septo-marginalis in the right ventricle; the LBB shows a more fan-shaped appearance over the interventricular septum in the left ventricle. Subsequently, the Purkinje fibers sprout from the bundle branches, connecting to individual cardiomyocytes to ensure a rapid electrical activation of the ventricles.[47]

1.4.1 The origin and development of the CCS

For many years the origin of the CCS has been studied. Initial debates focused on the origin of the cells, which contribute to the formation of this "specialized" network. Some postulated that the CCS had a neurogenic origin (the NCC lineage)[43] whereas others suggested a myocardial origin.[48] Lineage tracing studies however, demonstrated that the myocardium is the main source from which the CCS develops,[48] whereas the NCCs appeared to have a more inductive role.[42] Moreover, the cardiomyocytes of the CCS and those of the working myocardium (myocardium that is not part of the CCS) share the same four basic characteristics: 1. contraction, 2. auto-rhythmicity, 3. intercellular conduction and 4. electromechanical coupling, which also suggests a myocardial origin of CCS cells.[49]

Since it is established that the CCS is a myocardium derived structure, many researchers started to focus on the origin of the cardiomyocytes that contribute to formation of this system. In general two different approaches have been put forward: (1) "*the recruitment model*" puts forward that the CCS derives from a pool of multipotent undifferentiated cardiomyogenic

cells,[50-52] (2) "*the specification and ballooning model*" suggests that a population of differentiated pre-specified conduction cells located in the embryonic primary heart tube will develop into the CCS;[53] In this model the expression of specific genes / transcription factors in the primary heart tube myocardium prevents the differentiation of the pre-specified cardiomyocytes to a working myocardium phenotype. The individual heart chambers subsequently balloon-out of the primary heart tube,[54,55] after which the myocardium of the primary heart tube is restricted to specific areas (i.e. the sinu-atrial region, the AV region, the primary fold and the outflow tract area) in between the working myocardium. These areas will, under the control of several transcription factors, contribute to the developing CCS.[56] Interestingly, in early years, based on strictly histological criteria, the so-called "*ring theory*" has been proposed. This theory suggested that the precursors of the CCS could be identified by several rings of tissue that, after looping of the heart had been initiated, could be distinguished from the surrounding working myocardium by specific cellular characteristics.[57] This theory has been the subject of vivid discussions in the past decades and is regarded highly controversial nowadays. However, it is interesting to note that after looping of the heart has occurred, several zones of tissue (so-called transitional zones) that overlap with the areas mentioned under "*the specification and ballooning model*" can be distinguished based on expression patterns of several markers involved in CCS development.[58-61] Furthermore, these transitional zones largely correspond to the areas described in the "*ring theory*" including the sinu-atrial transition, the AV transition, the primary fold area and the ventriculo-arterial transitional zone (Figure 5).[62]

The development of the CCS can be studied either morphologically or electrophysiologically, the latter will be discussed in **Chapter 1.4.2 *"Action potential generation and propagation in the developing heart."*** Initial histological studies on CCS development demonstrated that cardiomyocytes of the CCS are characterized by reduced numbers of myofibrils and a high accumulation of glycogen as compared to the working myocardium in both human and animal.[63,64]

During the years increasing numbers of CCS specific markers have become available, which enabled detailed morphological analysis of the developing CCS at subsequent stages of development: *HNK-1*,[58] *mink-LacZ*,[61] CCS-*lacZ*,[59,60] *cGATA-6-lacZ*,[65]*cardiac troponin i-lacZ*,[66] *GATA-1*, *HCN4*[67] and homeodomain transcription factors Nkx2.5,[68,69] Hop,[70] Id2,[71] and T-box the transcription factors: Tbx2,[72] Tbx3[73] and Tbx5.[71] The individual role and temporarily expression of these marker genes during CCS development has recently been reviewed.[74] Based on the expression patterns during embryonic development of the different markers known to date, the embryonic CCS seems to be more extensive as compared to the mature CCS.[74] However, importantly, none of the markers solely stains the CCS.

In this thesis the expression of the homeodomain transcription factor *Shox2* (**Chapter 2 and 3**) and transmembrane protein *podoplanin* (**Chapter 4 and 5**) are described and added to the list of CCS developmental markers.

1.4.2 Action potential generation and propagation in the developing heart

The primary heart tube starts beating far before a specialized CCS can be recognized. At this stage the complete inflow tract in the tubular heart is able to generate action potentials, although optical mapping studies demonstrated in more detail that they mainly evoke from the dorsal side (initially more frequently left-sided) of the heart tube near the putative location of the sinus venosus.[75,76] The action potential subsequently spreads anteriorly and activates the heart tube towards the outflow tract region. At these stages no differences in conduction velocity in the heart tube can be discriminated[75,77,78] and action potential propagation is relatively slow due to poor intercellular coupling of the cardiomyocytes (Figure 6a).[78]
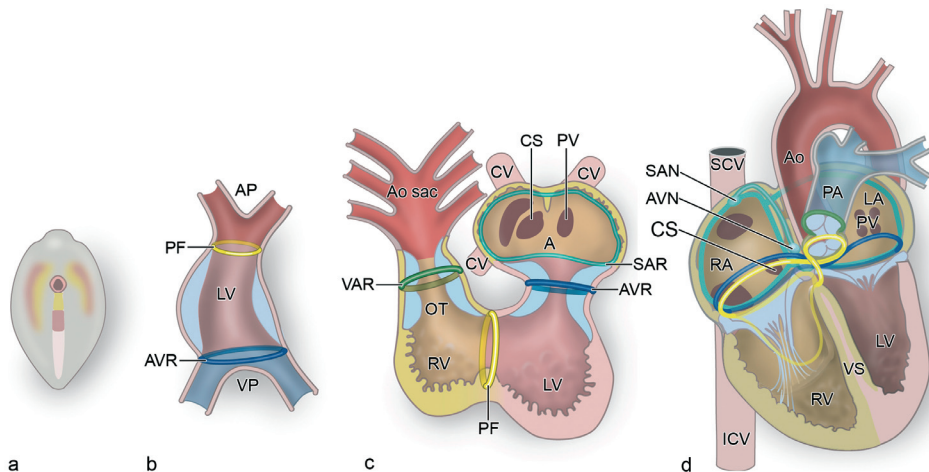
Figure 5. From primitive heart tube to a four-chambered heart including the transitional zones. (a) Represent the early embryonic body in which the splanchnic mesoderm is indicated along side the primitive streak, which will fuse to form a horseshoe-shaped heart primordium that subsequently transforms into the primitive heart tube. This primary heart tube depicted in (b) solely contains the myocardium of the future left ventricle (**LV**), AV canal and part of the atrium. At these stages two transitional zones can already be discriminated, at the venous pole (**VP**) the atrioventricular transitional zone (**AVR**) and the primary fold (**PF**) at the arterial pole (**AP**) of the heart. Subsequently, the heart will loop in a dextral manner, resulting in a looped heart tube as depicted in (c). Due to the addition of second heart field derived cardiomyocytes at the VP the atria (**A**) and sinus venosus area will appear, which include another transitional zone the sinu-atrial ring (**SAR**). The addition of second heart field derived cardiomyocytes at the AP will contribute to formation of the right ventricle (**RV**) that initiates from a groove in the PF. Furthermore, the myocardium of the outflow tract (**OT**) is added, which includes the ventriculo-arterial (**VAR**) transitional zone. Subsequently, by looping and septation a four chamber heart will appear in which the 4 transitional zones still can be recognized. Parts of these transitional zones show overlap with the mature CCS. **Ao** indicates aorta; **AVN**, atrioventricular node; **CS**, ostium of coronary sinus; **ICV**, inferior caval vein; **LA**, left atrium; **PA**, pulmonary artery; **PV**, pulmonary vein; **SAN**, sinoatrial node; **SCV**, superior caval vein; **VS**, ventricular septum. *Figures adapted and expanded from Gittenberger-de Groot et al.[62]*

| peristaltoid contracting tubular heart | base-to-apex | base-to-apex | apex-to-base |

Figure 6. Development of the action potential in the embryonic and fetal heart. (a) In the primary heart tube the cardiac impulse is generated near the venous pole (**VP**) of the heart and subsequently travels towards the arterial pole (**AP**) so that the heart tube contracts in a peristaltoid manner. In the looped-heart stage (b) and (c) the impulse is generated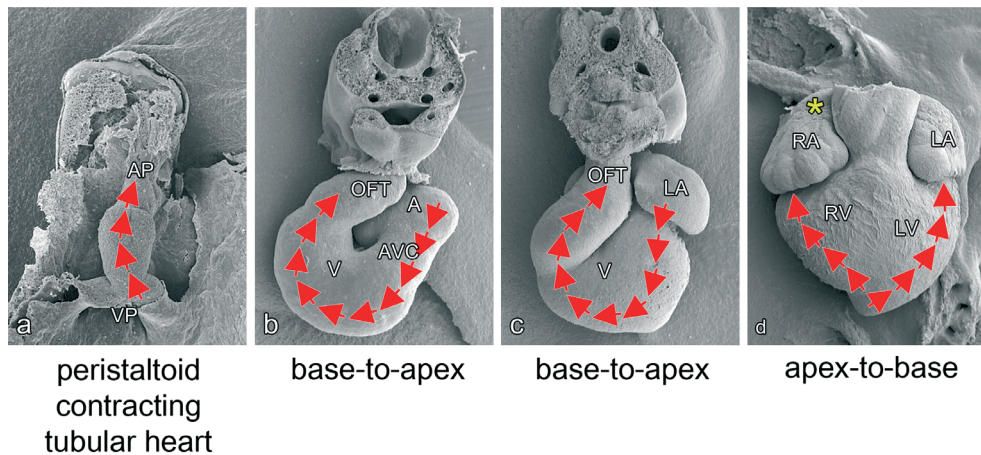 in the sinoatrial node, located near the entrance of the superior cardinal vein and the right atrium, from where it subsequently activates the atrial myocardium (**A**), the atrioventricular canal (**AVC**), the ventricular myocardium (**V**) and outflow tract (**OFT**). At these stages slow conducting zones are already present near the inflow tract (not depicted in this figure), the AVC and OFT. Furthermore, in (c) the ventricular part of the heart is still activated in a base-to-apex manner. (d) Represents the ventricular activation pattern in a mature apex-to-base manner, which is closely related to a functional cardiac conductions system and isolation of the AV junction. **LA** indicates left atrium; **LV**, left ventricle; **RA**, right atrium; **RV**, right ventricle; **asterisk**, location of impulse initiation by the sinoatrial node.

In the next step of heart development the primary heart tube starts to loop (Figure 6 b and c). At this looped stage, major changes occur in electrophysiological development. Initially, the entire sinus venosus myocardium has the potential to generate the action potential.[79] At the venous pole the SAN primordium gradually can be recognized near the right horn of the sinus venosus, which from then on will be the leading location to evoke the cardiac action potential (human ≈embryonic day 35; mouse ≈10 dpc; chick ≈HH 14-17). Primitive embryonic ECG recordings[77,78,80] as wells optical mapping studies[81] showed that fast and slow conducting areas can be discriminated in the looped heart. The slow conducting areas are located in the inflow tract (IFT), the AV canal (AVC) and outflow tract of the heart (OFT) separating the fast conducting future chamber myocardium,[78] thus mainly corresponding to the so-called "transitional zones" mentioned in **Chapter 1.4.1 *"The origin and development of the CCS."*** The areas of fast and slow conduction also can be confirmed morphologically by the specific expression pattern of ion channels important for the intercellular transfer of action potentials.[82-84] The presence of slow conducting myocardium in the AVC seem to be interesting, since this part of the heart (between future atria and ventricles) eventually will become the AVN area with similar slow or delaying conduction properties. The combination of electrophysiological

as well as morphological changes (i.e. formation of the AV-cushions) increase the pump efficiency of the looped heart, which results in a powerful blood flow from inflow towards outflow tract.

As cardiac development continues a switch in the activation pattern of the ventricles will take place (Figure 6d). Whereas ventricular activation initially occurs in a base-to-apex manner, during further development, a mature apex-to-base activation pattern arises,[78,85,86] which ensures effective pumping of the four-chambered heart. Basically, two important processes in cardiac development have been related to the appearance of an apex-to-base activation of the ventricles: (1) the maturated and electrophysiological functional HPS,[85,87-91] (2) The interruption of the AV myocardial continuity (except for the AV conduction axis) in the AVC region by the formation of the isolating annulus fibrosus **(Chapter 1.5.1 "*Annulus fibrosus: The isolating system*")**.[86,92 93]

In the early fetal four-chambered heart, the electrophysiological properties highly resemble those observed in mature hearts. The action potentials arise from the SAN and subsequently activate the atria, the AVN and HPS leading to a ventricular apex-to-base activation pattern.

1.4.3 Individual components of the CCS

1.4.3-a The sinoatrial node (SAN)

The SAN, the pacemaker of the heart was first identified in 1906 by the Scottisch anatomist Sir Arthur Keith (1866 - 1955) and one of his students Martin Flack (1882 - 1931) in a mole heart. The nodal structure that they observed in the right auricle of the heart near the location where the vena cava enters the right atrium was called: the sino-auricular node.[94]

During the years, multiple studies have shown that the SAN can be recognized in human as from the fifth week of development.[49] In mouse the first signs of the SAN primordium can be observed around 10.5 dpc, which was suggested to derive from an area of loose mesenchymal cells near the right atrium.[63] The development of the SAN and role of the PHF in formation of this structure are the topic of **Chapter 2-5** of this thesis. The anatomical "mature shape" of the SAN differs between several species.[95-97] In human and mouse the SAN appears to be comma-shaped with a "head" at the border of the superior caval vein and the right atrium and a "tail" along the terminal crest,[64,97,98] the adult derivative of the embryonic right venous valve that is an anatomical boundary between the right atrial appendage and the smooth walled sinus venosus part of the right atrium.

In the mature SAN, the myocardial cells show similar histological characteristics observed in the remainder of the CCS.[63,64] Early observations by James *et al*. discriminated two types of cells in the SAN: (1) the "P-cells" mainly located in the center portion of the SAN, which were believed to be the pacemaking cells and (2) the "Transitional cells," which can be found

throughout the complete SAN.[99] In the more recent years sophisticated electrophysiological mapping techniques have become available, and in line with that increasing knowledge about specific ionic currents important for the understanding of action potential generation. The SAN as demonstrated in rabbit hearts seems to be a very heterogeneous structure.[100] Differences are seen in ion channel expression between the center and periphery of the SAN. In the center, the leading site to evoke action potentials, electrical coupling by gap junction proteins is weak (in human: Cx40 and Cx45 positive; and Cx43 negative)[101] to protect this region from the inhibitory hyperpolarizing influences of the surrounding working (atrial) myocardium.[102] Furthermore, a specific subset of ion currents is present to enable action potential generation.[103,104] HCN4 (I_f or funny-current) a member of the Hyperpolarization-activated cyclic nucleotide-gated channel family appeared to have a key role in action potential generation.[105] For instance mutations in the human HCN4 gene have shown to result in SAN bradycardia.[106] Furthermore, the funny current inhibitor Ivabradine is increasingly being applied in clinical practice for heart rate reduction, targeting the spontaneous diastolic depolarization of the SAN.[107] The periphery of the SAN is characterized by a different subset of ionic currents and gap junction proteins.[104] This region is still able to evoke action potentials, but also has the capability to drive the more hyperpolarized atrial myocardium.[96]

1.4.3-b The internodal pathways

Many researchers have performed detailed morpho-histological studies of the atria, in attempt to understand the propagation of the action potential between the two specialized nodes of the CCS i.e. the SAN and AVN. In the mature heart, three individual pathways were proposed, which after their anatomical location in the atria were called: anterior, posterior (Thorel´s bundle) and middle (Wenckebach´s bundle) internodal pathway. Based on the original description by James, the individual tracts can be identified by three important atrial myocardial structures, being the crista terminalis, the Eustachian valve and Bachmann's bundle. The anterior pathway runs via the septum spurium into the Bachmann's bundle, which retro-aortically connects the right to the left atrium; the posterior pathway runs via the crista terminalis and the Eustachian valve; the middle pathway is a more poorly formed pathway and is anatomically more inconsistent (Figure 4).[108-110]

In embryonic and fetal hearts marker gene expression studies also demonstrated the presence of internodal tracts in both human[58] and animal models.[59,111-113] In the developing embryo the 3 internodal tracts correspond to: the right and left venous valves running in the dorsal wall of the right atrium in between the SAN and AVN, and the septum spurium the anterior fusion of the latter 2 valves. This suggests that the embryonic and fetal CCS is more extensive as compared to the mature CCS. These sinus venosus related structures may be involved in / or represent the predilection sites of adult atrial arrhythmogenic areas.[58,59] For instance, the adult

counterpart of the right venous valve can be recognized as the crista terminalis, a common site for atrial tachycardia.[114]

The initial, assumed role of the internodal tracts in fast conduction mainly derives from histological observations like the arrangements of the cardiomyocytes[110,115] and the suggested presence of Purkinje fibers.[108] Nowadays the functional role of the internodal pathways is still open to discussion. Most agree that impulse propagation through the atria solely depends on cardiac tissue alignment,[116] and not on specialized tracts. Furthermore, the absence of isolating tissue between the internodal tracts and the atrial working myocardium contradicts with the histological criteria, which can be used to define specialized conducting myocardial tracts in the heart, as were stated by Mönckeberg and Aschoff in 1910.[108] However, a critical remark towards these criteria is that they do not apply to the atrial parts of the CCS i.e. the SAN and the AVN. On the other hand, in the late seventies two individual studies did show preferential conduction of the cardiac impulse via pathways resembling to the internodal tracts as described by James.[108-110] In these studies, the administration of high doses of potassium in dog led to deprived electrical conduction in the atria except in sites corresponding with the internodal pathways and Bachman´s bundle.[117,118] These observations are further substantiated by more recent studies in atrial preparations of canine hearts in which exposure to elevated potassium levels also resulted in preferential conduction via the internodal pathways.[119]

1.4.3-c The atrioventricular node (AVN)

In 1906 Sunao Tawara (1873 – 1952) a Japanese pathologist who worked in the laboratory of Ludwig Aschoff (1866 – 1942; physician and pathologist) in Marburg Germany established the existence of an axis of histological specialized cells contained with fibrous sheaths as being responsible for rapid conduction from the atria to the ventricles. The AVN (also known as auriculoventricular node, Aschoff's node and node of Aschoff and Tawara) made part of this specialize conduction system.[120] During development the AVN can be identified as from approximately the fifth week in human ($\approx$ 11 dpc in mouse).[13,121]

Controversy still exists about the developmental origin of the AVN.[122,123] The last decades different theories based on histological observations in multiple species have been put forward: (1) The AVN completely derives from the primary AV canal myocardium (first heart field);[121] [124] (2) The existence of two AVN primordia located in the posterior wall in the common atrium, which then fuse to form the AVN primordium;[58,125,126] (3) The AVN develops as left sided counterpart of the SAN. Subsequently, by remodeling of the sinus venous area the AVN becomes positioned at its mature location in the heart;[127] (4) The AVN derives from a confluence of the sinu-atrial ring , AV ring and possibly the primary fold. By remodeling of this specialized ring tissue the AVN and other major parts of the CCS are formed.[40,57] In contrast to this, some suggested that the AVN solely derives from a single ring of specialized myocytes i.e. the primary interventricular ring.[128]

The maturation of the AVN seems not to be completed at the time of birth, as a number of structural changes with regard to rearrangement of myocardium as well as fibrous tissue occurs in the first year of life.[127,129] Persistence of a fetal phenotype of the AVN, so-called fetal dispersion,[129] has been related to the appearance of sudden cardiac death in the young.[130,131] With regard to anatomy and electrophysiological properties the AVN is a highly complex and heterogeneous structure in which several myocardial regions can be discriminated: (1) The compact node connecting to the bundle of His; (2) The transitional zone located between the compact node and the atrial working myocardium, in which transitional cells are located;[132-135] (3) Nodal extension originating from the AVN running towards the vestibules of the tricuspid and mitral valves. In literature, these nodal extensions have been referred to as: posterior,[136,137] inferior,[138,139] ostial,[140] leftward and rightward[141] nodal extensions. Some variances exist concerning the nodal extensions within and between species. In humans and rabbit hearts, the AVN (usually) has right sided nodal extensions, although left sided extensions can be observed in humans.[136,141 137,142]

All separate myocardial regions within the AVN show a different expression of gap-junction proteins (Cx43, Cx40, Cx45 and Cx30.2/31.9)[101,102,142] and ionic currents involved in action potential propagation and if mandatory initiation.[137,138,143] Modern electrophysiological mapping studies[144] as well as early electrode recordings[46] generally agree that two different conducting pathways fast (α) and slow (β) into the compact node can be discriminated. These α and β-pathway are involved in certain type of cardiac arrhythmias i.e. AV nodal reentry tachycardia (AVNRT).[145] There is still some debate on the exact anatomical structures, which encompass these α and β pathways. In immunohistochemical expression and optical mapping studies of the AV junction certain evidence was found that the β-pathway involves the isthmus between the coronary sinus and tricuspid valve. This region includes the right inferior nodal extension and the transitional cells located in that particular area.[146,147] The α-pathway seemed to be located more to a superior position and encompasses the transitional cells abundantly expressing Cx43 like the atrial myocardium, enabling fast action potential propagation.[148,149]

1.4.3-d The His-Purkinje system (HPS)
The HPS comprises the complete ventricular part of the conduction system, including the bundle of His, the LBB and RBB and the Purkinje system network. The bundle of His was first described in 1893 by Wilhelm His Jr (1863 – 1934), a Swiss born Cardiologist and Anatomist.[150] During development the bundle of His becomes recognizable in human around 5 to 6 weeks of development (mouse ≈ 10 dpc).[121] The exact developmental process of this structure is still not clear just like the mechanism, which solely prevents this bundle from being interrupted by fibrous tissue during annulus fibrosus formation in the AV junction. However, several studies on CCS development describing the expression of HNK-1,[151] G1N2,[152] Leu7[112] and CCS-Lacz,[59] indicate an important role for the primary ring (i.e. inter-ventricular

ring) myocardium in the anlage of the bundle of His and primary bundle branches.[55,59] The ultimate part of the CCS is the Purkinje fiber network. Purkinje fibers were first described in a sheep heart ventricle in 1839 by Jan Evangelista Purkinje (1787 – 1869; a Czech physiologist and Anatomist).[150] Purkinje fibers are mainly located (but not exclusively)[153] in the ventricles where they create an extensive conduction network. Their morphology and location in the ventricles differs between species.[154] During development Purkinje fibers become apparent around day 10 (HH 36) in chick in close association with coronary vessels and at a sub-endocardial position.[155] Purkinje fiber differentiation has shown to be narrowly regulated by activation of endothelial localized factors (i.e. endothelin-1 and endothelin converting enzyme-1) through hemodynamic alterations in the developing heart.[156] Furthermore, EPDCs have an essential role in proper differentiation of the Purkinje fibers in avian.[30] With regard to electrophysiological properties Purkinje fibers contain a specific subset of ionic currents,[157] which enables the capability of generating both automatic and triggered rhythms.[158,159]

1.4.3-e The right atrioventricular ringbundle (RAVRB) and retro aortic root branch (RAoRB)

The RAVRB and RAoRB are not part of the mature CCS, however based on their postulated origin related to CCS development, expression patterns of specific CCS markers[58,59,111] and possible involvement in certain types of arrhythmia[160] they will be mentioned shortly in this section. In human fetuses both histological[161] and marker gene expression studies[58] demonstrated the presence of "specialized" myocardial tracts around the tricuspid orifice, the so-called RAVRB (see also **Chapter 7**). At embryonic stages these tracts were also noticed near the aorta i.e. the RAoRB.[58] In animal hearts: avian,[162] chick,[163] mouse[59] rat and rabbit,[164] the complex of RAVRB and RAoRB is even more extensive and also encompasses a specialized tract around the mitral orifice, which will be referred to as the left AV ring bundle (i.e. LAVRB). With regard to the developmental origin of these structures, the RAVRB, RAoRB and the tract around the mitral orifice are believed to be remnants of the specialized ring tissue at the transitional zones in the developing heart.[40,49,152]

Up till now there are no electrophysiological studies, which prove that the RAVRB, LAVRB and RAoRB do have a role in normal action potential conduction, although their involvement in certain types of arrhythmia i.e. Mahaim tachycardia is postulated.[160,165] Interestingly, the immunohistochemical experiments in rat hearts demonstrated that the cardiomyocytes of the RAVRB and RAoRB show an expression pattern that is comparable to other parts of the CCS: Cx43 negative and HCN4 positive.[138] Moreover, the HCN4 positive RAVRB and LAVRB seem to be continuous with the two inferior nodal extensions of the AVN as described in **Chapter 1.4.3-c *"The atrioventricular node"***, which might indicate a role of these specialized tracts in AV conduction.[138]
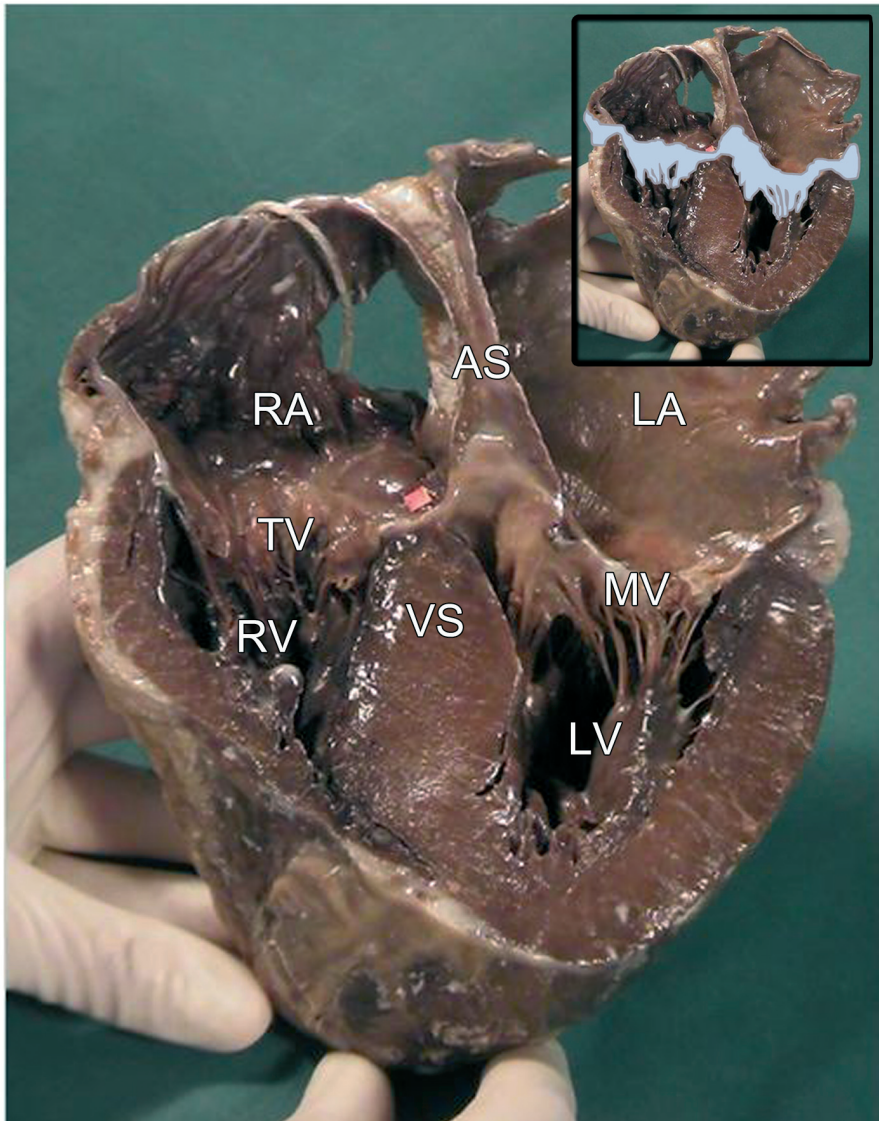
Figure 7. The fibrous heart skeleton. The annulus fibrosus creates a continuum of isolating fibrous tissue between the atrial and ventricular myocardium (light blue in detail upper right corner) as is depicted in this frontally sectioned specimen of a mature human heart. Furthermore, it can be appreciated that the fibrous tissue of the annulus fibrosus is continuous with the atrioventricular valves (light blue in detail upper right corner), i.e. the tricuspid valves (**TV**) at the right and mitral valves (**MV**) at the left AV junction. **AS** indicates atrial septum; **LA**, left atrium; **LV**, left ventricle; **RA**, right atrium; **RV**, right ventricle; **VS**, ventricular septum.

1.5 THE ANNULUS FIBROSUS AND ACCESSORY PATHWAYS (APs)

1.5.1 Annulus fibrosus: "The isolating system"

In a mature heart the AV conduction axis comprises the only myocardial continuity between the atria and ventricles the remainder being separated by a layer of fibrous tissue at the AV junction i.e. the annulus fibrosus. Morphologically, this fibrous structure is in continuity with the fibrous tissue of the AV valves (mitral and tricuspid valves; Figure 7). Early in development, at the stage of the primary heart tube, the atrial and ventricular myocardium is continuous in the AV junction. During cardiogenesis separation of the atrial and ventricular myocardium occurs, which leads to electrical isolation of the atria from the ventricles. Several specific structures have been described to have a role in annulus fibrosus development: The atrial and ventricular myocardium, the AV canal myocardium, AV cushion tissue, tissue of the AV groove[166] and recently an important role of EPDCs has been demonstrated.[92,167]

Two different theories have been put forward underlying the process of annulus fibrosus formation. The first postulates that the annulus fibrosus completely derives from the invagination of AV sulcus tissue into the myocardium of the AV canal. Furthermore, this theory states that major parts of the AV cushions derive from this sulcus tissue.[166] The second theory states that development of the AV junction involves the fusion of the AV sulcus tissue from the epicardial side with the endocardially located cushion tissue of the developing heart. In this theory the endocardial cushion tissue substantially contributes to formation of the AV valves.[93,168-170] With regard to human annulus fibrosus development the study of Wessels *et al.* supports the latter theory, in which both AV sulcus and AV cushion tissue have an important role. This study demonstrated that formation of AV isolation starts around 7 weeks of human development near the antero-lateral portion of the future tricuspid valve orifice. By twelve weeks the complete AV junction has become isolated except for the AV conduction axis.[93]

In **Chapter 6** and **7** of this thesis the development of the annulus fibrosus in mouse and human are described, respectively. Furthermore, these chapters describe the role of periostin, which is able to regulate collagen-I fibrillogenesis,[171] in the development of this isolating structure.

1.5.2 Accessory pathways (APs): "substrate for arrhythmia"

The identification of the individual components of the CCS, particularly those involving the AV conduction axis, indirectly launched the discussion about APs. It was Stanly Kent (1863 - 1958, British physiologist) who (wrongly) defined that the lateral myocardial connections through the AV groove, which he observed in a mammalian heart, were the pathways for normal AV conduction.[172] However, this theory did not have much impact, since at the same time period the true AV conduction axis became well established by Tawara and His.[150] Nowadays, APs are defined as accessory bundles of cardiomyocytes, which interconnect the atrial and ventricular part of heart next to the AV conduction axis. These APs may either

conduct the action potential in an antegrade (atrium-to-ventricle) or a retrograde (ventricle-to-atrium) manner. Furthermore, APs may form the substrate for certain types of supraventricular arrhythmias i.e. Wolff-Parkinson-White (WPW) syndrome and Mahaim tachycardia (**Chapter 1.6 *"Cardiac arrhythmias in the young"***).

Studies in both human and animal have shown that APs can be located anywhere at the AV junction and might be positioned endocardially or epicardially. Although it has been well established that abnormal development of the AV junction as observed in patients with Ebstein's anomaly coincide with high numbers of APs,[173,174] there is still debate on the exact origin of APs. Electrophysiological studies in human[175,176] and animal[177] demonstrated that not all APs share the same electrophysiological conducting properties, some APs even have decremental properties resembling to those of specialized CCS tissue,[175] whereas others demonstrate a working myocardium phenotype. Moreover, morphological analysis of APs indicated that not all APs show the same cellular morphology.[178-180] In clinical practice not all APs in patients suffering from AV reentry tachycardia (AVRT; **Chapter 1.6 *"Cardiac arrhythmias in the young"***) react similar to anti-arrhythmic drugs.[181] All these arguments may indicate that not all APs share a common developmental origin.

In the late fifties it was already postulated that APs are remnants of the primary AV canal myocardium. Due to incomplete AV insulation i.e. annulus fibrosus development the atrial and ventricular myocardium are not completely separated, the myocardial substrate left in the AV canal composes the AP.[182] Animal experiments performed in developing quail hearts contributed to this hypothesis. Electrophysiological recordings in embryonic and fetal quail heart showed presence of antegrade conducting APs in otherwise normal developing hearts.[86,92] These APs decreased in number and size at subsequent stage of development. From this was concluded that APs are part of the normal maturation process of the annulus fibrosus.[86] Moreover, in human two-thirds of newborns diagnosed with AVRT based on the presence of APs remain free of symptoms before the age of one year without invasive treatment strategies.[183,184] This might suggest that annulus fibrosus formation and maturation is not finished by the time of birth and extends into the first year of life. The postnatal maturation of the heart also has been described for the AVN region,[127] which is closely related to the annulus fibrosus.

In the more recent years genetic mutations have been identified that coincide with high percentage of APs. Mutations in the gene encoding the gamma2 regulatory subunit of AMP-activated kinase (*PRKAG-2*) have been found in families with WPW-syndrome. Patients carrying this mutation suffer from ventricular pre-excitation, atrial fibrillation, conduction defects and cardiac hypertrophy.[185,186] Mouse models with this specific mutation demonstrated postnatal development of APs responsible for ventricular pre-excitation.[187] Another mutation recently related to AP etiology is in the Bone Morphogenetic Protein (BMP) receptor *Alk3*. Mouse embryos lacking *Alk3* showed abnormal development of the AV valves and anlage of

the annulus fibrosus resulting in antegradely conducting APs.[188]

APs may also be related to parts of the CCS. In rare cases APs interconnect the AVN and ventricular myocardium. More frequently APs are found between the fascicles and the ventricular myocardium, which were first reported by Mahaim (1897 – 1965; Belgian MD) and are therefore frequently referred to as Mahaim-fibers.[189,190] Conduction via this specific type of APs show electrophysiological properties similar to the AVN, including automaticity.[191] Contemporary animal experiments studying CCS development by means of CCS-*LacZ* expression demonstrated a possible link between right ventricular inflow tract formation and atrio-fascicular tract via the trabecula septomarginalis i.e. moderator band.[165]

More uncommon causes of APs are intracardiac tumours i.e. rhabdomyomas (sarcomas), producing myocardial substrates in the AV junction that serve as AP for AVRT.[192,193] Although this cause of an AP is rare sometimes AVRT is the initial presentation of intracardiac tumours.

Up till now it is not known whether "physiological" APs, similar to those observed during normal avian heart development,[86] can also be found in mammals including human. Furthermore, if APs are present during normal mammalian heart development, do they show a similar course at the developing annulus fibrosus? Are they electrophysiologically functional and do they have a relationship with the developing CCS? Answers to these questions can be studied in **Chapter 6** and **7** of this thesis, where we for the first time describe the presence of APs during normal mammalian heart development.

1.6 CARDIAC ARRHYTHMIAS IN THE YOUNG

1.6.1 Arrhythmia in the fetus

Fetal arrhythmias occur in 1-3% of all pregnancies.[194-196] Prenatally detection and monitoring of fetal arrhythmias requires echocardiographic techniques like M-mode, pulse-wave and Doppler-flow measurements.[197,198] Furthermore, other new techniques like fetal magnetocardiography (MCG) and transabdominal fetal ECG can be performed to evaluate fetal arrhythmias.

In general three different types of fetal arrhythmia can be discriminated: irregular ectopic beats, tachycardia (heartrate >180 beats per minute (bpm)) and bradycardia (heartrate <100 bpm).[199] While arrhythmias may be well-tolerated in the fetus, at the severe end of the spectrum they may cause low cardiac output, fetal hydrops, and death. The presence of arrhythmia-related hydrops is an important predictor of an adverse outcome, associated with a high risk of mortality.[184,200] Furthermore, neurological complications can occur based on a dysfunction of the cerebrovascular autoregulation.[201-203]

Supraventricular tachycardia (SVT) and atrial flutter (AF) are the most common causes of

fetal tachycardia.[204] Fetal AF is characterized by a fast atrial heart rate, ranging between 300 up to 550 bpm and is usually associated with 2:1 AV conduction, but AV conduction can range between 1:1 to 4:1. AF results from an intra-atrial electrical macro-reentrant circuit in the atrium around fixed or functional anatomical conduction barriers.[196] Furthermore, fetuses with AF frequently appear to have APs and may also develop AVRT pre- and or post-natally.[184,205] AVRT is the most common type of SVT in the fetus and is characterized by the presence of electrophysiological functional APs crossing the isolating annulus fibrosus next to the AV conduction axis. Almost all causes of fetal and neonatal SVT are orthodromic AVRT, in which the action potential is conducted via the AV conduction axis and retrogradely (ventricle-to-atrium) via the AP, creating a circus movement between the atria and ventricles. In the fetus and neonate antidromic AVRT are rare and characterized by antegrade (atrium-to-ventricle) conduction via the AP and retrograde conduction via the AV conduction axis. In fetal SVT cases ventricular pre-excitation (WPW-syndrome) is present in approximately 10% of postnatal ECG recordings, indicating that the majority of fetal SVT is caused by so-called concealed APs.[195,206] Due to new techniques, WPW-syndrome has also been documented in the fetus. A number of case reports showed similar characteristics on fetal MCG recordings as observed in post-natal ECG recordings from WPW-syndrome patients i.e. (1) short PR-interval, (2) long QRS-complex duration, and (3) a delta-wave.[207,208] It is postulated that (as is the case in adults) fetal ectopic atrial contractions (present in 1 to 2% of pregnancies) may trigger AVRT.[209] Other rare forms of fetal tachycardia are, permanent junctional reciprocating tachycardia (PJRT), atrial ectopic tachycardia (AET), congenital junctional ectopic tachycardia and ventricular tachycardia.[196]

Treatment of fetal SVT and AF includes anti-arrhythmic drug therapy, which can be administered either transplacentally or directly to the fetus through injections in the umbilical vein. Throughout the years several anti-arrhythmic drug agents have proven to be effective in treatment of fetal SVT and AF, including: Digoxin, Flecainide, Sotalol and Amiodarone. Success rates in suppression of SVT are highly variable between 32% and 100% of SVT and AF cases.[196,210] Furthermore, there is not one single guideline for anti-arrhythmic drug therapy in fetal tachycardias and variances exists in treatment protocols between individual institutions. Later in pregnancy, after 34-35 weeks of gestation, a good alternative treatment option is delivery, by caesarean section, with postnatal SVT conversion i.e. anti-arrhythmic drug therapy or even radiofrequency ablation in exceptional cases in which drug therapy fails.

In the fetus the majority of brady-arrhythmias are caused by an AV block (AVB). In case of AVB the AV conduction axis is interrupted resulting in hampered impulse propagation to the ventricles. Congenital AVB can be associated with congenital structural heart malformations and frequently has a poor prognosis.[211,212] Furthermore, AVB can be auto-immune mediated by maternal anti-Ro (SS-A), anti-La (SS-B),[213] anti-U1 RNP[214] and anti-cardiolipin[215] antibodies, which cross the placenta and enter the fetal circulation. The exact mechanism by which these

antibodies cause AVB remains unknown, although it has been suggested that an immune-mediated necrotizing arteritis and collagen changes in the AVN region results in focal degeneration and fibrosus of that specific area.[216,217] The auto-immune mediated AVB usually develops between the eighteenth and twenty-fourth week of development.[218] Furthermore, progress of auto-immune AVB frequently occurs within days, and most of these fetuses (>95%) are diagnosed with established complete AVB.[219] Another rare but important form of fetal bradycardia can occur in long QT-syndrome (LQTS) due to either functional 2:1 AVB or sinus bradycardia.[220] Furthermore, a common and benign form of fetal bradycardia is caused by blocked atrial premature (ectopic) beats in bigeminy or trigeminy.[196]

Treatment of AVB mediated fetal brady-arrhythmia includes drug therapy or early delivery by cesarean section for postnatal interventions like pacemaker therapy. Prenatal steroid therapy focuses on improvement of fetal AVB, myocardial contractility, and fetal hydrops but its efficacy seems limited. Furthermore, beta sympathomimetic agents like Ritodrine and Fenoterol can be administered increasing fetal heart rate and myocardial contractility.[196,219]

Despite treatment, the outcome of fetal AVB is poor in fetuses with hydrops, heart rates below 55 bpm or structural heart malformations,[211,212] which can be appreciated in **Chapter 8** of this thesis that discusses the early and late outcome of severe fetal arrhythmia.

1.6.2 SVT in children

SVT is the most common type of arrhythmias in children, with an estimated incidence of 1 per 250-1000 of otherwise healthy children.[221] AF and atrial fibrillation in children are attributed largely to structural heart disease. In the pediatric age group, ventricular tachycardia, including LQTS, and brady-arrhythmias i.e. sinus bradycardia and AVB are less frequently observed. A large retrospective review of emergency department visits showed that 55.1 per 100.000 of pediatric visitors (<18 years of age) presented with significant arrhythmias, of which the majority had SVT.[222]

In children with structurally normal hearts AVRT is by far the most common mechanism of SVT in childhood occurring both in children with WPW-syndrome and in children with a concealed AP (concealed-WPW). The incidence of AVRT seems to vary within the young age group, which has been described in multiple studies. The first episode of SVT occurs, whether or not before birth, in approximately half of the cases before the age of one year.[223,224] Furthermore, incidence peaks have been observed in early childhood (6-9 years) and in adolescence.[224,225] It seems that in infants SVT in the majority of cases resolves without invasive treatment before the age of one year (**Chapter 8**),[183,184] nevertheless one third will have recurrences around the age of 8 years.[224] In children diagnosed with SVT after the age of one year, spontaneous resolution only occurs in 15% of cases.[223]

Another common category of SVT, AVNRT is rarely observed at fetal and neonatal stages, whereas postnatally the incidence gradually increases with age. In AVNRT, tachycardia is

mediated by a reentry circuit, which is created by a fast (α) and a slow (β) conducting pathway within the AVN **(Chapter 1.4.3-c *"The atrioventricular node"*)**.

The spontaneous disappearance as well as occurrence of arrhythmias in the young might be related to postnatal cardiac maturation. After birth, morphological[127,226] as well as electrophysiological[227,228] changes within the heart have been described. These changes may create specific circumstances for cardiac arrhythmias to occur in one child or to resolve in another. This thesis focuses on cardiac development including that of the CCS, in relation to cardiac arrhythmias in fetuses and neonates.

1.7 AIM OF THIS THESIS

This thesis is separated in two parts, **Part I** and **Part II** in which normal and abnormal heart development are studied and related to congenital heart disease, in particular to the etiology of supraventricular arrhythmias. The aim of **Part I** is to describe the important role of the PHF in development of the venous pole, parts of the CCS and the epicardium of the heart. In **Part II** normal heart development, mainly with respect to anlage and maturation of the AV junction including the CCS and the isolating annulus fibrosus, is related to clinically observed AVRTs at perinatal stages of development.

1.8 CHAPTER OUTLINE

Part I

In **Chapter 2** the important role of the homeobox gene *Shox2* in development of the PHF derived sinus venosus myocardium is demonstrated, with special focus on the anlage and differentiation of the primary pacemaker (i.e. SAN) of the heart.

In **Chapter 3** the role of *Shox2* in SAN development is further studied by means of electrophysiological recordings in wildtype and *Shox2* mutant hearts. Furthermore, a role of the PHF in epicardial lineage development is substantiated by demonstrating an abrogated epicardial development in *Shox2* mutants.

Chapter 4 further delineates the formation of the PHF derived sinus venosus myocardium including major parts of the CCS by means of spatio-temporal expression of the transmembrane protein *podoplanin*.

In **Chapter 5** abnormal anlage of the PHF was demonstrated in *podoplanin* mutants. In these

mutants the abnormal formation of the venous pole of the heart could be linked to an abrogated EMT process in the coelomic epithelium from where the PHF cells presumably derive.

Part II

In **Chapter 6** the development of the AV junction specifically with regard to the formation of the isolating annulus fibrosus is demonstrated during normal embryonic and fetal mouse heart development. Furthermore, the presence, location and course of functional APs crossing the annulus fibrosus is demonstrated at subsequent developmental stages.

Chapter 7 shows the presence and course of APs in otherwise normal developing human embryonic, fetal and neonatal hearts. The presence of the APs were related to clinically observed perinatal AVRTs that in majority of cases are self-limiting before the age of one year.

Chapter 8 retrospectively evaluates the perinatal management, outcome and long-term cardiac follow-up in severe case of fetal brady- and tachyarrhythmias.

In the general discussion, **Chapter 9** the results of **Part I** and **Part II** of this thesis are individually discussed and related to congenital heart disease and supraventricular arrhythmias.

REFERENCES

1. Hoffman JI, Kaplan S. The incidence of congenital heart disease. *J Am Coll Cardiol*. 2002;39:1890-1900.
2. Larsen WJ. *Human Embryology*. third ed. Pennsylvania, USA: Churchill Livingstone; 2001.
3. Frasch M. Intersecting signalling and transcriptional pathways in Drosophila heart specification. *Semin Cell Dev Biol*. 1999;10:61-71.
4. Schultheiss TM, Xydas S, Lassar AB. Induction of avian cardiac myogenesis by anterior endoderm. *Development*. 1995;121:4203-4214.
5. Laverriere AC, MacNeill C, Mueller C, Poelmann RE, Burch JB, Evans T. GATA-4/5/6, a subfamily of three transcription factors transcribed in developing heart and gut. *J Biol Chem*. 1994;269:23177-23184.
6. Deruiter MC, Poelmann RE, VanderPlas-de V, I, Mentink MM, Gittenberger-de Groot AC. The development of the myocardium and endocardium in mouse embryos. Fusion of two heart tubes? *Anat Embryol (Berl)*. 1992;185:461-473.
7. Lough J, Sugi Y. Endoderm and heart development. *Dev Dyn*. 2000;217:327-342.
8. Schier AF. Nodal signaling in vertebrate development. *Annu Rev Cell Dev Biol*. 2003;19:589-621.
9. Hamada H, Meno C, Watanabe D, Saijoh Y. Establishment of vertebrate left-right asymmetry. *Nat Rev Genet*. 2002;3:103-113.
10. Bamforth SD, Braganca J, Farthing CR, Schneider JE, Broadbent C, Michell AC, Clarke K, Neubauer S, Norris D, Brown NA, Anderson RH, Bhattacharya S. Cited2 controls left-right patterning and heart development through

a Nodal-Pitx2c pathway. *Nat Genet*. 2004;36:1189-1196.

11. Manasek FJ. Embryonic development of the heart. I. A light and electron microscopic study of myocardial development in the early chick embryo. *J Morphol*. 1968;125:329-365.

12. Stalsberg H, DeHaan RL. The precardiac areas and formation of the tubular heart in the chick embryo. *Dev Biol*. 1969;19:128-159.

13. Viragh S, Challice CE. Origin and differentiation of cardiac muscle cells in the mouse. *J Ultrastruct Res*. 1973;42:1-24.

14. Kelly RG, Buckingham ME. The anterior heart-forming field: voyage to the arterial pole of the heart. *Trends Genet*. 2002;18:210-216.

15. Dodou E, Verzi MP, Anderson JP, Xu SM, Black BL. Mef2c is a direct transcriptional target of ISL1 and GATA factors in the anterior heart field during mouse embryonic development. *Development*. 2004;131:3931-3942.

16. Kelly RG, Brown NA, Buckingham ME. The arterial pole of the mouse heart forms from Fgf10-expressing cells in pharyngeal mesoderm. *Dev Cell*. 2001;1:435-440.

17. Waldo KL, Kumiski DH, Wallis KT, Stadt HA, Hutson MR, Platt DH, Kirby ML. Conotruncal myocardium arises from a secondary heart field. *Development*. 2001;128:3179-3188.

18. de la Cruz MV, Sanchez GC, Arteaga MM, Arguello C. Experimental study of the development of the truncus and the conus in the chick embryo. *J Anat*. 1977;123:661-686.

19. Cai CL, Liang X, Shi Y, Chu PH, Pfaff SL, Chen J, Evans S. Isl1 identifies a cardiac progenitor population that proliferates prior to differentiation and contributes a majority of cells to the heart. *Dev Cell*. 2003;5:877-889.

20. Mjaatvedt CH, Nakaoka T, Moreno-Rodriguez R, Norris RA, Kern MJ, Eisenberg CA, Turner D, Markwald RR. The outflow tract of the heart is recruited from a novel heart-forming field. *Dev Biol*. 2001;238:97-109.

21. Perez-Pomares JM, Phelps A, Sedmerova M, Wessels A. Epicardial-like cells on the distal arterial end of the cardiac outflow tract do not derive from the proepicardium but are derivatives of the cephalic pericardium. *Dev Dyn*. 2003;227:56-68.

22. Lie-Venema H, Van Den Akker NM, Bax NA, Winter EM, Maas S, Kekarainen T, Hoeben RC, Deruiter MC, Poelmann RE, Gittenberger-de Groot AC. Origin, fate, and function of epicardium-derived cells (EPDCs) in normal and abnormal cardiac development. *ScientificWorldJournal*. 2007;7:1777-1798.

23. Jenkins SJ, Hutson DR, Kubalak SW. Analysis of the proepicardium-epicardium transition during the malformation of the RXRalpha-/- epicardium. *Dev Dyn*. 2005;233:1091-1101.

24. Lavine KJ, Yu K, White AC, Zhang X, Smith C, Partanen J, Ornitz DM. Endocardial and epicardial derived FGF signals regulate myocardial proliferation and differentiation in vivo. *Dev Cell*. 2005;8:85-95.

25. Kwee L, Baldwin HS, Shen HM, Stewart CL, Buck C, Buck CA, Labow MA. Defective development of the embryonic and extraembryonic circulatory systems in vascular cell adhesion molecule (VCAM-1) deficient mice. *Development*. 1995;121:489-503.

26. Hatcher CJ, Diman NY, Kim MS, Pennisi D, Song Y, Goldstein MM, Mikawa T, Basson CT. A role for Tbx5 in proepicardial cell migration during cardiogenesis. *Physiol Genomics*. 2004;18:129-140.

27. Dettman RW, Pae SH, Morabito C, Bristow J. Inhibition of alpha4-integrin stimulates epicardial-mesenchymal transformation and alters migration and cell fate of epicardially derived mesenchyme. *Dev Biol*. 2003;257:315-328.

28. Sengbusch JK, He W, Pinco KA, Yang JT. Dual functions of [alpha]4[beta]1 integrin in epicardial development: initial migration and long-term attachment. *J Cell Biol*. 2002;157:873-882.

29. Gittenberger-de Groot AC, Vrancken Peeters MP, Mentink MM, Gourdie RG, Poelmann RE. Epicardium-derived cells contribute a novel population to the myocardial wall and the atrioventricular cushions. *Circ Res*. 1998;82:1043-1052.

30. Eralp I, Lie-Venema H, Bax NA, Wijffels MC, van der Laarse A, Deruiter MC, Bogers AJ, Van Den Akker NM, Gourdie RG, Schalij MJ, Poelmann RE, Gittenberger-de Groot AC. Epicardium-derived cells are important for correct development of the Purkinje fibers in the avian heart. *Anat Rec A Discov Mol Cell Evol Biol*. 2006;288:1272-1280.

31. Winter EM, Gittenberger-de Groot AC. Epicardium-derived cells in cardiogenesis and cardiac regeneration.

Cell Mol Life Sci. 2007;64:692-703.

32.   Zhou B, Ma Q, Rajagopal S, Wu SM, Domian I, Rivera-Feliciano J, Jiang D, von GA, Ikeda S, Chien KR, Pu WT. Epicardial progenitors contribute to the cardiomyocyte lineage in the developing heart. *Nature*. 2008;454:109-113.

33.   Christoffels VM, Grieskamp T, Norden J, Mommersteeg MT, Rudat C, Kispert A. Tbx18 and the fate of epicardial progenitors. *Nature*. 2009;458:E8-E9.

34.   Kirby ML, Gale TF, Stewart DE. Neural crest cells contribute to normal aorticopulmonary septation. *Science*. 1983;220:1059-1061.

35.   Le Douarin N. Migration and differentiation of neural crest cells. *Curr Top Dev Biol*. 1980;16:31-85.

36.   Poelmann RE, Gittenberger-de Groot AC. A subpopulation of apoptosis-prone cardiac neural crest cells targets to the venous pole: multiple functions in heart development? *Dev Biol*. 1999;207:271-286.

37.   Waldo K, Miyagawa-Tomita S, Kumiski D, Kirby ML. Cardiac neural crest cells provide new insight into septation of the cardiac outflow tract: aortic sac to ventricular septal closure. *Dev Biol*. 1998;196:129-144.

38.   Nakamura T, Colbert MC, Robbins J. Neural crest cells retain multipotential characteristics in the developing valves and label the cardiac conduction system. *Circ Res*. 2006;98:1547-1554.

39.   Poelmann RE, Mikawa T, Gittenberger-de Groot AC. Neural crest cells in outflow tract septation of the embryonic chicken heart: differentiation and apoptosis. *Dev Dyn*. 1998;212:373-384.

40.   Gittenberger-de Groot AC, Bartelings MM, Deruiter MC, Poelmann RE. Basics of cardiac development for the understanding of congenital heart malformations. *Pediatr Res*. 2005;57:169-176.

41.   Verberne ME, Gittenberger-de Groot AC, Van Iperen L, Poelmann RE. Contribution of the cervical sympathetic ganglia to the innervation of the pharyngeal arch arteries and the heart in the chick embryo. *Anat Rec*. 1999;255:407-419.

42.   Poelmann RE, Jongbloed MR, Molin DG, Fekkes ML, Wang Z, Fishman GI, Doetschman T, Azhar M, Gittenberger-de Groot AC. The neural crest is contiguous with the cardiac conduction system in the mouse embryo: a role in induction? *Anat Embryol (Berl)*. 2004;208:389-393.

43.   Gorza L, Schiaffino S, Vitadello M. Heart conduction system: a neural crest derivative? *Brain Res*. 1988;457:360-366.

44.   Kozlowski D, Kozluk E, Adamowicz M, Grzybiak M, Walczak F, Walczak E. Histological examination of the topography of the atrioventricular nodal artery within the triangle of Koch. *Pacing Clin Electrophysiol*. 1998;21:163-167.

45.   Villain E. Indications for pacing in patients with congenital heart disease. *Pacing Clin Electrophysiol*. 2008;31 Suppl 1:S17-S20.

46.   Meijler FL, Janse MJ. Morphology and electrophysiology of the mammalian atrioventricular node. *Physiol Rev*. 1988;68:608-647.

47.   Mark GE, Rhim ES, Feldman AM, Pavri BB. Cardiac resynchronization therapy: from creation to evolution--an evidence-based review. *Congest Heart Fail*. 2007;13:84-92.

48.   Gourdie RG, Mima T, Thompson RP, Mikawa T. Terminal diversification of the myocyte lineage generates Purkinje fibers of the cardiac conduction system. *Development*. 1995;121:1423-1431.

49.   Moorman AF, de Jong F, Denyn MM, Lamers WH. Development of the cardiac conduction system. *Circ Res*. 1998;82:629-644.

50.   Pennisi DJ, Rentschler S, Gourdie RG, Fishman GI, Mikawa T. Induction and patterning of the cardiac conduction system. *Int J Dev Biol*. 2002;46:765-775.

51.   Gourdie RG, Harris BS, Bond J, Justus C, Hewett KW, O'Brien TX, Thompson RP, Sedmera D. Development of the cardiac pacemaking and conduction system. *Birth Defects Res C Embryo Today*. 2003;69:46-57.

52.   Cheng G, Litchenberg WH, Cole GJ, Mikawa T, Thompson RP, Gourdie RG. Development of the cardiac conduction system involves recruitment within a multipotent cardiomyogenic lineage. *Development*. 1999;126:5041-5049.

53.   Moorman AF, Christoffels VM. Cardiac chamber formation: development, genes, and evolution. *Physiol Rev*. 2003;83:1223-1267.

54. Christoffels VM, Habets PE, Franco D, Campione M, de Jong F, Lamers WH, Bao ZZ, Palmer S, Biben C, Harvey RP, Moorman AF. Chamber formation and morphogenesis in the developing mammalian heart. *Dev Biol*. 2000;223:266-278.

55. Christoffels VM, Burch JB, Moorman AF. Architectural plan for the heart: early patterning and delineation of the chambers and the nodes. *Trends Cardiovasc Med*. 2004;14:301-307.

56. Christoffels VM, Moorman AF. Development of the cardiac conduction system: why are some regions of the heart more arrhythmogenic than others? *Circ Arrhythm Electrophysiol*. 2009;2:195-207.

57. Wenink AC. Development of the human cardiac conducting system. *J Anat*. 1976;121:617-631.

58. Blom NA, Gittenberger-de Groot AC, Deruiter MC, Poelmann RE, Mentink MM, Ottenkamp J. Development of the cardiac conduction tissue in human embryos using HNK-1 antigen expression: possible relevance for understanding of abnormal atrial automaticity. *Circulation*. 1999;99:800-806.

59. Jongbloed MR, Schalij MJ, Poelmann RE, Blom NA, Fekkes ML, Wang Z, Fishman GI, Gittenberger-de Groot AC. Embryonic conduction tissue: a spatial correlation with adult arrhythmogenic areas. *J Cardiovasc Electrophysiol*. 2004;15:349-355.

60. Rentschler S, Vaidya DM, Tamaddon H, Degenhardt K, Sassoon D, Morley GE, Jalife J, Fishman GI. Visualization and functional characterization of the developing murine cardiac conduction system. *Development*. 2001;128:1785-1792.

61. Kondo RP, Anderson RH, Kupershmidt S, Roden DM, Evans SM. Development of the cardiac conduction system as delineated by minK-lacZ. *J Cardiovasc Electrophysiol*. 2003;14:383-391.

62. Gittenberger-de Groot AC, Jongbloed MR, Poelmann RE. Normal and Abnormal Cardiac development. In: Moller JH, Hoffman JIE (eds). *Pediatric Cardiovascular Medicine*. New York, USA: Churchill Livingstone; 2010:in press.

63. Viragh S, Challice CE. The development of the conduction system in the mouse embryo heart. *Dev Biol*. 1980;80:28-45.

64. James TN. Structure and function of the sinus node, AV node and His bundle of the human heart: part I-structure. *Prog Cardiovasc Dis*. 2002;45:235-267.

65. Davis DL, Edwards AV, Juraszek AL, Phelps A, Wessels A, Burch JB. A GATA-6 gene heart-region-specific enhancer provides a novel means to mark and probe a discrete component of the mouse cardiac conduction system. *Mech Dev*. 2001;108:105-119.

66. Di Lisi R, Sandri C, Franco D, Ausoni S, Moorman AF, Schiaffino S. An atrioventricular canal domain defined by cardiac troponin I transgene expression in the embryonic myocardium. *Anat Embryol (Berl)*. 2000;202:95-101.

67. Garcia-Frigola C, Shi Y, Evans SM. Expression of the hyperpolarization-activated cyclic nucleotide-gated cation channel HCN4 during mouse heart development. *Gene Expr Patterns*. 2003;3:777-783.

68. Thomas PS, Kasahara H, Edmonson AM, Izumo S, Yacoub MH, Barton PJ, Gourdie RG. Elevated expression of Nkx-2.5 in developing myocardial conduction cells. *Anat Rec*. 2001;263:307-313.

69. Jay PY, Harris BS, Buerger A, Rozhitskaya O, Maguire CT, Barbosky LA, McCusty E, Berul CI, O'Brien TX, Gourdie RG, Izumo S. Function follows form: cardiac conduction system defects in Nkx2-5 mutation. *Anat Rec A Discov Mol Cell Evol Biol*. 2004;280:966-972.

70. Ismat FA, Zhang M, Kook H, Huang B, Zhou R, Ferrari VA, Epstein JA, Patel VV. Homeobox protein Hop functions in the adult cardiac conduction system. *Circ Res*. 2005;96:898-903.

71. Moskowitz IP, Kim JB, Moore ML, Wolf CM, Peterson MA, Shendure J, Nobrega MA, Yokota Y, Berul C, Izumo S, Seidman JG, Seidman CE. A molecular pathway including Id2, Tbx5, and Nkx2-5 required for cardiac conduction system development. *Cell*. 2007;129:1365-1376.

72. Christoffels VM, Hoogaars WM, Tessari A, Clout DE, Moorman AF, Campione M. T-box transcription factor Tbx2 represses differentiation and formation of the cardiac chambers. *Dev Dyn*. 2004;229:763-770.

73. Bakker ML, Boukens BJ, Mommersteeg MT, Brons JF, Wakker V, Moorman AF, Christoffels VM. Transcription factor Tbx3 is required for the specification of the atrioventricular conduction system. *Circ Res*. 2008;102:1340-1349.

74. Jongbloed MR, Mahtab EA, Blom NA, Schalij MJ, Gittenberger-de Groot AC. Development of the cardiac conduction system and the possible relation to predilection sites of arrhythmogenesis. *ScientificWorldJournal*. 2008;8:239-269.

75. Kamino K, Hirota A, Fujii S. Localization of pacemaking activity in early embryonic heart monitored using voltage-sensitive dye. *Nature*. 1981;290:595-597.

76. Yada T, Sakai T, Komuro H, Hirota A, Kamino K. Development of electrical rhythmic activity in early embryonic cultured chick double-heart monitored optically with a voltage-sensitive dye. *Dev Biol*. 1985;110:455-466.

77. Van Mierop LH. Location of pacemaker in chick embryo heart at the time of initiation of heartbeat. *Am J Physiol*. 1967;212:407-415.

78. de Jong F, Opthof T, Wilde AA, Janse MJ, Charles R, Lamers WH, Moorman AF. Persisting zones of slow impulse conduction in developing chicken hearts. *Circ Res*. 1992;71:240-250.

79. Vicente-Steijn R, Kolditz DP, Mahtab EA, Askar SF, Bax NA, Van Der Graaf LM, Wisse LJ, Passier R, Pijnappels DA, Schalij MJ, Poelmann RE, Gittenberger-de Groot AC, Jongbloed MR. Electrical activation of sinus venosus myocardium and expression patterns of RhoA and Isl-1 in the chick embryo. *J Cardiovasc Electrophysiol*. 2010;21:1284-1292.

80. Paff GH, Boucek RJ, Harrell TC. Observations on the development of the electrocardiogram. *Anat Rec*. 1968;160:575-582.

81. Sedmera D, Reckova M, Rosengarten C, Torres MI, Gourdie RG, Thompson RP. Optical mapping of electrical activation in the developing heart. *Microsc Microanal*. 2005;11:209-215.

82. Arguello C, Alanis J, Valenzuela B. The early development of the atrioventricular node and bundle of His in the embryonic chick heart. An electrophysiological and morphological study. *Development*. 1988;102:623-637.

83. Delorme B, Dahl E, Jarry-Guichard T, Briand JP, Willecke K, Gros D, Theveniau-Ruissy M. Expression pattern of connexin gene products at the early developmental stages of the mouse cardiovascular system. *Circ Res*. 1997;81:423-437.

84. van Kempen MJ, Fromaget C, Gros D, Moorman AF, Lamers WH. Spatial distribution of connexin43, the major cardiac gap junction protein, in the developing and adult rat heart. *Circ Res*. 1991;68:1638-1651.

85. Chuck ET, Freeman DM, Watanabe M, Rosenbaum DS. Changing activation sequence in the embryonic chick heart. Implications for the development of the His-Purkinje system. *Circ Res*. 1997;81:470-476.

86. Kolditz DP, Wijffels MC, Blom NA, van der Laarse A, Markwald RR, Schalij MJ, Gittenberger-de Groot AC. Persistence of functional atrioventricular accessory pathways in postseptated embryonic avian hearts: implications for morphogenesis and functional maturation of the cardiac conduction system. *Circulation*. 2007;115:17-26.

87. Chuck ET, Meyers K, France D, Creazzo TL, Morley GE. Transitions in ventricular activation revealed by two-dimensional optical mapping. *Anat Rec A Discov Mol Cell Evol Biol*. 2004;280:990-1000.

88. Rothenberg F, Nikolski VP, Watanabe M, Efimov IR. Electrophysiology and anatomy of embryonic rabbit hearts before and after septation. *Am J Physiol Heart Circ Physiol*. 2005;288:344-351.

89. Rothenberg F, Watanabe M, Eloff B, Rosenbaum D. Emerging patterns of cardiac conduction in the chick embryo: waveform analysis with photodiode array-based optical imaging. *Dev Dyn*. 2005;233:456-465.

90. Sedmera D, Reckova M, Bigelow MR, Dealmeida A, Stanley CP, Mikawa T, Gourdie RG, Thompson RP. Developmental transitions in electrical activation patterns in chick embryonic heart. *Anat Rec A Discov Mol Cell Evol Biol*. 2004;280:1001-1009.

91. Sedmera D, Wessels A, Trusk TC, Thompson RP, Hewett KW, Gourdie RG. Changes in activation sequence of embryonic chick atria correlate with developing myocardial architecture. *Am J Physiol Heart Circ Physiol*. 2006.

92. Kolditz DP, Wijffels MC, Blom NA, van der Laarse A, Hahurij ND, Lie-Venema H, Markwald RR, Poelmann RE, Schalij MJ, Gittenberger-de Groot AC. Epicardium-derived cells in development of annulus fibrosus and persistence of accessory pathways. *Circulation*. 2008;117:1508-1517.

93. Wessels A, Markman MW, Vermeulen JL, Anderson RH, Moorman AF, Lamers WH. The development of the atrioventricular junction in the human heart. *Circ Res*. 1996;78:110-117.

94. Keith A, Flack M. The Form and Nature of the Muscular Connections between the Primary Divisions of the Vertebrate Heart. *J Anat Physiol*. 1907;41:172-189.

95. Opthof T. The mammalian sinoatrial node. *Cardiovasc Drugs Ther*. 1988;1:573-597.

96. Boyett MR, Honjo H, Kodama I. The sinoatrial node, a heterogeneous pacemaker structure. *Cardiovasc Res*. 2000;47:658-687.

97. Dobrzynski H, Boyett MR, Anderson RH. New insights into pacemaker activity: promoting understanding of sick sinus syndrome. *Circulation*. 2007;115:1921-1932.

98. Liu J, Dobrzynski H, Yanni J, Boyett MR, Lei M. Organisation of the mouse sinoatrial node: structure and expression of HCN channels. *Cardiovasc Res*. 2007;73:729-738.

99. James TN, Sherf L, Fine G, Morales AR. Comparative ultrastructure of the sinus node in man and dog. *Circulation*. 1966;34:139-163.

100. Dobrzynski H, Li J, Tellez J, Greener ID, Nikolski VP, Wright SE, Parson SH, Jones SA, Lancaster MK, Yamamoto M, Honjo H, Takagishi Y, Kodama I, Efimov IR, Billeter R, Boyett MR. Computer three-dimensional reconstruction of the sinoatrial node. *Circulation*. 2005;111:846-854.

101. Davis LM, Rodefeld ME, Green K, Beyer EC, Saffitz JE. Gap junction protein phenotypes of the human heart and conduction system. *J Cardiovasc Electrophysiol*. 1995;6:813-822.

102. Boyett MR, Inada S, Yoo S, Li J, Liu J, Tellez J, Greener ID, Honjo H, Billeter R, Lei M, Zhang H, Efimov IR, Dobrzynski H. Connexins in the sinoatrial and atrioventricular nodes. *Adv Cardiol*. 2006;42:175-197.

103. Irisawa H, Brown HF, Giles W. Cardiac pacemaking in the sinoatrial node. *Physiol Rev*. 1993;73:197-227.

104. Tellez JO, Dobrzynski H, Greener ID, Graham GM, Laing E, Honjo H, Hubbard SJ, Boyett MR, Billeter R. Differential expression of ion channel transcripts in atrial muscle and sinoatrial node in rabbit. *Circ Res*. 2006;99:1384-1393.

105. Stieber J, Herrmann S, Feil S, Loster J, Feil R, Biel M, Hofmann F, Ludwig A. The hyperpolarization-activated channel HCN4 is required for the generation of pacemaker action potentials in the embryonic heart. *Proc Natl Acad Sci U S A*. 2003;100:15235-15240.

106. Nof E, Luria D, Brass D, Marek D, Lahat H, Reznik-Wolf H, Pras E, Dascal N, Eldar M, Glikson M. Point mutation in the HCN4 cardiac ion channel pore affecting synthesis, trafficking, and functional expression is associated with familial asymptomatic sinus bradycardia. *Circulation*. 2007;116:463-470.

107. Bucchi A, Tognati A, Milanesi R, Baruscotti M, DiFrancesco D. Properties of ivabradine-induced block of HCN1 and HCN4 pacemaker channels. *J Physiol*. 2006;572:335-346.

108. James TN. The internodal pathways of the human heart. *Prog Cardiovasc Dis*. 2001;43:495-535.

109. James TN. The connecting pathways between the sinus node and A-V node and between the right and left atrium in the human heart. *Am Heart J*. 1963;66:498-508.

110. Sherf L, James TN. Fine structure of cells and their histologic organization within internodal pathways of the heart: clinical and electrocardiographic implications. *Am J Cardiol*. 1979;44:345-369.

111. Hoogaars WM, Tessari A, Moorman AF, de Boer PA, Hagoort J, Soufan AT, Campione M, Christoffels VM. The transcriptional repressor Tbx3 delineates the developing central conduction system of the heart. *Cardiovasc Res*. 2004;62:489-499.

112. Ikeda T, Iwasaki K, Shimokawa I, Sakai H, Ito H, Matsuo T. Leu-7 immunoreactivity in human and rat embryonic hearts, with special reference to the development of the conduction tissue. *Anat Embryol (Berl)*. 1990;182:553-562.

113. Chuck ET, Watanabe M. Differential expression of PSA-NCAM and HNK-1 epitopes in the developing cardiac conduction system of the chick. *Dev Dyn*. 1997;209:182-195.

114. Kalman JM, Olgin JE, Karch MR, Hamdan M, Lee RJ, Lesh MD. "Cristal tachycardias": origin of right atrial tachycardias from the crista terminalis identified by intracardiac echocardiography. *J Am Coll Cardiol*. 1998;31:451-459.

115. Ho SY, Anderson RH, Sanchez-Quintana D. Atrial structure and fibres: morphologic bases of atrial conduction. *Cardiovasc Res*. 2002;54:325-336.

116. Chung CY, Bien H, Entcheva E. The role of cardiac tissue alignment in modulating electrical function. *J Cardiovasc Electrophysiol*. 2007;18:1323-1329.

117. Vassalle M, Hoffman BF. The spread of sinus activation during potassium administration. *Circ Res*. 1965;17:285-295.

118. Wagner ML, Lazzara R, Weiss RM, Hoffman BF. Specialized conducting fibers in the interatrial band. *Circ Res*. 1966;18:502-518.

119. Racker DK. Sinoventricular transmission in 10 mM K+ by canine atrioventricular nodal inputs. Superior atrionodal bundle and proximal atrioventricular bundle. *Circulation*. 1991;83:1738-1753.

120. Suma K. Sunao Tawara: a father of modern cardiology. *Pacing Clin Electrophysiol*. 2001;24:88-96.

121. Viragh S, Challice CE. The development of the conduction system in the mouse embryo heart. II. Histogenesis of the atrioventricular node and bundle. *Dev Biol*. 1977;56:397-411.

122. Aanhaanen WT, Mommersteeg MT, Norden J, Wakker V, de Gier-de Vries C, Anderson RH, Kispert A, Moorman AF, Christoffels VM. Developmental Origin, Growth, and Three-Dimensional Architecture of the Atrioventricular Conduction Axis of the Mouse Heart. *Circ Res*. 2010;107:728-736.

123. Sun Y, Liang X, Najafi N, Cass M, Lin L, Cai CL, Chen J, Evans SM. Islet 1 is expressed in distinct cardiovascular lineages, including pacemaker and coronary vascular cells. *Dev Biol*. 2007;304:286-296.

124. Viragh S, Challice CE. The development of the conduction system in the mouse embryo heart. I. The first embryonic A-V conduction pathway. *Dev Biol*. 1977;56:382-396.

125. Truex RC, Marino TA, Marino DR. Observations on the development of the human atrioventricular node and bundle. *Anat Rec*. 1978;192:337-350.

126. Marino TA, Severdia J. The early development of the AV node and bundle in the ferret heart. *Am J Anat*. 1983;167:299-312.

127. James TN. Cardiac conduction system: fetal and postnatal development. *Am J Cardiol*. 1970;25:213-226.

128. Lamers WH, Wessels A, Verbeek FJ, Moorman AF, Viragh S, Wenink AC, Gittenberger-de Groot AC, Anderson RH. New findings concerning ventricular septation in the human heart. Implications for maldevelopment. *Circulation*. 1992;86:1194-1205.

129. James TN, Marshall TK. XVIII. Persistent fetal dispersion of the atrioventricular node and His bundle within the central fibrous body. *Circulation*. 1976;53:1026-1034.

130. James TN. Sudden death in babies: new observations in the heart. *Am J Cardiol*. 1968;22:479-506.

131. Suarez-Mier MP, Gamallo C. Atrioventricular node fetal dispersion and His bundle fragmentation of the cardiac conduction system in sudden cardiac death. *J Am Coll Cardiol*. 1998;32:1885-1890.

132. Gittenberger-de Groot AC, Wenink AC. The specialized myocardium in the fetal heart. In: Van Mierop LHS, Oppenheimer-Dekker A, Bruins C (eds) *Embryology and teratology of the heart and the great arteries*. Vol 13. The Hague, The Netherlands: Leiden University press; 1978:pp15-24.

133. Anderson RH, Becker AE, Brechenmacher C, Davies MJ, Rossi L. The human atrioventricular junctional area. A morphological study of the A-V node and bundle. *Eur J Cardiol*. 1975;3:11-25.

134. Truex RC, Smythe MQ. Reconstruction of the human atrioventricular node. Anat Rec. 1967;158:11-19.

135. Truex RC, Smythe MQ. Comparative morphology of the cardiac conduction tissue in animals. *Ann N Y Acad Sci*. 1965;127:19-33.

136. Inoue S, Becker AE. Posterior extensions of the human compact atrioventricular node: a neglected anatomic feature of potential clinical significance. *Circulation*. 1998;97:188-193.

137. Dobrzynski H, Nikolski VP, Sambelashvili AT, Greener ID, Yamamoto M, Boyett MR, Efimov IR. Site of origin and molecular substrate of atrioventricular junctional rhythm in the rabbit heart. *Circ Res*. 2003;93:1102-1110.

138. Yanni J, Boyett MR, Anderson RH, Dobrzynski H. The extent of the specialized atrioventricular ring tissues. *Heart Rhythm*. 2009;6:672-680.

139. Cosio FG, Anderson RH, Kuck KH, Becker A, Borggrefe M, Campbell RW, Gaita F, Guiraudon GM, Haissaguerre M, Rufilanchas JJ, Thiene G, Wellens HJ, Langberg J, Benditt DG, Bharati S, Klein G, Marchlinski F, Saksena S. Living anatomy of the atrioventricular junctions. A guide to electrophysiologic mapping. A Consensus Statement

from the Cardiac Nomenclature Study Group, Working Group of Arrhythmias, European Society of Cardiology, and the Task Force on Cardiac Nomenclature from NASPE. *Circulation*. 1999;100:31-37.

140. Billette J. What is the atrioventricular node? Some clues in sorting out its structure-function relationship. *J Cardiovasc Electrophysiol*. 2002;13:515-518.

141. Hucker WJ, McCain ML, Laughner JI, Iaizzo PA, Efimov IR. Connexin 43 expression delineates two discrete pathways in the human atrioventricular junction. *Anat Rec (Hoboken)*. 2008;291:204-215.

142. Ko YS, Yeh HI, Ko YL, Hsu YC, Chen CF, Wu S, Lee YS, Severs NJ. Three-dimensional reconstruction of the rabbit atrioventricular conduction axis by combining histological, desmin, and connexin mapping data. *Circulation*. 2004;109:1172-1179.

143. Liu J, Noble PJ, Xiao G, Abdelrahman M, Dobrzynski H, Boyett MR, Lei M, Noble D. Role of pacemaking current in cardiac nodes: insights from a comparative study of sinoatrial node and atrioventricular node. *Prog Biophys Mol Biol*. 2008;96:294-304.

144. Nikolski V, Efimov I. Fluorescent imaging of a dual-pathway atrioventricular-nodal conduction system. *Circ Res*. 2001;88:E23-E30.

145. Moe GK, Preston JB, Burlington H. Physiologic evidence for a dual A-V transmission system. *Circ Res*. 1956;4:357-375.

146. Nikolski VP, Jones SA, Lancaster MK, Boyett MR, Efimov IR. Cx43 and dual-pathway electrophysiology of the atrioventricular node and atrioventricular nodal reentry. *Circ Res*. 2003;92:469-475.

147. Inoue S, Becker AE, Riccardi R, Gaita F. Interruption of the inferior extension of the compact atrioventricular node underlies successful radio frequency ablation of atrioventricular nodal reentrant tachycardia. *J Interv Card Electrophysiol*. 1999;3:273-277.

148. Anderson RH, Janse MJ, van Capelle FJ, Billette J, Becker AE, Durrer D. A combined morphological and electrophysiological study of the atrioventricular node of the rabbit heart. *Circ Res*. 1974;35:909-922.

149. Li J, Greener ID, Inada S, Nikolski VP, Yamamoto M, Hancox JC, Zhang H, Billeter R, Efimov IR, Dobrzynski H, Boyett MR. Computer three-dimensional reconstruction of the atrioventricular node. *Circ Res*. 2008;102:975-985.

150. Boyett MR. 'And the beat goes on.' The cardiac conduction system: the wiring system of the heart. *Exp Physiol*. 2009;94:1035-1049.

151. Nakagawa M, Thompson RP, Terracio L, Borg TK. Developmental anatomy of HNK-1 immunoreactivity in the embryonic rat heart: co-distribution with early conduction tissue. *Anat Embryol (Berl)*. 1993;187:445-460.

152. Wessels A, Vermeulen JL, Verbeek FJ, Viragh S, Kalman F, Lamers WH, Moorman AF. Spatial distribution of "tissue-specific" antigens in the developing human heart and skeletal muscle. III. An immunohistochemical analysis of the distribution of the neural tissue antigen G1N2 in the embryonic heart; implications for the development of the atrioventricular conduction system. *Anat Rec*. 1992;232:97-111.

153. Bogusch G. The innervation of Purkinje fibres in the atrium of the avian heart. *Cell Tissue Res*. 1974;150:57-66.

154. Ono N, Yamaguchi T, Ishikawa H, Arakawa M, Takahashi N, Saikawa T, Shimada T. Morphological varieties of the Purkinje fiber network in mammalian hearts, as revealed by light and electron microscopy. *Arch Histol Cytol*. 2009;72:139-149.

155. Gourdie RG, Green CR, Severs NJ, Anderson RH, Thompson RP. Evidence for a distinct gap-junctional phenotype in ventricular conduction tissues of the developing and mature avian heart. *Circ Res*. 1993;72:278-289.

156. Takebayashi-Suzuki K, Yanagisawa M, Gourdie RG, Kanzawa N, Mikawa T. In vivo induction of cardiac Purkinje fiber differentiation by coexpression of preproendothelin-1 and endothelin converting enzyme-1. *Development*. 2000;127:3523-3532.

157. Dun W, Boyden PA. The Purkinje cell; 2008 style. *J Mol Cell Cardiol*. 2008;45:617-624.

158. Sipido KR. Calcium overload, spontaneous calcium release, and ventricular arrhythmias. *Heart Rhythm*. 2006;3:977-979.

159. Boyden PA, Pu J, Pinto J, Keurs HE. Ca(2+) transients and Ca(2+) waves in purkinje cells : role in action potential initiation. *Circ Res*. 2000;86:448-455.

160. Anderson RH, Ho SY, Gillette PC, Becker AE. Mahaim, Kent and abnormal atrioventricular conduction. *Cardiovasc Res*. 1996;31:480-491.

161. Anderson RH, Taylor IM. Development of atrioventricular specialized tissue in human heart. *Br Heart J*. 1972;34:1205-1214.

162. Davies F. The Conducting System of the Bird's Heart. *J Anat*. 1930;64:129-146.

163. Lu Y, James TN, Yamamoto S, Terasaki F. Cardiac conduction system in the chicken: gross anatomy plus light and electron microscopy. *Anat Rec*. 1993;236:493-510.

164. Anderson RH. The disposition and innervation of atrioventricular ring specialized tissue in rats and rabbits. *J Anat*. 1972;113:197-211.

165. Jongbloed MR, Wijffels MC, Schalij MJ, Blom NA, Poelmann RE, van der Laarse A, Mentink MM, Wang Z, Fishman GI, Gittenberger-de Groot AC. Development of the right ventricular inflow tract and moderator band: a possible morphological and functional explanation for Mahaim tachycardia. *Circ Res*. 2005;96:776-783.

166. Wenink AC, Gittenberger-de Groot AC, Brom AG. Developmental considerations of mitral valve anomalies. *Int J Cardiol*. 1986;11:85-101.

167. Lie-Venema H, Eralp I, Markwald RR, Van Den Akker NM, Wijffels MC, Kolditz DP, van der Laarse A, Schalij MJ, Poelmann RE, Bogers AJ, Gittenberger-de Groot AC. Periostin expression by epicardium-derived cells is involved in the development of the atrioventricular valves and fibrous heart skeleton. *Differentiation*. 2008;76:809-819.

168. Van Mierop LH, Alley RD, Kausel HW, Stranahan A. The anatomy and embryology of endocardial cushion defects. *J Thorac Cardiovasc Surg*. 1962;43:71-83.

169. Odgers PN. The development of the atrio-ventricular valves in man. *J Anat*. 1939;73:643-657.

170. Oosthoek PW, Wenink AC, Vrolijk BC, Wisse LJ, Deruiter MC, Poelmann RE, Gittenberger-de Groot AC. Development of the atrioventricular valve tension apparatus in the human heart. *Anat Embryol (Berl)*. 1998;198:317-329.

171. Norris RA, Damon B, Mironov V, Kasyanov V, Ramamurthi A, Moreno-Rodriguez R, Trusk T, Potts JD, Goodwin RL, Davis J, Hoffman S, Wen X, Sugi Y, Kern CB, Mjaatvedt CH, Turner DK, Oka T, Conway SJ, Molkentin JD, Forgacs G, Markwald RR. Periostin regulates collagen fibrillogenesis and the biomechanical properties of connective tissues. *J Cell Biochem*. 2007;101:695-711.

172. Kent AF. Researches on the Structure and Function of the Mammalian Heart. *J Physiol*. 1893;14:2-254.

173. Oh JK, Holmes DR, Jr., Hayes DL, Porter CB, Danielson GK. Cardiac arrhythmias in patients with surgical repair of Ebstein's anomaly. *J Am Coll Cardiol*. 1985;6:1351-1357.

174. Kiernan TJ, Fahy G. Multiple accessory pathways, dual AV nodal physiology, non-compacted myocardium and patent foramen ovale in a patient with Ebstein's anomaly: report of a case. *Int J Cardiol*. 2007;114:412-413.

175. Bohora S, Dora SK, Namboodiri N, Valaparambil A, Tharakan J. Electrophysiology study and radiofrequency catheter ablation of atriofascicular tracts with decremental properties (Mahaim fibre) at the tricuspid annulus. *Europace*. 2008;10:1428-1433.

176. Haghjoo M, Kharazi A, Fazelifar AF, Alizadeh A, Emkanjoo Z, Sadr-Ameli MA. Electrocardiographic and electrophysiologic characteristics of anteroseptal, midseptal, and posteroseptal accessory pathways. *Heart Rhythm*. 2007;4:1411-1419.

177. Santilli RA, Spadacini G, Moretti P, Perego M, Perini A, Crosara S, Tarducci A. Anatomic distribution and electrophysiologic properties of accessory atrioventricular pathways in dogs. *J Am Vet Med Assoc*. 2007;231:393-398.

178. Peters NS, Rowland E, Bennett JG, Green CR, Anderson RH, Severs NJ. The Wolff-Parkinson-White syndrome: the cellular substrate for conduction in the accessory atrioventricular pathway. *Eur Heart J*. 1994;15:981-987.

179. Becker AE, Anderson RH, Durrer D, Wellens HJ. The anatomical substrates of wolff-parkinson-white syndrome. A clinicopathologic correlation in seven patients. *Circulation*. 1978;57:870-879.

180. Klein GJ, Hackel DB, Gallagher JJ. Anatomic substrate of impaired antegrade conduction over an accessory atrioventricular pathway in the Wolff-Parkinson-White syndrome. *Circulation*. 1980;61:1249-1256.

181. Chen SA, Tai CT, Chiang CE, Lee SH, Wen ZC, Chiou CW, Ueng KC, Chen YJ, Yu WC, Huang JL, Chang MS. Electrophysiologic characteristics, electropharmacologic responses and radiofrequency ablation in patients with decremental accessory pathway. *J Am Coll Cardiol*. 1996;28:732-737.

182. Truex RC, Bishof JK, Hoffman EL. Accessory atrioventricular muscle bundles of the developing human heart. *Anat Rec*. 1958;131:45-59.

183. Ko JK, Deal BJ, Strasburger JF, Benson DW, Jr. Supraventricular tachycardia mechanisms and their age distribution in pediatric patients. *Am J Cardiol*. 1992;69:1028-1032.

184. Naheed ZJ, Strasburger JF, Deal BJ, Benson DW, Jr., Gidding SS. Fetal tachycardia: mechanisms and predictors of hydrops fetalis. *J Am Coll Cardiol*. 1996;27:1736-1740.

185. Gollob MH, Green MS, Tang AS, Gollob T, Karibe A, Ali Hassan AS, Ahmad F, Lozado R, Shah G, Fananapazir L, Bachinski LL, Roberts R. Identification of a gene responsible for familial Wolff-Parkinson-White syndrome. *N Engl J Med*. 2001;344:1823-1831.

186. Gollob MH, Seger JJ, Gollob TN, Tapscott T, Gonzales O, Bachinski L, Roberts R. Novel PRKAG2 mutation responsible for the genetic syndrome of ventricular preexcitation and conduction system disease with childhood onset and absence of cardiac hypertrophy. *Circulation*. 2001;104:3030-3033.

187. Patel VV, Arad M, Moskowitz IP, Maguire CT, Branco D, Seidman JG, Seidman CE, Berul CI. Electrophysiologic characterization and postnatal development of ventricular pre-excitation in a mouse model of cardiac hypertrophy and Wolff-Parkinson-White syndrome. *J Am Coll Cardiol*. 2003;42:942-951.

188. Gaussin V, Morley GE, Cox L, Zwijsen A, Vance KM, Emile L, Tian Y, Liu J, Hong C, Myers D, Conway SJ, Depre C, Mishina Y, Behringer RR, Hanks MC, Schneider MD, Huylebroeck D, Fishman GI, Burch JB, Vatner SF. Alk3/Bmpr1a receptor is required for development of the atrioventricular canal into valves and annulus fibrosus. *Circ Res*. 2005;97:219-226.

189. Luderitz B. Ivan Mahaim (1897-1965). *J Interv Card Electrophysiol*. 2003;8:155.

190. Aliot E, de Chillou C, Revault d'Allones G, Mabo P, Sadoul N. Mahaim tachycardias. *Eur Heart J*. 1998;19 Suppl E:E25-31.

191. Sternick EB, Sosa EA, Timmermans C, Cruz Filho FE, Rodriguez LM, Gerken LM, Scanavacca MI, Fagundes ML, Bueno SC, Vrandecic MO, Wellens HJ. Automaticity in Mahaim fibers. *J Cardiovasc Electrophysiol*. 2004;15:738-744.

192. Van Hare GF, Phoon CK, Munkenbeck F, Patel CR, Fink DL, Silverman NH. Electrophysiologic study and radiofrequency ablation in patients with intracardiac tumors and accessory pathways: is the tumor the pathway? *J Cardiovasc Electrophysiol*. 1996;7:1204-1210.

193. Emmel M, Brockmeier K, Sreeram N. Rhabdomyoma as accessory pathway: electrophysiologic and morphologic confirmation. *Heart*. 2004;90:43.

194. Vlagsma R, Hallensleben E, Meijboom EJ. Supraventricular tachycardia and premature atrial contractions in fetus. *Ned Tijdschr Geneeskd*. 2001;145:295-299.

195. Simpson JM, Sharland GK. Fetal tachycardias: management and outcome of 127 consecutive cases. *Heart*. 1998;79:576-581.

196. Jaeggi ET, Nii M. Fetal brady- and tachyarrhythmias: new and accepted diagnostic and treatment methods. *Semin Fetal Neonatal Med*. 2005;10:504-514.

197. Kleinman CS, Hobbins JC, Jaffe CC, Lynch DC, Talner NS. Echocardiographic studies of the human fetus: prenatal diagnosis of congenital heart disease and cardiac dysrhythmias. *Pediatrics*. 1980;65:1059-1067.

198. Rein AJ, O'Donnell C, Geva T, Nir A, Perles Z, Hashimoto I, Li XK, Sahn DJ. Use of tissue velocity imaging in the diagnosis of fetal cardiac arrhythmias. *Circulation*. 2002;106:1827-1833.

199. Maeno Y, Hirose A, Kanbe T, Hori D. Fetal arrhythmia: prenatal diagnosis and perinatal management. J Obstet *Gynaecol Res*. 2009;35:623-629.

200. Schmidt KG, Ulmer HE, Silverman NH, Kleinman CS, Copel JA. Perinatal outcome of fetal complete atrioventricular block: a multicenter experience. *J Am Coll Cardiol*. 1991;17:1360-1366.

201. Oudijk MA, Gooskens RH, Stoutenbeek P, de Vries LS, Visser GH, Meijboom EJ. Neurological outcome of children who were treated for fetal tachycardia complicated by hydrops. *Ultrasound Obstet Gynecol*. 2004;24:154-158.

202. Schade RP, Stoutenbeek P, de Vries LS, Meijboom EJ. Neurological morbidity after fetal supraventricular tachyarrhythmia. *Ultrasound Obstet Gynecol*. 1999;13:43-47.

203. Lopriore E, Aziz MI, Nagel HT, Blom NA, Rozendaal L, Kanhai HH, Vandenbussche FP. Long-term neurodevelopmental outcome after fetal arrhythmia. *Am J Obstet Gynecol*. 2009;201:46-51.

204. Kleinman CS, Nehgme RA. Cardiac arrhythmias in the human fetus. *Pediatr Cardiol*. 2004;25:234-251.

205. Johnson WH, Jr., Dunnigan A, Fehr P, Benson DW, Jr. Association of atrial flutter with orthodromic reciprocating fetal tachycardia. *Am J Cardiol*. 1987;59:374-375.

206. van Engelen AD, Weijtens O, Brenner JI, Kleinman CS, Copel JA, Stoutenbeek P, Meijboom EJ. Management outcome and follow-up of fetal tachycardia. *J Am Coll Cardiol*. 1994;24:1371-1375.

207. Hosono T, Chiba Y, Shinto M, Kandori A, Tsukada K. A fetal Wolff-Parkinson-White syndrome diagnosed prenatally by magnetocardiography. *Fetal Diagn Ther*. 2001;16:215-217.

208. Pirie AM, Wright J. Prenatal diagnosis of the Wolf-Parkinson-White syndrome by fetal magnetocardiography. *BJOG*. 2003;110:710.

209. Strasburger JF, Wakai RT. Fetal cardiac arrhythmia detection and in utero therapy. *Nat Rev Cardiol*. 2010;7:277-290.

210. Oudijk MA, Ruskamp JM, Ambachtsheer BE, Ververs TF, Stoutenbeek P, Visser GH, Meijboom EJ. Drug treatment of fetal tachycardias. *Paediatr Drugs*. 2002;4:49-63.

211. Jaeggi ET, Hamilton RM, Silverman ED, Zamora SA, Hornberger LK. Outcome of children with fetal, neonatal or childhood diagnosis of isolated congenital atrioventricular block. A single institution's experience of 30 years. *J Am Coll Cardiol*. 2002;39:130-137.

212. Baschat AA, Gembruch U, Knopfle G, Hansmann M. First-trimester fetal heart block: a marker for cardiac anomaly. *Ultrasound Obstet Gynecol*. 1999;14:311-314.

213. Ho SY, Esscher E, Anderson RH, Michaelsson M. Anatomy of congenital complete heart block and relation to maternal anti-Ro antibodies. *Am J Cardiol*. 1986;58:291-294.

214. Bilazarian SD, Taylor AJ, Brezinski D, Hochberg MC, Guarnieri T, Provost TT. High-grade atrioventricular heart block in an adult with systemic lupus erythematosus: the association of nuclear RNP (U1 RNP) antibodies, a case report, and review of the literature. *Arthritis Rheum*. 1989;32:1170-1174.

215. Lockshin MD, Druzin ML, Goei S, Qamar T, Magid MS, Jovanovic L, Ferenc M. Antibody to cardiolipin as a predictor of fetal distress or death in pregnant patients with systemic lupus erythematosus. *N Engl J Med*. 1985;313:152-156.

216. Bharati S, de la Fuente DJ, Kallen RJ, Freij Y, Lev M. Conduction system in systemic lupus erythematosus with atrioventricular block. *Am J Cardiol*. 1975;35:299-304.

217. James TN, Rupe CE, Monto RW. Pathology of the cardiac conduction system in systemic lupus erythematosus. *Ann Intern Med*. 1965;63:402-410.

218. Buyon JP, Hiebert R, Copel J, Craft J, Friedman D, Katholi M, Lee LA, Provost TT, Reichlin M, Rider L, Rupel A, Saleeb S, Weston WL, Skovron ML. Autoimmune-associated congenital heart block: demographics, mortality, morbidity and recurrence rates obtained from a national neonatal lupus registry. *J Am Coll Cardiol*. 1998;31:1658-1666.

219. Jaeggi ET, Friedberg MK. Diagnosis and management of fetal bradyarrhythmias. *Pacing Clin Electrophysiol*. 2008;31 Suppl 1:S50-S53.

220. Hofbeck M, Ulmer H, Beinder E, Sieber E, Singer H. Prenatal findings in patients with prolonged QT interval in the neonatal period. *Heart*. 1997;77:198-204.

221. Salerno JC, Seslar SP. Supraventricular tachycardia. *Arch Pediatr Adolesc Med*. 2009;163:268-274.

222. Sacchetti A, Moyer V, Baricella R, Cameron J, Moakes ME. Primary cardiac arrhythmias in children. *Pediatr Emerg Care*. 1999;15:95-98.

223. Nadas AS, Daeschner CW, Roth A, Blumenthal SL. Paroxysmal tachycardia in infants and children; study of 41 cases. *Pediatrics*. 1952;9:167-181.

224. Perry JC, Garson A, Jr. Supraventricular tachycardia due to Wolff-Parkinson-White syndrome in children: early disappearance and late recurrence. *J Am Coll Cardiol*. 1990;16:1215-1220.

225. Deal BJ, Keane JF, Gillette PC, Garson A, Jr. Wolff-Parkinson-White syndrome and supraventricular tachycardia

during infancy: management and follow-up. *J Am Coll Cardiol*. 1985;5:130-135.

226. James TN. Normal and abnormal consequences of apoptosis in the human heart. From postnatal morphogenesis to paroxysmal arrhythmias. *Circulation*. 1994;90:556-573.

227. Blaufox AD, Rhodes JF, Fishberger SB. Age related changes in dual AV nodal physiology. *Pacing Clin Electrophysiol*. 2000;23:477-480.

228. Cohen MI, Wieand TS, Rhodes LA, Vetter VL. Electrophysiologic properties of the atrioventricular node in pediatric patients. *J Am Coll Cardiol*. 1997;29:403-407.

229. Gittenberger-de Groot AC, Poelmann RE. Cardiac Morphogenesis. In: Yagel S, Silverman NH, Gembruch U (eds) *Fetal Cardiology*. second ed. New york, USA: Informa Healthcare; 2009:pp9-17.

230. Netter F.H. *HEART*. eight ed. Cincinnati, USA: The Hennegan Co; 1992.

Part I

The Posterior Heart Field in Cardiac Development

Rüdiger J. Blaschke[1]
Nathan D. Hahurij[2]
Sanne Kuijper[3,*]
Steffen Just[4,*]
Lambertus J. Wisse[2]
Kirsten Deissler[5]
Tina Maxelon[1]
Konstantinos Anastassiadis[6]
Jessica Spitzer[1]
Stefan E. Hardt[4]
Hans Schöler[7]
Harma Feitsma[3]
Wolfgang Rottbauer[4]
Martin Blum[5]
Frist Meijlink[3]
Gudrun Rappold[1,#]
Adriana C. Gittenberger-de Groot[2,#]

[1] Institute of Human Genetics, University of Heidelberg, Heidelberg, Germany.
[2] Department of Anatomy & Embryology, Leiden University Medical Center, Leiden, The Netherlands.
[3] Hubrecht Institute, KNAW & University Medical Center Utrecht, Utrecht, The Netherlands.
[4] Department of Internal Medicine III, University of Heidelberg, Heidelberg, Germany.
[5] Institute for Zoology, University Hohenheim, Stuttgart, Germany.
[6] Max-Planck-Institute for Molecular Cell Biology and Genetics MPI-CBG, BIOTEC TU Dresden, Dresden, Germany.
[7] Max-Planck-Institute of Molecular Biomedecine, Műnster, Germany.

* Authors have equally contributed
# Considered joint senior authors

2

Targeted mutation reveals essential functions of the homeodomain transcription factor *Shox2* in sinoatrial and pacemaking development

ABSTRACT

Background
The identification of molecular pathways regulating the development of pacemaking and coordinated heartbeat is crucial for a comprehensive mechanistic understanding of arrhythmia related diseases. Elucidation of these pathways has mainly been complicated by an insufficient definition of the developmental structures involved in these processes and the unavailability of animal models specifically targeting the relevant tissues. We here report on a highly restricted expression pattern of the homeodomain transcription factor *Shox2* in the sinus venosus myocardium, including the sinoatrial nodal region and the venous valves.

Methods and Results
To investigate its function *in vivo*, we have generated mouse lines carrying a targeted mutation of the *Shox2* gene. While heterozygous animals did not exhibit obvious defects, homozygosity of the targeted allele led to embryonic lethality at 11.5 to 13.5 dpc. *Shox2*^{-/-} embryos exhibited severe hypoplasia of the sinus venosus myocardium in the posterior heart field including the sinoatrial nodal region and venous valves. We furthermore demonstrate aberrant expression of Connexin40 and Connexin43 and the transcription factor *Nkx2.5 in vivo* specifically within the sinoatrial nodal region, and show that *Shox2* deficiency interferes with pacemaking function in Zebrafish embryos.

Conclusion
From these results, we postulate a critical function of *Shox2* in the recruitment of sinus venosus myocardium comprising the sinoatrial nodal region.

INTRODUCTION

Shox2 encodes a member of a small subfamily of paired-related homeodomain transcription factors[1,2] that has been identified by virtue of its sequence similarity to the short stature homeobox gene *SHOX*[3] causing various short stature syndromes. Human phenotypes caused by *SHOX*[2] deficiency have not been identified so far. According to the complex embryonic expression pattern of *Shox2*, it has initially been implicated in craniofacial, limb, brain and heart development.[1,2] This assumption has recently been confirmed by analyses of independently generated knockout mouse models that revealed crucial functions of *Shox2* in palate formation[4] and chondrocyte maturation during bone development.[5] In the current study we describe the expression of *Shox2* and its crucial role in the developing venous pole of the embryonic mouse heart.

The development of the vertebrate heart comprises multiple cell fate decisions that are necessary to create the diverse cell types required for an integrated function of the mature organ. Recently, new insights have shown that during cardiac development new myocardium is added at the arterial as well as the venous pole of the primary heart tube. The venous pole of the heart, also known as sinus venosus, is the location where blood drains into the heart. It is suggested that the sinus venosus myocardium in which the sinus venosus is incorporated predominantly derives from a second lineage of cardiomyocytes.[6] We refer to this population, in contrast to the anterior heart field at the arterial pole, as the posterior heart field (PHF).[7] The sinus venosus myocardium compromises at the borderline of the right cardinal vein and the right atrium a sinoatrial nodal (SAN) region that can be both morphologically and immunohistochemically defined.[8]

Nkx2.5 is an early precardiac marker and we have investigated its expression in the development of the PHF. *Nkx2.5*, the vertebrate homolog of the *Drosophila tinman*,[9-11] encodes a homeodomain transcription factor, that amongst other functions is essential for normal development of the cardiac conduction system (CCS). Patients diagnosed with *Nkx2.5* haploinsufficiences exhibit several progressive heart defects including atrial and ventricular septal defects as well as atrioventricular conduction system abnormalities.[12-16]

To substantiate our hypothesis that *Shox2* has an essential role in heart development, we have established the detailed expression pattern within the developing heart, examined the effects of *Shox2* depletion in *Zebrafish* embryos and generated mouse lines carrying a targeted mutation of *Shox2*. Furthermore, atrial myosin light chain (MLC-2a), Nkx2.5, Connexin40 (Cx40) and Connexin43 (Cx43)[17] were used to investigate the differentiation and possible aberrant formation of the PHF derived sinus venosus myocardium compromising the SAN region of *Shox2*^{-/-} embryos. The results were evaluated with 3D reconstruction techniques.

MATERIAL AND METHODS

All animal experiments were conducted according to German animal protection laws and approved by the regional board of Baden Württemberg (permission no. 35-9185.81/G-64/05). A short summary of the techniques is provided, which is supported by the expanded Material and Methods section for routine procedures.

We generated chimeras and mutant mice by a replacement of the targeting vector aiming at the *Shox2* locus. Genomic DNA was prepared from tail biopsies and yolk sac as previously described.[18] The details for construction of the targeting vector and the primer design of both DNA and RNA are provided in the expanded Material and Methods section.

Whole mount and sectioned mouse embryos (9.5 dpc n=10; 10.5 dpc n=2; 11.5 dpc n=3; 12.5 dpc n=2; 13.5 dpc n=1) were studied by *in situ* hybridization (ISH) using previously described protocols,[19] and sections were subjected to immunohistochemistry using antibodies against MLC-2a and Nkx2.5 as well as markers for the developing CCS: Cx40 and Cx43. The standard procedures for immunohistochemistry are provided in the expanded Material and Methods section. For 3D visualisation we generated reconstructions of the developing sinus venosus area using AMIRA software.

To establish a possible hypoplastic development of the SAN region we performed volume measurements of this region in wildtype (n=3) and *Shox2$^{-/-}$* (n=3) embryos of 11.5 dpc according to the Cavalieri method.[20] Statistical analysis was performed with an independent samples *t*-test ($P<0.05$), using the SPSS 11.0 software program.

For Zebrafish studies we isolated the full-length Zebrafish *Shox2* cDNA sequence, which was followed by whole-mount RNA ISH as previously described[21] and are elaborated in the expanded Material and Methods section.

To compare the heart rate in age matched resting conscious animals, electrocardiograms were recorded using a custom made mouse jacket and silver electrode clips attached to the paws (Föhr Medical Instruments, Germany). Electrocardiograms were recorded on a Schwarzer Cardioscript (Schwarzer-Picker, Germany).
The Authors had full access to and take responsibility for the integrity of the data. All authors have read and agree to the manuscript as written.

RESULTS

Shox2 expression during heart development
An initial insight into the possible functions of *Shox2* during heart development was derived from expression analyses by antisense ISH on wildtype whole mount embryos, isolated embryonic hearts and serial sections. These analyses revealed *Shox2* transcripts as early as 8.5 dpc in the posterior region of the primitive heart tube. At 9.5 dpc, *Shox2* expression was restricted to the inflow tract (Figure 1a), particularly to the mesenchyme of the transitional zone between the sinus venosus and the common atrium (Figure 1b), where the sinus venosus myocardium is formed. While the atrial and ventricular myocardium itself were negative for *Shox2* expression at 10.5 dpc, both leaflets of the sinus venosus myocardium derived venous valves showed strong expression of *Shox2* at this stage (Figure 1c). At 11.5 dpc *Shox2* expression had expanded and now included the SAN region, as well as the venous

valves, two parallel bundles spanning the longitudinal axis of the atria (Figure 1d, e). These structures have previously been demonstrated to constitute an integral part of the developing conduction system by analyses of *lacZ* expression in the CCS-*LacZ* mouse.[22,23] In addition, we observed a distinct staining in the upper ventricular region, which resembled the ventricular expression of CCS-*LacZ* and the primitive stages of left and right bundle branch formation (Figure 1d, e). This pattern of expression observed at 11.5 dpc was retained at later stages up to 13.5 dpc.
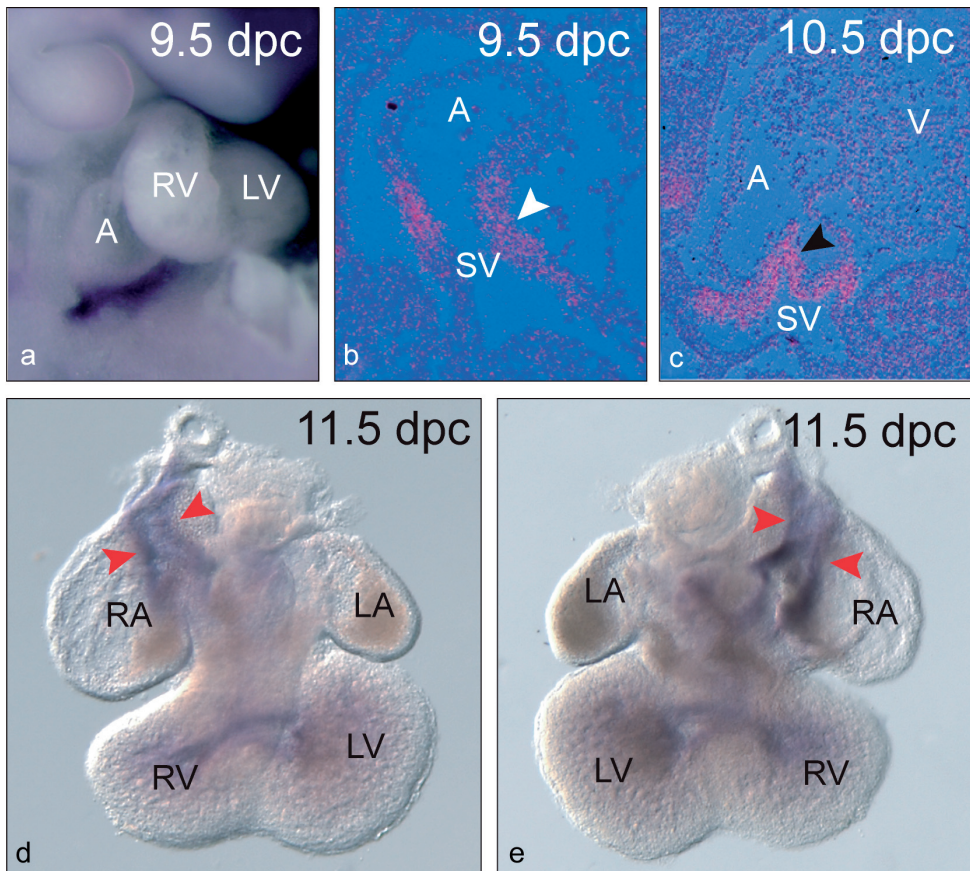

Figure 1. *Shox2* expression is highly restricted within the developing heart. Whole mount *in situ* hybridization on 9.5 dpc embryos shows that *Shox2* expression in the developing heart is restricted to the posterior region (a). Expression is confined to the myocardium of the transitional zone where the sinus venosus (**SV**) connects to the common atrium at 9.5 dpc (**white arrowhead** in b) and the venous valves that originate from this myocardium at 10.5 dpc (**black arrowhead** in c) as shown by *in situ* hybridization on serial sections. Whole mount analyses on hearts isolated at 11.5 dpc (d and e) reveal specific expression in the sinoatrial nodal region, including the venous valves, two bundles spanning the atria along their longitudinal axes (**red arrowheads** in d and e). At this stage, positive staining can also be detected in the primitive left and right bundle branches of the cardiac conduction system. **A** indicates atrium; **V**, ventricle; **LA**, left atrium; **RA**, right atrium; **LV**, left ventricle; **RV**, right ventricle.

The homozygous loss of *Shox2* functions is lethal

To investigate the functions of *Shox2 in vivo*, we have inactivated its mouse equivalent by gene targeting. Targeted mutation of *Shox2* was performed in a classical homologous recombination approach using the replacement vector depicted in Figure 2a. In the targeted locus a PGK-neo cassette replaces 2282 bp of genomic DNA including the entire second exon of the *Shox2* gene that encodes the majority of the homeodomain. This strategy allows concomitant disruption of both *Shox2* isoforms, *Shox2a* and *Shox2b*, that have been described so far.[1,2] While expression from the *Shox2a* promoter produces a compromised mRNA missing the major part of the homeodomain, utilization of the *Shox2b* promoter results in a non-coding mRNA missing the *Shox2b* ATG start codon. The resulting locus is therefore likely to represent a null allele. Targeted alleles were generated in two different ES cell lines (RI and E14), their presence confirmed by Southern-blot analyses and germ line transmission verified by PCR analysis of chimera offspring (Figure 2b, c). Furthermore, RT-PCR analysis using total RNA
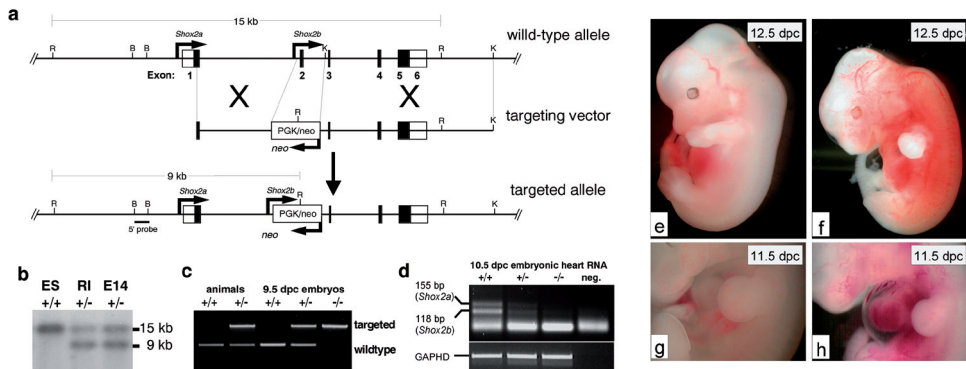

Figure 2. Targeted disruption of the *Shox2* locus and morphological heart defects in *Shox2*^{-/-} embryos. The structure of the *Shox2* gene locus, the replacement vector and the targeted allele are depicted in (a). Black boxes represent the exons of the *Shox2* gene. Positions of relevant restriction sites are given on top and the 5' and 3' homology regions for homologous recombination are denoted by dashed lines. *Shox2a* and *Shox2b* represent different isoforms generated by alternative transcriptional initiation and splicing. *Shox2a* comprises exons 1-6 while *Shox2b* is encoded by exons 2, 3, 4 and 6. Exon numbers are indicated. The predicted positions of the *Shox2a* and *Shox2b* promoters and the direction of neo[r] transcription are indicated by arrows. Southern-blot analysis of EcoRI digested genomic DNA from parental and targeted embryonic stem (**ES**) cells (b). The 5' probe (black bar in a) detects 15 kb and 9 kb fragments in wildtype and targeted DNA, respectively. ES, parental ES cell line; RI and E14 respective targeted ES cell clones. PCR analysis of yolk sac DNA isolated from 9.5 dpc embryos (c). The products correspond to wildtype and targeted alleles, respectively and genotyped embryos were phenotypically normal at this stage. RT-PCR results performed with primers flanking the alternatively spliced exon 5 and RNA from 10.5 dpc hearts reveals that both isoforms are affected in targeted embryos (d). Compared to wildtype embryos of 12.5 dpc (e), *Shox2*^{-/-} embryos of similar age (f) show a severely hemorrhagic phenotype. Furthermore, pericardial oedema are frequently observed in homozygous *Shox2*^{-/-} embryos of 11.5 dpc (h), compared to wildtype embryos (g). This suggests cardiovascular failure as the principle cause of death. **R** indicates EcoRI; **B**, BamHI; **K**, KpnI; **AN**, animals; **EM**, embryos; +/+, wildtype; +/-, heterozygous; -/-, homozygous.

from 10.5 dpc hearts revealed that both described isoforms, *Shox2a* and *Shox2b*, are affected in heterozygous embryos and could not be detected in homozygous embryos (Figure 2d).

Heterozygous mouse lines were bred into and maintained on both, C57BL/6 and CD1 backgrounds. In both genetic backgrounds heterozygous animals were fertile, had comparable bodyweight and did not exhibit any obvious abnormalities. Furthermore, genotype analysis of 276 animals from three generations revealed frequencies of 51.8% and 48.2% for the *Shox2*$^{+/+}$ and *Shox2*$^{+/-}$ alleles respectively (Table 1). We therefore concluded that *Shox2*$^{+/-}$ animals do not carry any gross abnormalities affecting overall integrity and body growth. Assessment of resting heart rates by ECG recordings furthermore revealed that there was no difference between wildtype and heterozygous animals. We observed some PR variability but no differences between the groups as for PQ-intervals, QRS duration or QT-intervals (Figure 3).

While *Shox2*$^{+/-}$ animals did not exhibit any obvious phenotype, heterozygote inter-crosses yielded 38% *Shox2*$^{+/+}$ and 62% *Shox2*$^{+/-}$ animals but no *Shox2*$^{-/-}$ offspring (n=87) although *Shox2*$^{-/-}$ embryos dissected at 9.5 dpc were viable and did not exhibit any obvious abnormalities. However, analyses of embryos at different developmental stages revealed that homozygous mutants died between 11.5 and 13.5 dpc. A normal Mendelian frequency for *Shox2*$^{-/-}$ embryos was observed up to 10.5 dpc (29%). At 12.5 dpc this frequency dropped to 13% with all *Shox2*$^{-/-}$ embryos exhibiting distinctive phenotypical features and at 14.5 dpc, only two homozygous embryos could be recovered (4.3%), both of which were dead at the time of dissection.

This embryonic lethality, combined with the highly restricted *Shox2* expression in the developing heart, suggested a heart defect as the most likely cause of death.

Table 1. Frequencies of heterozygous animals observed in mouse lines generated from two independently targeted embryonic stem cell clones.

	E14 derived mouse line			RI derived mouse line		
Animals	**Shox2$^{+/+}$**	**Shox2$^{+/-}$**	**Animals**	**Shox2$^{+/+}$**	**Shox2$^{+/-}$**
F$_2$ (n=79)	48 (61%)	31 (39%)	F$_2$ (n=32)	14 (44%)	18 (56%)
F$_3$ (n=34)	18 (53%)	16 (47%)	F$_3$ (n=52)	21 (41%)	31 (59%)
F$_4$ (n=27)	11 (41%)	16 (59%)	F$_4$ (n=52)	31 (59%)	21 (41%)
total (n=140)	**77 (55%)**	**65 (45%)**	**total (n=136)**	**66 (49%)**	**70 (51%)**

Genotype frequencies were calculated for 276 animals from three generations. Both mouse lines are comparable and exhibit the expected *Shox2*$^{-/+}$ frequencies.

Shox2 deficient embryos exhibit heart defects

Consistent with the observed *Shox2* expression in the developing heart, we observed several signs of cardiovascular failure in homozygous *Shox2^{-/-}* embryos compared to wildtype embryos of similar age (Figure 2e-h). These included pericardial oedema (Figure 2g, h) and massive externally visible blood vessels throughout the embryo (Figure 2f). Immunohistochemical staining analyses with the MLC-2a, Nkx2.5, Cx40 and Cx43 specific antibodies were performed to reveal specific differences between wildtype and *Shox2^{-/-}* embryonic hearts from 9.5 to 11.5 dpc.

Animal ID	Genotype	Heart Rate
B10 F9-30	wt	696
B10 F9-31	wt	672
B16 F9-26	wt	684
B16 F9-24	wt	600
B16 F9-25	wt	660
B16 F9-23	wt	564
Mean		**646**
SEM		**21**
SD		**52**
number of animals		**6**

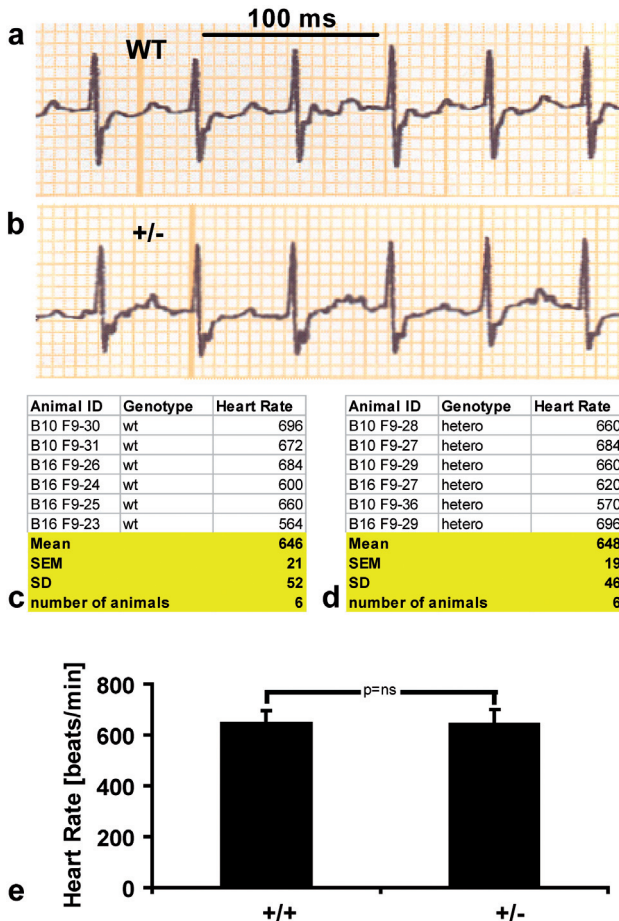| Animal ID	Genotype	Heart Rate
B10 F9-28	hetero	660
B10 F9-27	hetero	684
B10 F9-29	hetero	660
B16 F9-27	hetero	620
B10 F9-36	hetero	570
B16 F9-29	hetero	696
Mean		**648**
SEM		**19**
SD		**46**
number of animals		**6**

Figure 3. Except for some PR variability, the ECG recordings did not reveal any obvious differences between wildtype (a) and heterozygous animals (b) and resting heart rates of wildtype (c) and heterozygous knockout mice (d). Graphic representation of mean values calculated from six independent measurements of each genotype reveals identical heart rates between wildtype and heterozygous animals at a highly significant level (e). **SEM** indicates standard error of means; **SD**, standard deviation.

Wildtype embryos

9.5 dpc

At this stage, the shape of the primary heart tube was still clearly discernible and the looping process of the heart was not completed yet (data not shown).

10.5 dpc

The embryonic heart clearly showed the common atrium and primitive left and right ventricle (Figure 4a,c). The atrial myocardium showed strong expression of MLC-2a, while the expression of MLC-2a in the ventricles was less strong (Figure 4c). Expression of Nkx2.5 was observed both in the common atrium and primitive ventricles. The developing venous valves were positive for MLC-2a and Nkx2.5 (data not shown).

The sinus venosus, was located caudo-dorsally to the common atrium and formed the inflow tract of the heart. At this stage two large vessels drain into the left and right horn of the sinus venosus, called the left and right common cardinal vein respectively. The pulmonary vein, which drains into the common atria, was clearly discernible but not enclosed by myocardium yet (Figure 4a).
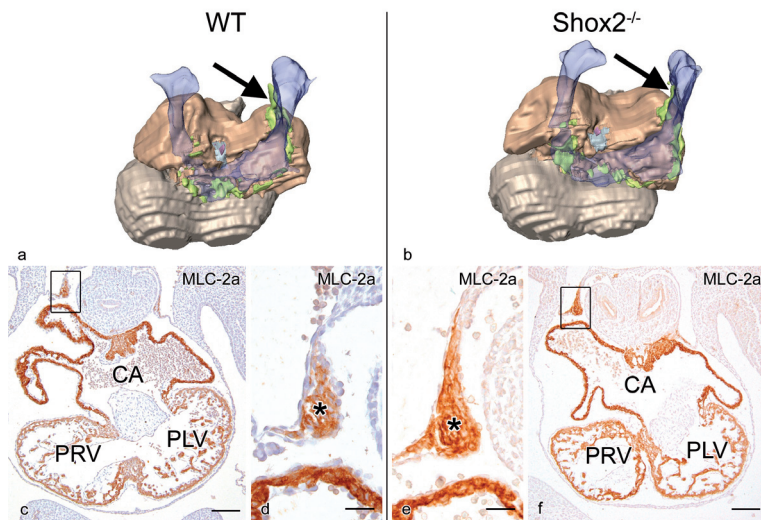

Figure 4. Three dimensional reconstructions of MLC-2a and Nkx2.5 expression patterns of a dorsal view of a wildtype (WT) and a *Shox2-/-* embryonic heart of 10.5 dpc. The MLC-2a and Nkx2.5 positive myocardium of the common atrium (**CA**) and primitive left and right ventricle (**PLV** and **PRV**) are indicated in **brown** and **grey** respectively (a, b). At this stage the pulmonary vein (**pink**) is not enclosed by myocardium yet (**grey**). The CA of the *Shox2-/-* embryo appeared to be slightly enlarged (compare a and b). The MLC-2a positive and Nkx2.5 negative sinus venosus myocardium in which the sinus venosus (**blue transparent**) is incorporated is indicated in **lime green** (a,b). The size of the sinoatrial node region (**black arrow** in a and b; **asterisk** in d and e, which are enlargements of boxes in c and f respectively) is identical. Scale bars: (c), (f) = 300μm; (d), (e) = 70μm.
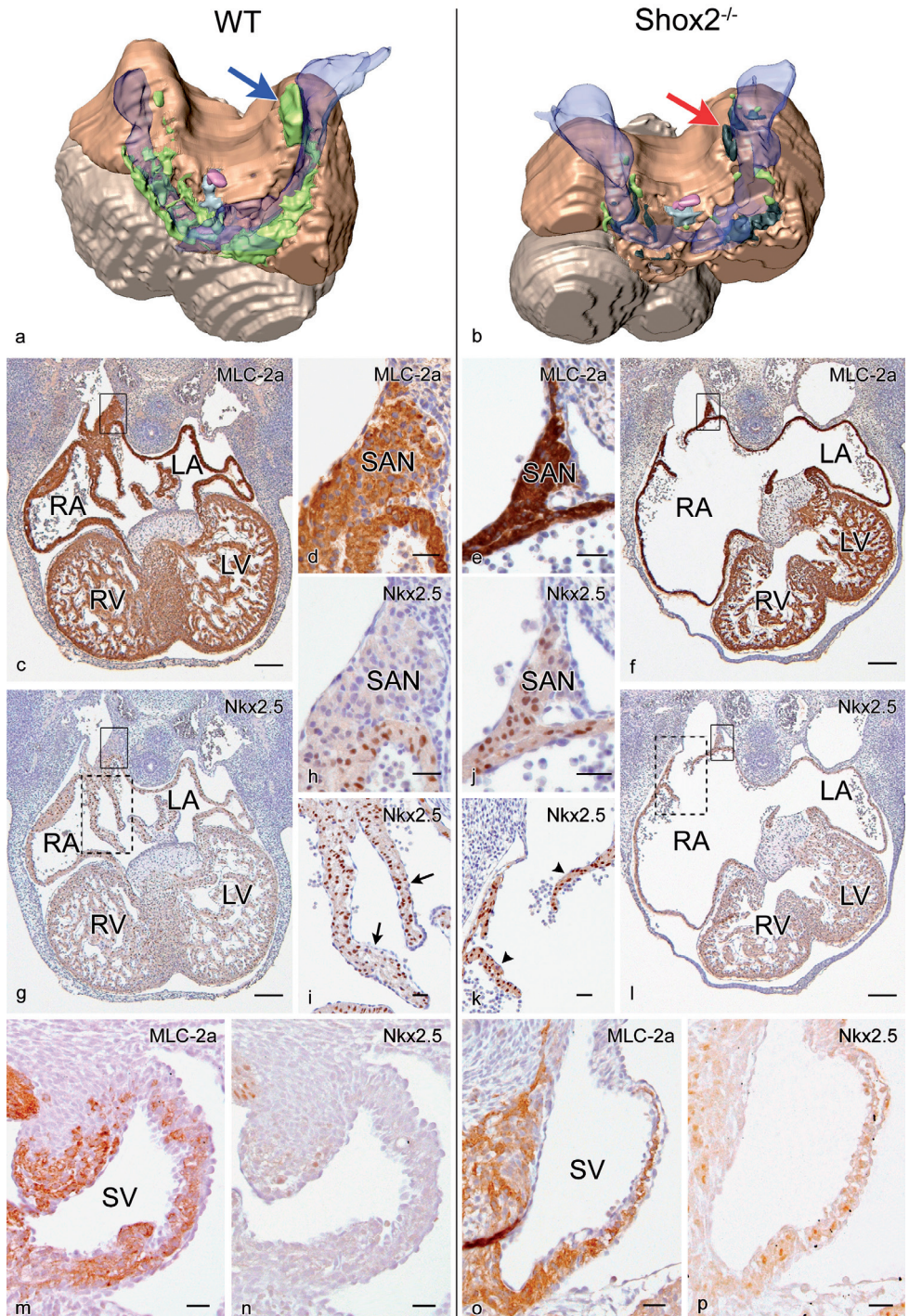
A U-shaped band of myocardium, which formed the wall of the sinus venosus adjacent to the atrial myocardium was positive for MLC-2a and showed negative Nkx2.5 expression. This comprises the SAN region, which is located in the medial wall of the right cardinal vein (Figure 4a).

11.5 dpc

The embryonic heart showed further maturation, the septation of the atria and the ventricles was still not completed at this stage. The future left and right atria as well as the future left and right ventricle were clearly discernible. Both, the atrial and ventricular myocardium were positive for MLC-2a, and also showed expression of Nkx2.5 (Figure 5c, g). The more developed venous valves were positive for MLC-2a and also showed expression of Nkx2.5 (Figure 5c, i). Compared to earlier stages, the intensity of the expression of MLC-2a and Nkx2.5 appeared to be stronger at 11.5 dpc. The sinus venosus myocardium was positive for MLC-2a but negative for Nkx2.5 (Figure 5m, n) and Cx40 and Cx43 (Figure 6a, c, e).

A 3D reconstruction of the embryonic heart showed that the MLC-2a positive and Nkx2.5 negative sinus venosus myocardium, formed a U-shaped structure, which is situated caudo-dorsally to the atria (Figure 5a, m, n). In addition, the pulmonary vein showed further maturation nevertheless it was not enclosed by myocardium yet (Figure 5a).

Figure 5. *Shox2* **deficient mice exhibit a different expression pattern of Nkx2.5 in the myocardium of the developing sinus venosus (SV) including the sinoatrial node (SAN) region.** The three dimensional reconstructions show the dorsal view of a wildtype (**WT**) (a) and a *Shox2⁻/⁻* (b) embryonic heart of 11.5 dpc, in which the MLC-2a and Nkx2.5 positive myocardium of the atria and ventricles are indicated in **brown** and **grey** respectively (a, b). The MLC-2a positive myocardium of the SV is indicated in **lime green** where there is Nkx2.5 negativity (a, b) and **black** where Nkx2.5 is aberrantly positive (b). The **blue arrow** in (a) indicates the region of the SAN in a WT embryo and the **red arrow** in (b) indicates the same region in a *Shox2⁻/⁻* embryo. Immunohistochemical analysis demonstrates that the SAN region both in WT (d detail of box in c) and *Shox2⁻/⁻* hearts (e detail of box in f) is positive for MLC-2a. (g) Section of a WT heart in which the box indicates the region of the SAN, which is negative for Nkx2.5 (h enlargement of box in g). In WT hearts, the venous valves (**arrow** in i, enlargement of dotted box in g) are positive for Nkx2.5. Remarkably, in *Shox2⁻/⁻* embryos the hypoplastic SAN region (j enlargement of box in l) is positive for Nkx2.5. Furthermore, the Nkx2.5 positive venous valves in *Shox2⁻/⁻* embryos appeared to be severely hypoplastic (**arrow heads** in k, enlargement of dotted box in l). In WT embryonic hearts, the MLC-2a positive myocardium in which the SV is incorporated (m) is negative for Nkx2.5 (n). Conversely, in *Shox2⁻/⁻* embryos this specific myocardium is both positive for MLC-2a (o) and Nkx2.5 (p). **LA** indicates left atrium; **RA**, right atrium; **LV**, left ventricle; **RV**, right ventricle; in the 3D reconstruction: **light grey** indicates region negative for myocardium surrounding the pulmonary veins; **blue transparent**, lumen of the SV; **pink**, pulmonary veins. Scale bars: (c), (f), (g), (l) = 300μm, all others 60μm.

Shox2⁻ᐟ⁻ embryos

9.5 dpc

Compared to wildtype hearts of similar age, the region of the common atrium seemed to be slightly enlarged. Besides this atrial enlargement, no major abnormalities were observed (data not shown).

10.5 dpc

By comparing 3D reconstructions of wildtype and *Shox2⁻ᐟ⁻* embryonic hearts, the morphology appeared comparable with only the exception of a slightly dilated common atrium (compare Figure 4a and b). As in wildtype embryos, MLC-2a expression was found in the common atrium and primitive left and right ventricle, with strongest expression in atrial myocardium (Figure 4f). In addition, the atrial and ventricular myocardium showed expression of Nkx2.5. The sections showed that the venous valves in *Shox2⁻ᐟ⁻* embryos were hypoplastic, which were still MLC-2a positive and also showed expression of Nkx2.5.
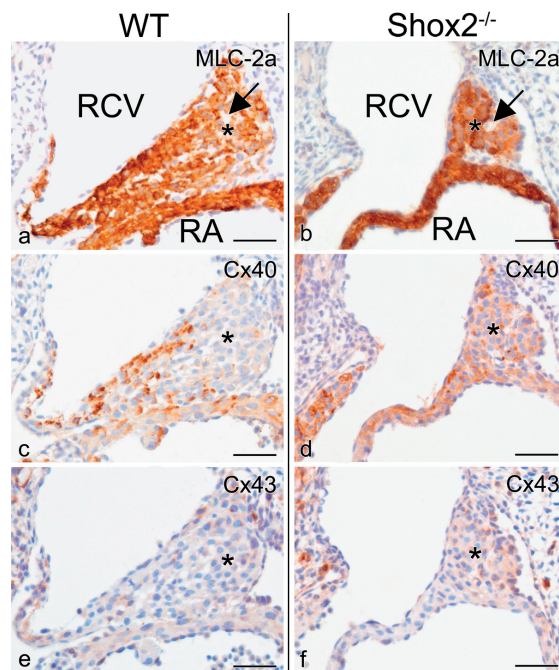

Figure 6. Compared to wildtype (WT), the sinoatrial node (SAN) region of *Shox2⁻ᐟ⁻* embryos showed an aberrant expression of Cx40 and Cx43 at 11.5 dpc. The SAN region (**asterisk** in a-f) including the artery for that region (**black arrow** in a and b) located in de medial wall of the right cardinal vein (**RCV**) is both in WT (a) and *Shox2⁻ᐟ⁻* (b) embryos positive for MLC-2a. (c, d) Sections stained with the Cx40 specific antibody, show that the SAN region in WT hearts is negative for Cx40 (c) and in *Shox2⁻ᐟ⁻* hearts positive (d). (e, f) Sections stained with the Cx43 specific antibody show that the SAN region in WT hearts is negative for Cx43 (e) and in *Shox2⁻ᐟ⁻* hearts moderately positive (f). RA indicates right atrium. Scale bars = 30μm.

The MLC-2a positive and Nkx2.5 negative myocardium lining the the sinus venosus and the cardinal veins did not differ essentially from that seen in the wildtype embryo. The SAN region was also MLC-2a positive but Nkx2.5 negative and did not show any malformations in development (Figure 4b, e, f).

11.5 dpc

3D reconstructions of *Shox2*$^{-/-}$ embryonic hearts showed that the morphology of these hearts was altered dramatically. Compared to wildtype hearts, the left and right ventricles were markedly dislocated in *Shox2*$^{-/-}$ embryos (compare Figure 5a and b). The atria were severely dilated and the myocardial wall of the atria seemed to be much thinner. The atrial and ventricular myocardium was positive for MLC-2a (Figure 5f) and also showed expression of Nkx2.5 (Figure 5l). Here also, the atria showed the strongest expression of MLC-2a. The venous valves were severely hypoplastic and in some embryos even completely absent. Remnants of these valves were positive for MLC-2a and Nkx2.5 (Figure 5f, k).

In *Shox2*$^{-/-}$ embryos the myocardium of the sinus venosus appeared less well developed. At a few locations where myocardium was lining the sinus venosus the myocardium was positive for MLC-2a and also showed expression of Nkx2.5 (Figure 5o, p). Interestingly, compared to wildtype embryos not only the size of the SAN region was markedly decreased (P=0.018, Power of 81.9%; compare Figure 5d and e) but this hypoplastic SAN region in contrast to wildtype embryos was positive for Nkx2.5 (Figure 5j). In addition, an aberrant expression of connexins was observed in the myocardium of the SAN region, which turned out to be positive for Cx40 (Figure 6d) and moderately positive for Cx43 (Figure 6f).

Figure 7. Alignment of *Danio rerio* and *Mus musculus* Shox2a Amino acid. The overall identity and similarity of the longest *Shox2* isoform (*Shox2a*) between the two species is 76% and 82% respectively. The differences in both proteins are mainly due to amino acid exchanges in the N-terminal part and the absence of a poly-glycine stretch in the Zebrafish protein.

3D reconstructions furthermore revealed that the U-shaped MLC-2a positive and Nkx2.5 negative myocardial structure was almost absent (Figure 5b).

Shox2 antisense morpholino injected Zebrafish embryos develop severe sinus bradycardia

Since the loss of *Shox2* functions directly affects the developing sinus venosus myocardium, which includes the SAN region, we addressed the possibility that a loss of *Shox2* functions may lead to pacemaking and conduction deficiencies using an antisense morpholino based approach in Zebrafish embryos. The Zebrafish *Shox2* gene encodes a protein that exhibits a similarity of 82% to the mouse protein (Figure 7) and expression of the Zebrafish *Shox2* gene mirrors expression in human and mouse in the central and peripheral nervous system, the pectoral fin buds and the inflow tract of the heart (data not shown). Injection of morpholino-modified antisense oligonucleotides specifically targeting the exon 3 splice site of *Shox2* (Figure 8) into early embryos led to severe cardiac dysfunction, with a pronounced sinus bradycardia (70 ± 15 versus 165 ± 25 beats per minute) and intermittent sinus exit block after 72 hours of development, when the embryo is still able to survive on passive diffusion of oxygen and nutrients (see online movie 1 and 2*). Identical results were obtained with a morpholino-oligo targeting the ATG start codon.
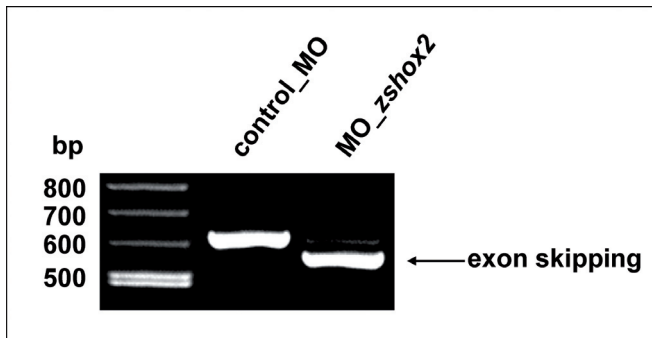
Figure 8. Specificity of injected anti-Shox2 morpholino. The injection of MO-*zshox2*, targeting the splice donor site of intron 3 results in an abnormal splice product (skipping of exon 3), leading to premature termination of translation.

__Online video material 1 and 2.__ Compared to the wildtype (movie 1), Shox2 deficient Zebrafish embryos exhibit severe sinus bradycardia and intermittent sinus exit blocks 72 hours post fertilization (movie 2).

DISCUSSION

In the present study we have investigated the expression pattern of *Shox2* during cardiogenesis and its crucial function in sinus venosus myocardial development. *Shox2* belongs to a small subfamily of homeodomain transcription factors and has previously been suggested to play a role in early heart development.[1] Reevaluation of the embryonic expression pattern showed that the initial description of *Shox2* expression in the outflow tract region of the developing heart could not be confirmed.[1] The detailed analyses presented here, clearly demonstrates that *Shox2* is expressed in the myocardium surrounding the developing sinus venosus as well as in a myocardial band on top of the ventricular septum. This sinus venosus myocardium is added to the venous pole of the heart and is recruited after formation of the primary heart tube.[6] We will refer to the sinus venosus area as the PHF located at both, the right and left side of the developing atrium.[7] For this study we concentrated on the right sided *Shox2* expression that is prominent in the sinus venosus myocardium compromising the developing SAN region and the venous valves within the right atrium.

To elucidate the predicted functions of *Shox2* in sinus venosus myocardium development, we have generated mice carrying a targeted mutation of the *Shox2* gene and observed embryonic lethality in *Shox2*^{-/-} embryos at 11.5 to 13.5 dpc due to cardiovascular failure. We have shown that there is a functional relationship between *Shox2* and the formation of the myocardium of the PHF being evident from the observation that the PHF myocardial areas that normally express *Shox2* are severely hypoplastic in *Shox2*^{-/-} embryos. This leads to diminished myocardium surrounding the cardinal veins and a marked hypoplasia of the venous valves and the SAN region. As it is not known exactly where and to what degree the sinus venosus myocardium is incorporated in normal atrial development, it is possible that the observed thin dilated atrial wall is also a result of the insufficient recruitment of sinus venosus myocardium, or improper replication and differentiation of the existing or newly added myocardium. Alternatively, it can also be explained by ultimately failing heart functions. The latter could be attributed to a deficient function of the hypoplastic and abnormally differentiated SAN region.

Identification of regulatory pathways involved in CCS formation has been impeded mainly due to an insufficient definition of the developmental origin of structures involved in these processes and the unavailability of animal models specifically targeting these structures. The transition from descriptive to molecular analyses of CCS development has recently gained momentum with the generation of *minK-lacZ* and CCS-*lacZ* transgenic mice.[22-24] Interestingly, the specific pattern of expression observed for *Shox2* strongly correlates with the *lacZ* expression in the SAN region and venous valves in these transgenic animals. *Shox2* therefore

represents an example of a homeodomain transcription factor with an expression pattern that overlaps with part of the developing CCS.

It is therefore appealing to not only show a role for *Shox2* in the formation of the PHF myocardium but to also postulate a function in the differentiation of the SAN region, the future pacemaking area. We were able to verify this hypothesis by analysing the physiological effects of a specific downregulation of *Shox2* expression by antisense morpholino injections into Zebrafish embryos. Indeed, anti-*Shox2* injected embryos exhibited severe bradycardia and intermitted sinus exit blocks suggesting severe sinus arrhythmia and / or pacemaking system malfunction as the primary cause of death in *Shox2* deficient animals.

To gain more insight into the cellular and molecular mechanisms underlying the proposed *Shox2* related SAN region malfunction, we have investigated the expression of Nkx2.5, Cx40 and Cx43 in this area in wildtype and knockout embryos. In our model we confirm that Nkx2.5 expression is absent in the cardiomyocytes of the normal developing SAN region[7,25] that are destined to acquire pacemaking properties. It can be postulated that the aberrant Nkx2.5 positivity in the SAN region of the *Shox2* knockout mouse interferes with its normal pacemaking function. This result is supported by recent data showing that transgenic mice ectopically expressing *Nkx2.5* under the control of an *α-MHC* promoter present sinus bradycardia and prolonged PR-intervals.[26] It seems tempting to postulate that the molecular pathway underlying the observed sinus bradycardia in our Zebrafish is identical in *Shox2*^{-/-} and *α-MHC-Nkx2.5* transgenic animals. It can furthermore be presumed that this mechanism acts in a stringent regional manner, since *Nkx2.5* driven pathways have recently been shown indispensable for maturation and maintenance of other conduction system components including atrioventricular nodal cardiomyocyte lineage specification.[27] The aberrant spatiotemporal *Nkx2.5* regulation in *Shox2*^{-/-} embryos was observed only within the hypoplastic SAN region but not within other regions exhibiting high levels of *Shox2* expression, including the venous valves that in normal development do not show a lack of Nkx2.5 expression. Also, Nkx2.5 expression is present in the myocardium of the atrioventricular conduction system in both, normal and *Shox2*^{-/-} embryos. Interestingly, this phenomenon also sheds light on the observation that patients diagnosed with *Nkx2.5* haploinsufficiences exhibit atrioventricular but no SAN dysfunction.[12-16] With our model, we can for the first time sufficiently explain both aspects of this phenotype. While the absent or abrogated *Nkx2.5* expression explains atrioventricular conduction problems, these patients may not exhibit SAN disease because the developing SAN region is not primarily hampered as this area normally does not express *Nkx2.5*.

Cx40 and Cx43 have mainly been used for the characterisation of the adult SAN but also have value as markers for earlier differentiation stages.[17] We have shown aberrant expression of these markers in the mutant SAN region. As Nkx2.5 has been reported to be involved in the regulation of connexins,[9,28,29] the aberrant expression of Nkx2.5 might be linked to the abnormal expression patterns of Cx40 and Cx43 and thus explain a postulated disturbed pacemaking function in *Shox2*^{-/-} embryos.

It is not clear at this stage if Nkx2.5 expression is directly regulated by *Shox2* in the SAN region or if this is a downstream event within a more elaborate pathway. It is evident however that a complete understanding of the molecular mechanisms underlying the observed *Nkx2.5* regulation requires the identification of additional regulatory molecules specifically expressed within the SAN region and investigation of their potential to interact with and modulate the functional properties of *Shox2*.

In summary, our data demonstrated the essential role of *Shox2* in the developing embryonic heart. We have shown that *Shox2* is necessary for the normal anlage of the PHF myocardium, which is uniquely Nkx2.5 negative. Furthermore, we have established a functional link between *Shox2* and the expression of Nkx2.5 that itself was shown to play an important role in the development and maturation of the SAN region. This observation provides a working hypothesis to further investigate the recruitment of sinus venosus myocardium and the molecular pathways underlying critical cell fate decisions that are required for pacemaking differentiation.

FUNDING SOURCES

REFERENCES

1. Blaschke RJ, Monaghan AP, Schiller S, Schechinger B, Rao E, Padilla-Nash H, Ried T, Rappold GA. SHOT, a SHOX-related homeobox gene, is implicated in craniofacial, brain, heart, and limb development. *Proc Natl Acad Sci U S A*. 1998;95:2406-2411.
2. Rovescalli AC, Asoh S, Nirenberg M. Cloning and characterization of four murine homeobox genes. *Proc Natl Acad Sci U S A*. 1996;93:10691-10696.

3. Rao E, Weiss B, Fukami M, Rump A, Niesler B, Mertz A, Muroya K, Binder G, Kirsch S, Winkelmann M, Nordsiek G, Heinrich U, Breuning MH, Ranke MB, Rosenthal A, Ogata T, Rappold GA. Pseudoautosomal deletions encompassing a novel homeobox gene cause growth failure in idiopathic short stature and Turner syndrome. *Nat Genet*. 1997;16:54-63.

4. Yu L, Gu S, Alappat S, Song Y, Yan M, Zhang X, Zhang G, Jiang Y, Zhang Z, Zhang Y, Chen Y. Shox2-deficient mice exhibit a rare type of incomplete clefting of the secondary palate. *Development*. 2005;132:4397-4406.

5. Cobb J, Dierich A, Huss-Garcia Y, Duboule D. A mouse model for human short-stature syndromes identifies Shox2 as an upstream regulator of Runx2 during long-bone development. *Proc Natl Acad Sci U S A*. 2006;103:4511-4515.

6. Kelly RG. Molecular inroads into the anterior heart field. *Trends Cardiovasc Med*. 2005;15:51-56.

7. Gittenberger-de Groot AC, Mahtab EA, Hahurij ND, Wisse LJ, Deruiter MC, Wijffels MC, Poelmann RE. Nkx2.5-negative myocardium of the posterior heart field and its correlation with podoplanin expression in cells from the developing cardiac pacemaking and conduction system. *Anat Rec (Hoboken)*. 2007;290:115-122.

8. Ebert SN, Taylor DG. Catecholamines and development of cardiac pacemaking: an intrinsically intimate relationship. *Cardiovasc Res*. 2006;72:364-374.

9. Bruneau BG. Transcriptional regulation of vertebrate cardiac morphogenesis. *Circ Res*. 2002;90:509-519.

10. Harvey RP. NK-2 homeobox genes and heart development. *Dev Biol*. 1996;178:203-216.

11. Srivastava D, Olson EN. A genetic blueprint for cardiac development. *Nature*. 2000;407:221-226.

12. Jay PY, Berul CI, Tanaka M, Ishii M, Kurachi Y, Izumo S. Cardiac conduction and arrhythmia: insights from Nkx2.5 mutations in mouse and humans. *Novartis Found Symp*. 2003;250:227-238.

13. Jay PY, Harris BS, Maguire CT, Buerger A, Wakimoto H, Tanaka M, Kupershmidt S, Roden DM, Schultheiss TM, O'Brien TX, Gourdie RG, Berul CI, Izumo S. Nkx2-5 mutation causes anatomic hypoplasia of the cardiac conduction system. *J Clin Invest*. 2004;113:1130-1137.

14. Benson DW, Silberbach GM, Kavanaugh-McHugh A, Cottrill C, Zhang Y, Riggs S, Smalls O, Johnson MC, Watson MS, Seidman JG, Seidman CE, Plowden J, Kugler JD. Mutations in the cardiac transcription factor NKX2.5 affect diverse cardiac developmental pathways. *J Clin Invest*. 1999;104:1567-1573.

15. Kasahara H, Lee B, Schott JJ, Benson DW, Seidman JG, Seidman CE, Izumo S. Loss of function and inhibitory effects of human CSX/NKX2.5 homeoprotein mutations associated with congenital heart disease. *J Clin Invest*. 2000;106:299-308.

16. Schott JJ, Benson DW, Basson CT, Pease W, Silberbach GM, Moak JP, Maron BJ, Seidman CE, Seidman JG. Congenital heart disease caused by mutations in the transcription factor NKX2-5. *Science*. 1998;281:108-111.

17. Miquerol L, Dupays L, Theveniau-Ruissy M, Alcolea S, Jarry-Guichard T, Abran P, Gros D. Gap junctional connexins in the developing mouse cardiac conduction system. *Novartis Found Symp*. 2003;250:80-98.

18. Hogan BLM, Beddington R, Constantini F, Lacy E. *Manipulating the Mouse Embryo*: A Laboratory Manual. New York, NY: Cold Spring Harbor Press; 1994.

19. Wilkinson DG. *Whole Mount In Situ Hybridisation of Vertabrate Embryos*. Oxford, UK: Oxford IRL Press; 1992.

20. Gundersen HJ, Jensen EB. The efficiency of systematic sampling in stereology and its prediction. *J Microsc*. 1987;147:229-263.

21. Rottbauer W, Saurin AJ, Lickert H, Shen X, Burns CG, Wo ZG, Kemler R, Kingston R, Wu C, Fishman M. Reptin and pontin antagonistically regulate heart growth in zebrafish embryos. *Cell*. 2002;111:661-672.

22. Rentschler S, Vaidya DM, Tamaddon H, Degenhardt K, Sassoon D, Morley GE, Jalife J, Fishman GI. Visualization and functional characterization of the developing murine cardiac conduction system. *Development*. 2001;128:1785-1792.

23. Jongbloed MR, Schalij MJ, Poelmann RE, Blom NA, Fekkes ML, Wang Z, Fishman GI, Gittenberger-de Groot AC. Embryonic conduction tissue: a spatial correlation with adult arrhythmogenic areas. *J Cardiovasc Electrophysiol*. 2004;15:349-355.

24. Kondo RP, Anderson RH, Kupershmidt S, Roden DM, Evans SM. Development of the cardiac conduction system as delineated by minK-lacZ. *J Cardiovasc Electrophysiol*. 2003;14:383-391.

25. Christoffels VM, Mommersteeg MT, Trowe MO, Prall OW, Gier-de Vries C, Soufan AT, Bussen M, Schuster-Gossler K, Harvey RP, Moorman AF, Kispert A. Formation of the Venous Pole of the Heart From an Nkx2-5-Negative Precursor Population Requires Tbx18. *Circ Res*. 2006;98:1555-1563.

26. Wakimoto H, Kasahara H, Maguire CT, Moskowitz IP, Izumo S, Berul CI. Cardiac electrophysiological phenotypes in postnatal expression of Nkx2.5 transgenic mice. *Genesis*. 2003;37:144-150.

27. Pashmforoush M, Lu JT, Chen H, Amand TS, Kondo R, Pradervand S, Evans SM, Clark B, Feramisco JR, Giles W, Ho SY, Benson DW, Silberbach M, Shou W, Chien KR. Nkx2-5 pathways and congenital heart disease; loss of ventricular myocyte lineage specification leads to progressive cardiomyopathy and complete heart block. *Cell*. 2004;117:373-386.

28. Bruneau BG, Nemer G, Schmitt JP, Charron F, Robitaille L, Caron S, Conner DA, Gessler M, Nemer M, Seidman CE, Seidman JG. A murine model of Holt-Oram syndrome defines roles of the T-box transcription factor Tbx5 in cardiogenesis and disease. *Cell*. 2001;106:709-721.

29. Dupays L, Jarry-Guichard T, Mazurais D, Calmels T, Izumo S, Gros D, Theveniau-Ruissy M. Dysregulation of connexins and inactivation of NFATc1 in the cardiovascular system of Nkx2-5 null mutants. *J Mol Cell Cardiol*. 2005;38:787-798.

2

CLINICAL PERSPECTIVE

We have shown that in early cardiac development the venous pole of the heart is subjected to extensive remodeling. Recruitment of second heart field sinus venosus myocardium is seen. This myocardium forms a U-shaped band lining the base of the left and right cardinal vein through the area of the dorsal mesocardium. This sinus venosus myocardium is unique in that it does not express the precardial marker *Nkx2.5*. Pacemaking activity is already functional in the sinus venosus myocardium during development and is restricted in adult life to the sinoatrial node. *Shox2*, a homeobox gene highly homologous to *SHOX*, which is involved in short stature syndrome in humans, is a novel marker for the sinus venosus myocardium. To unravel the role of *Shox2* in heart development, *Shox2* knockout mice were made. These mice showed embryonic lethality between 11.5 and 13.5 dpc, and the sinus venosus myocardium was markedly hypoplastic, including the sinoatrial nodal region. This latter region also showed abnormal differentiation in that genes that are normally negative in the developing node (Nkx2.5, Cx40 and Cx43) were now aberrantly positive. *Shox2* downregulation in Zebrafish resulted in marked bradycardia because of diminished pacemaking function. Therefore, we assume that the embryonic lethality in the *Shox2* mutant mice might result from a comparable process. The hypoplasia and abnormal differentiation of the sinoatrial nodal region could lead to a disturbed pacemaking function and resultant cardiac failure.

EXPANDED MATERIAL AND METHODS

Construction of the targeting vector, generation of chimeras and mutant mice

The replacement targeting vector aiming at the *Shox2* locus was generated by inserting genomic DNA fragments into the plasmid pHR68. The 5' homology region was amplified from the cosmid B212cos1 using primers *Shox2* ATG-for: 5'-GGGAGAGCTTGAGCGCGAGGTTG-3' and *Shox2* int1-rev: 5'-GCAAGACAGTCTCATTACCAGAT-3'. The 3' homology region represents a *Kpn*I restriction fragment isolated from the cosmid B212cos. Correct insertion of the 5' and 3' homology fragments was verified by sequence analysis. The *Sal*I digested targeting plasmid was electroporated into RI and E14 ES cells respectively. Homologous recombination was confirmed by Southern-blot analysis using a 578 bp *Bam*HI fragment from the 5' upstream region of the targeted locus (Figure 2a). ES cells from one correctly targeted RI and E14 clone were injected into C57BL/6 blastocysts that were implanted into pseudopregnant females as described.[18] Heterozygous animals were sequentially bred into a C57BL/6 genetic background at least to F_4.

DNA and RNA analysis

Genomic DNA was prepared from tail biopsies and yolk sacs as previously described. Animals were genotyped using the primer neo-for: 5'-TGAGCGGGACTCTGGGGTTCGA-3' and *Shox2*-int1/2-for: 5'-CAGGGTTAGGAGTCTCTAGCCT'-3' (Figure 2a). For embryo genotyping, these primers were used in combination with the primer *Shox2*-ex2-rev: 5'-TGCT TGATTTTGGTCTGGCCTTCGT-3' residing within the replaced second *Shox2* exon. RNA from whole embryos or isolated embryonic hearts was isolated using a QIAGEN RNAeasy Mini-Kit and RT-PCRs were carried out with the primers SO3- for: 5`GTGTTCT-CATAGGGGCCGCCAGC 3` and *Shox2*-rev: 5`ACAGCGCTGTCCAGCTGCAGCTGCG 3`. These primers flank the alternatively spliced exon 5 and allow discriminating between *Shox2*a and *Shox2*b.

Immunohistochemistry and 3-D reconstructions

Immunohistochemistry with the MLC-2a, Nkx2.5, Cx40 and Cx43 specific antibodies were performed by routine procedures. All embryos (wildtype 10.5 dpc n=1 and *Shox2*^{-/-} 10.5 dpc n=1; wildtype 11.5 dpc n=4 and *Shox2*^{-/-} 11.5 dpc n=4) were fixed in 4% paraformaldehyde (PFA), after dehydration they were embedded in paraffin. The embedded embryos were 5 μm sectioned and mounted 1 to 5 onto protein /glycerin coated slides so 5 different staining procedures could be performed on one embryo. After dehydration of the slides, inhibition of the endogenous peroxidase was performed for MLC-2a and Nkx2.5 with a solution of 0.3% H_2O_2 in PBS for 20 min. For Cx40 and Cx43 antigen retrieval was performed in 0.01M Citric buffer of pH 6.0 at 97˚C for 12 min. Overnight incubation of the slides was completed with

the following primary antibodies: 1/2000 anti-atrial myosin light chain 2 (MLC-2a, gift from S.W. Kubalak) and 1/4000 anti-NK2 transcription factor related locus 5 (Nkx2.5, Santa Cruz Biotechnology, sc-8697), 1/100 anti-Connexin40 (Cx40, Santa Cruz Biotechnology, sc-20466) and 1/200 anti-Connexin43 (Cx43, Sigma, C6219). The primary antibodies were dissolved in PBS-Tween-20 with 1% Bovine Serum Albumin (BSA, Sigma Aldrich, USA). All slides were rinsed between subsequent incubation steps: PBS (2x) and PBS-Tween-20 (1x). Incubation with the secondary antibodies was performed for 40 min: for MLC-2a and Cx43 1/200 goat-anti-rabbit-biotin (Vector Laboratories, USA, BA-1000) and 1/66 goat serum (Vector Laboratories,USA, S1000); for Nkx2.5 and Cx40 1/200 horse-anti-goat-biotin (Vector Laboratories, USA, BA-9500) and 1/66 horse serum (Brunschwig Chemie, Germany, S-2000) in PBS-Tween-20. Thereafter, a 40 min incubation with ABC-reagent (Vector-Laboratories, USA, PK 6100) was performed. For visualisation, all slides were incubated with 400 µg/ml 3-3'di-aminobenzidin tetrahydrochloride (DAB, Sigma-Aldrich Chemie, USA, D5637) dissolved in Tris-maleate buffer pH7.6 to which 20 µl H_2O_2 was added: MLC-2a 5 min and Nkx2.5, Cx40 and Cx43 10 min. 0.1% Haematoxylin (Merck, Darmstadt, Germany) was used to counterstain the slides for 10 sec, followed by rinsing with tap water for 10 min. After dehydration, all slides were mounted with Entellan (Merck, Darmstadt, Germany).

We made 3D reconstructions of the atrial and ventricular myocardium of MLC-2a stained sections of 10.5 and 11.5 dpc wildtype and *Shox2*^{-/-} embryonic hearts, in which Nkx2.5 negative myocardium was manually added. The reconstructions were made as described earlier,[23] using the AMIRA software package (Template Graphics Software, San Diego, USA).

Zebrafish *in situ* hybridization and Morpholino injection

Whole-mount RNA *in situ* hybridization was essentially carried out as described.[21] The full length Zebrafish *Shox2* mRNA sequence was amplified and cloned into pCR II (Invitrogen) for *in vitro* transcription (Roche). Morpholino modified antisense oligonucleotides were designed against the splice donor site 5´-TGTATCCACGCACCTTTATGCAACT-3´ and the translational start site of *Zebrafish Shox2* 5´- ACGCTGTAAGTTCTTCC ATCACTGC-3´ and injected as described.[21]

Nathan D. Hahurij[1, 2]
Nico A. Blom[1]
Frits Meijlink[3]
Edris A.F. Mahtab[2]
Lambertus J. Wisse[2]
Regina Bökenkamp[1]
Denise P. Kolditz[4]
Martin J. Schalij[4]
Robert E. Poelmann[2]
Monique R.M. Jongbloed[2, 4]
Adriana C. Gittenberger-de Groot[2]

[1] Department of Pediatric Cardiology, Leiden University Medical Center, Leiden, The Netherlands.
[2] Department of Anatomy & Embryology, Leiden University Medical Center, Leiden, The Netherlands.
[3] Hubrecht Institute, KNAW & University Medical Center Utrecht, Utrecht, The Netherlands.
[4] Department of Cardiology, Leiden University Medical Center, Leiden, The Netherlands.

3

Shox2 in pacemaker and epicardial development

Functional implications

ABSTRACT

Background

Shox2 has an important role in formation of the posterior heart field (PHF). The PHF contributes to major parts of the inflow tract of the heart including the cardiac conduction system and the epicardium. Here we hypothesize that mutation of the *Shox2* gene leads to abnormal sinoatrial node (SAN) / pacemaking function as well as abnormal epicardial development in the heart.

Methods and Results

Electrophysiological recordings were performed in wildtype and *Shox2−/−* embryos of 12.5 days post conception (dpc). Compared to wildtype the electrophysiological assessments in *Shox2−/−* embryos showed a significant (*P*=0.032) lower heart rate (105±36 bpm vs 74±15 bpm), no differences were observed in atrioventricular conduction time (76±24 ms vs 80±14 ms, respectively). Immunohistochemical analysis and 3D reconstructions with MLC-2a, Nkx2.5 and HCN4 specific antibodies, showed hypoplasia and aberrant differentiation of the PHF derived sinus venosus myocardium in *Shox2−/−* embryos of 12.5 dpc. In both wildtype and *Shox2−/−* HCN4 was widely expressed throughout the complete sinus venosus myocardium including the SAN, albeit decreased in *Shox2−/−* due to hypoplasia of this area. Expression of Wt1 and 3D reconstructions of the pro-epicardial organ (PEO) in *Shox2−/−* embryos showed a decreased PEO size at 9.5 dpc with normal epicardial spreading at 12.5 dpc. At latter stages the ventricles showed decreased numbers of epicardium derived cells and an abnormal ventricular wall morphology.

Conclusions

Shox2 has a crucial role in development of the venous pole of the heart including the SAN and its pacemaking function. Furthermore, we, for the first time show that *Shox2* is essential for proper epicardial lineage development.

INTRODUCTION

The last decennium it has been well established that the heart generates from two large cardiogenic fields in the dorsal mesocardium: the first and second heart field.[1] The first heart field gives rise to the primary heart tube and the second heart field contributes cardiomyocytes at the venous as well as the arterial pole of this tube. At the venous pole these cardiomyocytes are derived from a subgroup of the second heart field, the so-called posterior heart field (PHF). The PHF derived myocardium is characterized by specific expression patterns of several markers like the early cardiomyocyte marker NK2 transcription factor related locus 5 (Nkx2.5)

and gives rise to major parts of the developing cardiac conduction system (CCS).[2,3]

The homeobox gene *Shox2* was shown to be indispensable in the formation of the PHF and mice lacking *Shox2* die at early embryonic stages most probably due to severe cardiac failure.[4] Previously, we showed that mutations of *Shox2* lead to a diminished anlage and aberrant differentiation of the PHF myocardium including the sinoatrial node (SAN), the posterior atrial wall and the venous valves. In the hypoplastic SAN an up-regulation of Nkx2.5, Connexin 40 (Cx40), Connexin 43 (Cx43),[4] Nppa and Tbx3 was observed.[5] Although SAN / pacemaker dysfunction might be expected in *Shox2*^{-/-} embryos, electrophysiological studies have not yet been performed in this specific mouse model.

Contemporary studies identified specialized pacemaking channels in the developing SAN essential for action potential generation.[6] The hyperpolarization-activated cyclic nucleotide-gated channel (HCN) 4 is believed to be one of the most important currents involved in pacemaking. Human mutations in the *HCN4* gene cause marked bradycardia.[7,8] Immunohistochemical analysis in mice showed that at early stages of cardiac development HCN4 is highly expressed in the PHF derived sinus venosus myocardium, including the region of the SAN. In addition, both *Shox2* and *Nkx2.5* seem to have an imperative role in the regulation of HCN4 expression during cardiogenesis.[5,9]

Recently, we demonstrated that abnormal sinus venosus development might also coincide with an abnormal anlage of the epicardium of the heart.[10] Aberrant epicardial development may also be expected in *Shox2* mutants, since: (1) *Shox2* expression is known to be highly restricted in the sinus venosus area including the pro-epicardial organ (PEO), a cauliflower-like protrusion of mesothelial cells from which the epicardial cells derive[11] and (2) both the cardiomyocytes of the inflow tract (derived from the PHF) and the PEO seem to originate from a common Tbx-18 expressing cardiac progenitor pool in the dorsal mesocardium.[12,13] As from approximately 9.5 days post conception (dpc), epicardial cells start to migrate from the PEO over the developing heart thus forming a layer of epicardium. Subsequently, by epithelial-to-mesenchymal-transformation (EMT) of epicardial cells, the so-called epicardium derived cells (EPDCs) are generated.[11] EPDCs migrate into the myocardium fulfilling several important roles in development and maturation of the heart.[14-16]

In the current study we hypothesize that *Shox2* has an important role in pacemaker function and epicardial development. To substantiate this hypothesis electrophysiological assessments and immunohistochemical analysis with the HCN4 specific antibody were performed in isolated wildtype and *Shox2*^{-/-} hearts of 12.5 dpc. The role of *Shox2* in epicardial development was studied by 3D reconstructions of the PEO of wildtype and *Shox2*^{-/-} hearts. Furthermore, immunohistochemistry was performed with Wilm's tumor 1 (Wt1), a specific marker for both epicardial cells and EPDCs.[17]

MATERIAL AND METHODS

Animals and preparation of the hearts

All animal experiments were approved by the local medical ethical committee and conducted according to the Dutch animal protection law (Leiden, DEC No 6679). Mutant mice were bred by The Netherlands Institute of Developmental Biology (Hubrecht laboratory, Utrecht, The Netherlands) after replacing the targeted vector aiming at the *Shox2* locus in a CD1 mouse strain as described previously.[4] The presence of a vaginal plug one day after breeding was considered to be 0.5 dpc. For harvesting of the embryos, pregnant mice were sacrificed by cervical dislocation at 12.5 dpc. Thereafter an incision was made in the mid-abdominal region, followed by the extraction of the two laterally located uterus horns. The uterus was place in a Petri dish filled with heated Tyrode's solution containing (in mmol/l) 130 NaCl, 4 KCl, 1,2 KH_2PO_4, 0,6 $MgSO_47H_2O$, 20 $NaHCO_3$, 1,5 $CaCl_22H_2O$ and 10 glucose at 37˚Celsius (C). Subsequently in Tyrode´s solution of 0˚C the embryonic hearts were dissected one-by-one for electrophysiological recordings. The individual embryonic tails were harvested for standard genotyping of the embryos as described previously.[4]

Table 1. Electrophysiological recordings in Wildtype and *Shox2$^{-/-}$* embryos of 12.5 dpc

Embryo (number)	Age (dpc)	Genotype (Wildtype / *Shox2$^{-/-}$*)	Heart rate (BPM)	AV conduction Time (msec)
E8597A	12.5	WT	68	112.3
E8597B	12.5	WT	76	83
E8597C	12.5	*Shox2$^{-/-}$*	67	84.3
E8598B	12.5	WT	80	61.1
E8598C	12.5	*Shox2$^{-/-}$*	110	79.6
E8598D	12.5	*Shox2$^{-/-}$*	80	102.9
E8599C	12.5	WT	85	79.5
E8599E	12.5	WT	151	84
E8601A	12.5	*Shox2$^{-/-}$*	98	82
E8601C	12.5	WT	143	78.3
E8601D	12.5	*Shox2$^{-/-}$*	60	64.7
E8601E	12.5	*Shox2$^{-/-}$*	75	81
E8601F	12.5	*Shox2$^{-/-}$*	87	73.8
E8601I	12.5	WT	145	48.1
E8418A	12.5	*Shox2$^{-/-}$*	71	99.4
E8418C	12.5	*Shox2$^{-/-}$*	59	62.9
E8418K	12.5	*Shox2$^{-/-}$*	63	65.3

Electrophysiological recordings and genotyping

Electrophysiological recordings were conducted in isolated wildtype (n=7) and *Shox2*^{-/-} (n=10) embryonic mouse hearts of 12.5 dpc (Table 1). Since genotyping of the embryos was performed after the electrophysiological experiments, all recordings are considered to be performed blind. For a detailed description of the recording equipment and the recording protocol we refer to the Expanded Material and Methods section. After recordings, all embryonic hearts were fixed in 4% paraformaldehyde (PFA) for further immunohistochemical processing.

Immunohistochemistry and in situ hybridization (ISH)

Immunohistochemistry was performed with antibodies specifically against atrial myosin light chain 2 (MLC-2a, gift from S.W. Kubalak), Nkx2.5 (Santa Cruz Biotechnology, sc-8697), HCN4 (Alomon labs, APS-052) and Wt1 (Santa Cruz Biotechnology, SC-192). The preparation of sections and detailed descriptions of the immunohistochemical staining as well as ISH protocols can be found in previous publications.[4,18]

3D reconstructions

3D reconstructions were made of the PEO and developing venous pole of the heart as described before,[19] using the AMIRA software package (Template Graphics Software, San Diego, USA).

Statistical Analyses

Statistical analysis was performed using the SPSS 15.0 software package (SPSS Inc, Chicago, Ill). A students-*t*-test was executed if values were equally distributed (skew ness is |-1|), otherwise a Mann Whitney *U*-test was performed. Statistical significant results are defined as: $P < 0.05$.

The authors had full access to and take responsibility for the integrity of the data. All authors have read and agree to the manuscript as written.

RESULTS

During the dissection of the embryos no visible differences were observed between wildtype, *Shox2*^{+/-} and *Shox2*^{-/-} embryos before the age of 12.5 dpc. After that age *Shox2*^{-/-} embryos did not have a spontaneous heart beat anymore and showed a severely hemorrhagic phenotype. In addition, around 16.5 - 17.5 dpc only apoptotic remnants of *Shox2*^{-/-} embryos were detected. Previous reports showed no differences between wildtype and *Shox2*^{+/-} embryos.[4,5] Therefore, the current study only described differences between wildtype and *Shox2*^{-/-} embryos up to 12.5 dpc.

Expression of *Shox2*

The expression of *Shox2* was studied by antisense in situ hybridization in whole mount embryos, isolated hearts and serial sections of wildtype hearts as described previously.[4] At 9.5 dpc, expression of *Shox2* was limited to the venous pole of the heart, including the region of the PEO, where formation of the sinus venosus occurs. From 10.5 to 12.5 dpc expression of *Shox2* is clearly visible in the myocardium surrounding the left and right horn of the sinus venosus including the SAN, which is located at the medial border of the right sinus horn. Furthermore, *Shox2* expression was clearly present in the developing venous valves, and at the top of the ventricular septum in the area of the putative left and right bundle branches.[4]
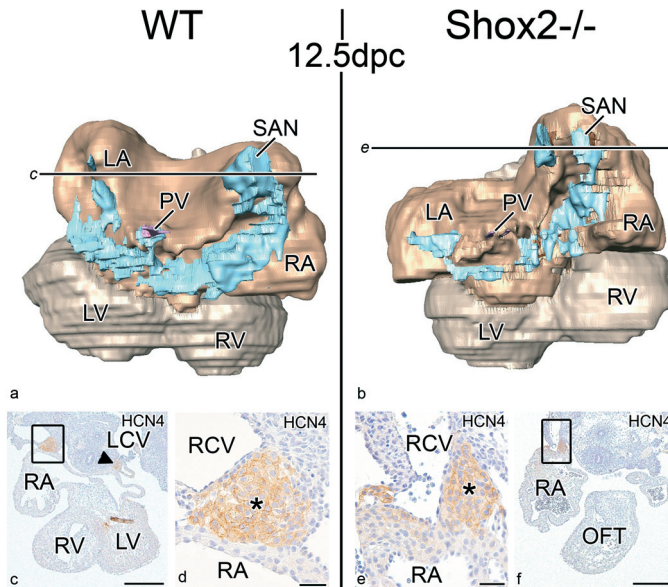

Figure 1. Expression of HCN4 in wildtype (WT) and *Shox2-/-* heart of 12.5 dpc. (a) and (b) show reconstructions of the dorsal side of embryonic WT and *Shox2-/-* hearts of 12.5 dpc respectively, in which the HCN4 expression pattern in the sinus venosus area is indicated (**light blue**). Both in WT and *Shox2-/-* hearts the light blue HCN4 positive myocardium is continuous between the left and right horn of the sinus venosus. (c) HCN4 stained section through the WT heart indicated at the specific level in (a) showing that the SAN (**asterisk** in d boxed area in c) is positive for HCN4. At these stages HCN4 expression is also observed in the left sinus horn as indicated by the **arrow head** in (c). (e) Magnification of the boxed area in (f) which is a HCN4 stained section through the *Shox2-/-* heart at the level indicated in (b) clearly showing that the SAN (asterisk) expresses HCN4. **LA** indicates left atrium; **LCV**, left cardinal vein; **LV**, left ventricle; **OFT**, outflow tract; **RCV**, right cardinal vein; **RV**, right ventricle; **VS**, ventricular septum. In the reconstructions: **pink** indicates pulmonary vein; **dark brown**, atrial myocardium; **light brown**, ventricular myocardium. Scale bars: (c) and (f) = 300µm; (d) and (e) = 30µm.

Electrophysiological recordings and HCN4 expression at 12.5 dpc

All recordings were performed after a three minute calibration period of the hearts in the experimental setup. Table 1 summarizes the electrophysiological data of each individual heart. In total 7 wildtype and 10 *Shox2*^{-/-} hearts of 12.5 dpc were assessed. In wildtype as well as in *Shox2*^{-/-} embryos stable heart rates were recorded, and no sinus arrests or sinus exit blocks were observed in the mutant embryos. The mean recorded heart rate in wildtype and *Shox2*^{-/-} embryonic hearts was 105±36 bpm and 74±15 bpm, respectively. Statistical analysis showed a significant decrease (*P*=0.032) of the heart rate in *Shox2*^{-/-} embryos as compared to wildtype. No significant differences were recorded in mean AV conduction time between wildtype (76±24 ms) and *Shox2*^{-/-} (80±14 ms) hearts.

In wildtype hearts of 12.5 dpc the expression of the main cardiac pacemaker channel HCN4 was present in the complete MLC-2a positive and Nkx2.5 negative U-shaped region of sinus venosus myocardium including the SAN (Figure 1a, c, d; Figure 2a, c-e). Furthermore, weak HCN4 expression was observed in the region surrounding the developing pulmonary vein and at the base of both the venous valves and the primary interatrial septum. In all embryonic hearts HCN4 expression in the left and right sinus venosus horns could be followed from section to section towards a direct connection to the developing atrioventricular node (AVN) region at the base of the AV groove (Figure 1a).

In *Shox2*^{-/-} embryos of similar age HCN4 expression was observed in the hypoplastic MLC-2a positive and Nkx2.5 negative sinus venosus myocardium. Expression of HCN4 was also present in the aberrantly Nkx2.5 positive areas of the U-shaped sinus venosus myocardium (Figure 1b; Figure 2b). The same accounts for the hypoplastic MLC-2a and Nkx2.5 positive SAN (Figure 1b, e, f; Figure 2b, f-h) and for the base of the hypoplastic venous valves. The continuum of HCN4 positive myocardium between the SAN and the developing AVN region was still present.

Myocardial and epicardial development 9.5 dpc – 12.5 dpc

At 9.5 dpc both in wildtype and *Shox2*^{-/-} hearts, the PEO located in close proximity to the sinus venosus, stained positive for Wt1. However, in *Shox2*^{-/-} the size of this structure appeared to be decreased (Figure 3a-h).

At 10.5 dpc, in *Shox2*^{-/-} embryos the common atrium was slightly dilated and the venous valves were hypoplastic. At these stages, the sinus venosus myocardium including the SAN was MLC-2a positive and Nkx2.5 negative in both wildtype and *Shox2*^{-/-} embryos. In addition, in both wildtype and *Shox2*^{-/-} embryos Wt1 stained sections showed normal epicardial spreading by formation of a single layer of Wt1 positive epicardium over the complete developing heart (data not shown).

At 11.5 dpc major differences were observed between wildtype and *Shox2*^{-/-} hearts. In *Shox2*^{-/-} the atria were dilated and the sinus venosus myocardium was hypoplastic including the SAN, the dorsal atrial wall and venous valves. In wildtypes the sinus venosus myocardium including the SAN stained positive for MLC-2a and negative for Nkx2.5.

In *Shox2*^{-/-} however, an aberrant differentiation of this area was observed staining positive for both MLC-2a and Nkx2.5. Both in wildtype and *Shox2*^{-/-} AV cushions and outflow tract cushions could be discriminated in the AV canal and outflow tract region respectively. Compared to wildtype, the ventricles in *Shox2*^{-/-} embryos seemed to be aberrantly positioned, with the right ventricle in a more superior position. At this stage no differences were observed in ventricular wall thickness and trabecular development between wildtype and *Shox2*^{-/-} hearts (data not shown).
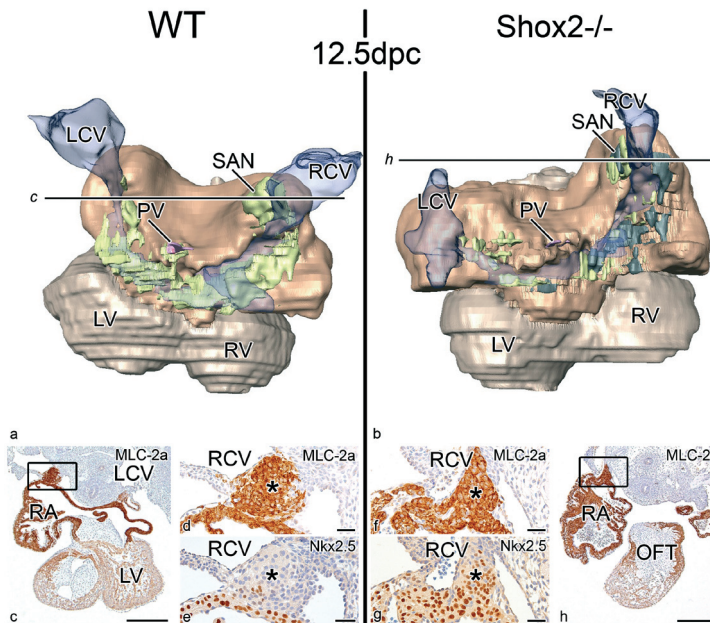

Figure 2. Expression of MLC-2a and Nkx2.5 in the PHF in wildtype (WT) and *Shox2*^{-/-} at 12.5 dpc. Three dimensional reconstructions of the dorsal side of WT and *Shox2*^{-/-} embryonic hearts of 12.5 dpc are shown in (a) and (b) respectively. Compared to WT (a) the PHF derived MLC-2a positive and Nkx2.5 negative sinus venosus myocardium (**green**) is severely hypoplastic in *Shox2*^{-/-} embryos (b). The aberrant differentiated, Nkx2.5 expressing sinus venosus myocardium in *Shox2*^{-/-} is indicated in **black** (b). (c) Shows a transverse MLC-2a stained section through the embryonic heart as indicated in (a). In WT the sinoatrial node (**SAN**, **asterisk** in d-e) is positive for MLC-2a (d, magnification of boxed area in c) and negative for Nkx2.5 (e, consecutive section of d). In *Shox2*^{-/-} the hypoplastic SAN is positive for MLC-2a (f, magnification of boxed area in h, which is transverse MLC-2a stained section through the *Shox2*^{-/-} heart as indicated in b) and positive for Nkx2.5 (g, consecutive section of f). **LCV** indicates left cardinal vein; **LV**, left ventricle; **OFT**, outflow tract; **PV**, pulmonary vein; **RA**, right atrium; **RCV**, right cardinal vein; **RV**, right ventricle; In the reconstruction: **light brown**, ventricular myocardium; **dark brown**, atrial myocardium; **blue transparent**, sinus venosus. Scale bars: (c) and (h) = 300μm; (d-g) = 30μm.

At 12.5 dpc the structural abnormalities between wildtype and *Shox2*^{-/-} became more pronounced. In wildtype hearts the volume of the sinus venosus myocardium including the SAN increased and retained its MLC-2a positive and negative Nkx2.5 expression pattern (Figure 2a, c-e). In *Shox2*^{-/-} hearts the same area was severely hypoplastic and at many locations abnormally positive for Nkx2.5 (Figure 2b, f-h). At these stages in wildtype the pulmonary vein was almost completely surrounded by myocardium, which was MLC-2a positive and showed a mosaic expression pattern for Nkx2.5. In *Shox2*^{-/-} the myocardium in this area was hypoplastic, stained positive for MLC-2a and also showed Nkx2.5 mosaic expression (data not shown). At this stage the aberrant positioning of the ventricles in *Shox2*^{-/-} hearts became even more apparent. The 3D reconstructions of *Shox2* mutants clearly show that the right ventricle is dilated and aberrantly positioned to a more superior region. Similar to previous stages AV and outflow tract cushions could be discriminated both in wildtype and *Shox2*^{-/-} hearts (Figure 4a-d).
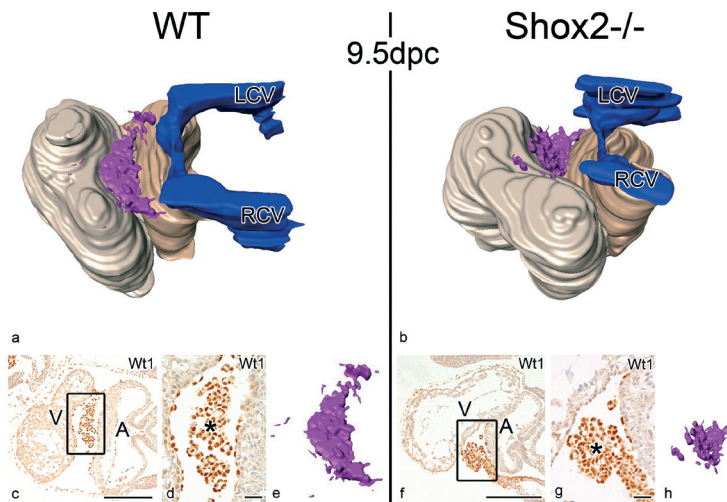

Figure 3. PEO formation in wildtype (WT) and *Shox2*^{-/-} embryos. Caudo-dorsal views of 3D reconstructions of WT (a) and *Shox2*^{-/-} (b) embryonic hearts of 9.5 dpc. (c) Wt1 stained section of the WT heart reconstructed in (a). (d) Magnification of the boxed area in (c) of the PEO (**asterisk**) staining positive for Wt1. (e) Isolated reconstruction of the PEO of the WT heart indicated in (a). (f) Wt1 stained section of the *Shox2*^{-/-} heart reconstructed in (b). (g) Magnification of boxed area in (f) shows the PEO (**asterisk**) positive for Wt1. (h) Isolated reconstruction of the PEO of the *Shox2*^{-/-} heart in (b), clearly showing that the size of the PEO is decreased (compare e and h). **A** indicates common atrium; **LCV**, left cardinal vein; **RCV**, right cardinal vein; **V**, ventricular part of the heart; In the reconstructions: **light brown** indicates ventricular myocardium; **dark brown**, atrial myocardium; **blue**, sinus venosus lumen. Scale bars: (c) and (f) = 200μm; (d) and (g) = 30μm.

At 12.5 dpc, for the first time differences in the thickness of the ventricular wall and the anlage of ventricular trabeculation were observed between wildtype and *Shox2-/-* embryos. Compared to wildtype embryos *Shox2-/-* embryos appeared to have a thinner ventricular wall at many locations. In addition, the ventricles showed less trabeculation (Figure 5a, b). At these stages in wildtype as well as in *Shox2-/-* hearts the Wt1 stained sections showed that the complete atrial and ventricular walls were covered with a layer of Wt1 positive epicardial cells (Figure 5a, c, b, e). In wildtype hearts many EPDCs were already discriminated, however in *Shox2-/-* hearts the number of EPDCs seemed to be decreased. Especially at locations adjacent to a thin ventricular myocardial wall less EPDCs in the subepicardial space were observed (Figure 5a-f).
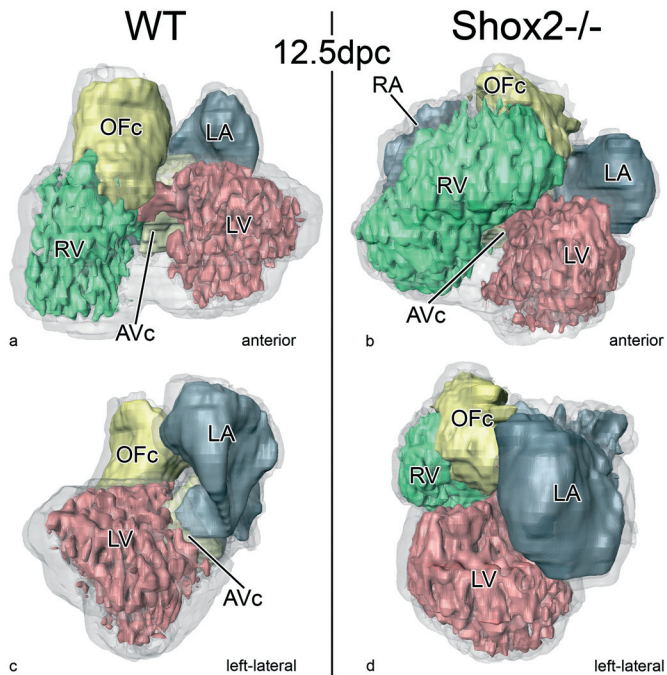

Figure 4. Cardiac morphology of wildtype (WT) and *Shox2-/-* hearts at 12.5 dpc. Reconstructions of frontal views of WT (a) and *Shox2-/-* (b) hearts of 12.5 dpc are demonstrated in which the lumen of the right ventricle (**RV; green**), left ventricle (**LV; red**) and left atrium (**LA; dark grey**) are indicated, in *Shox2-/-* the right atrial lumen (**RA; dark grey**) can also be observed. Furthermore, the atrioventricular cushions (**AVc; light yellow**) and Outflow cushions (**OFc; dark yellow**) are designated. In *Shox2-/-* hearts the RV is severely dilated and positioned in a more superior position (b) as compared to WT (a). (c) and (d) show left-lateral views of hearts in (a) and (b) respectively, clearly indicating that the dilated RV in *Shox2-/-* is located superiorly to the LV; **light grey** indicates contours of atrial as well as ventricular myocardium.
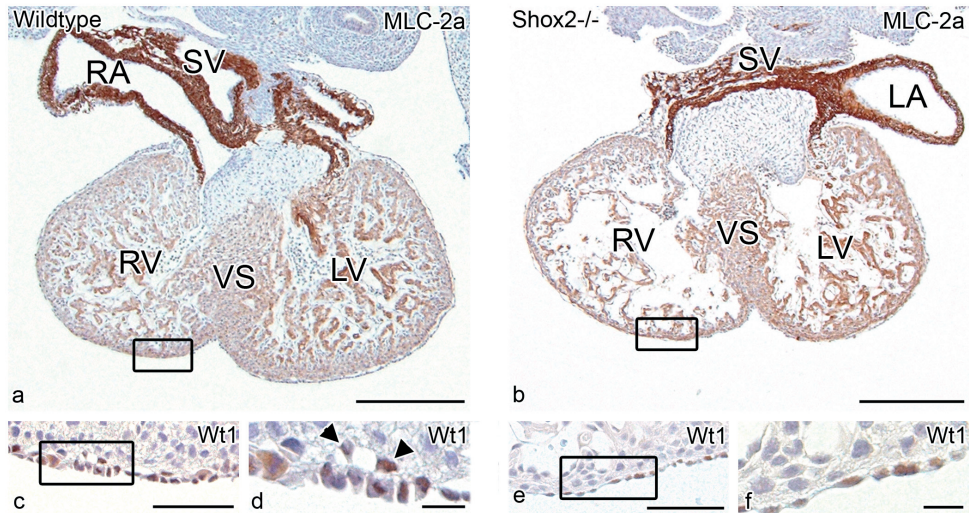
Figure 5. Expression of Wt1 in wildtype (WT) and *Shox2*^{-/-} hearts of 12.5 dpc. Compared to the ventricular morphology of WT hearts as indicated by the MLC-2a stained section in (a), the ventricular morphology is abnormal in *Shox2*^{-/-} hearts of similar age showing a thin ventricular wall and less trabeculae (b). (c) Consecutive Wt1 stained section of the boxed area in (a) clearly shows that the epicardium is Wt1 positive. Wt1 positive EPDCs can be discriminated and are indicated by the **arrowheads** in (d), which is a magnification of the boxed area in (c). (e) Consecutive Wt1 stained section of the boxed area in (b) showing a single layer of Wt1 positive epicardium in the *Shox2*^{-/-} heart. In *Shox2*^{-/-} hearts almost no EPDCs were observed in the subepicardial layer as indicated in (f), which is a magnification of the boxed area in (e); Scale bars: (a) and (b) = 300μm; (c-f) = 30μm.

DISCUSSION

The development and maturation of the venous pole of the heart has been a matter of debate for years. However, contemporary studies gained more insight in the formation of this rather complex cardiac region. It was shown that the PHF adds newly formed cardiomyocytes to the venous pole of the primary heart tube, and that major parts of the CCS, including the SAN are derived from this group of secondarily added myocytes.[2,4,9] It has been even postulated that the PHF plays a role in the development of the AVN.[2,20]

Mutations in several genes like *podoplanin*,[18] *Tbx18*[21,22], *Tbx3*[22,23] and *Shox2*[4,5] can result in a disturbed anlage and / or differentiation of the venous pole (i.e. sinus venosus) of the heart. Furthermore, we recently demonstrated in *podoplanin*[10] and *Pdgfrα*[24] mutant mice that abnormal epicardial development may also coincide with hampered PHF anlage.

In the present study we examined the pacemaking function of the SAN as well as epicardial development in *Shox2* mutants. We confirmed hypoplasia and aberrant differentiation of the venous pole of the heart including the SAN in *Shox2* mutant mice of 12.5 dpc. At these stages electrophysiological recordings demonstrated a regular but significantly slower sinus rhythm

in *Shox2*^{-/-} embryos as compared to controls. The AVN function remained intact in the mutant mice as indicated by normal AV conduction times. Remarkably, the expression of pacemaker channel HCN4 could clearly be observed in the hypoplastic SAN. The epicardial lineage development indeed appeared to be abnormal in *Shox2* mutants, including a diminished size of the PEO and a decreased numbers of EPDCs in the subepicardial space.

Shox2, HCN4 and decreased pacemaking.

HCN4 is considered to be the most important channel for cardiac pacemaking,[6] especially in the maintenance of a stable heart rate. Recent studies in humans demonstrated that mutation in the *HCN4* gene causes marked sinus bradycardia.[7,8] In mouse heart development, HCN4 can already be detected at the complete venous pole of the heart at very early embryonic stages.[9] During development the expression pattern of HCN4 becomes more restricted and is predominantly observed in the SAN. However, in the hearts of two months old mice HCN4 is also observed in the AVN region and the right atrioventricular ring bundle, which has been suggested to enable action potential generation at other regions outside the SAN.[25]

The regulation of *HCN4* expression during embryonic development has not yet been elucidated. Mommersteeg *et al.* recently postulated that in early embryonic development (<14.5 dpc) *Nkx2.5* represses expression of *HCN4*.[9] The current study confirms this relation, with respect to the sinus venosus myocardium in wildtype embryos of 12.5 dpc. At later stages (>14.5 dpc), except for the SAN the complete sinus venosus myocardium gains an atrial differentiation program, becoming positive for Nkx2.5, Cx43, Cx40 and losing expression of HCN4.[9,18]

The regulation of HCN4 in the SAN region seems to be more controversial. Espinoza-Lewis *et al.* showed absence of HCN4 expression in *Shox2*^{-/-} embryos of 11.5 dpc.[5] They suggested that an *Shox2* mediated aberrant up-regulation of Nkx2.5 in the SAN, down regulates HCN4, which bears resemblance to the atrial differentiation program of the remainder of sinus venosus myocardium in wildtype hearts (>14.5 dpc). This is in contrast to the findings in our study that clearly showed that HCN4 is still expressed in the hypoplastic Nkx2.5 positive sinus venosus myocardium including the SAN in *Shox2*^{-/-} embryos of 12.5 dpc. Recent findings on the role of *Tbx3* in SAN development also demonstrated that Nkx2.5 positive and HCN4 positive areas do have overlap in some parts of the SAN, i.e. the SAN-tail.[22] Therefore, we postulate that HCN4 is not solely regulated by Nkx2.5 and that the transcriptional regulation of the main cardiac pacemaking channel involves a more elaborate pathway.

Initial morphological[26] and modern immunohistochemical marker studies[22,27] both demonstrated that different areas within the developing SAN can be discriminated, i.e. a solid node and a tail extending on the endocardial surface of the terminal crest. From developmental origin

point-of-view it has recently been shown that the solid node derives from *Tbx18* and *Isl1* expressing precursor cells of the SHF.[13] Moreover, *Tbx18* mutants fail to develop a solid node. Less however is known about the development of the SAN-tail, which is a Tbx18 negative and Nkx2.5 and HCN4 positive structure.[22] Examination of the structure-function relationship within the SAN of human and animal models[28] showed that the solid node as wells as the tail of the SAN is able to generate action potentials.[27] The solid node is the main pacemaker location within the SAN, however if heart rate decreases the dominant pacemaking area tends to shift towards the SAN-tail.[28] Moreover, the different areas within this "pacemaking complex" react differently to neuronal and adrenal signaling.[29] For instance stimulation of the sympathic nervous system leads to a superior shift of the main pacemaker site resulting in an increase of heart rate.[30]

The significant lower heart rate in *Shox2*^{-/-} hearts observed in the current study might be related to abnormal anlage of the pacemaking complex and not solely to absence of HCN4 as stated by others.[5] We postulate that in *Shox2*^{-/-} hearts, due to aberrant anlage of the PHF, the majority of the solid node is absent. Therefore, pacemaking in *Shox2*^{-/-} hearts might occur in a lower SAN region (i.e. tail), which may explain the slower heart rate since under physiological circumstances this area renders slower pacemaking properties as compared to the solid nodal area of the SAN.[28] A second explanation might of course be the aberrant differentiation of the SAN in *Shox2*^{-/-} showing up-regulation of Nkx2.5, Cx40, Cx43,[4] Nppa and down-regulation of Tbx3.[5] The latter one has shown to be important for maintaining a SAN gene differentiation program during development.[22,23] Normally, markers like Cx40 and Cx43 are weakly expressed or absent in the SAN[31] to prevent the SAN from the inhibitory hyperpolarizing influences of the surrounding atrial myocardium.[32] Although arrhythmias related to abnormal expression of these markers has been described in patients,[33,34] isolated up-regulation in the SAN and aberrant pacemaking has not yet been documented.

Shox2 and epicardial development

The epicardium covers the outer layer of the heart and derives from the PEO, which is located in the area of the developing sinus venosus.[11] Studies in mouse embryos have shown that the formation of the PEO occurs around 9.5 dpc. As from that moment *Wt1* positive epicardial cells start to migrate over the complete surface of the embryonic heart. Subsequently, EMT of the epicardium gives rise to the so-called EPDCs which temporarily express *Wt1*.[17] EPDCs then invade the myocardium contributing to several essential processes of heart development.[10,11,24]

Mechanical manipulation of the PEO in chick / quail embryos results in several cardiac malformations related to an abrogated epicardial spreading and EPDC formation, such as

myocardial non-compaction and abnormal development of the coronary arteries, the Purkinje system and AV valves.[14,15,35] Furthermore, a disturbed AV isolation is observed resulting in high numbers of accessory AV myocardial connections causing pre-mature electrical activation of the ventricles.[15,16] Moreover, the epicardium has an important role in stimulation of myocardial proliferation in the developing ventricles by secretion of several myotrophic factors.[36] Therefore, we postulate that the ventricular abnormalities observed in *Shox2*^{-/-} i.e. thin myocardium, abnormal ventricular trabecularization and right ventricular dilatation and dislocation are related to abnormal epicardial development. Due to a decreased PEO size less epicardial cells spread over the surface of the developing *Shox2*^{-/-} heart. Subsequently, a hampered EMT process will lead to a reduced amount of EPDCs in these hearts causing the ventricular abnormalities that were observed.

Recently we demonstrated in *podoplanin*[10] and *Pdgfrα*[24] mutants a disturbed epicardial lineage development. Interestingly, more or less identical to the *Shox2* gene, *podoplanin* and *Pdgfrα* also have an essential role in development of the PHF derived sinus venosus myocardium. Therefore, we postulated that the PHF contributes to formation of both the sinus venosus myocardium and the PEO,[10] since the coelomic epithelium contributes mesenchyme to the PEO[12,13,37] as well as the PHF-derived structures at the venous pole of the heart.[1,2]
The disturbed epicardial development observed in *Pdgfrα* as well as *podoplanin* knockouts highly correspond to that observed in *Shox2* mutants. However, the *Pdgfrα* and *podoplanin* mutants not only showed decreased numbers of EPDCs and a decreased PEO size, but also hampered epicardial adhesion and spreading.[10,24] The epicardial abnormalities may be related to the specific role that these genes have in the EMT process. Unlike the expression pattern of *Shox2*, both *podoplanin* and *Pdgfrα* are also present in the complete epicardial layer covering the heart suggesting a local involvement in EMT. Interestingly, for *Pdgfrα* a functional link in regulation of *Wt1* expression has recently been demonstrated.[24] *Wt1*, expressed in the epicardium and EPDCs,[17] is known to regulate expression of several important factors in EMT like Snail and the cell-to-cell adhesion protein E-cadherin.[38] Moreover, *podoplanin* mutants showed an aberrant up-regulation of E-cadherin, which was postulated to be the underlying mechanism of the epicardial abnormalities in that particular mouse model.[10] Thus far, similar mechanisms have not been identified in *Shox2* mutants.

CONCLUSION

The current study confirms the hypoplasia and aberrant differentiation of the PHF derived sinus venosus myocardium in *Shox2*^{-/-} embryos of 12.5 dpc. We show that knocking out the *Shox2* gene causes sinus bradycardia despite the persistence of the pacemaker channel HCN4

in the hypoplastic SAN. Furthermore, we for the first time showed that *Shox2* has an important role in epicardial lineage development. Our results support the hypothesis that the sinus venous myocardium and the PEO derive from a common pool of progenitor cells (i.e. the PHF), since *Shox2* mutants show defects of the venous pole as well as the epicardium. Finally, the current study also sheds new light on the etiology of the early embryonic death observed in *Shox2* mutants. We suggest that two mechanisms are involved: (1) disturbed cardiac pacemaking due to abnormal anlage and differentiation of the SAN and (2) abnormal ventricular maturation caused by abnormal epicardial lineage development, which results in ventricular dysfunction.

FUNDING SOURCES

REFERENCES

1. Cai CL, Liang X, Shi Y, Chu PH, Pfaff SL, Chen J, Evans S. Isl1 identifies a cardiac progenitor population that proliferates prior to differentiation and contributes a majority of cells to the heart. *Dev Cell*. 2003;5:877-889.
2. Gittenberger-de Groot AC, Mahtab EA, Hahurij ND, Wisse LJ, Deruiter MC, Wijffels MC, Poelmann RE. Nkx2.5-negative myocardium of the posterior heart field and its correlation with podoplanin expression in cells from the developing cardiac pacemaking and conduction system. *Anat Rec (Hoboken)*. 2007;290:115-122.
3. Christoffels VM, Mommersteeg MT, Trowe MO, Prall OW, Gier-de Vries C, Soufan AT, Bussen M, Schuster-Gossler K, Harvey RP, Moorman AF, Kispert A. Formation of the Venous Pole of the Heart From an Nkx2-5-Negative Precursor Population Requires Tbx18. *Circ Res*. 2006;98:1555-1563.
4. Blaschke RJ, Hahurij ND, Kuijper S, Just S, Wisse LJ, Deissler K, Maxelon T, Anastassiadis K, Spitzer J, Hardt SE, Scholer H, Feitsma H, Rottbauer W, Blum M, Meijlink F, Rappold G, Gittenberger-de Groot AC. Targeted mutation reveals essential functions of the homeodomain transcription factor Shox2 in sinoatrial and pacemaking development. *Circulation*. 2007;115:1830-1838.
5. Espinoza-Lewis RA, Yu L, He F, Liu H, Tang R, Shi J, Sun X, Martin JF, Wang D, Yang J, Chen Y. Shox2 is essential for the differentiation of cardiac pacemaker cells by repressing Nkx2-5. *Dev Biol*. 2009;327:376-385.
6. Stieber J, Herrmann S, Feil S, Loster J, Feil R, Biel M, Hofmann F, Ludwig A. The hyperpolarization-activated channel HCN4 is required for the generation of pacemaker action potentials in the embryonic heart. *Proc Natl Acad Sci U S A*. 2003;100:15235-15240.
7. Nof E, Luria D, Brass D, Marek D, Lahat H, Reznik-Wolf H, Pras E, Dascal N, Eldar M, Glikson M. Point mutation in the HCN4 cardiac ion channel pore affecting synthesis, trafficking, and functional expression is associated with familial asymptomatic sinus bradycardia. *Circulation*. 2007;116:463-470.
8. Milanesi R, Baruscotti M, Gnecchi-Ruscone T, DiFrancesco D. Familial sinus bradycardia associated with a mutation in the cardiac pacemaker channel. *N Engl J Med*. 2006;354:151-157.
9. Mommersteeg MT, Hoogaars WM, Prall OW, de Gier-de Vries C, Wiese C, Clout DE, Papaioannou VE, Brown NA, Harvey RP, Moorman AF, Christoffels VM. Molecular pathway for the localized formation of the sinoatrial node. *Circ Res*. 2007;100:354-362.

10. Mahtab EA, Wijffels MC, Van Den Akker NM, Hahurij ND, Lie-Venema H, Wisse LJ, Deruiter MC, Uhrin P, Zaujec J, Binder BR, Schalij MJ, Poelmann RE, Gittenberger-de Groot AC. Cardiac malformations and myocardial abnormalities in podoplanin knockout mouse embryos: Correlation with abnormal epicardial development. *Dev Dyn*. 2008;237:847-857.

11. Lie-Venema H, Van Den Akker NM, Bax NA, Winter EM, Maas S, Kekarainen T, Hoeben RC, Deruiter MC, Poelmann RE, Gittenberger-de Groot AC. Origin, fate, and function of epicardium-derived cells (EPDCs) in normal and abnormal cardiac development. *ScientificWorldJournal*. 2007;7:1777-1798.

12. van Wijk B, van den Berg G, Abu-Issa R, Barnett P, van der Velden S, Schmidt M, Ruijter JM, Kirby ML, Moorman AF, Van Den Hoff MJ. Epicardium and myocardium separate from a common precursor pool by crosstalk between bone morphogenetic protein- and fibroblast growth factor-signaling pathways. *Circ Res*. 2009;105:431-441.

13. Mommersteeg MT, Dominguez JN, Wiese C, Norden J, de Gier-de Vries C, Burch JB, Kispert A, Brown NA, Moorman AF, Christoffels VM. The sinus venosus progenitors separate and diversify from the first and second heart fields early in development. *Cardiovasc Res*. 2010;87:92-101.

14. Eralp I, Lie-Venema H, Bax NA, Wijffels MC, van der Laarse A, Deruiter MC, Bogers AJ, Van Den Akker NM, Gourdie RG, Schalij MJ, Poelmann RE, Gittenberger-de Groot AC. Epicardium-derived cells are important for correct development of the Purkinje fibers in the avian heart. *Anat Rec A Discov Mol Cell Evol Biol*. 2006;288:1272-1280.

15. Lie-Venema H, Eralp I, Markwald RR, Van Den Akker NM, Wijffels MC, Kolditz DP, van der Laarse A, Schalij MJ, Poelmann RE, Bogers AJ, Gittenberger-de Groot AC. Periostin expression by epicardium-derived cells is involved in the development of the atrioventricular valves and fibrous heart skeleton. *Differentiation*. 2008;76:809-819.

16. Kolditz DP, Wijffels MC, Blom NA, van der Laarse A, Hahurij ND, Lie-Venema H, Markwald RR, Poelmann RE, Schalij MJ, Gittenberger-de Groot AC. Epicardium-derived cells in development of annulus fibrosus and persistence of accessory pathways. *Circulation*. 2008;117:1508-1517.

17. Moore AW, McInnes L, Kreidberg J, Hastie ND, Schedl A. YAC complementation shows a requirement for Wt1 in the development of epicardium, adrenal gland and throughout nephrogenesis. *Development*. 1999;126:1845-1857.

18. Mahtab EA, Vicente-Steijn R, Hahurij ND, Jongbloed MR, Wisse LJ, Deruiter MC, Uhrin P, Zaujec J, Binder BR, Schalij MJ, Poelmann RE, Gittenberger-de Groot AC. Podoplanin deficient mice show a rhoa-related hypoplasia of the sinus venosus myocardium including the sinoatrial node. *Dev Dyn*. 2009;238:183-193.

19. Jongbloed MR, Wijffels MC, Schalij MJ, Blom NA, Poelmann RE, van der Laarse A, Mentink MM, Wang Z, Fishman GI, Gittenberger-de Groot AC. Development of the right ventricular inflow tract and moderator band: a possible morphological and functional explanation for Mahaim tachycardia. *Circ Res*. 2005;96:776-783.

20. Sun Y, Liang X, Najafi N, Cass M, Lin L, Cai CL, Chen J, Evans SM. Islet 1 is expressed in distinct cardiovascular lineages, including pacemaker and coronary vascular cells. *Dev Biol*. 2007;304:286-296.

21. Christoffels VM, Mommersteeg MT, Trowe MO, Prall OW, de Gier-de Vries C, Soufan AT, Bussen M, Schuster-Gossler K, Harvey RP, Moorman AF, Kispert A. Formation of the venous pole of the heart from an Nkx2-5-negative precursor population requires Tbx18. *Circ Res*. 2006;98:1555-1563.

22. Wiese C, Grieskamp T, Airik R, Mommersteeg MT, Gardiwal A, de Gier-de Vries C, Schuster-Gossler K, Moorman AF, Kispert A, Christoffels VM. Formation of the sinus node head and differentiation of sinus node myocardium are independently regulated by Tbx18 and Tbx3. *Circ Res*. 2009;104:388-397.

23. Hoogaars WM, Engel A, Brons JF, Verkerk AO, de Lange FJ, Wong LY, Bakker ML, Clout DE, Wakker V, Barnett P, Ravesloot JH, Moorman AF, Verheijck EE, Christoffels VM. Tbx3 controls the sinoatrial node gene program and imposes pacemaker function on the atria. *Genes Dev*. 2007;21:1098-1112.

24. Bax NA, Bleyl SB, Gallini R, Wisse LJ, Hunter J, Van Oorschot AA, Mahtab EA, Lie-Venema H, Goumans MJ, Betsholtz C, Gittenberger-de Groot AC. Cardiac malformations in Pdgfralpha mutant embryos are associated with increased expression of WT1 and Nkx2.5 in the second heart field. *Dev Dyn*. 2010;239:2307-2317.

25. Yanni J, Boyett MR, Anderson RH, Dobrzynski H. The extent of the specialized atrioventricular ring tissues. *Heart Rhythm*. 2009;6:672-680.

26. Viragh S, Challice CE. The development of the conduction system in the mouse embryo heart. *Dev Biol*. 1980;80:28-45.

27. Liu J, Dobrzynski H, Yanni J, Boyett MR, Lei M. Organisation of the mouse sinoatrial node: structure and expression of HCN channels. *Cardiovasc Res*. 2007;73:729-738.

28. Boineau JP, Schuessler RB, Roeske WR, Autry LJ, Miller CB, Wylds AC. Quantitative relation between sites of atrial impulse origin and cycle length. *Am J Physiol*. 1983;245:781-789.

29. Boineau JP, Canavan TE, Schuessler RB, Cain ME, Corr PB, Cox JL. Demonstration of a widely distributed atrial pacemaker complex in the human heart. *Circulation*. 1988;77:1221-1237.

30. Schuessler RB, Boineau JP, Bromberg BI. Origin of the sinus impulse. *J Cardiovasc Electrophysiol*. 1996;7:263-274.

31. Miquerol L, Dupays L, Theveniau-Ruissy M, Alcolea S, Jarry-Guichard T, Abran P, Gros D. Gap junctional connexins in the developing mouse cardiac conduction system. *Novartis Found Symp*. 2003;250:80-98.

32. Boyett MR, Inada S, Yoo S, Li J, Liu J, Tellez J, Greener ID, Honjo H, Billeter R, Lei M, Zhang H, Efimov IR, Dobrzynski H. Connexins in the sinoatrial and atrioventricular nodes. *Adv Cardiol*. 2006;42:175-197.

33. Schott JJ, Benson DW, Basson CT, Pease W, Silberbach GM, Moak JP, Maron BJ, Seidman CE, Seidman JG. Congenital heart disease caused by mutations in the transcription factor NKX2-5. *Science*. 1998;281:108-111.

34. Gollob MH. Begetting atrial fibrillation: Connexins and arrhythmogenesis. *Heart Rhythm*. 2008;5:888-891.

35. Eralp I, Lie-Venema H, Deruiter MC, Van Den Akker NM, Bogers AJ, Mentink MM, Poelmann RE, Gittenberger-de Groot AC. Coronary artery and orifice development is associated with proper timing of epicardial outgrowth and correlated Fas-ligand-associated apoptosis patterns. *Circ Res*. 2005;96:526-534.

36. Stuckmann I, Evans S, Lassar AB. Erythropoietin and retinoic acid, secreted from the epicardium, are required for cardiac myocyte proliferation. *Dev Biol*. 2003;255:334-349.

37. Kruithof BP, van WB, Somi S, Kruithof-de JM, Perez Pomares JM, Weesie F, Wessels A, Moorman AF, Van Den Hoff MJ. BMP and FGF regulate the differentiation of multipotential pericardial mesoderm into the myocardial or epicardial lineage. *Dev Biol*. 2006;295:507-522.

38. Martinez-Estrada OM, Lettice LA, Essafi A, Guadix JA, Slight J, Velecela V, Hall E, Reichmann J, Devenney PS, Hohenstein P, Hosen N, Hill RE, Munoz-Chapuli R, Hastie ND. Wt1 is required for cardiovascular progenitor cell formation through transcriptional control of Snail and E-cadherin. *Nat Genet*. 2010;42:89-93.

3

EXPANDED MATERIAL AND METHODS

Electrophysiology recording protocol

The embryonic hearts were attached with fine wires through extra-cardiac tissue in a fluid heated, temperature controlled (Physitemp instruments Inc, Clifton NJ, USA) petridish of 35.5-37˚Celsius onto a layer of agarose gel (Roche Diagnostics GmbH, Mannheim, Germany). During the equilibration period of 3 minutes and the subsequent electrophysiological recordings the hearts were constantly super-perfused with Carbogenated (95% O_2 and 5% CO_2) Tyrode's solution containing (in mmol/l) 130 NaCl, 4 KCl, 1,2 KH_2PO_4, 0,6 $MgSO_4 7H_2O$, 20 $NaHCO_3$, 1,5 $CaCl_2 2H_2O$ and 10 glucose of 37˚Celsius.

For electrophysiological extracellular recordings 4 unipolar tungsten electrodes (tip: 1-2µm; impedance 0.9-1.0MΩ; WPI Inc, Sarasota FL, USA) were placed on the right atrium (RA), right ventricular base (RVB), left ventricular base (LVB) and left ventricular apex (LVA) using microscopic guided micromanipulators (Wild Heerbrugg, M7A, Switzerland). Furthermore, an Ag/AgCl electrode in the Petri dish served as reference electrode. The complete experimental setting was located in a Faraday cage to prevent the recordings from exterior electrophysiological disturbances.

All electrograms were recorded with a high-gain, low-noise, direct-current bioamplifier system (Iso-DAM8A; WPI Inc) with 4 isolated preamplifier modules with an output impedance of >10^{12}Ω. The signals were band-pass (300Hz-1kHz) and notch filtered (50Hz) before being digitized at a sample rate of 1≥kHz with a computerized recording system (Prucka Engineering Inc, Houston, Tex) and stored on optical disks for offline analysis.

All electrophysiological recordings were performed under stable sinus rhythm after a 3 minute calibration period. The basal cycle length/HR of each heart was calculated by the average of 10 consecutive beats. The AV conduction time is defined as the time interval between atrial activation and the first ventricular activation either at the LVA or at the LVB / RVB.

After EP recording all hearts were fixed in 4% paraformaldehyde for immunohistochemical processing.

Adriana C. Gittenberger-de Groot[1]
Edris A.F. Mahtab[1]
Nathan D. Hahurij[1]
Lambertus J. Wisse[1]
Marco C. DeRuiter[1]
Maurits C.E.F. Wijffels[2]
Robert E. Poelmann[1]

[1] Department of Anatomy & Embryology, Leiden University Medical Center, Leiden, The Netherlands.
[2] Department of Cardiology, Leiden University Medical Center, Leiden, The Netherlands.

4

Nkx2.5 negative myocardium of the posterior heart field and its correlation with podoplanin expression in cells from the developing cardiac pacemaking and conduction system

ABSTRACT

Recent advances in the study of cardiac development have shown the relevance of addition of myocardium to the primary myocardial heart tube. In wildtype mouse embryos (9.5-15.5 days post conception) we have studied the myocardium at the venous pole of the heart using immunohistochemistry and 3D reconstructions of expression patterns of MLC-2a, Nkx2.5 and podoplanin, a novel coelomic and myocardial marker. Podoplanin positive coelomic epithelium was continuous with adjacent podoplanin and MLC-2a positive myocardium that formed a conspicuous band along the left cardinal vein extending through the base of the atrial septum to the posterior myocardium of the atrioventricular canal, the atrioventricular nodal region and the His-Purkinje system. Later on podoplanin expression was also found in the myocardium surrounding the pulmonary vein. On the right side podoplanin positive cells were seen along the right cardinal vein, which during development persisted in the sinoatrial node and part of the venous valves. In the MLC-2a and podoplanin positive myocardium Nkx2.5 expression was absent in the sinoatrial node and the wall of the cardinal veins. There was a mosaic positivity in the wall of the common pulmonary vein and the atrioventricular conduction system as opposed to the overall Nkx2.5 expression seen in the chamber myocardium. We conclude that we have found podoplanin as a marker that links a novel Nkx2.5 negative sinus venosus myocardial area, which we refer to as the posterior heart field, with the cardiac conduction system.

INTRODUCTION

In early cardiac development the myocardium of the heart tube develops from two bilateral cardiogenic plates (primary heart field) that fuse to a common primary heart tube.[1,2] The earlier observations by cell marker research in chicken embryos of De La Cruz[3] that myocardium is added to this primary heart field, is now supported by several studies that in most cases refer to addition of myocardium at the outflow tract of the heart, being from the anterior[4] or secondary[5] heart field. Newly recruited myocardium is not only added at the outflow tract but also at the inflow tract. This myocardium is derived from the splanchnic mesoderm running from the arterial pole (outflow tract) to the venous pole (inflow tract) which is also referred to as second heart field,[6] or second lineage.[6,7] Recently a number of genes / proteins, considered as early markers of the second lineage, have been reported, such as fibroblast growth factor 8 and 10,[8] Isl1,[6] inhibitor of differentiation Id2,[9] GATA factors targeting Mef2c[10,11] and Tbx1 and Tbx18.[12,13]

Terminology in this rapidly evolving area of recruitment of new myocardium is still somewhat confusing as most cell differentiation markers and sometimes there lineage tracing have different spatio-temporal boundaries.

From 9.5 days post conception (dpc) onwards we have become particularly interested in recruitment of myocardium at the venous pole, which we refer to by the new positional term: posterior heart field (PHF), as an addition to the anterior heart field at the outflow tract. We have discovered that a novel gene in heart development, called *podoplanin*, not only demarcates a specific area of myocardium at the sinus venosus of the heart, but is also expressed in major parts of the cardiac conduction system (CCS). In the differentiation of the CCS a number of markers have already been reported that are expressed in the sinoatrial and atrioventricular conduction system such as HNK1 and Leu7,[14-16] PSA-NCAM,[17] Msx2[18] and the reporter genes CCS-*LacZ*,[19-21] *MinK*,[22] *Tbx3*[23] and cardiomyocytes – antigens.[24] Very recently a Mesp-1 non-expressing myocardial population was reported in the ventricular conduction system.[25] All these studies, however, concentrate on the differentiation of the CCS myocardium as opposed to the chamber myocardium and do not, as is suggested by our present findings, provide a link with the recruitment of second lineage myocardium.

Podoplanin is a 43-kd mucin type transmembrane glycoprotein,[26] which has not been described during heart development. It was first called E11 antigen by Wetterwald as a new marker for an osteoblastic cell line. The protein is also found in other cell types including the nervous system, the epithelia of the lung, eye, oesophagus and intestine,[27] the mesothelium of the visceral peritoneum[26] and podocytes in the kidney.[28] Furthermore, it has recently been investigated as a marker for lymphatic endothelium.[29]

Our study of podoplanin expression in the developing myocardium of the PHF is combined with a novel finding regarding *Nkx2.5*, which is an early marker of cardiac progenitor cells[30] and demarcates the cardiac field[31] in concert with GATA-4/5/6.[32] *Nkx2.5* is also shown to be essential for normal differentiation and function of the CCS in both human[33] and mouse studies.[34]

In this study we will describe development of novel sinus venosus myocardium, in close correlation with the mesothelial lining of the pericardio-peritoneal coelomic cavity that is demarcated by positive podoplanin expression and Nkx2.5 non-expression. The podoplanin expression in the CCS provides a possible link between this novel myocardium from the PHF with the development of the sinoatrial node and other parts of the CCS.

MATERIAL AND METHODS

We studied the lining of the thoracic cavity and heart in wildtype mouse embryos of 9.5 dpc (n=8), 10.5 dpc (n=8), 11.5 dpc (n=7), 12.5 dpc (n=8), 13.5 dpc (n=8), 14.5 dpc (n=9) and 15.5 dpc (n=2). The embryos were fixed in 4% paraformaldehyde (PFA) and routinely processed for paraffin immunohistochemical investigation. The 5 μm transverse sections were mounted onto egg-white / glycerin coated glass slides in a 1 to 5 order, so that 5 different stainings from subsequent sections could be compared.

Immunohistochemistry

After rehydration of the slides, inhibition of endogenous peroxidase was performed with a solution of 0.3% H_2O_2 in PBS for 20 min. The slides were incubated overnight with the following primary antibodies: 1/2000 anti-atrial myosin light chain 2 (MLC-2a, which was kindly provided by S.W. Kubalak, Charleston, SC, USA), 1/4000 anti-human Nkx2.5 (Santa Cruz Biotechnology, Inc.,CA, USA) and 1/1000 anti-podoplanin (clone 8.1.1. Hybridomabank, Iowa, USA). All primary antibodies were dissolved in PBS-Tween-20 with 1% Bovine Serum Albumin (BSA, Sigma Aldrich, USA). Between subsequent incubation steps all slides were rinsed as follows: PBS (2x) and PBS-Tween-20 (1x). The slides were incubated with secondary antibodies for 40 min: for MLC-2a 1/200 goat-anti-rabbit-biotin (Vector Laboratories, USA, BA-1000) and 1/66 goat serum (Vector Laboratories, USA, S1000) in PBS-Tween-20; for Nkx2.5 1/200 horse-anti-goat-biotin (Vector Laboratories, USA, BA-9500) and 1/66 horse serum (Brunschwig Chemie, Switserland, S-2000) in PBS-Tween-20; for podoplanin 1/200 goat-anti-Syrian hamster-biotin (Jackson Imunno research, USA, 107-065-142) with 1/66 goat serum (Vector Laboratories, USA, S1000) in PBS-Tween-20. Subsequently, all slides were incubated with ABC-reagent (Vector Laboratories,USA, PK 6100) for 40 min. For visualisation, the slides were incubated with 400 μg/ml 3-3'di-aminobenzidin tetrahydrochloride (DAB, Sigma-Aldrich Chemie, USA, D5637) dissolved in Tris-maleate buffer pH7.6 to which 20 μl H_2O_2 was added: MLC-2a 5 min; Nkx2.5 and podoplanin 10 min. Counterstaining was performed with 0.1% haematoxylin (Merck, Darmstadt, Germany) for 10 sec, followed by rinsing with tap water for 10 min. Finally, all slides were dehydrated and mounted with Entellan (Merck, Darmstadt, Germany).

3D reconstructions

We made 3D reconstructions of the atrial and ventricular myocardium of MLC-2a stained sections of 11.5 dpc and 13.5 dpc embryos in which podoplanin positive and Nkx2.5 negative myocardium from adjacent sections were manually superimposed to show overlapping areas. The reconstructions were made as described earlier[20] using the AMIRA software package (Template Graphics Software, San Diego, USA).

RESULTS

Below we will describe the expression patterns of MLC-2a, podoplanin and Nkx2.5 in the PHF in several subsequent stages of heart development (9.5-15.5 dpc), while in Figures 1-3 typical examples and 3D reconstructions of the expression patterns of these proteins are provided.

Stage 9.5 dpc

At this stage the heart is still in the looping phase and the boundaries of the primary heart tube can easily be demarcated by immunohistochemistry. The MLC-2a and Nkx2.5 staining of the myocardium stops at the transition with the negatively stained coelomic epithelium at the dorsal mesocardium. This squamous coelomic epithelium is part of the lining of the pericardio-peritoneal cavities, which are laterally flanked by the cardinal veins. Podoplanin is slightly positive at the left side and negative at the right side on the medial border of the cardinal veins wall. There is no podoplanin staining discernable at other sides at this stage yet.

Stages 10.5 dpc and 11.5 dpc

Serial MLC-2a stained sections have been reconstructed to form a 3D image. Figures 1a and 1b show the dorsal face of the heart in which the various staining patterns are depicted. The line in Figure 1a shows the level of the sections depicted in c-k. Septation of the ventricular inlet and atrium has started. On the right side the venous valves are already recognizable (Figure 1c). Podoplanin expression is observed in the coelomic lining and in the mesenchyme adjoining the medial wall of the left superior cardinal vein (Figure 1b and k) with light staining alongside the right superior cardinal vein at the position of the developing right sinoatrial node (Figure 1b, i and j). The left sided expression envelops the sinus venosus confluence of the cardinal veins (Figure 1b) and extends in the myocardium to the posterior region of the atrioventricular canal (Figure 1i and k), which is the site of the future atrioventricular node. The podoplanin positive mesenchyme is differentiating into myocardium as indicated by the overlapping expression with MLC-2a (compare Figure 1a and c-e with 1b and i-k). These overlapping areas are Nkx2.5 negative in contrast to the marked Nkx2.5 staining in the MLC-2a positive myocardium of the atria and the ventricles (Figure 1a and f-h).

Stages 12.5 dpc and 13.5 dpc

The 3D reconstruction of MLC-2a stained sections from an 13.5 dpc embryonic heart (dorsal face shown) are depicted in Figures 2a and 2b. The cardiac chambers are now clearly discernable. As expected the MLC-2a is more markedly expressed in the atrial and sinus venosus myocardium than in the ventricular myocardium (Figure 2c and e). The coelomic cavity is separated in pleural and pericardial cavities.
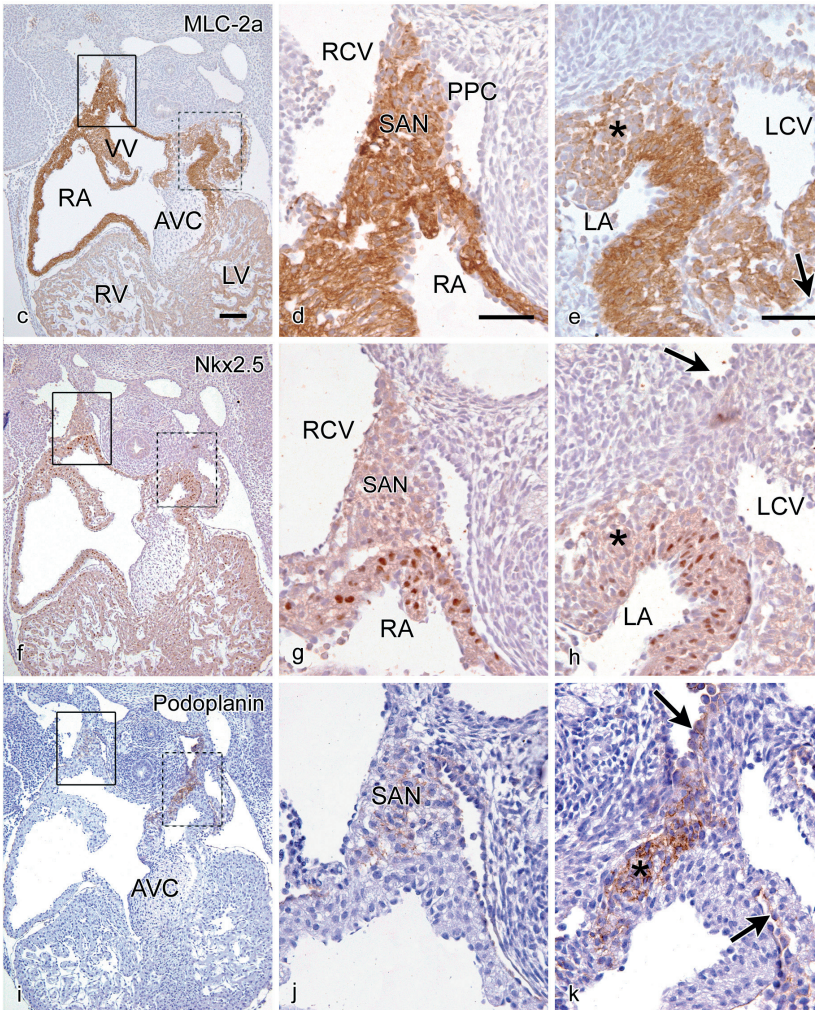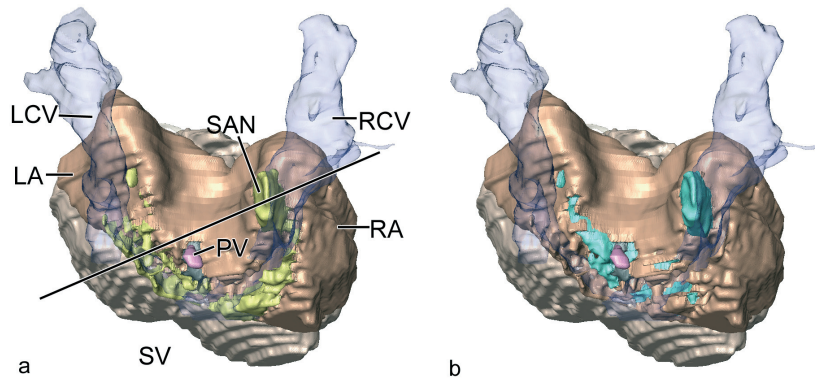
At the venous pole we now discern marked podoplanin expression in the myocardium of the developing right sided sinoatrial node and the patchy staining in the venous valves, while the adjoining atrial myocardium is podoplanin negative (Figure 2k and l). The sinoatrial nodal myocardium is still in close contact with the adjacent markedly podoplanin positive coelomic lining (Figure 2k and l). Bordering the left cardinal vein a similar podoplanin positive cell cluster is seen, as well as podoplanin positive myocardial strands running along the posterior left atrial wall that merge with the myocardial cells of the common pulmonary vein (Figure 2m and n). The continuity of these strands is obvious with patches of cuboidal podoplanin positive cells, as opposed to squamous podoplanin positive epithelial cells, lining both the pleural (Figure 2k-n) and pericardial cavity (Figure 2k-n). Both left and right sided podoplanin positive cell clusters as well as the myocardium of the wall of both cardinal veins are positive for MLC-2a although the staining is somewhat less intense compared to the main body of the atrial wall (Figure 2c-f).

The expression of Nkx2.5 (Figure 2a and g-j) does not overlap completely with the MLC-2a or the podoplanin staining. Nkx2.5 is negative in the right sinoatrial node, the posterior cell cluster between the left cardinal vein and the pulmonary vein and in the wall of the right and left cardinal veins (Figure 2g-j). A podoplanin and MLC-2a positive myocardial cell strand extends from the left side of the sinus venosus and stretches by way of the dorsal mesocardium and the spina vestibulum deep into the crux of the heart (Figure 2e, i and m). The staining encircles the orifice of the left cardinal vein, which opens into the right atrial cavity (not shown). This myocardial strand extends through the basis of the atrial septum to the position of the atrioventricular node and can be followed to the common bundle (Figure 2e, i and m), bundle branches (Figure 3a-d), the moderator band and the Purkinje system (not shown). Up to the level of the bundle branches this strand shows a mosaic Nkx2.5 staining which is

Figure 1. Dorsal view of a reconstruction (a, b) of an 11.5 dpc wildtype mouse heart of the myocardium stained with MLC-2a (atria brown and ventricles grey). In (a) the Nkx2.5 negative pattern is added (**lime green**) and (b) shows the podoplanin positive pattern (**turquoise**). The left (**LCV**) and right (**RCV**) cardinal veins and their sinus venosus (**SV**) confluence are **transparent blue**. (c-e): Sections stained with MLC-2a (c: overview and details d: line box and e: dotted box) show marked expression in the myocardium of the wall of the atria (**RA** and **LA**). Also the anlage of the sinoatrial node (**SAN**) and a left sided mesenchymal population (**asterisk** in e) as well as the wall of the LCV show MLC-2a expression. (f-h): Staining in consecutive sections with Nkx2.5 (lime green in reconstruction (a) and overview in (f), with higher magnification in (g) and (h), show a marked expression in the atrial wall (g) and negativity in the mesenchyme (asterisk in h) and the SAN (g). There is no staining in the wall of the LCV. Podoplanin staining is positive in some parts of the coelomic cavities (**arrows** in h and k). This is not shown in the reconstruction (b) where only the overlap of MLC-2a and podoplanin (turquoise) is shown. Podoplanin is more intense at the left side at this stage of development (k) specifically in the pre-myocardial mesenchyme running from the left pericardio-peritoneal canal, caudal of the anlage of the common pulmonary vein (**PV**; **pink** in a and b) through the base of the atrial septum to the posterior part of the atrioventricular canal dorsal of the inferior atrioventricular cushion (**AVC**) (i and k). Scale bars: (c-k) = 100μm.

therefore less marked than the surrounding myocardium (Figure 2i). A mosaic Nkx2.5 staining is also observed in the venous valves (not shown).

At stage 13.5 dpc the common pulmonary vein for the first time is clearly discernable with a myocardial sheath in which podoplanin positive cells are extending (Figure 2m and n).
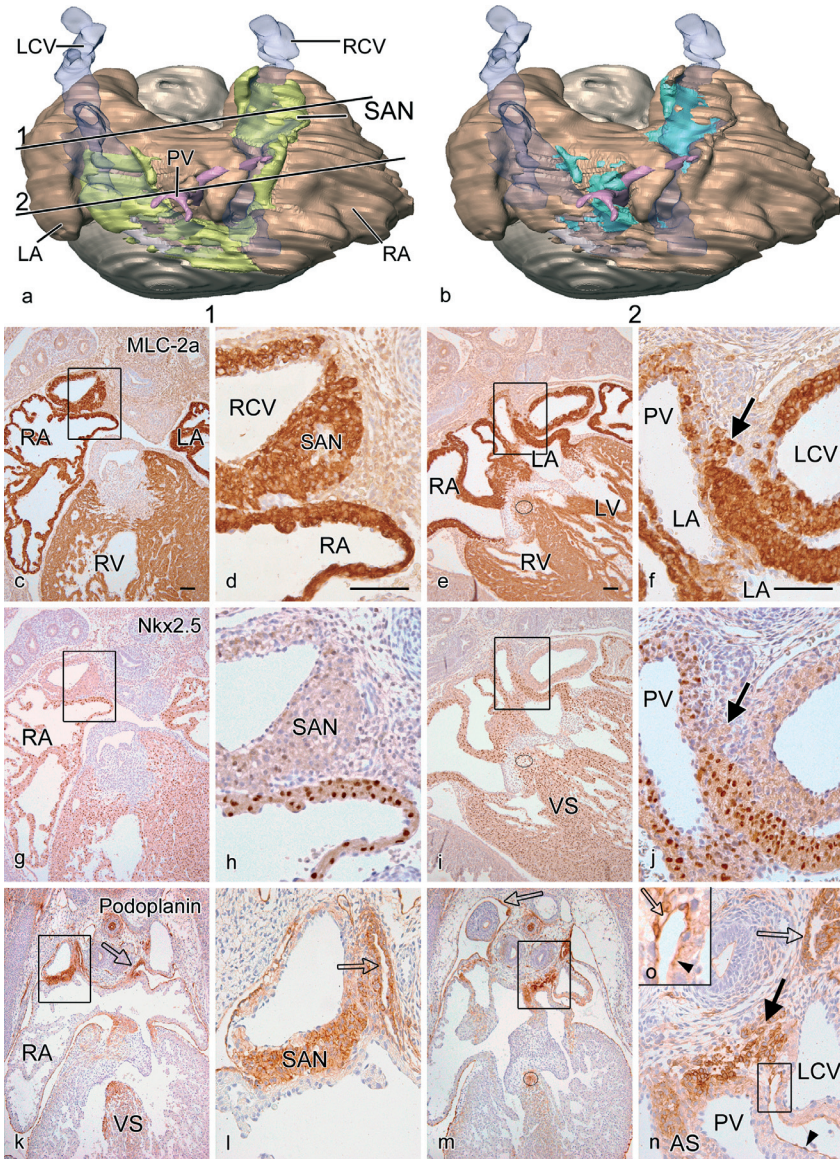
MLC-2a and Nkx2.5 are positive in the pulmonary wall although both are less marked as compared to the adjacent atrial wall (Figure 2f and j). Between the left cardinal vein and the myocardial pulmonary venous wall a small cluster of podoplanin and MLC-2a positive and Nkx2.5 negative myocardial cells is still present (Figure 2f, j and n).

Stages 14.5 dpc and 15.5 dpc

The left sided podoplanin expression in the myocardium is disappearing. The staining is only retained in the right sinoatrial node and it has become more marked in the common and right and left bundle branches (Figure 3e and f).

Figure 2. Dorsal view of a reconstruction (a, b) of an 13.5 dpc wildtype mouse heart of the myocardium stained with MLC-2a (atria brown and ventricles grey). The Nkx2.5 negative region is superimposed in (a), whereas the podoplanin positive region is presented in (b). The left (**LCV**) and right (**RCV**) cardinal veins which have an independent entrance into the right atrium are **transparent blue**. The transsection (1) for the sinoatrial node (**SAN**) and the left sided podoplanin expression and pulmonary vein (**PV** in **pink**) (2) are indicated. (c-f): Sections stained with MLC-2a antibody (c and e: overviews at transsections 1 and 2 and magnifications d and f: boxed areas) show marked expression in the myocardium of the wall the atria (**RA** and **LA**) and somewhat lesser in the right (**RV**) and left (**LV**) ventricle. The LCV in (f), RCV in (d) and the SAN in (d) are positive. A cluster of moderately MLC-2a positive cells (**arrow** in f) is positioned in the mesenchyme between the LCV and PV. Nkx2.5 staining is markedly positive in all major components of the heart. Absence of staining (**lime green** in a) is seen in the wall of the RCV (h), the SAN (g and h), the LCV and the mesenchymal cell cluster (arrow in j). The PV has a less marked Nkx2.5 (mosaic) staining (j). The same accounts for a circular structure situated at the site of the common bundle at the top of the ventricular septum (**VS**) (dotted circle in e, i and m). Podoplanin staining is observed on both right and left sided MLC-2a areas (**turquoise** in b). This encomprises the SAN (k and l) and the left sided cluster between LCV, partly merging with the PV wall (arrow in n) and extending into the base of the atrial septum (**AS**). It is also positive in the common bundle (dotted circle in m) extending over the top of the VS (k). Podoplanin is also positive in the lining of the coelomic cavity. In areas with underlying podoplanin positive myocardial cells the coelomic cells are cuboid (**open arrow** in k-n). In the remaining coelomic lining, like the epicardium (**arrowhead** in n and o) the epithelium is squamous. The coelomic lining is always MLC-2a and Nkx2.5 negative. Scale bars: (c-n) = 100μm.
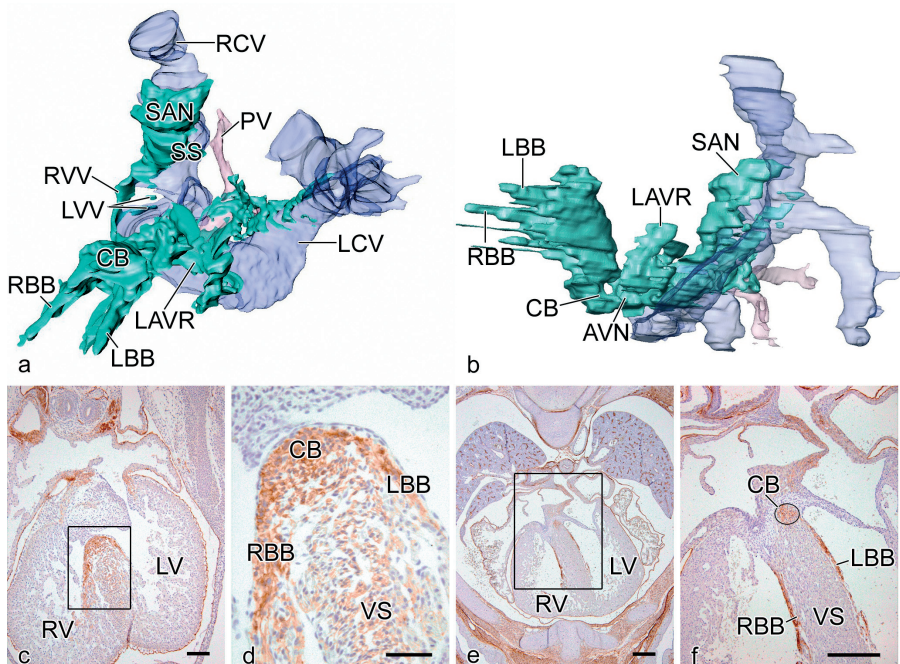
Figure 3. Reconstruction of the podoplanin expression (turquois) depicting the various parts of the myocardium of the conduction system in the same 13.5 dpc embryo depicted in Figure 2a. Left frontal view shows the position of the sinoatrial node (**SAN**) next to the right cardinal vein (**RCV**), the presence in the right (**RVV**) and left (**LVV**) venous valves (b) merges in the region of the atrioventricular node (**AVN**) visible in the left lateral view. The expression is also found in a left atrioventricular ring of myocardium (**LAVR**). The AVN myocardium continues as a common bundle (**CB**) in the right (**RBB**) and left (**LBB**) bundle branches. (c-f): Sections of the thorax and heart of wildtype mouse embryos of 13.5 dpc (c with box magnified in d) and 15.5 dpc (e with box magnified in f) stained for podoplanin which is clearly visible in the common bundle (**CB**) in (c, d, e and dotted circle in f), as well as in the RBB and LBB (e and f) on top of the ventricular septum (**VS**). **PV** indicates Pulmonary vein; **SS**, Septum spurium. Scale bars: (c-f) = 100μm.

DISCUSSION

The contribution of myocardium to the primary heart tube has been acknowledged for many years by tracing cells with marker constructs[3,35] as well as molecularly based tracing techniques using reporter mice.[7,10-12,36] From these studies the addition of myocardium to, in particular the outflow tract, is obvious. Moreover, Kelly[7] described the recruitment of cardiomyocytes from the splanchnic mesoderm to the outflow and inflow tract of the heart as a second myocardial lineage adding to the first lineage. The regulation of continued cardiogenesis at the inflow tract of the heart, which already starts at 8.5 dpc, is far from unravelled and has to fit in the multiple transcriptional domains of i.e. atrial chambers.[37] This process will be complicated if

it is comparable with the situation at the outflow tract in which many genes are involved such as *Isl1*,[6] GATA factors targeting *Mef2c*,[10,11] *Tbx1*,[12] *Tbx4*,[38] *Id2*,[9] and many others including members of the fibroblast growth factor and TGF beta family.[39] Our study adds podoplanin to this list for the PHF, which is most probably a subpopulation of the second lineage.[6,7]

Podoplanin and MLC-2a in the posterior heart field

Podoplanin is expressed in several tissues in the developing embryo but for this study the reported expression in the coelomic lining,[26] the underlying mesenchyme and the myocardium of the CCS is important. Expression in other tissues did not pose problems in interpretation as patterns are well separated in time and space. The coelomic epithelium was clearly activated at specific sites, being irregular and cuboidal which might indicate an ongoing process of epithelial-mesenchymal transformation (EMT). Similar EMT events have been described for the endocardium of the atrioventricular cushions[40,41] as well as epicardium derived cells (EPDCs)[42,43] expressing Wt1;[44-46] and cytokeratin.[47] As a podoplanin reporter mouse has not been developed we cannot unequivocally prove EMT. It is remarkable that the podoplanin expression is retained in the mesenchyme underlying the coelomic epithelium and that we have shown that we are dealing with a myocardial progenitor cell by the overlapping expression with MLC-2a. Although MLC-2a is described to be specific for atrial myocardium,[48] it also stains the myocardium of the sinus venosus and somewhat weaker the ventricular cardiomyocytes. The contribution of novel myocardium to the PHF at the sinus venosus seems to stop after 15.5 dpc as the podoplanin expression diminishes and the coelomic epithelium becomes quiescent resuming a squamous phenotype.

A functional role for podoplanin is still to be found. Data are emerging describing an EMT process of podoplanin dependent downregulation of E-cadherin in invasive and migratory cells of oral mucosal cancer cells.[49] Also an EMT independent process in adult tissues has been described, where podoplanin induces the reorganisation of ezrin-radixin-moesin (ERM) proteins and the actin cytoskeleton via downregulation of RhoA signal, resulting in collective tumor cell migration and conelike invasion.[50] For our study it would support a possible role for podoplanin in migration and invasion of the PHF myocardium into parts of the CCS.

Nkx2.5 expression and the posterior heart field

As a marker for pre-cardiac mesoderm and myocardial cells we also used an antibody against human Nkx2.5.[51,52] We found that the U-shaped PHF myocardium was negative for Nkx2.5. During development this resulted in a Nkx2.5 negative right sided sinoatrial node. In the podoplanin positive venous valves, the base of the atrial septum and the atrioventricular conduction system, there seemed to be a mosaic Nkx2.5 expression as opposed to the overall expression in the atrial and ventricular wall comparable to the heterogeneous pattern of Nkx2.5

expression pattern described previously.[53] The myocardial contribution to the sinus venosus from precursors that are Nkx2.5 negative was also recently described.[13]

The function of *Nkx2.5* in cardiogenesis seems very important but is still far from clear. Different noggin-sensitive *Nkx2.5* enhancers are found in various segments of the heart during development, indicative for chamber-specific functions,[54] whereas cofactors such as GATA-4 are equally important. Furthermore, the differentiation of cardiac Purkinje fibers requires precise spatiotemporal regulation of Nkx2.5 expression,[52] probably in a dose-dependent way.[54] The mechanism of Nkx2.5 regulation is probably dependent on repressor systems for which strong candidates include Tbox family members, such as *Tbx2* and *Tbx5*.[55] Most studies have concentrated on Nkx2.5 in intracardiac patterning and differentiation. The implications of a population of Nkx2.5 negative myocardial cells in the PHF have to be evaluated further, while at least Tbx18 plays a role.[13]

The posterior heart field and development of the cardiac conduction system
Several marker studies have linked sinus venosus myocardium to the development of the cardiac conduction system. These include HNK1 and Leu7,[14-16] PSA-NCAM[17] and more recently the transgenic reporter mice for CCS-*LacZ*[19-21] and *MinK*.[22] Our own studies on HNK1 and Leu7[14-16] provide in general the same pattern for the CCS as now found in our study for podoplanin. The CCS-*LacZ* mouse shows that the complete cardiac conduction system myocardium is positive. CCS-LacZ does not differentiate between Nkx2.5 expressing and non-expressing myocardial cells as the right sinoatrial node is CCS-LacZ positive. Also other reported markers as Tbx3[23] do not reflect the described podoplanin positive PHF myocardium. In this respect the recent elegant reporter gene study of Mesp-1 expressing and non-expressing myocardial cells in the heart is of great interest.[25] These authors show that there is a myocardial heterogeneity in the atrioventricular conduction system. They also show that this does not refer to a neural crest derived population. The latter origin was shown by our group to align with the CCS,[56] although we never found the neural crest cells to attain a myocardial phenotype. The Mesp-1 study does speculate on the origin of the non-expressing Mesp-1 cells but has not traced them to the PHF. There are no data on their contribution to the sinoatrial and atrioventricular node.

In literature there are two main concepts for development of the CCS. The first one provides evidence for an autonomous origin of the central conduction system from cardiomyocytes residing in the primary heart tube.[57] This myocardium retains a primitive phenotype after ballooning of the atrial and ventricular cavities has started. *Tbx2* and *Tbx3*, and *ANF* are important genes guiding this process.[58] In this concept the atrioventricular node derives from the primitive myocardium of the atrioventricular canal. The origin of the cells of the conduction

system and specifically the atrioventricular node is still under debate. It seems evident that part of the posterior atrioventricular node originates from the myocardium[59] of the primary heart tube. Our current findings, supported by the Mesp-1 study do not exclude a contribution of myocardium from the PHF to the CCS, which is further strengthened by the extensive clonal cell tracing study of the Buckingham group.[60]

The second concept on conduction system differentiation works along local differentiation pathways of the myocardium of the heart tube[61] by induction and signaling. This concept is more in line with our data on secondary differentiation of the conduction system in which both EPDCs[62] and neural crest cells[63] might play the inductive role. It does not exclude secondary sources of myocardium, which in part correlate with migration pathways of EPDCs and neural crest cells.

The posterior heart field and functional clinical implications

Our data show an early and transient left sided counterpart of the sinoatrial node. In the early embryonic heart using voltage-sensitive dye, the pacemaking activity has initially been located to originate at the left side,[64] which would fit with our observations. It also supports the reports on the anlage of a left sinoatrial node, which is found as an anomaly in left atrial isomerism.[65] A possible role for podoplanin in the electrophysiology of CCS still has to be investigated. It has been reported, however, to be essential for water transport,[27] Ca dependent cell adhesiveness[49] and cationic, anionic and amino acid transport.[66] These aspects might be linked to cellular communications important for cardiac conduction.

Mutations of the *Nkx2.5* gene in human patients lead to conduction system disturbances and atrial septal defects.[33,67] Comparable to these mutations in human patients is the *Nkx2.5* haploinsufficiency in mice embryos. The effects of *Nkx2.5* haploinsufficiency, described above, are weaker in mice but convergent with those in human.[68] Our study provides a new insight in that Nkx2.5 negative PHF myocardium is continuously added to the already Nkx2.5 positive myocardium of the primary heart tube. We show that PHF myocardium forms the sinoatrial node, which is Nkx2.5 negative. PHF myocardium might also add cells through the base of the atrial septum to the region of the atrioventricular conduction system and to the venous valves, which play a role in development of the conduction system[20] as well as in the formation of the atrial septum.[69] In this way atrial septal defects[33] found in *Nkx2.5* human mutation patients may relate to a deficient contribution from the PHF myocardium to the venous valves. Most studies are dealing with *Nkx2.5* mutations with ensuing underexpression. In an overexpression study, which would influence the Nkx2.5 negative sinoatrial node, defects in pacemaker activity with bradycardia have been described.[34] In conclusion the temporo-spatial information in this study on the late contribution of Nkx2.5 negative as well as positive myocardium might explain the cardiac abnormalities found in the human population.[67]

ACKOWLEDGEMETS

REFERENCES

1. Deruiter MC, Poelmann RE, VanderPlas-de V, I, Mentink MM, Gittenberger-de Groot AC. The development of the myocardium and endocardium in mouse embryos. Fusion of two heart tubes? *Anat Embryol (Berl)*. 1992;185:461-473.
2. Moreno-Rodriguez RA, Krug EL, Reyes L, Villavicencio L, Mjaatvedt CH, Markwald RR. Bidirectional fusion of the heart-forming fields in the developing chick embryo. *Dev Dyn*. 2006;235:191-202.
3. de la Cruz MV, Castillo MM, Villavicencio L, Valencia A, Moreno-Rodriguez RA. Primitive interventricular septum, its primordium, and its contribution in the definitive interventricular septum: in vivo labelling study in the chick embryo heart. *Anat Rec*. 1997;247:512-520.
4. Mjaatvedt CH, Nakaoka T, Moreno-Rodriguez R, Norris RA, Kern MJ, Eisenberg CA, Turner D, Markwald RR. The outflow tract of the heart is recruited from a novel heart-forming field. *Dev Biol*. 2001;238:97-109.
5. Waldo KL, Kumiski DH, Wallis KT, Stadt HA, Hutson MR, Platt DH, Kirby ML. Conotruncal myocardium arises from a secondary heart field. *Development*. 2001;128:3179-3188.
6. Cai CL, Liang X, Shi Y, Chu PH, Pfaff SL, Chen J, Evans S. Isl1 identifies a cardiac progenitor population that proliferates prior to differentiation and contributes a majority of cells to the heart. *Dev Cell*. 2003;5:877-889.
7. Kelly RG. Molecular inroads into the anterior heart field. *Trends Cardiovasc Med*. 2005;15:51-56.
8. Kelly RG, Brown NA, Buckingham ME. The arterial pole of the mouse heart forms from Fgf10-expressing cells in pharyngeal mesoderm. *Dev Cell*. 2001;1:435-440.
9. Martinsen BJ, Frasier AJ, Baker CV, Lohr JL. Cardiac neural crest ablation alters Id2 gene expression in the developing heart. *Dev Biol*. 2004;272:176-190.
10. Dodou E, Verzi MP, Anderson JP, Xu SM, Black BL. Mef2c is a direct transcriptional target of ISL1 and GATA factors in the anterior heart field during mouse embryonic development. *Development*. 2004;131:3931-3942.
11. Verzi MP, McCulley DJ, De VS, Dodou E, Black BL. The right ventricle, outflow tract, and ventricular septum comprise a restricted expression domain within the secondary/anterior heart field. *Dev Biol*. 2005;287:134-145.
12. Xu H, Morishima M, Wylie JN, Schwartz RJ, Bruneau BG, Lindsay EA, Baldini A. Tbx1 has a dual role in the morphogenesis of the cardiac outflow tract. *Development*. 2004;131:3217-3227.
13. Christoffels VM, Mommersteeg MT, Trowe MO, Prall OW, de Gier-de Vries C, Soufan AT, Bussen M, Schuster-Gossler K, Harvey RP, Moorman AF, Kispert A. Formation of the venous pole of the heart from an Nkx2-5-negative precursor population requires Tbx18. *Circ Res*. 2006;98:1555-1563.
14. Deruiter MC, Gittenberger-de Groot AC, Wenink AC, Poelmann RE, Mentink MM. In normal development pulmonary veins are connected to the sinus venosus segment in the left atrium. *Anat Rec*. 1995;243:84-92.
15. Blom NA, Gittenberger-de Groot AC, Deruiter MC, Poelmann RE, Mentink MM, Ottenkamp J. Development of the cardiac conduction tissue in human embryos using HNK-1 antigen expression: possible relevance for understanding of abnormal atrial automaticity. *Circulation*. 1999;99:800-806.
16. Wenink AC, Symersky P, Ikeda T, Deruiter MC, Poelmann RE, Gittenberger-de Groot AC. HNK-1 expression patterns in the embryonic rat heart distinguish between sinuatrial tissues and atrial myocardium. *Anat Embryol (Berl)*. 2000;201:39-50.
17. Watanabe M, Timm M, Fallah-Najmabadi H. Cardiac expression of polysialylated NCAM in the chicken embryo: correlation with the ventricular conduction system. *Dev Dyn*. 1992;194:128-141.

18. Chan-Thomas PS, Thompson RP, Robert B, Yacoub MH, Barton PJ. Expression of homeobox genes Msx-1 (Hox-7) and Msx-2 (Hox-8) during cardiac development in the chick. *Dev Dyn*. 1993;197:203-216.

19. Rentschler S, Vaidya DM, Tamaddon H, Degenhardt K, Sassoon D, Morley GE, Jalife J, Fishman GI. Visualization and functional characterization of the developing murine cardiac conduction system. *Development*. 2001;128:1785-1792.

20. Jongbloed MR, Schalij MJ, Poelmann RE, Blom NA, Fekkes ML, Wang Z, Fishman GI, Gittenberger-de Groot AC. Embryonic conduction tissue: a spatial correlation with adult arrhythmogenic areas. *J Cardiovasc Electrophysiol*. 2004;15:349-355.

21. Jongbloed MR, Wijffels MC, Schalij MJ, Blom NA, Poelmann RE, van der Laarse A, Mentink MM, Wang Z, Fishman GI, Gittenberger-de Groot AC. Development of the right ventricular inflow tract and moderator band: a possible morphological and functional explanation for Mahaim tachycardia. *Circ Res*. 2005;96:776-783.

22. Kondo RP, Anderson RH, Kupershmidt S, Roden DM, Evans SM. Development of the cardiac conduction system as delineated by minK-lacZ. *J Cardiovasc Electrophysiol*. 2003;14:383-391.

23. Hoogaars WM, Tessari A, Moorman AF, de Boer PA, Hagoort J, Soufan AT, Campione M, Christoffels VM. The transcriptional repressor Tbx3 delineates the developing central conduction system of the heart. *Cardiovasc Res*. 2004;62:489-499.

24. Franco D, Icardo JM. Molecular characterization of the ventricular conduction system in the developing mouse heart: topographical correlation in normal and congenitally malformed hearts. *Cardiovasc Res*. 2001;49:417-429.

25. Kitajima S, Miyagawa-Tomita S, Inoue T, Kanno J, Saga Y. Mesp1-nonexpressing cells contribute to the ventricular cardiac conduction system. *Dev Dyn*. 2006;235:395-402.

26. Wetterwald A, Hoffstetter W, Cecchini MG, Lanske B, Wagner C, Fleisch H, Atkinson M. Characterization and cloning of the E11 antigen, a marker expressed by rat osteoblasts and osteocytes. *Bone*. 1996;18:125-132.

27. Williams MC, Cao Y, Hinds A, Rishi AK, Wetterwald A. T1 alpha protein is developmentally regulated and expressed by alveolar type I cells, choroid plexus, and ciliary epithelia of adult rats. *Am J Respir Cell Mol Biol*. 1996;14:577-585.

28. Breiteneder-Geleff S, Matsui K, Soleiman A, Meraner P, Poczewski H, Kalt R, Schaffner G, Kerjaschki D. Podoplanin, novel 43-kd membrane protein of glomerular epithelial cells, is down-regulated in puromycin nephrosis. *Am J Pathol*. 1997;151:1141-1152.

29. Schacht V, Ramirez MI, Hong YK, Hirakawa S, Feng D, Harvey N, Williams M, Dvorak AM, Dvorak HF, Oliver G, Detmar M. T1alpha/podoplanin deficiency disrupts normal lymphatic vasculature formation and causes lymphedema. *EMBO J*. 2003;22:3546-3556.

30. Harvey RP. NK-2 homeobox genes and heart development. *Dev Biol*. 1996;178:203-216.

31. Chen CY, Schwartz RJ. Identification of novel DNA binding targets and regulatory domains of a murine tinman homeodomain factor, nkx-2.5. *J Biol Chem*. 1995;270:15628-15633.

32. Laverriere AC, MacNeill C, Mueller C, Poelmann RE, Burch JB, Evans T. GATA-4/5/6, a subfamily of three transcription factors transcribed in developing heart and gut. *J Biol Chem*. 1994;269:23177-23184.

33. Schott JJ, Benson DW, Basson CT, Pease W, Silberbach GM, Moak JP, Maron BJ, Seidman CE, Seidman JG. Congenital heart disease caused by mutations in the transcription factor NKX2-5. *Science*. 1998;281:108-111.

34. Pashmforoush M, Lu JT, Chen H, Amand TS, Kondo R, Pradervand S, Evans SM, Clark B, Feramisco JR, Giles W, Ho SY, Benson DW, Silberbach M, Shou W, Chien KR. Nkx2-5 pathways and congenital heart disease; loss of ventricular myocyte lineage specification leads to progressive cardiomyopathy and complete heart block. *Cell*. 2004;117:373-386.

35. Moreno-Rodriguez RA, de la Cruz MV, Krug EL. Temporal and spatial asymmetries in the initial distribution of mesenchyme cells in the atrioventricular canal cushions of the developing chick heart. *Anat Rec*. 1997;248:84-92.

36. Baldini A. DiGeorge syndrome: an update. *Curr Opin Cardiol*. 2004;19:201-204.

37. Franco D, Campione M, Kelly R, Zammit PS, Buckingham M, Lamers WH, Moorman AF. Multiple transcriptional domains, with distinct left and right components, in the atrial chambers of the developing heart. *Circ Res*. 2000;87:984-991.

38. Krause A, Zacharias W, Camarata T, Linkhart B, Law E, Lischke A, Miljan E, Simon HG. Tbx5 and Tbx4 transcription factors interact with a new chicken PDZ-LIM protein in limb and heart development. *Dev Biol*. 2004;273:106-120.

39. Brand T, Schneider MD. The TGF beta superfamily in myocardium: ligands, receptors, transduction, and function. *J Mol Cell Cardiol*. 1995;27:5-18.

40. Markwald R, Eisenberg C, Eisenberg L, Trusk T, Sugi Y. Epithelial-mesenchymal transformations in early avian heart development. *Acta Anat (Basel)*. 1996;156:173-186.

41. Potts JD, Runyan RB. Epithelial-mesenchymal cell transformation in the embryonic heart can be mediated, in part, by transforming growth factor beta. *Dev Biol*. 1989;134:392-401.

42. Vrancken Peeters MP, Gittenberger-de Groot AC, Mentink MM, Poelmann RE. Smooth muscle cells and fibroblasts of the coronary arteries derive from epithelial-mesenchymal transformation of the epicardium. *Anat Embryol (Berl)*. 1999;199:367-378.

43. Lie-Venema H, Gittenberger-de Groot AC, van Empel LJ, Boot MJ, Kerkdijk H, de Kant E, Deruiter MC. Ets-1 and Ets-2 transcription factors are essential for normal coronary and myocardial development in chicken embryos. *Circ Res*. 2003;92:749-756.

44. Moore AW, McInnes L, Kreidberg J, Hastie ND, Schedl A. YAC complementation shows a requirement for Wt1 in the development of epicardium, adrenal gland and throughout nephrogenesis. *Development*. 1999;126:1845-1857.

45. Perez-Pomares JM, Phelps A, Sedmerova M, Carmona R, Gonzalez-Iriarte M, Munoz-Chapuli R, Wessels A. Experimental studies on the spatiotemporal expression of WT1 and RALDH2 in the embryonic avian heart: a model for the regulation of myocardial and valvuloseptal development by epicardially derived cells (EPDCs). *Dev Biol*. 2002;247:307-326.

46. Carmona R, Gonzalez-Iriarte M, Perez-Pomares JM, Munoz-Chapuli R. Localization of the Wilm's tumour protein WT1 in avian embryos. *Cell Tissue Res*. 2001;303:173-186.

47. Vrancken Peeters MP, Mentink MM, Poelmann RE, Gittenberger-de Groot AC. Cytokeratins as a marker for epicardial formation in the quail embryo. *Anat Embryol (Berl)*. 1995;191:503-508.

48. Kubalak SW, Miller-Hance WC, O'Brien TX, Dyson E, Chien KR. Chamber specification of atrial myosin light chain-2 expression precedes septation during murine cardiogenesis. *J Biol Chem*. 1994;269:16961-16970.

49. Martin-Villar E, Scholl FG, Gamallo C, Yurrita MM, Munoz-Guerra M, Cruces J, Quintanilla M. Characterization of human PA2.26 antigen (T1alpha-2, podoplanin), a small membrane mucin induced in oral squamous cell carcinomas. *Int J Cancer*. 2005;113:899-910.

50. Wicki A, Lehembre F, Wick N, Hantusch B, Kerjaschki D, Christofori G. Tumor invasion in the absence of epithelial-mesenchymal transition: Podoplanin-mediated remodeling of the actin cytoskeleton. *Cancer Cell*. 2006;9:261-272.

51. Komuro I, Izumo S. Csx: a murine homeobox-containing gene specifically expressed in the developing heart. *Proc Natl Acad Sci U S A*. 1993;90:8145-8149.

52. Harris BS, Gourdie RG, O'Brien TX. Atrioventricular conduction system and transcription factors Nkx2.5 and Msx2. *J Cardiovasc Electrophysiol*. 2005;16:86-87.

53. Thomas PS, Kasahara H, Edmonson AM, Izumo S, Yacoub MH, Barton PJ, Gourdie RG. Elevated expression of Nkx-2.5 in developing myocardial conduction cells. *Anat Rec*. 2001;263:307-313.

54. Chi X, Chatterjee PK, Wilson W, III, Zhang SX, DeMayo FJ, Schwartz RJ. Complex cardiac Nkx2-5 gene expression activated by noggin-sensitive enhancers followed by chamber-specific modules. *Proc Natl Acad Sci U S A*. 2005;102:13490-13495.

55. Habets PE, Moorman AF, Clout DE, van Roon MA, Lingbeek M, van Lohuizen M, Campione M, Christoffels VM. Cooperative action of Tbx2 and Nkx2.5 inhibits ANF expression in the atrioventricular canal: implications for cardiac chamber formation. *Genes Dev*. 2002;16:1234-1246.

56. Poelmann RE, Jongbloed MR, Molin DG, Fekkes ML, Wang Z, Fishman GI, Doetschman T, Azhar M, Gittenberger-de Groot AC. The neural crest is contiguous with the cardiac conduction system in the mouse embryo: a role in induction? *Anat Embryol (Berl)*. 2004;208:389-393.

57. Moorman AF, de Jong F, Denyn MM, Lamers WH. Development of the cardiac conduction system. *Circ Res*. 1998;82:629-644.

58. Christoffels VM, Hoogaars WM, Tessari A, Clout DE, Moorman AF, Campione M. T-box transcription factor Tbx2 represses differentiation and formation of the cardiac chambers. *Dev Dyn*. 2004;229:763-770.

59. Moorman AF, Christoffels VM. Cardiac chamber formation: development, genes, and evolution. *Physiol Rev*. 2003;83:1223-1267.

60. Meilhac SM, Esner M, Kerszberg M, Moss JE, Buckingham ME. Oriented clonal cell growth in the developing mouse myocardium underlies cardiac morphogenesis. *J Cell Biol*. 2004;164:97-109.

61. Gourdie RG, Harris BS, Bond J, Justus C, Hewett KW, O'Brien TX, Thompson RP, Sedmera D. Development of the cardiac pacemaking and conduction system. *Birth Defects Res C Embryo Today*. 2003;69:46-57.

62. Gittenberger-de Groot AC, Vrancken Peeters MP, Mentink MM, Gourdie RG, Poelmann RE. Epicardium-derived cells contribute a novel population to the myocardial wall and the atrioventricular cushions. *Circ Res*. 1998;82:1043-1052.

63. Poelmann RE, Gittenberger-de Groot AC. A subpopulation of apoptosis-prone cardiac neural crest cells targets to the venous pole: multiple functions in heart development? *Dev Biol*. 1999;207:271-286.

64. Kamino K, Hirota A, Fujii S. Localization of pacemaking activity in early embryonic heart monitored using voltage-sensitive dye. *Nature*. 1981;290:595-597.

65. Dickinson DF, Wilkinson JL, Anderson KR, Smith A, Ho SY, Anderson RH. The cardiac conduction system in situs ambiguus. *Circulation*. 1979;59:879-885.

66. Boucherot A, Schreiber R, Pavenstadt H, Kunzelmann K. Cloning and expression of the mouse glomerular podoplanin homologue gp38P. *Nephrol Dial Transplant*. 2002;17:978-984.

67. Kasahara H, Benson DW. Biochemical analyses of eight NKX2.5 homeodomain missense mutations causing atrioventricular block and cardiac anomalies. *Cardiovasc Res*. 2004;64:40-51.

68. Biben C, Weber R, Kesteven S, Stanley E, McDonald L, Elliott DA, Barnett L, Koentgen F, Robb L, Feneley M, Harvey RP. Cardiac septal and valvular dysmorphogenesis in mice heterozygous for mutations in the homeobox gene Nkx2-5. *Circ Res*. 2000;87:888-895.

69. Blom NA, Gittenberger-de Groot AC, Jongeneel TH, Deruiter MC, Poelmann RE, Ottenkamp J. Normal development of the pulmonary veins in human embryos and formulation of a morphogenetic concept for sinus venosus defects. *Am J Cardiol*. 2001;87:305-309.

4

Edris A.F. Mahtab[1]
Nathan D. Hahurij[1, 2, #]
Rebecca Vicente-Steijn[1, #]
Monique R.M. Jongbloed[1, 3]
Lambertus J. Wisse[1]
Marco C. DeRuiter[1]
Pavel Uhrin[4]
Jan Zaujec[4]
Bernd R. Binder[4]
Martin J. Schalij[3]
Robert E. Poelmann[1]
Adriana C. Gittenberger-de Groot[1]

[1] Department of Anatomy & Embryology, Leiden University Medical Center, Leiden, The Netherlands.
[2] Department of Pediatric Cardiology, Leiden University Medical Center, Leiden, The Netherlands.
[3] Department of Cardiology, Leiden University Medical Center, Leiden, The Netherlands.
[4] Department of Vascular Biology and Thrombosis Research, Center for Biomolecular Medicine and Pharmacology,
  Medical University of Vienna, Austria.

[#] *Authors have equally contributed*

5

Podoplanin deficient mice show a Rhoa related hypoplasia of the sinus venosus myocardium including the sinoatrial node

ABSTRACT

We investigated the role of *podoplanin* in development of the sinus venosus myocardium comprising the sinoatrial node, the dorsal atrial wall and the primary atrial septum as well as the myocardium of the cardinal and pulmonary veins. We analyzed *podoplanin* wildtype and knockout mouse embryos between 9.5-15.5 days post conception (dpc) using immunohistochemical marker podoplanin, sinoatrial node marker HCN4, myocardial markers MLC-2a, Nkx2.5 as well as Cx43, coelomic marker WT-1 and epithelial-to-mesenchymal transformation markers E-cadherin and RhoA. 3D reconstructions were made and myocardial morphometry were performed. *Podoplanin* mutants showed hypoplasia of the sinoatrial node, the primary atrial septum and dorsal atrial wall. Myocardium lining the wall of the cardinal and pulmonary veins was thin and perforated. Impaired myocardial formation is correlated with abnormal epithelial-to-mesenchymal transformation of the coelomic epithelium due to upregulated E-cadherin and downregulated RhoA, which are controlled by *podoplanin*. Our results demonstrate an important role for *podoplanin* in development of sinus venosus myocardium.

INTRODUCTION

During early embryogenesis the lateral plate mesoderm splits into two layers: the somatic and the splanchnic mesoderm forming the outer and the inner layer of the coelomic cavity.[1,2] The somatic mesoderm is involved in development of the body wall and extremities while myocardial precursors are restricted to the splanchnic mesoderm.[3,4] Subsequently, the left and right primary heart fields (cardiogenic plates) fuse at the ventral midline resulting in the primary linear heart tube, which starts looping at 8.5 days post conception (dpc).[1,2,5]

Previous studies of heart development[5-7] have shown that further development of the heart tube is related to the addition of cells at both the arterial and venous pole of the heart, forming the outflow and the inflow tract myocardium, respectively. These early observations on the addition of the secondary myocardium have recently been supported by several studies describing the addition of myocardium at the arterial pole, being secondary[8] and anterior heart fields[9-12] and the posterior heart field (PHF) at the venous pole[12-15] of the developing heart. The complete length of the splanchnic mesoderm contributing to the addition of myocardium at both poles of the heart was called second heart field[14] or second lineage.[10,12,14]

A number of genes and proteins, considered as early markers of the second heart field at the outflow and inflow tract, have been reported, such as *MesP1*,[16] *Fibroblast growth factor (Fgf)*

8 and *10*,[9] *BMP-2* and Nkx2.5,[8,13,15] *Isl1*,[14] inhibitor of differentiation Id2,[17] GATA factors targeting *Mef2c*,[18,19] *Tbx1*, *Tbx3* and *Tbx18*[15,20] and *Shox2*.[21] Recently we have added *podoplanin* to this list as a novel gene in cardiac development.

As a coelomic and myocardial marker, podoplanin is specifically expressed in the mesenchyme and in the myocardium at the venous pole.[13,22] Studying the mesenchymal population, podoplanin expression was observed in the proepicardial organ and epicardium.[13,22,23] In the cardiomyocyte population podoplanin staining was seen in major parts of the developing atrioventricular cardiac conduction system, in sinus venosus myocardium including the sinoatrial node, the venous valves, the dorsal mesocardium, the dorsal atrial wall and primary atrial septum. Also the myocardium surrounding the cardinal veins and the common pulmonary vein belongs to this population.[13,22] In earlier publications, podoplanin, a 43-kd mucin type transmembrane glycoprotein, first named E11 antigen as a new marker for an osteoblastic cell line,[24] was also reported in the nervous system, the epithelia of lung, eye, oesophagus and intestine,[25] the mesothelium of the visceral peritoneum,[24] the coelomic wall (pericardium) lining the pericardial cavity[13] and the epicardium,[22] the podocytes of the kidney[26] and the lymphatic endothelium.[27]

To elucidate a possible functional role of *podoplanin* in cardiac development and more specifically in the development of the sinus venosus myocardium, we studied *podoplanin* knockout mouse embryos and used several immunohistochemical markers. To investigate the sinus venosus myocardium including the sinoatrial node we have used hyperpolarization-activated, cyclic nucleotide-gated cation 4 (HCN4).[28-30] In addition, atrial myosin light chain 2 (MLC-2a), NK2 transcription factor related locus 5 (Nkx2.5) and connexin 43 (Cx43) were used. Furthermore, we studied E-cadherin, a cell to cell adhesion protein, and RhoA important for epithelial-to-mesenchymal transformation (EMT) of the coelomic epithelium, a process that allows epithelial cells to become mobile mesenchymal cells.[31] To visualize the epithelium and mesothelium of the coelomic cavity, the epicardium and sites of active EMT we have used Wilm's tumor suppressor protein (WT-1).[32-34] It has been described that the PHF and resulting myocardium are derived from the epithelial lining of the coelomic cavity (splanchnic mesothelium) by EMT.[13] During normal development, loss of E-cadherin is needed for proper EMT resulting in loss of epithelial features[35] and consecutive development into migratory mesenchymal cells. During abnormal development, an upregulated state of E-cadherin, by e.g. lack of *podoplanin*, causes an altered EMT.[22,36] Podoplanin can, therefore, be considered as an inhibitor of E-cadherin stimulating EMT. In addition, RhoA activation by podoplanin and ezrin interaction have been described to lead into podoplanin-induced EMT.[37] Similar to E-cadherin, lack of *podoplanin* might lead to downregulated RhoA and altered EMT.

In the current paper we studied the role of *podoplanin* in the development of the sinus venosus myocardium derived from the PHF, which is a part of the more extensive second heart field. We demonstrate that knocking out the *podoplanin* gene leads to myocardial abnormalities in sinus venosus myocardium at the venous pole of the developing mouse heart.

MATERIAL AND METHODS

Generation of *podoplanin*^{-/-} mice and harvesting of embryos

The *podoplanin* knockout mice were generated by homologous recombination in embryonic stem cells from the 129S/v mouse line by inserting a neomycin phosphotransferase cassette in a 7.7kb genomic fragment encompassing exons II to V. The complete description of this model was reported previously.[22] Briefly, the heterozygous ES cell clones were test-bred for germline transmission with Swiss mice to generate *podoplanin*^{+/-} offspring (50% 129S/v: 50% Swiss genetic background) using standard procedures. These mice were crossed to obtain *podoplanin*^{-/-} embryos and *podoplanin*^{+/+} (wildtype) littermates. The morning of the vaginal plug was stated 0.5 dpc. Pregnant females were sacrificed and embryos were harvested.

General description

We investigated the lining of the coelomic cavity and the morphology of the sinus venosus myocardium of the heart in 27 wildtype mouse embryos of 9.5 dpc (n=4), 10.5 dpc (n=4), 11.5 dpc (n=3), 12.5 dpc (n=4), 13.5 dpc (n=5), 14.5 dpc (n=4) and 15.5 dpc (n=3) and compared these with 37 *podoplanin* knockout mouse embryos of 9.5 dpc (n=4), 10.5 dpc (n=4), 11.5 dpc (n=6), 12.5 dpc (n=8), 13.5 dpc (n=6), 14.5 dpc (n=5) and 15.5 dpc (n=4). All embryos were fixed in 4% paraformaldehyde (PFA) and routinely processed for paraffin immunohistochemical investigation.

Immunohistochemistry

Immunohistochemistry was performed with antibodies against MLC-2a (1/6000, kindly provided by S.W. Kubalak, Charleston, SC, USA), Nkx2.5 (1/4000, Santa Cruz Biotechnology, Inc., CA, USA, SC-8697), podoplanin (clone 8.1.1., 1/500, Hybridomabank, Iowa, USA), WT-1 (1/1000, Santa Cruz Biotechnology, Inc., CA, USA, sc-192), E-cadherin (1/150, Santa Cruz Biotechnology, Inc., CA, USA, SC-7870), HCN4 (1/1000, Alomone labs, The Netherlands, APC-052), RhoA (1/2000, Santa Cruz Biotechnology, Inc., CA, USA, SC-418) and Cx43 (1/200, Sigma-Aldrich Chemie, USA, C6219). The primary antibodies were dissolved in phosphate buffered saline (PBS)-Tween-20 with 1% Bovine Serum Albumin (BSA, Sigma Aldrich, USA). Between subsequent incubation steps all slides were rinsed in PBS (2x) and PBS-Tween-20 (1x). The slides were incubated with the secondary antibody for 45 min: for

MLC-2a, WT-1, E-cadherin, HCN4 and Cx43 with 1/200 goat-anti-rabbit-biotin (Vector Laboratories, USA, BA-1000) and 1/66 goat serum (Vector Laboratories, USA, S1000) in PBS-Tween-20; for Nkx2.5 with 1/200 horse-anti-goat-biotin (Vector Laboratories, USA, BA-9500) and 1/66 horse serum (Brunschwig Chemie, Switserland, S-2000) in PBS-Tween-20; for podoplanin with 1/200 goat-anti-Syrian hamster-biotin (Jackson Imunno research, USA, 107-065-142) and 1/66 goat serum (Vector Laboratories, USA, S1000) in PBS-Tween-20 and for RhoA with 1/200 horse-anti-mouse-biotin (Santa Cruz Biotechnology, Inc., CA, USA, SC-9996-FITC) and 1/66 horse serum (Brunschwig Chemie, Switserland, S-2000) in PBS-Tween-20. The slides were incubated with ABC-reagent (Vector Laboratories,USA, PK 6100) for 45 min. For visualization the slides were incubated with 400 μg/ml 3-3'di-aminobenzidin tetrahydrochloride (DAB, Sigma-Aldrich Chemie, USA, D5637) dissolved in Tris-maleate buffer pH 7.6 to which 20 μl H_2O_2 was added: MLC-2a, and E-cadherin 5 min; Nkx2.5, HCN4, Cx43, WT-1 and podoplanin 10 min. Counterstaining was performed with 0.1% haematoxylin (Merck, Darmstadt, Germany) for 5 sec, followed by rinsing with tap water for 10 min. All slides were dehydrated and mounted with Entellan (Merck, Darmstadt, Germany).

3D reconstructions

We made 3D reconstructions of the sinus venousus myocardium based on MLC-2a, Nkx2.5 and HCN4 stained sections of wildtype as well as *podoplanin* knockout embryos of 12.5 dpc in which the morphological differences were shown. The reconstructions were made as previously described[38] using the AMIRA software package (Template Graphics Software, San Diego, USA).

Morphometry of the myocardium

Based on HCN4, MLC-2a and Nkx2.5 stained sections, sinus venosus and separately sinoatrial node myocardial volume estimation was performed of 12 wildtype mouse hearts of 11.5 dpc (n=3), 12.5 dpc (n=3), 13.5 dpc (n=3), 14.5 dpc (n=3) and 12 *podoplanin* knockout mouse hearts of 11.5 dpc (n=3), 12.5 dpc (n=3), 13.5 dpc (n=3), 14.5 dpc (n=3) based on Cavalieri's principle as described previously.[39] Statistical analysis was performed with an independent sample-*t*-test (*P*<0.05) using the SPSS 11.0 software program (SPSS Inc, Chicago, III). In summary, regularly spaced points (100 mm^2 for sinus venosus myocardium and 49 mm^2 for sinoatrial node myocardium) were randomly positioned on the HCN4 stained myocardium. The distance between the subsequent sections of the slides was 0.075 mm for sinus venosus myocardium and 0.025 mm for the sinoatrial node. The volume measurement was done using the HB2 Olympus microscope with a 100x magnification objective for the sinus venosus myocardium and 200x for the sinoatrial node.

RESULTS

General description

We studied the embryonic phenotype of the *podoplanin* knockout mice, which show an increased embryonic death of approximately 40% of the homozygote embryos between 10-16 dpc. Additionally, 50% of the neonatal homozygote knockout mice die within the first weeks of life, while heterozygous mutants reach sexual maturity. The cause of embryonic death has been correlated to the cardiac defects[22] while the cause of neonatal death is still unknown.
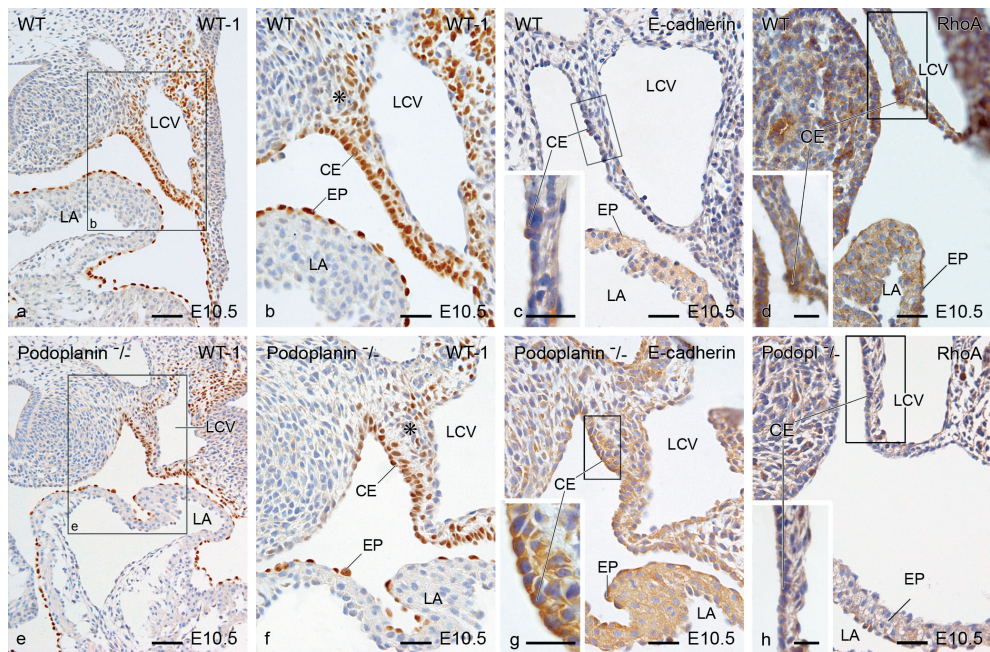

Figure 1. Transverse sections showing EMT sites of the coelomic cavity epithelium in the hearts of 10.5 dpc wildtype (WT) and *podoplanin* knockout (*podoplanin*⁻ᐟ⁻) mouse embryos. To demarcate the coelomic mesothelium and sites of active EMT, we studied WT-1 staining (a, b, e and f) and E-cadherin staining (c and g). WT-1 positivity was found in the mesothelium (**asterisk** in b and f) and epithelium (**CE**) of the coelomic cavity and epicardium (**EP**) of the WT embryos (a and b). WT-1 staining was more extensive at the corners of the coelomic cavity (asterisk) below the left cardinal vein (**LCV**), where the CE appeared to be cuboidal and well organized (b). In the *podoplanin*⁻ᐟ⁻ embryos WT-1 was also present in these regions (e and f), however, the CE was disorganized and the cells were irregular in shape and size (compare a and b with e and f). E-cadherin staining appeared stronger in both the EP and CE of the *podoplanin*⁻ᐟ⁻ embryos (g) as compared to the WT mouse embryos (c). Remarkably, in the *podoplanin*⁻ᐟ⁻ E-cadherin staining was not only upregulated in the CE but also in the underlying mesothelial cells (c and g). In WT embryos RhoA expression was seen in the coelomic mesenchyme, CE and epicardium (d). In the mutants overall expression of RhoA was downregulated (h). **LA** indicates left atrium. Scale bars: (a), (e) = 60μm; (b-d), (f-h) = 30μm; magnification box in (c), (d), (g) and (h) = 20μm.

Several marked morphological cardiac abnormalities were observed in the knockout mouse embryos. In the younger stages a hypoplastic proepicardial organ (10.5 dpc) as well as ventricular myocardium were observed with discontinuous epicardium, a thin layer of the subepicardial mesenchyme and a diminished amount of epicardium derived cells (EPDCs).[22] These hearts also presented with outflow tract abnormalities such as severe dextroposition of the aorta, coronary artery abnormalities, spongious myocardium of the developing interventricular septum and impaired formation and fusion of the atrioventricular cushions. At the sinus venosus region, which is the area of our focus, myocardial hypoplasia and morphological abnormalities were observed. In general, the sinus venosus myocardial abnormalities, mentioned below, were seen in the sinoatrial node, the dorsal atrial wall, the atrial septum as well as the myocardium of the cardinal and pulmonary veins.

Morphology and immunohistochemical expression patterns of the sinus venosus myocardium will be described in the knockout embryos and compared to wildtype embryos, in subsequent stages of heart development.

Podoplanin expression in the heart
In wildtype mice the first expression of podoplanin can be recognized as early as 9.5 dpc in the coelomic mesothelium and in the proepicardial organ.[13,22] Moreover, podoplanin was observed in the myocardium of the medial wall of the left cardinal vein shortly before entering the sinus venosus. At 10.5 dpc podoplanin staining in this region was more extensive and extended into the dorsal mesocardium. At the right side the staining is evaluated for the first time at the level of the future sinoatrial node, in the medial wall of the right cardinal vein. The venous valves showed also podoplanin positivity. At 12.5 dpc podoplanin was clearly observed in the pericardium, epicardium, sinoatrial node, venous valves, dorsal mesocardium, myocardium of the pulmonary vein, atrial septum and ventricular conduction system. Remarkably, podoplanin staining was also observed at the left side bordering the medial contour of the left cardinal vein. The pattern and intensity of this region was similar to the sinoatrial node region at the right side, although the left-sided region was smaller at this stage.[13]

Sites of epithelial-to-mesenchymal transformation
To demarcate the coelomic mesothelium and sites of active EMT, we used WT-1 staining as a coelomic mesothelial marker, E-cadherin staining as a cell-to-cell adhesion marker and RhoA playing a crucial role in EMT at specific sites of the venous pole. WT-1 was observed in both the coelomic mesothelium and proepicardial organ at 9.5 dpc in the wildtype. In the mutants, compared to the wildtype embryos, these regions were smaller and E-cadherin was upregulated. At 10.5 dpc in wildtype embryos WT-1 positivity was found in the single layer of mesothelium of the coelomic cavity and epicardium (Figure 1a and b). Marked staining was seen at the

WT
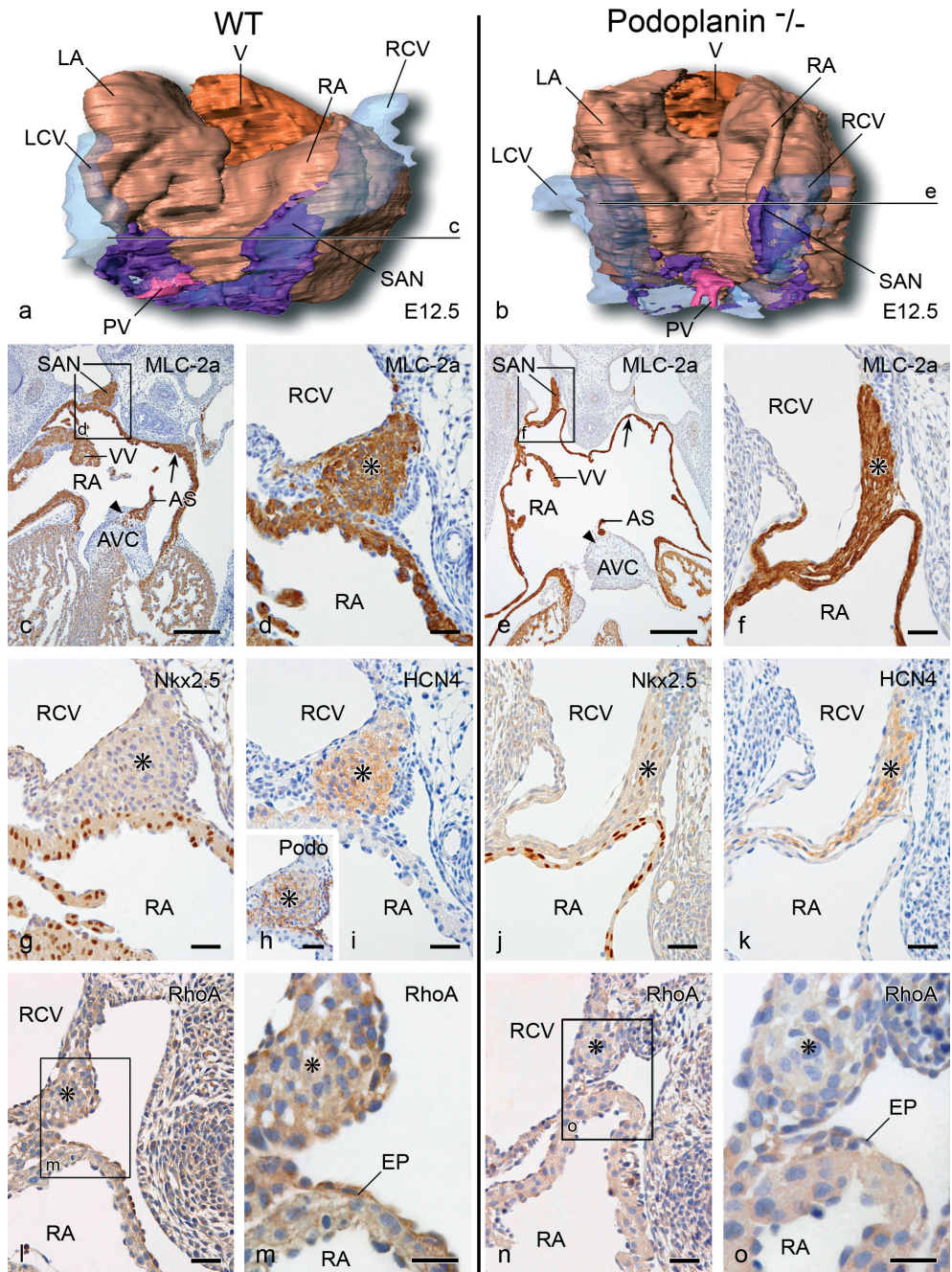
Podoplanin ⁻/⁻

corners of the coelomic cavity at both sides adjacent to the cardinal veins, where the expression of WT-1 was more extensive and the cells of the coelomic mesothelium appeared to be cuboidal and well organized (Figure 1b). In the *podoplanin* knockout embryos WT-1 was also present in these regions (Figure 1e and f), however, the coelomic mesothelium was disorganized, the cells were irregular in shape and size and seemed to have maintained their epithelial confinement (Figure 1, compare a and b with e and f). The defective spreading of the epicardium at several locations was shown after WT-1 staining that followed this pattern and did not normally cover the myocardium in the knockout mouse embryos (Figure 1a and e). Increased E-cadherin staining has been observed clearly in both the epicardium and mesothelium lining the coelomic wall in the *podoplanin* knockout embryos (Figure 1g) compared to the wildtype mouse embryos (Figure 1c). Remarkably, in the mutants E-cadherin staining was not only upregulated in the epithelium of the coelomic cavity but also in the underlying mesenchymal cells (Figure 1c and g), supporting the observation of disturbed EMT. At 10.5 dpc in wildtype embryos major RhoA expression was seen in the mesenchyme and epithelium of the coelomic cavity and epicardium (Figure 1d). In the mutants overall expression of RhoA was downregulated (Figure 1h).

The sinus venosus myocardium

To evaluate the extent of sinus venosus myocardium we studied the expression of HCN4 in the wildtype and *podoplanin* knockout embryos between 9.5-14.5 dpc. The HCN4 positive region of the sinus venosus area (Figure 2i, k and Figure 3d, f, m, o) overlaps the Nkx2.5 negative (Figure 2g, j and Figure 3h-k) and MLC-2a positive sinus venosus region (Figure 2c-f and Figure 3c, e, l, n). Podoplanin is also expressed in these regions of the sinus venosus myocardium, almost completely overlapping with the Nkx2.5 negative and HCN4 positive regions.

Figure 2. Cranio-dorsal view of 3D reconstructions (a and b) and transverse sections (c-o) showing at 12.5 dpc the hypoplasia of the sinoatrial nodal (SAN) region in the *podoplanin* knockout (*podoplanin*$^{-/-}$) mouse embryos compared to the wildtype (WT) embryos. The intersection line c refers to sections (c) and (d) and the intersection line e refers to sections (e) and (f). In the SAN (**asterisks**) the expression level of MLC-2a (c-f), Nkx2.5 (g and j), and HCN4 (i and k) was unaltered in the WT (c, d, g and i) and *podoplanin*$^{-/-}$ embryos (e, f, j and k). Section h shows podoplanin (**Podo**) expression in the SAN of the WT heart. The SAN in the *podoplanin*$^{-/-}$ is thin and hypoplastic compared to WT (compare d with f). In the mutants the venous valves (**VV**), dorsal atrial wall (**arrows** in c and e) and primary atrial septum (**AS**) were also small and hypoplastic (compare c with e). Because of the deficient AS the mutant hearts showed a large atrial septum defect (compare c with e) and the AS myocardium was not properly embedded in the atrioventricular cushion (**AVC**, **arrow heads** in c and e). The AVC was not fused properly with the ventricular septum resulting into a ventricular septum defect (compare c with e). In WT embryos, RhoA expression was seen in coelomic mesenchyme, CE as well as in SAN and epicardium (**EP**) (l, m). In the mutants, RhoA expression was downregulated in SAN as well as in CE and EP (n, o). **LA** indicates left atrium; **LCV**, left cardinal vein; **RA**, right atrium; **RCV**, right cardinal vein. In the 3D reconstructions: atrial myocardium, **light brown**; cardinal veins lumen, **transparent blue**; common pulmonary vein (**PV**) lumen, **pink**; sinus venosus myocardium, **purple**; ventricular myocardium (**V**), **brown**. Scale bars: (c), (e) = 200μm; (d), (f-l), (n) = 30μm; (m), (o) = 20μm.
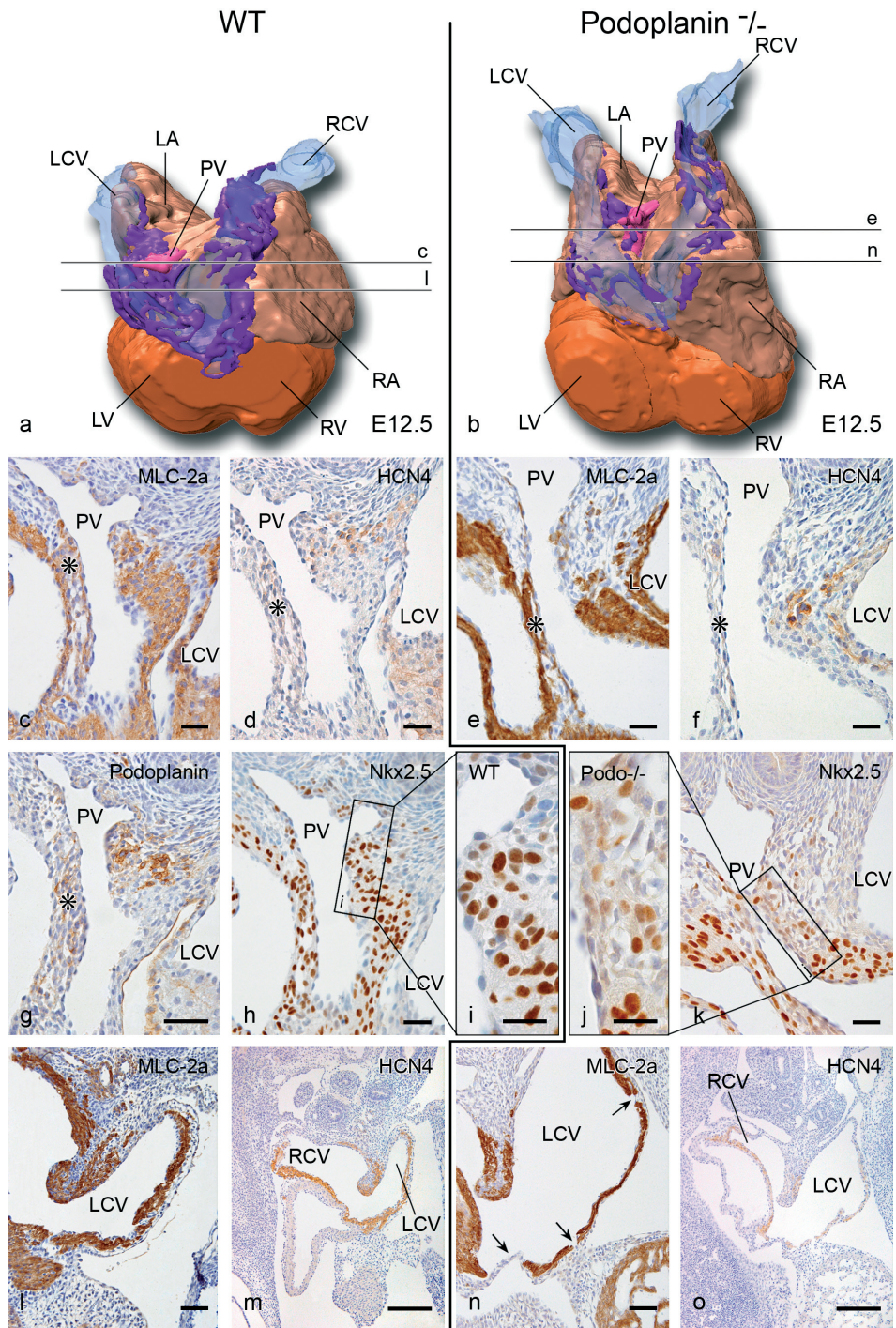
Sinoatrial node and venous valves

In the sinoatrial node the MLC-2a positive (Figure 2c-f) and Nkx2.5 negative (Figure 2g, j) region were identical to the HCN4 (Figure 2i, k) and podoplanin (Figure 2h) positive areas. In contrast to the remaining sinus venosus myocardial structures, in the sinoatrial node HCN4 remained positive while Nkx2.5 negative staining was maintained. In the knockout mice the sinoatrial node was hypoplastic (Figure 2a, b, d, f) and the venous valves were shorter and thinner (Figure 2c, e), however, the expression pattern of MLC2a, Nkx2.5 HCN4 and Cx43 (not shown), was not changed compared to the wildtype (Figure 2c-k). Comparable to 10.5 dpc in wildtype embryos, RhoA expression was seen in coelomic mesenchyme and epithelium as well as in sinoatrial node and epicardium (Figure 2l, m). In the mutants, RhoA expression was downregulated in sinoatrial node as well as in coelomic epithelium and epicardium (Figure 2n, o).

Primary atrial septum and dorsal atrial wall

In both wildtype and *podoplanin* knockout embryos MLC-2a expression was present in the sinus venosus myocardium and the myocardium of the atrial and ventricular wall (Figure 2a-f and Figure 3a-c, e, l, n). Similar to the sinoatrial node and venous valves, the expression pattern of the mentioned markers was unchanged in the mutants compared to the wildtype embryos. In the mutants, myocardial hypoplasia was seen of the dorsal atrial wall (Figure 2c-f). The atrial septum was thin (Figure 3c-f) and deficient (Figure 2c, e) with a large secondary foramen (Figure 2c, e). The myocardialization process at the base of the atrial septum was almost absent (Figure 2c, e). Additionally in the knockout embryos, the atrioventricular cushion was not fused properly to the top of the ventricular septum resulting into a persisting interventricular communication (Figure 2c, e). There is marked dilatation of the atria in the mutant embryos compared to the wildtype (Figure 2c, e).

Figure 3. Cranio-dorsal view of 3D reconstructions (a and b) and transverse sections (c-o) showing the myocardial hypoplasia of the common pulmonary vein (PV), atrial septum (asterisk) and the wall of the cardinal veins of 12.5 dpc wildtype (WT) and *podoplanin* knockout (*podoplanin*^{-/-}) embryonic mouse hearts. The intersection lines c, l, e and n refer to the sections (c), (l), (e) and (n) respectively. In the MLC-2a sections (c, e) the hypoplasia of the myocardium around the PV in the *podoplanin*^{-/-} is clearly visible. Moreover, parts of myocardium around the PV, which are also positive for HCN4 (d) and *podoplanin* (g) are missing in the *podoplanin*^{-/-} (compare c, d with e, f). This lack of myocardium around the PV is also seen in the sections stained with Nkx2.5 (h-k) where the Nkx2.5 mosaic myocardium of the PV is missing in the *podoplanin*^{-/-} (k, j) compared with the WT (h, i). The hypoplasia of the atrial septum (**asterisk**) is seen in the *podoplanin*^{-/-} (e) compared to the WT (c). Sections (l) and (n) are stained with MLC-2a and sections (m) and (o) show HCN4 expression of the same region demonstrating the hypoplasia and the perforations (**arrows** in n) of the myocardium of the cardinal veins in the *podoplanin*^{-/-}. **LA** indicates left atrium; **LCV**, left cardinal vein; **LV**, left ventricle; **RA**, right atrium; **RCV**, right cardinal vein; **RV**, right ventricle. In the 3D reconstructions: atrial myocardium, **light brown**; cardinal veins lumen, **transparent blue**; PV lumen, **pink**; sinus venosus myocardium, **purple**; ventricular myocardium, **brown**. Scale bars: (c), (e), (l), (n) = 60µm; (d), (f-h), (k) = 30µm; (i), (j) = 20µm; (m), (o) = 200µm.

Pulmonary and cardinal veins

In wildtype embryos the wall of the pulmonary and cardinal veins showed MLC-2a (Figure 3c, l) and HCN4 (Figure 3a, d, m) expression while the Nkx2.5 expression pattern was mosaic in the myocardium lining the pulmonary vein (Figure 3h, i) and negative in the wall of the cardinal veins (Figure 3h). The staining for HCN4 was diminished at 15.5 dpc compared to earlier stages whereas the initially Nkx2.5 negative myocardium of the cardinal veins and Nkx2.5 mosaic myocardium of the pulmonary vein wall became positive.

In the knockout embryos, myocardium of the pulmonary vein wall was hypoplastic and almost absent compared to the wildtype (Figure 3c, e). The extent of hypoplasia and lack of myocardium of the pulmonary vein corresponded with the regions normally expressing HCN4
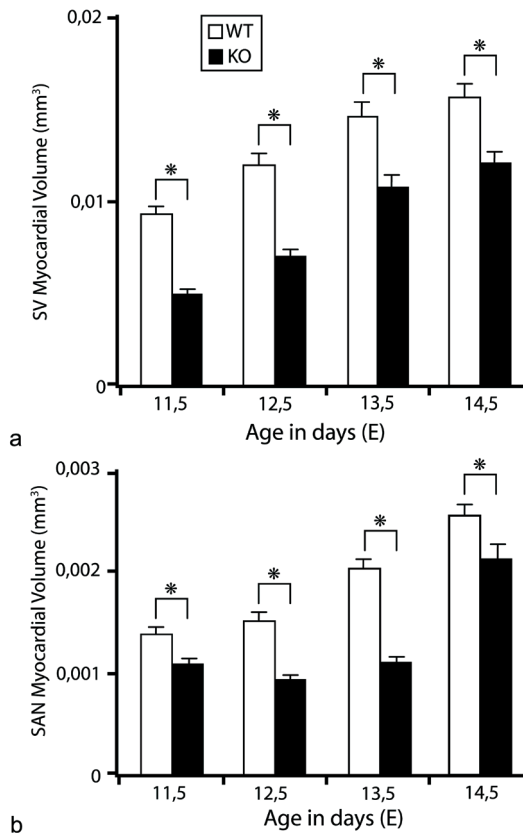

Figure 4. Sinus venosus (**SV**, a) and sinoatrial node (**SAN**, b) myocardial volume estimation of 12 wildtype (**WT**) mouse hearts of 11.5 dpc (n=3), 12.5 dpc (n=3), 13.5 dpc (n=3) and 14.5 dpc (n=3) and 12 podoplanin knockout (**KO**) mouse hearts 11.5 dpc (n=3), 12.5 dpc (n=3), 13.5 dpc (n=3) and 14.5 dpc (n=3). *Podoplanin* knockout embryos have a significant smaller SV and SAN myocardial volume (*$P<0.05$) compared to WT embryos.

(Figure 3d, f) and podoplanin (Figure 3g). Comparable to the MLC-2a stained myocardium around the pulmonary vein as described above, the Nkx2.5 mosaic area was hypoplastic and almost absent in the knockout mice (compare Figure 3h, i with j, k).

The myocardium of the cardinal veins was also hypoplastic and showed several fenestrations (Figure 3l-o). Both the atrial lumen and the lumen of the cardinal veins were dilated. The sinus venosus (Figure 4a) and separately the sinoatrial node (Figure 4b) myocardial volume, which was estimated by myocardial morphometry, showed a significant ($P<0.05$) decrease of myocardial volume in the knockout embryos compared to the wildtype embryos.

DISCUSSION

This study was conducted to elucidate the role of *podoplanin* in the development of the sinus venosus myocardium derived from the specific area of the second heart field which we have named PHF.[13,22] Previous studies have shown that mesodermal progenitor cells from the second heart field contribute to the formation and addition of myocardium both at the arterial and the venous pole of the developing heart.[10,13,14,40,41] Our observations are based on the study of the *podoplanin* gene and its protein expression in different embryonic stages during cardiac development. We have generated *podoplanin* knockout mouse embryos and used several immunohistochemical markers to study the mutants and wildtypes. We observed that the mutant embryos present severe cardiac malformations and show hypoplasia of the sinus venosus myocardium. These findings have consequences for the development and contribution of the PHF to the sinus venosus myocardium.

Sinoatrial node and venous valves

The sinoatrial node is a complex structure that plays a fundamental role in cardiac pacemaker activity.[28] Despite its essential role in cardiac conduction the origin of the sinoatrial node is still not well understood. Recently the formation and differentiation of the sinoatrial node at the venous pole of the heart has been described from the novel Nkx2.5 negative and Tbx18 positive precursor cells,[15] which were positive for podoplanin.[13] In the current study we report HCN4 expression in the podoplanin positive and Nkx2.5 negative sinoatrial node in accordance with observations in other studies.[15,30,42] The specific combination of Nkx2.5 negative and podoplanin and HCN4 positive expression in the sinoatrial node during early heart development is in contrast with the expression of these markers in the primary atrial myocardium. The latter suggests a different precursor for the sinoatrial node and the primary atrial myocardium. In contrast to the primary atrial myocardium, which derives from the primary heart field, the sinus venosus myocardium including the sinoatrial node originates from the second heart field,

as concluded from Isl1, Tbx3 and Tbx18 expression at the venous pole of the heart.[14,15,30,43] To clarify the functional role of *podoplanin* in the development of the sinus venosus myocardium we have studied *podoplanin* mutants and found a hypoplastic sinus venosus myocardium including the sinoatrial node and the venous valves. Another interesting gene involved in the development of the sinus venosus myocardium is *Shox2*.[21] *Shox2* mutants showed severe hypoplasia of the sinus venosus myocardium comparable to our observations in the *podoplanin* null mice. Moreover, the hypoplastic sinoatrial node in *Shox2* mutants showed aberrant expression of Cx43 combined with abnormal Nkx2.5 positivity. In contrast to the *Shox2* mutants, Nkx2.5 and Cx43 expression patterns remained unchanged in the *podoplanin* knockout mouse hearts, suggesting a different role for *podoplanin* in sinoatrial node / pacemaking development than *Shox2*. Electrophysiological experiments will be carried out to investigate possible arrhythmias in these mutants to solve the mentioned neonatal death.

Primary atrial septum and dorsal atrial wall

Lineage tracing experiments studying *Isl1*,[14] *Fgf 10*[10] and *Tbx5*,[44,45] *Tbx18*[15] and *Shox2*[21] have demonstrated the contribution of the second heart field at the venous pole to the formation of the atrial myocardium, which has a distinct molecular composition compared to the heart tube derived from the primary heart field.[10,14,46]

Podoplanin is expressed in PHF as well and not only stains the proepicardial organ derivatives but also the Nkx2.5 negative myocardium in the dorsal mesocardium.[13] This myocardium is supposed to form part of the dorsal atrial wall as well as the atrial septum. In the *podoplanin* mutant mouse this myocardium is hypoplastic, probably due to diminished PHF-derived myocardial contribution. Another option, is that abnormal epicardial-myocardial interaction plays a role in development of deficient myocardium as is seen in *SP3* mutant mouse.[47] We already described the deficient EPDC contribution in the *podoplanin* mutant.[22,23] Therefore, both the hypoplasia of the atrial septum as well as the dorsal atrial wall observed in the current study, are related to the altered contribution of myocardial and epicardial cells from the PHF.

Pulmonary and cardinal veins

A controversy regarding the development of the venous pole concerns the origin of the pulmonary vein. The pulmonary pit develops either in the dorsal mesocardium at the midline,[48-50] at the left[51] or the right[51-53] side of the embryo as a solitary unpaired structure that arises from the sinus venosus[51-53] or primitive atrium.[46,48,54] Recently, Männer and Merkel[55] have described the pulmonary pit as a bilaterally paired structure. We have described that the early common pulmonary vein is surrounded by Nkx2.5 mosaic cells, which are positive for MLC-2a and podoplanin.[13] Part of this myocardium has also been reported as mediastinal

myocardium.[54] The Nkx2.5 mosaic area forms a myocardial sleeve around the pulmonary vein extending to the atrial septum and Nkx2.5 negative cardinal veins in contrast to the primary atrial myocardium, which is completely Nkx2.5 positive. These data support the formation of the wall of the pulmonary vein to be from the surrounding mesodermal precursor cells at the dorsal mesocardium, which is postulated to derived from the PHF.[13] Concomitant with the higher proliferation rate of the pulmonary vein myocardium,[56] the Nkx2.5 mosaic area became Nkx2.5 positive in contrast to the sinoatrial node and cardinal vein myocardium that remained Nkx2.5 negative but HCN4 positive. This suggests a distinct differentiation rate of the pulmonary vein myocardium compared to the sinoatrial node and cardinal vein myocardium. At 15.5 dpc the cardinal vein myocardium became gradually positive for Nkx2.5, whereas the HCN4 expression was diminished suggesting the gradual completion of the differentiation process at the venous pole.

In the mutant embryos, the diminished myocardial contribution to the wall of the pulmonary vein and cardinal veins is evident. It is not clear whether MLC-2a and Nkx2.5 are directly regulated by *podoplanin* or whether this is due to altered addition of secondary myocardium from the PHF region by lack of *podoplanin*.

The role of podoplanin in EMT of the coelomic epithelium

EMT of the coelomic epithelium plays an important role in the addition of cells to the developing heart. An important feature of EMT is downregulation of cell-to-cell adhesion molecule E-cadherin,[35,57,58] which is correlated with *podoplanin*.[36] We have observed upregulation of E-cadherin in the coelomic cavity epithelium of the *podoplanin* knockout embryos. Regarding the addition of myocardium from the second heart field, the observed hypoplasia at the sinus venosus region might be caused by upregulated E-cadherin in the *podoplanin* knockout embryos, which causes abnormal EMT of the coelomic epithelium at specific sites of the sinus venosus myocardium.[22]

Moreover, *podoplanin* is involved in motility of cells where it colocalizes with the ezrin, radixin and moesin (ERM) protein family.[36,59] ERM proteins bind to the podoplanin ERM - binding site to activate RhoA, a member of the Rho GTPase protein family controlling a wide variety of cellular processes including proliferation, differentiation, cell morphology and motility.[60,61] The increased RhoA activity leads to '*podoplanin*-induced' EMT.[37] With regard to this mechanism, lack of *podoplanin* has resulted in diminished expression of RhoA protein, which may prevent the '*podoplanin*-induced' EMT with subsequent myocardial abnormalities of the venous pole.

Taken together, we show severe hypoplasia and myocardial abnormalities of the sinus venosus myocardium by lack of *podoplanin*. In addition, we postulate not only a common origin of

the sinoatrial node, dorsal atrial wall, atrial septum, pulmonary and cardinal veins deriving from the PHF, but also provide a link between the pulmonary vein and sinus venosus myocardium rather than the pulmonary vein and primary atrial myocardium.

Clinical implications

Parts of the cardiac conduction system derive from the second heart field, which may imply a role in the etiology of clinical syndromes. Several transgenic mice present with sick sinus syndrome, occurring in a familial form, are due to the lack of Ca^{2+} and other ion channels as well as gap junctions.[62] The dysfunctions include bradycardia, sinus dysrhythmia and sinus node exit block.[62] In our mutant embryos we have observed a hypoplastic sinoatrial node. While podoplanin is involved in water transport,[25] cationic, anionic and amino acid transport[63] and $Ca2^+$ dependent cell adhesiveness,[36] it is relevant to perform functional studies in these hearts in future to show dysfunctions such as bradycardia (sick sinus syndrome) comparable to *Shox2* mutants.[21]

Several studies suggested an embryonic background of atrial fibrillation originating from the pulmonary and caval veins, based on expression patterns of molecular and immunohistochemical markers.[50,64,65] In the current study we observed HCN4 expression in the sinoatrial node and in the myocardium of the wall of the cardinal veins and the pulmonary vein. In the mutant mice this population of HCN4 positive cells is diminished in the sinus venosus myocardium, which may provide a developmental background of arrhythmias originating from this area. Next to disturbances in cardiac conduction the observed deficient myocardial as well as epicardial contribution results in atrial and ventricular septal defects in addition to the already observed myocardial and coronary vascular abnormalities.[22]

REFERENCES

1. Deruiter MC, Poelmann RE, VanderPlas-de Vries, I, Mentink MM, Gittenberger-de Groot AC. The development of the myocardium and endocardium in mouse embryos. Fusion of two heart tubes? *Anat Embryol (Berl)*. 1992;185:461-473.
2. Moreno-Rodriguez RA, Krug EL, Reyes L, Villavicencio L, Mjaatvedt CH, Markwald RR. Bidirectional fusion of the heart-forming fields in the developing chick embryo. *Dev Dyn*. 2006;235:191-202.
3. Linask KK. N-cadherin localization in early heart development and polar expression of Na+,K(+)-ATPase, and integrin during pericardial coelom formation and epithelialization of the differentiating myocardium. *Dev Biol*. 1992;151:213-224.

4. Linask KK, Knudsen KA, Gui YH. N-cadherin-catenin interaction: necessary component of cardiac cell compartmentalization during early vertebrate heart development. *Dev Biol*. 1997;185:148-164.

5. Stalsberg H, DeHaan RL. The precardiac areas and formation of the tubular heart in the chick embryo. *Dev Biol*. 1969;19:128-159.

6. Viragh S, Challice CE. Origin and differentiation of cardiac muscle cells in the mouse. *J Ultrastruct Res*. 1973;42:1-24.

7. de la Cruz MV, Sanchez GC, Arteaga MM, Arguello C. Experimental study of the development of the truncus and the conus in the chick embryo. *J Anat*. 1977;123:661-686.

8. Waldo KL, Kumiski DH, Wallis KT, Stadt HA, Hutson MR, Platt DH, Kirby ML. Conotruncal myocardium arises from a secondary heart field. *Development*. 2001;128:3179-3188.

9. Kelly RG, Brown NA, Buckingham ME. The arterial pole of the mouse heart forms from Fgf10-expressing cells in pharyngeal mesoderm. *Dev Cell*. 2001;1:435-440.

10. Kelly RG. Molecular inroads into the anterior heart field. *Trends Cardiovasc Med*. 2005;15:51-56.

11. Mjaatvedt CH, Nakaoka T, Moreno-Rodriguez R, Norris RA, Kern MJ, Eisenberg CA, Turner D, Markwald RR. The outflow tract of the heart is recruited from a novel heart-forming field. *Dev Biol*. 2001;238:97-109.

12. Meilhac SM, Esner M, Kelly RG, Nicolas JF, Buckingham ME. The clonal origin of myocardial cells in different regions of the embryonic mouse heart. *Dev Cell*. 2004;6:685-698.

13. Gittenberger-de Groot AC, Mahtab EA, Hahurij ND, Wisse LJ, Deruiter MC, Wijffels MC, Poelmann RE. Nkx2.5-negative myocardium of the posterior heart field and its correlation with podoplanin expression in cells from the developing cardiac pacemaking and conduction system. *Anat Rec (Hoboken)*. 2007;290:115-122.

14. Cai CL, Liang X, Shi Y, Chu PH, Pfaff SL, Chen J, Evans S. Isl1 identifies a cardiac progenitor population that proliferates prior to differentiation and contributes a majority of cells to the heart. *Dev Cell*. 2003;5:877-889.

15. Christoffels VM, Mommersteeg MT, Trowe MO, Prall OW, de Gier-de Vries C, Soufan AT, Bussen M, Schuster-Gossler K, Harvey RP, Moorman AF, Kispert A. Formation of the venous pole of the heart from an Nkx2-5-negative precursor population requires Tbx18. *Circ Res*. 2006;98:1555-1563.

16. Saga Y, Miyagawa-Tomita S, Takagi A, Kitajima S, Miyazaki J, Inoue T. MesP1 is expressed in the heart precursor cells and required for the formation of a single heart tube. *Development*. 1999;126:3437-3447.

17. Martinsen BJ, Frasier AJ, Baker CV, Lohr JL. Cardiac neural crest ablation alters Id2 gene expression in the developing heart. *Dev Biol*. 2004;272:176-190.

18. Dodou E, Verzi MP, Anderson JP, Xu SM, Black BL. Mef2c is a direct transcriptional target of ISL1 and GATA factors in the anterior heart field during mouse embryonic development. *Development*. 2004;131:3931-3942.

19. Verzi MP, McCulley DJ, De VS, Dodou E, Black BL. The right ventricle, outflow tract, and ventricular septum comprise a restricted expression domain within the secondary/anterior heart field. *Dev Biol*. 2005;287:134-145.

20. Xu H, Morishima M, Wylie JN, Schwartz RJ, Bruneau BG, Lindsay EA, Baldini A. Tbx1 has a dual role in the morphogenesis of the cardiac outflow tract. *Development*. 2004;131:3217-3227.

21. Blaschke RJ, Hahurij ND, Kuijper S, Just S, Wisse LJ, Deissler K, Maxelon T, Anastassiadis K, Spitzer J, Hardt SE, Scholer H, Feitsma H, Rottbauer W, Blum M, Meijlink F, Rappold G, Gittenberger-de Groot AC. Targeted mutation reveals essential functions of the homeodomain transcription factor Shox2 in sinoatrial and pacemaking development. *Circulation*. 2007;115:1830-1838.

22. Mahtab EA, Wijffels MC, Van Den Akker NM, Hahurij ND, Lie-Venema H, Wisse LJ, Deruiter MC, Uhrin P, Zaujec J, Binder BR, Schalij MJ, Poelmann RE, Gittenberger-de Groot AC. Cardiac malformations and myocardial abnormalities in podoplanin knockout mouse embryos: Correlation with abnormal epicardial development. *Dev Dyn*. 2008;237:847-857.

23. Lie-Venema H, Van Den Akker NM, Bax NA, Winter EM, Maas S, Kekarainen T, Hoeben RC, Deruiter MC, Poelmann RE, Gittenberger-de Groot AC. Origin, fate, and function of epicardium-derived cells (EPDCs) in normal and abnormal cardiac development. *ScientificWorldJournal*. 2007;7:1777-1798.

24. Wetterwald A, Hoffstetter W, Cecchini MG, Lanske B, Wagner C, Fleisch H, Atkinson M. Characterization and cloning of the E11 antigen, a marker expressed by rat osteoblasts and osteocytes. *Bone*. 1996;18:125-132.

5

25. Williams MC, Cao Y, Hinds A, Rishi AK, Wetterwald A. T1 alpha protein is developmentally regulated and expressed by alveolar type I cells, choroid plexus, and ciliary epithelia of adult rats. *Am J Respir Cell Mol Biol*. 1996;14:577-585.

26. Breiteneder-Geleff S, Matsui K, Soleiman A, Meraner P, Poczewski H, Kalt R, Schaffner G, Kerjaschki D. Podoplanin, novel 43-kd membrane protein of glomerular epithelial cells, is down-regulated in puromycin nephrosis. *Am J Pathol*. 1997;151:1141-1152.

27. Schacht V, Ramirez MI, Hong YK, Hirakawa S, Feng D, Harvey N, Williams M, Dvorak AM, Dvorak HF, Oliver G, Detmar M. T1alpha/podoplanin deficiency disrupts normal lymphatic vasculature formation and causes lymphedema. *EMBO J*. 2003;22:3546-3556.

28. Boyett MR, Honjo H, Kodama I. The sinoatrial node, a heterogeneous pacemaker structure. *Cardiovasc Res*. 2000;47:658-687.

29. Liu J, Dobrzynski H, Yanni J, Boyett MR, Lei M. Organisation of the mouse sinoatrial node: structure and expression of HCN channels. *Cardiovasc Res*. 2007;73:729-738.

30. Mommersteeg MT, Hoogaars WM, Prall OW, de Gier-de Vries C, Wiese C, Clout DE, Papaioannou VE, Brown NA, Harvey RP, Moorman AF, Christoffels VM. Molecular pathway for the localized formation of the sinoatrial node. *Circ Res*. 2007;100:354-362.

31. Hay ED. The mesenchymal cell, its role in the embryo, and the remarkable signaling mechanisms that create it. *Dev Dyn*. 2005;233:706-720.

32. Moore AW, McInnes L, Kreidberg J, Hastie ND, Schedl A. YAC complementation shows a requirement for Wt1 in the development of epicardium, adrenal gland and throughout nephrogenesis. *Development*. 1999;126:1845-1857.

33. Perez-Pomares JM, Phelps A, Sedmerova M, Carmona R, Gonzalez-Iriarte M, Munoz-Chapuli R, Wessels A. Experimental studies on the spatiotemporal expression of WT1 and RALDH2 in the embryonic avian heart: a model for the regulation of myocardial and valvuloseptal development by epicardially derived cells (EPDCs). *Dev Biol*. 2002;247:307-326.

34. Carmona R, Gonzalez-Iriarte M, Perez-Pomares JM, Munoz-Chapuli R. Localization of the Wilm's tumour protein WT1 in avian embryos. *Cell Tissue Res*. 2001;303:173-186.

35. Cano A, Perez-Moreno MA, Rodrigo I, Locascio A, Blanco MJ, del Barrio MG, Portillo F, Nieto MA. The transcription factor snail controls epithelial-mesenchymal transitions by repressing E-cadherin expression. *Nat Cell Biol*. 2000;2:76-83.

36. Martin-Villar E, Scholl FG, Gamallo C, Yurrita MM, Munoz-Guerra M, Cruces J, Quintanilla M. Characterization of human PA2.26 antigen (T1alpha-2, podoplanin), a small membrane mucin induced in oral squamous cell carcinomas. *Int J Cancer*. 2005;113:899-910.

37. Martin-Villar E, Megias D, Castel S, Yurrita MM, Vilaro S, Quintanilla M. Podoplanin binds ERM proteins to activate RhoA and promote epithelial-mesenchymal transition. *J Cell Sci*. 2006;119:4541-4553.

38. Jongbloed MR, Wijffels MC, Schalij MJ, Blom NA, Poelmann RE, van der Laarse A, Mentink MM, Wang Z, Fishman GI, Gittenberger-de Groot AC. Development of the right ventricular inflow tract and moderator band: a possible morphological and functional explanation for Mahaim tachycardia. *Circ Res*. 2005;96:776-783.

39. Gundersen HJ, Jensen EB. The efficiency of systematic sampling in stereology and its prediction. *J Microsc*. 1987;147:229-263.

40. Lin L, Cui L, Zhou W, Dufort D, Zhang X, Cai CL, Bu L, Yang L, Martin J, Kemler R, Rosenfeld MG, Chen J, Evans SM. Beta-catenin directly regulates Islet1 expression in cardiovascular progenitors and is required for multiple aspects of cardiogenesis. *Proc Natl Acad Sci U S A*. 2007;104:9313-9318.

41. Moorman AF, Christoffels VM, Anderson RH, Van Den Hoff MJ. The heart-forming fields: one or multiple? *Philos Trans R Soc Lond B Biol Sci*. 2007;362:1257-1265.

42. Garcia-Frigola C, Shi Y, Evans SM. Expression of the hyperpolarization-activated cyclic nucleotide-gated cation channel HCN4 during mouse heart development. *Gene Expr Patterns*. 2003;3:777-783.

43. Hoogaars WM, Engel A, Brons JF, Verkerk AO, de Lange FJ, Wong LY, Bakker ML, Clout DE, Wakker V, Barnett P, Ravesloot JH, Moorman AF, Verheijck EE, Christoffels VM. Tbx3 controls the sinoatrial node gene program

and imposes pacemaker function on the atria. *Genes Dev*. 2007;21:1098-1112.

44. Bruneau BG, Logan M, Davis N, Levi T, Tabin CJ, Seidman JG, Seidman CE. Chamber-specific cardiac expression of Tbx5 and heart defects in Holt-Oram syndrome. *Dev Biol*. 1999;211:100-108.

45. Liberatore CM, Searcy-Schrick RD, Yutzey KE. Ventricular expression of tbx5 inhibits normal heart chamber development. *Dev Biol*. 2000;223:169-180.

46. Anderson RH, Brown NA, Moorman AF. Development and structures of the venous pole of the heart. *Dev Dyn*. 2006;235:2-9.

47. van Loo PF, Mahtab EA, Wisse LJ, Hou J, Grosveld F, Suske G, Philipsen S, Gittenberger-de Groot AC. Transcription factor Sp3 knockout mice display serious cardiac malformations. *Mol Cell Biol*. 2007;27:8571-8582.

48. Webb S, Brown NA, Wessels A, Anderson RH. Development of the murine pulmonary vein and its relationship to the embryonic venous sinus. *Anat Rec*. 1998;250:325-334.

49. Wessels A, Anderson RH, Markwald RR, Webb S, Brown NA, Viragh S, Moorman AF, Lamers WH. Atrial development in the human heart: an immunohistochemical study with emphasis on the role of mesenchymal tissues. *Anat Rec*. 2000;259:288-300.

50. Jongbloed MR, Schalij MJ, Poelmann RE, Blom NA, Fekkes ML, Wang Z, Fishman GI, Gittenberger-de Groot AC. Embryonic conduction tissue: a spatial correlation with adult arrhythmogenic areas. *J Cardiovasc Electrophysiol*. 2004;15:349-355.

51. Tasaka H, Krug EL, Markwald RR. Origin of the pulmonary venous orifice in the mouse and its relation to the morphogenesis of the sinus venosus, extracardiac mesenchyme (spina vestibuli), and atrium. *Anat Rec*. 1996;246:107-113.

52. Deruiter MC, Gittenberger-de Groot AC, Wenink AC, Poelmann RE, Mentink MM. In normal development pulmonary veins are connected to the sinus venosus segment in the left atrium. *Anat Rec*. 1995;243:84-92.

53. Blom NA, Gittenberger-de Groot AC, Jongeneel TH, Deruiter MC, Poelmann RE, Ottenkamp J. Normal development of the pulmonary veins in human embryos and formulation of a morphogenetic concept for sinus venosus defects. *Am J Cardiol*. 2001;87:305-309.

54. Soufan AT, Van Den Hoff MJ, Ruijter JM, de Boer PA, Hagoort J, Webb S, Anderson RH, Moorman AF. Reconstruction of the patterns of gene expression in the developing mouse heart reveals an architectural arrangement that facilitates the understanding of atrial malformations and arrhythmias. *Circ Res*. 2004;95:1207-1215.

55. Manner J, Merkel N. Early morphogenesis of the sinuatrial region of the chick heart: a contribution to the understanding of the pathogenesis of direct pulmonary venous connections to the right atrium and atrial septal defects in hearts with right isomerism of the atrial appendages. *Anat Rec (Hoboken)*. 2007;290:168-180.

56. Mommersteeg MT, Brown NA, Prall OW, de Gier-de Vries C, Harvey RP, Moorman AF, Christoffels VM. Pitx2c and Nkx2-5 are required for the formation and identity of the pulmonary myocardium. *Circ Res*. 2007;101:902-909.

57. Batlle E, Sancho E, Franci C, Dominguez D, Monfar M, Baulida J, Garcia De HA. The transcription factor snail is a repressor of E-cadherin gene expression in epithelial tumour cells. *Nat Cell Biol*. 2000;2:84-89.

58. Carmona R, Gonzalez-Iriarte M, Macias D, Perez-Pomares JM, Garcia-Garrido L, Munoz-Chapuli R. Immunolocalization of the transcription factor Slug in the developing avian heart. *Anat Embryol (Berl)*. 2000;201:103-109.

59. Scholl FG, Gamallo C, Vilaro S, Quintanilla M. Identification of PA2.26 antigen as a novel cell-surface mucin-type glycoprotein that induces plasma membrane extensions and increased motility in keratinocytes. *J Cell Sci*. 1999;112:4601-4613.

60. Hall A. Small GTP-binding proteins and the regulation of the actin cytoskeleton. *Annu Rev Cell Biol*. 1994;10:31-54.

61. Van Aelst, D'Souza-Schorey C. Rho GTPases and signaling networks. *Genes Dev*. 1997;11:2295-2322.

62. Dobrzynski H, Boyett MR, Anderson RH. New insights into pacemaker activity: promoting understanding of sick sinus syndrome. *Circulation*. 2007;115:1921-1932.

5

63. Boucherot A, Schreiber R, Pavenstadt H, Kunzelmann K. Cloning and expression of the mouse glomerular podoplanin homologue gp38P. *Nephrol Dial Transplant*. 2002;17:978-984.

64. Blom NA, Gittenberger-de Groot AC, Deruiter MC, Poelmann RE, Mentink MM, Ottenkamp J. Development of the cardiac conduction tissue in human embryos using HNK-1 antigen expression: possible relevance for understanding of abnormal atrial automaticity. *Circulation*. 1999;99:800-806.

65. Melnyk P, Ehrlich JR, Pourrier M, Villeneuve L, Cha TJ, Nattel S. Comparison of ion channel distribution and expression in cardiomyocytes of canine pulmonary veins versus left atrium. *Cardiovasc Res*. 2005;65:104-116.

Part II

Cardiac Development and Atrioventricular Reentry

Tachycardia

Nathan D. Hahurij[1, 2]
Denise P. Kolditz[2, 3]
Regina Bökenkamp[1]
Roger R. Markwald[4]
Martin J. Schalij[3]
Robert E. Poelmann[2]
Adriana C. Gittenberger-de Groot[2]
Nico A. Blom[1]

[1] Department of Pediatric Cardiology, Leiden University Medical Center, Leiden, The Netherlands.
[2] Department of Anatomy & Embryology, Leiden University Medical Center, Leiden, The Netherlands.
[3] Department of Cardiology, Leiden University Medical Center, Leiden, The Netherlands.
[4] Cardiovascular Developmental Biology Center, Children's Research Institute, Medical University of
  South Carolina, Charleston SC, USA.

6

Accessory atrioventricular myocardial pathways

in mouse heart development;

substrate for supraventricular tachycardias

ABSTRACT

Atrioventricular Reentry Tachycardia (AVRT) requiring an accessory atrioventricular pathway (AP) is the most common type of arrhythmia in the perinatal period. The etiology of these arrhythmias is not fully understood as well as their capability to dissipate spontaneously in the first year of life. Temporary presence of APs during annulus fibrosus development might cause this specific type of arrhythmias. To study the presence of APs electrophysiological recordings of ventricular activation patterns and immunohistochemical analyses with antibodies specifically against MLC-2a, Periostin, Nkx2.5 and Connexin-43 were performed in embryonic mouse hearts ranging from 11.5-18.5 days post conception (dpc). The electrophysiological recordings revealed the presence of functional APs in early (13.5-15.5 dpc) and late (16.5-18.5 dpc) post-septated stages of mouse heart development. These APs stained positive for MLC-2a and Nkx2.5 and negative for Periostin and Connexin-43. Longitudinal analyses showed that APs gradually decreased in number (*P*=0.003) and size (*P*=0.035) at subsequent developmental stages (13.5-18.5 dpc). Expression of periostin was observed in the developing annulus fibrosus, adjacent to APs and other locations where formation of fibrous tissue is essential. We conclude that functional APs are present during normal mouse heart development. These APs can serve as transient substrate for AVRTs in the perinatal period of development.

INTRODUCTION

In the fetus and newborn Atrioventricular (AV) Reentry Tachycardia (AVRT) is a relatively common tachyarrhythmia. AVRT requires the presence of an accessory AV pathway (AP) that crosses the isolating annulus fibrosus. Initial management of AVRT can be difficult but the natural course is benign and most children remain symptom free without medication after the age of one year.[1-3]

Annulus fibrosus formation plays a key role in the separation of atrial and ventricular myocardium in the AV canal[4] and encompasses interactions between several molecular pathways,[5,6] which have not yet been completely identified. Periostin, a member of the fascilin gene family,[7] is highly expressed in collagen rich-fibrous connective tissue in the developing heart that is subjected to high mechanical stress.[8,9] Recently, it has been revealed that periostin directly regulates collagen-I fibrillogenesis.[8] The inductive role of periostin on fibrous tissue formation seems to be of special interest in annulus fibrosus anlage.[10,11]

In mature hearts the atrial and ventricular myocardium are electrically separated in two myocardial compartments, which are interconnected via the AV conduction axis i.e. the AV node and bundle of His.[5] At early embryonic stages however, the atrial and ventricular

myocardium are continuous in the primitive AV canal establishing a ventricular base-to-apex activation pattern. At later stages, ventricular conduction transforms into the mature apex-to-base activation. The switch from ventricular base-to-apex in apex-to-base activation is suggested to be closely related to the completion of ventricular septation and annulus fibrosus development.[12,13] Nevertheless, contemporary electrophysiological studies in embryonic mouse hearts have shown that before ventricular septation is completed a mature apex-to-base activation is already present, suggesting that the AV conduction axis is functional far before ventricular septation has finished.[14,15]

It has been hypothesized that temporary persistence of the embryonic AV myocardial continuity during annulus fibrosus development might serve as APs. Consequently, these transient APs may provide the substrate for AVRT in the perinatal period and explain its self-limiting character. Studies in avian demonstrated that antegrade conducting APs are present at late post-septated stages of heart development, which gradually diminish during fetal life.[12] In mammalian hearts,[15,16] including human,[17,18] APs have also been described throughout cardiac development. Thus far, the description of APs in mammals mainly focused on the electrophysiological properties of primitive AV canal myocardium in pre-septated hearts[15] and neither late stages of fetal heart development nor the exact course of APs at the developing annulus fibrosus were provided.

The current study for the first time describes the presence of "functional" APs in early and late post-septated stages of mouse heart development. Furthermore, we show that periostin is highly expressed in the developing annulus fibrosus at locations where separation of atrial and ventricular myocardium is mandatory.

MATERIAL AND METHODS

Animals and preparation of hearts

Animal experiments were approved by the Institutional Animal Care and Use Committee of the Leiden University Medical Center. Embryonic hearts were obtained from two separate wildtype mouse strains, C57Bl6/Jico and CD1. The presence of a vaginal plug one day after breeding was considered to be 0.5 days post conception (dpc). Embryos of subsequent stages were used, ranging from 11.5-18.5 dpc (n=48). After cervical dislocation of the pregnant mouse, the uterus horns containing the embryos were harvested and placed in a Petri dish filled with Tyrode's solution containing in mmol/L: 130 NaCl, 4 KCL, 1.2 KH_2PO_4, 0.6 $MgSO_4 \cdot 7H_2O$, 20 $NaHCO_3$, 1.5 $CaCL_2 \cdot 2H_2O$ and 10 glucose (chemicals derive from: Merck, Darmstad, Germany) at 37°Celsius (°C). Subsequently, in Tyrode's solution of 0°C one-by-one the embryonic hearts were dissected.

Electrophysiologic recordings

In the electrophysiology setup the embryonic hearts were attached with fine wires through extra-cardiac tissue in a fluid heated, temperature controlled (Physitemp instruments Inc, Clifton, NJ, USA) Petri dish of 35.5-37°C onto a layer of agarose gel (Roche Diagnostics, Mannheim, Germany). During the 3 minute equilibration period and subsequent electrophysiological recordings the hearts were constantly super-perfused with Carbogenated (95% O_2 and 5% CO_2) Tyrode's solution at 37°C. Unipolar tungsten electrodes (tip: 1-2μm; impedance 0.9-1.0MΩ; WPI Inc, Sarasota, FL, USA) were positioned on the right atrium (RA), right ventricular base (RVB), left ventricular base (LVB) and left ventricular apex (LVA) (Figure 1), using microscopic guided micromanipulators (Wild Heerbrugg, M7A, Switzerland). An Ag/AgCl electrode in the Petri dish served as reference electrode.

All electrograms were recorded under stable sinus rhythm with a high-gain, low-noise, direct-current bioamplifier system (Iso-DAM8A; WPI Inc, Berlin, Germany) with 4 isolated preamplifier modules with an output impedance of $>10^{12}$ Ω. The signals were band-passed (300Hz-1kHz) and notch filtered (50Hz) before being digitized at a sample rate of $1\geq$ kHz with a computerized recording system (Prucka Engineering Inc, Houston, Tex, USA) and stored on optical disks for offline analysis.
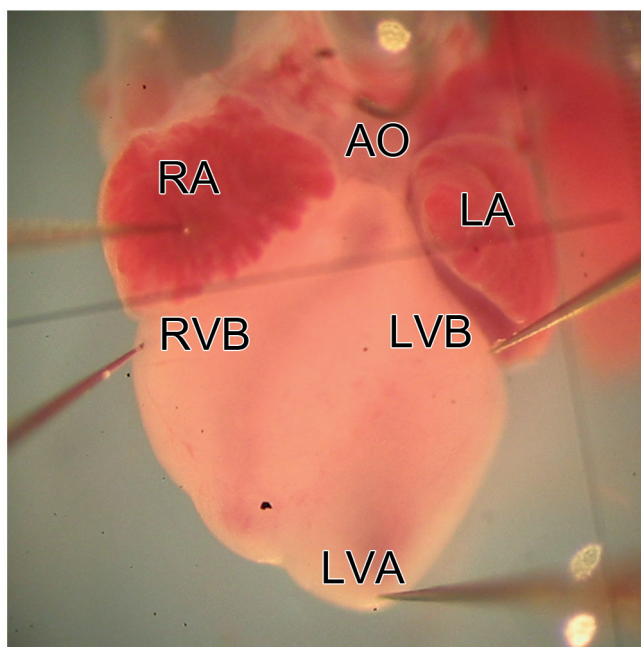

Figure 1. Positioning of the unipolar electrodes for electrophysiological recordings. Four Tungsten electrodes were placed on the epicardial surface of the embryonic hearts, at the right atrium (**RA**), right ventricular base (**RVB**), left ventricular base (**LVB**) and left ventricular apex (**LVA**); **AO** indicates Aorta.

The basal cycle length / Heart Rate (HR) of each heart and local depolarization time of each electrode, defined as maximal negative deflection on the unipolar electrogram, were calculated by the average of 10 consecutive beats. Subsequently, ventricular activation patterns of each heart were determined: base-to-apex if the RVB or LVB depolarized 1≥ ms prior to the LVA; apex-to-base if the LVA depolarized 1≥ ms prior to the RVB or LVB; concurrent if the depolarization time between the LVA and LVB or RVB was <1 ms. After recordings all hearts were fixed in 4% paraformaldehyde for immunohistochemical processing.

Immunohistochemistry and Immunofluoresence
Standard immunohistochemistry was performed with: 1/2000 atrial myosin light chain 2 (MLC-2a, gift from S.W. Kubalak, Charleston, SC, USA), 1/1000 Periostin (R.R. Markwald, Charleston, SC, USA) and 1/200 Connexin-43 (Cx43, Sigma, C6219, St. Louise, MO, USA) specific antibodies. Immunofluorescent double staining procedures were performed combining 1/250 periostin and 1/2000 NK2 transcription factor related locus 5 (Nkx2.5, Santa Cruz Biotechnology, sc-8697, Heidelberg, Germany) specific antibodies. Detailed description of the staining procedures can be found in previous publications.[10-12]

Morphology and Statistics
All hearts were studied for the presence of APs including their location at the developing annulus fibrosus using an Olympus BH-2 lighting microscope. AP-width was calculated by counting the number of subsequent MLC-2a stained sections through which a single accessory connection could be followed and multiplied by 25 μm (distance between subsequent MLC-2a stained sections).

Statistical analysis of HR and AV conduction time was performed with a students-t-test if values were equally distributed (skewness is |-1|) otherwise a Mann-Whitney U test was used. Analyses of AP-number and AP-width were performed with a univariate analyses of variance (unianova). A P value of <0.05 (2-tailed) was considered to be significant. The SPSS15.0 software package (SPSS Inc, Chicago, Ill, USA) was used for all analyses.

RESULTS

Electrophysiological recordings
Pre-septated hearts (11.5-13.5 dpc; n=6)
The mean recorded HR in pre-septated hearts was 94±24 beats per minute (bpm) with a mean AV interval of 84±13 ms. Comparable to previous studies,[14,15] most pre-septated hearts (67%) already showed LVA activation prior to RVB or LVB activation,

indicating that the AV conduction axis is functional before ventricular septation has been completed. In 2 hearts concurrent ventricular apex and base activation patterns were observed (Table 1).

Early post-septated hearts (13.5-15.5 dpc; n=29)

In early post-septated hearts a mean HR of 115±41 bpm was recorded with a mean AV interval of 80±17 ms. Interestingly, only 38% of early post-septated hearts showed an apex-to-base ventricular activation pattern, the largest group showed base-to-apex and concurrent ventricular activation patterns (62%). Concurrent apex and base activation was recorded in the majority of early post-septated hearts (48%). More detailed analyses of concurrent activated hearts showed that in most of these hearts (41%) concurrent activation occurred between the LVB and LVA. In two hearts (7%) the RVB was activated prior to the LVA and also in two hearts (7%) the LVB was activated prior to LVA (Table 1). Statistical analyses of AV conduction time showed no significant differences (*P*=NS) between the mean AV conduction time in apex-to-base (78±12 ms; n=11) and base-to-apex and concurrent (81±20 ms; n=14) activated hearts.

Table 1. Summary of ventricular activation patterns in pre-, early post- and late post-septated hearts

Group,age,(n)	HR (bpm) mean±SD (range)	AV-interval (ms) mean±SD (range)	Ventricular Activation pattern n (%)	
Pre-septated 11.5-13.5dpc (n=6)	94±24 (66-135)	83±13 (64-105)	LVA>LVB/RVB	4 (67)
			Concurrent	2 (33)
			LVA=RVB	2 (33)
Early post-septated 13.5-15.5dpc (n=29)	115±41 (67-246)	80±17 (44-112)	LVA>LVB/RVB	11 (38)
			LVB>LVA	2 (7)
			RVB>LVA	2 (7)
			Concurrent	14 (48)
			LVA=LVB	12 (41)
			LVA=RVB	2 (7)
Late post-septated 16.5-18.5dpc (n=13)	95±27 (63-146)	81±18 (56-110)	LVA>LVB/RVB	6 (46)
			LVB>LVA	4 (31)
			RVB>LVA	1 (8)
			Concurrent	2 (15)
			LVA=LVB	2 (15)

Late post-septated hearts (16.5-18.5 dpc; n=13)

The mean HR recorded in these hearts was 95±27 bpm with a mean AV interval of 81±18 ms. A mature apex-to-base activation pattern was observed in only 46% of the hearts (n=6). In a relatively large group of hearts activation of the LVB prior to the LVA was recorded (31%). Concurrent apex and base activation was observed in 15%, by which concurrent activation only occurred between the LVB and LVA. Furthermore, activation of the RVB prior to the LVA was observed in one heart (Table 1). Analyses of the mean AV conduction time showed no significant difference (*P*=NS) in apex-to-base (80±22 ms; n=6) and base-to-apex and concurrent (82±16 ms; n=7) activated hearts.

Examples of unipolar-electrophysiological recordings of apex-to-base, base-to-apex and concurrent activated hearts are shown in Figures 2 and 3.

APs during cardiac development

In all pre-septated hearts (n=6) the MLC-2a stained sections showed a myocardial continuity between the atria and ventricles over the primitive AV canal. At several locations in the left and right AV ring separation of atrial and ventricular myocardium by the developing annulus fibrosus was observed (Figure 4a, b, d). The primitive ventricular septum was already present at 11.5 dpc and ventricular septation was completed between 13.5-14.5 dpc. At the dorsal side of the heart a broad myocardial continuity between the atria and ventricles was observed i.e. the AV conduction axis (data not shown).
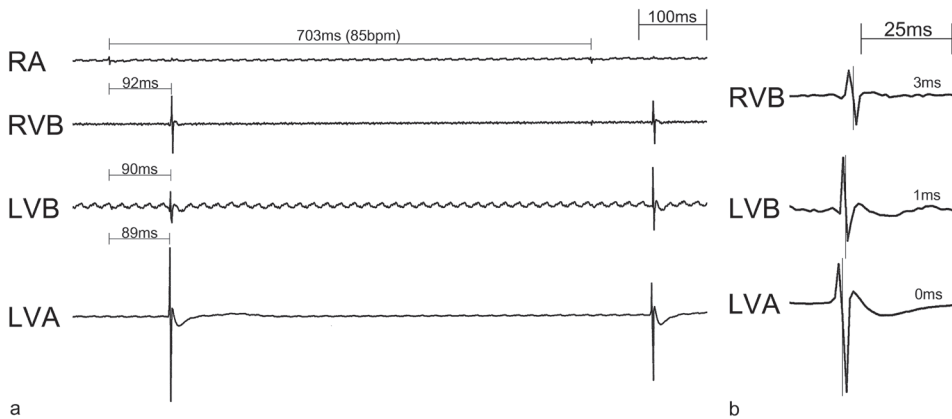

Figure 2. Representative electrophysiological recording of an Apex-to-Base activated heart. (a) Recording of an early post-septated embryonic heart of 13.5 dpc with a cycle length of 703 ms (85 bpm). The left ventricular apex (**LVA**) is activated 89 ms after the right atrium (**RA**), followed by the left ventricular base (**LVB**; 90 ms) and right ventricular base (**RVB**; 92 ms). (b) Magnification of ventricular activation patterns, showing that the maximal negative deflection at the LVA precedes 1 ms prior to LVB and 3 ms prior to RVB activation, thereby creating a ventricular apex-to-base activation.

At 12.5 dpc expression of Cx43 was present in the working myocardium of both atria and ventricles, whereas Cx43 expression was absent in the myocardium of the complete AV canal (Figure 4c, e).
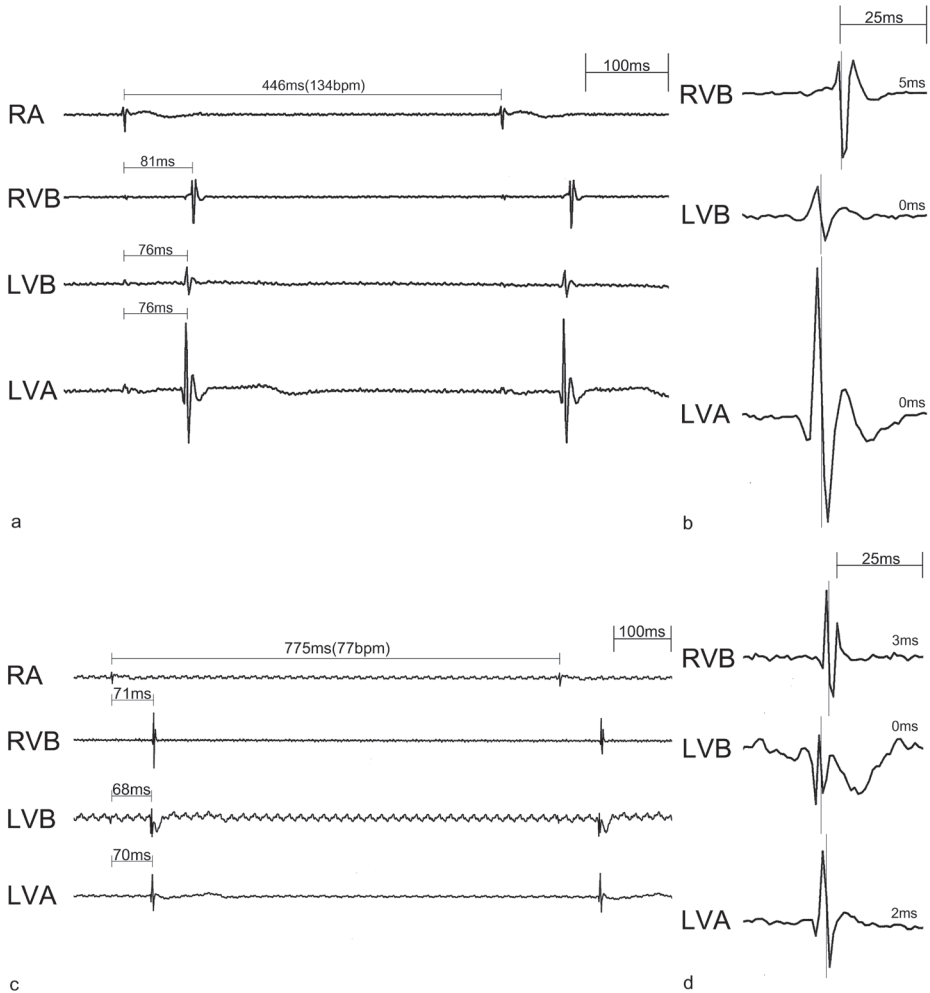

Figure 3. Representative electrophysiological recordings of concurrent Apex and Base and Base-to-Apex activated hearts. (a) Recording of an early post-septated heart of 15.5 dpc with a cycle length of 446 ms (134 bpm). 76 ms after right atrial (**RA**) activation, first ventricular activation occurs at both the left ventricular apex (**LVA**) and left ventricular base (**LVB**), followed by right ventricular base (**RVB**) activation (81 ms). (b) Magnification of ventricular activation patterns, showing that the maximal negative deflection of the RVB is 5 ms after LVA and LVB activation. Consequently this heart shows a concurrent LVA and LVB activation pattern. (c) Recording of a late post-septated heart of 16.5 dpc with a cycle length of 775 ms (77 bpm). First ventricular activation was observed 68 ms after RA activation at the LVB. Subsequently, the LVA and RVB were activated at 70 ms and 71 ms, respectively. (d) Magnification of ventricular activation patterns, indicating that the maximal negative deflection at the LVB precedes 2 ms prior to LVA and 3 ms prior to RVB activation, thereby creating a base-to-apex ventricular activation.

In all early post-septated hearts (13.5-15.5 dpc; n=29) APs were found around both the mitral and tricuspid orifice of the AV canal. Some of the APs consisted of a single strand of cardiomyocytes whereas others comprised broad myocardial continuities. At these stages Cx43 was clearly present in the working myocardium of the atria and ventricles, however all APs were negative for Cx43 (Figure 4g, h). At early post-septated stages APs were more often located around the mitral orifice (63%; *P*=0.000), and analyses of the AP-width also showed a larger mean total AP-width at that specific region (*P*=0.000) (Table 2). Interestingly, in almost all early post-septated hearts (24/29) a broad Cx43 negative AP was present at the antero-lateral position of the left AV junction connecting the left atrial myocardium and left ventricular myocardium along its free wall (Figure 4f-h).

In all late post-septated hearts (16.5-18.5 dpc; n=13) APs were still observed around the mitral and tricuspid orifice. The expressions pattern of Cx43 was similar as compared to earlier stages and all APs were still Cx43 negative (data not shown). Although the mean total AP-width at these stages was largest at the mitral orifice (*P*=0.028), no differences were found between the mean number of APs at the mitral and tricuspid orifice (*P*=NS). Compared to earlier stages the mean number of APs per heart around the mitral orifice had decreased significantly (*P*=0.000), whereas no significant decrease was observed at the tricuspid orifice (*P*=0.136) (Table 2). Furthermore, the antero-lateral AP at the left AV junction was present in all hearts (13/13).

Longitudinal analyses of AP-number and AP-width in all post-septated hearts of subsequent developmental stages (13.5-18.5 dpc; n=42) showed significant decrease both in mean number of APs (*P*=0.003) (Figure 5) and mean total AP-width (*P*=0.035).

Table 2. Summary of morphological analyses of APs in early and late post-septated hearts.

	Early post-septated 13.5-15.5dpc (n=29)	Late post-septated 16.5-18.5dpc (n=13)	Statistics (early vs late)
Mean number of APs	8.1	5.2	P=0.003
Mean number left sided APs	5.1	3.1	P=0.000
Mean number right sided APs	3.0	2.1	*P*=NS
Statistics mean AP number (left vs right)	*P*=0.000	*P*=NS	-
Mean width (μm) of APs	347	214	P=0.035
Mean width (μm) left sided APs	238	138	P=0.000
Mean width (μm) right sided APs	109	76	*P*=NS
Statistics mean AP-width (left vs right)	*P*=0.000	*P*=0.028	-

Furthermore, differences were observed in the rate by which APs disappeared around the mitral and tricuspid orifice, which appeared significantly faster at the left side of the AV junction (*P*=0.015).

Periostin expression in relation to annulus fibrosus development and APs

Expression of periostin was present in all embryonic and fetal stages (11.5-18.5 dpc) and specifically limited to the epicardium, the endothelial lining of atrial and ventricular trabeculae, the subendocardial region of both outflow and AV cushions and the interstitial fibroblasts flanked by working myocardium in the atria and ventricles. At later stages (>14.5 dpc) strong expression was also observed in the AV cushion derived AV valves including their tension apparatus as well as in the endothelial lining of the developing coronary vessels.
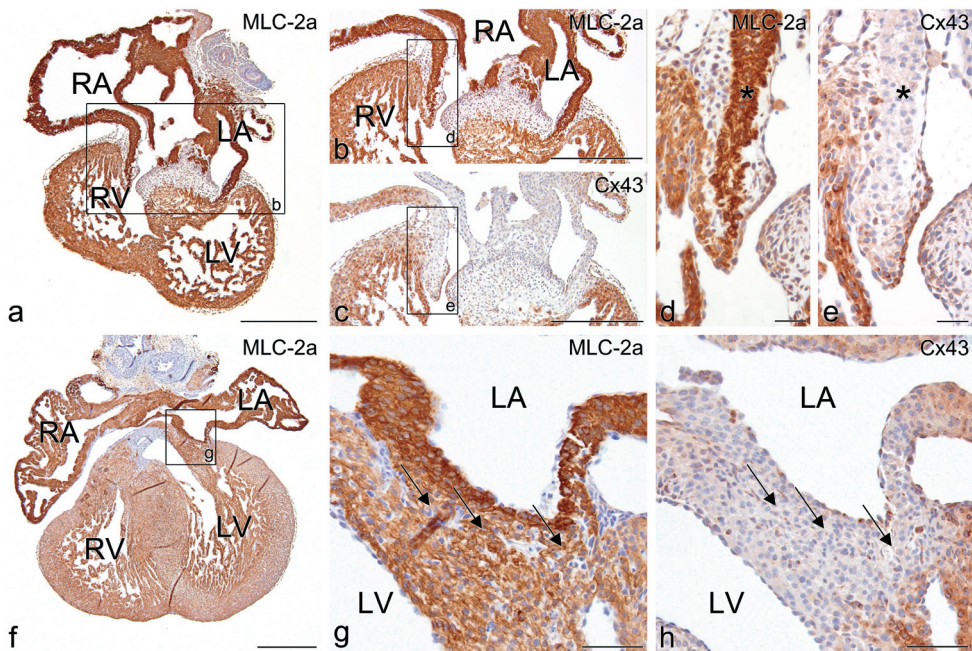

Figure 4. Connexin-43 (Cx43) expression in the AV junction in pre- and post-septated hearts. (a) Frontal MLC-2a stained section of a pre-septated heart of 12.5 dpc. In the AV junctional area (b magnification of boxed area in a) Cx43 expression was absent (c consecutive section of a), whereas Cx43 was clearly present in the working myocardium of atria and ventricles (c). (d) And (e) magnifications of boxed areas in (b) and (c) respectively, show details of the right AV junctional myocardium positive for MLC-2a (**asterisk** in d) and negative for Cx43 (**asterisk** in e). (g) Frontal section of a 15.5 dpc MLC-2a stained heart. (g) Magnification of boxed area in (f) shows the large antero-lateral AP observed in n=37 of total n=42 post-septated hearts. **Arrows** in (g) indicate the exact locations of myocardial AV connections. The myocardium of the AV junction including these connections is negative for Cx43 (**arrows** in h). **RV** indicates right ventricle; **LA**, left atrium; **LV**, left ventricle; Scale bars: (a-c) and (f) = 300µm; (d), (e) = 30µm; (g), (h) = 60µm.

Remarkably, periostin was absent in parts of the AV conduction axis, especially in the atrioventricular node (data not shown). Periostin expression was clearly present in the developing annulus fibrosus. Strongest expression was observed at the immediate border between the developing annulus fibrosus and AV canal myocardium (Figure 6a-c, g-i). Furthermore, high expression of periostin seemed to overlap with the MLC-2a positive APs around both the mitral and tricuspid orifice (Figure 6i).

Immunofluorescent double stained sections with periostin and Nkx2.5 were used to study the developing annulus fibrosus in relation to the AP cardiomyocytes (Figure 6d-f, j-l). At all developmental stages periostin was strongly expressed in fibroblasts bordering AP cardiomyocytes (11.5-18.5 dpc), however no periostin expression could be demonstrated in Nkx2.5 positive cardiomyocytes themselves (Figure 6f, l).

At early post-septated stages (13.5 dpc) low periostin expression was observed at the anterior side of the left AV junction in almost all hearts, corresponding to the location of the left antero-lateral APs. These broad APs were positive for the myocardial markers MLC-2a and Nkx2.5 but negative for periostin (Figure 6a-f). At later post-septated stages (>16.5 dpc), expression of periostin increased at these specific areas (Figure 6g-l).
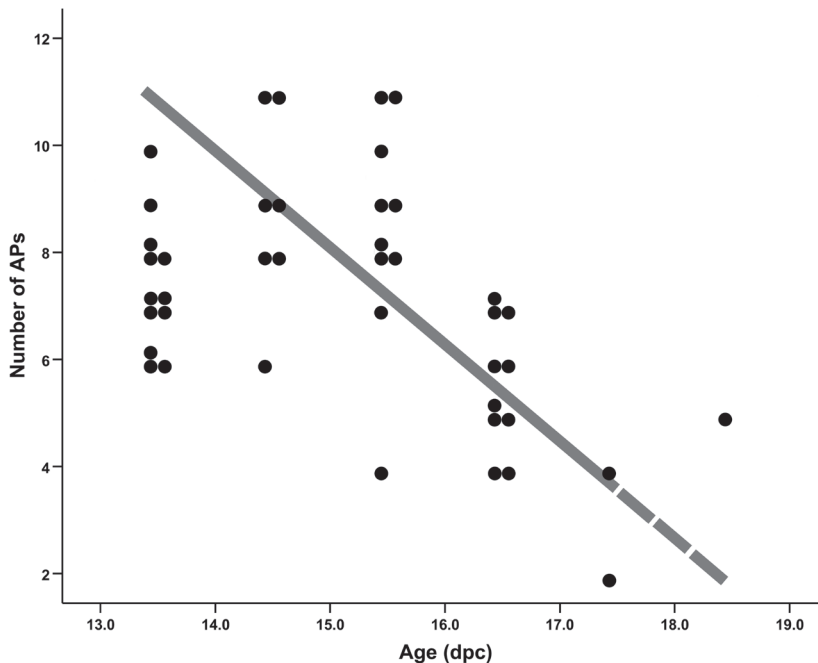

Figure 5. The course of APs in post-septated mouse hearts. The graph schematically represents the course of APs around both the developing tricuspid and mitral valve orifice in post-septated mouse hearts (n=42). Each black circle represents a heart in which a specific number of APs was observed as indicated on the Y-axis, at subsequent developmental stages (X-axis). The gray transparent line indicates the hypothesized course of APs at the developing annulus fibrosus.
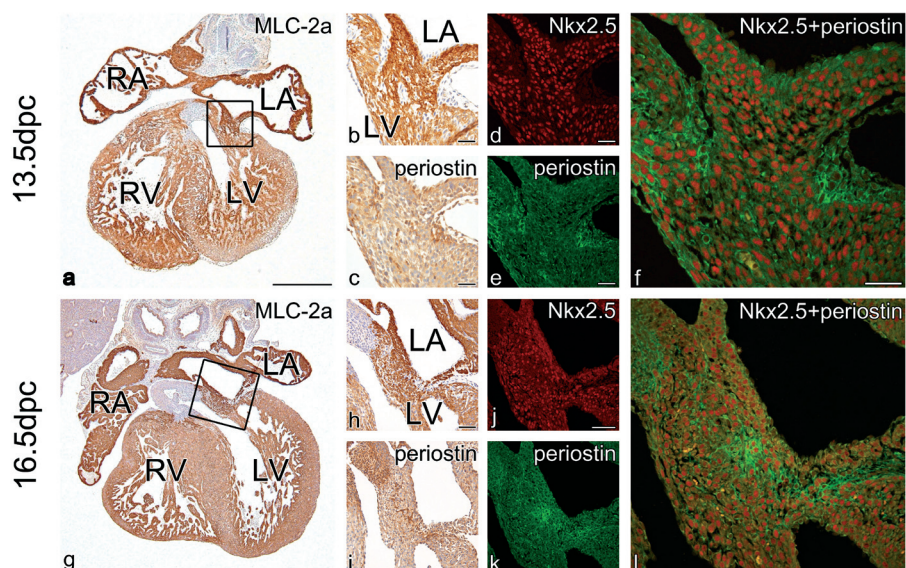
Figure 6. Nkx2.5 and periostin double expression in the developing annulus fibrosus and persistent APs. (a) Frontal MLC-2a stained section of an early post-septated heart of 13.5 dpc. The boxed area in (a) shows a left sided antero-lateral AP magnified in (b). Periostin expression was observed next to the MLC-2a positive AP (c consecutive of a). An immunofluorescent double-stained section shows that this AP (f consecutive section of a) was positive for Nkx2.5 (d) and negative for periostin (e). (g) Frontal section of almost the same area in (a) of a late post-septated MLC-2a stained heart of 16.5 dpc. (h) Magnification of the boxed area in (g), showing an MLC-2a positive AP, which also is positive for periostin (i consecutive section of g). Compared to early post-septated stages (f), this AP (l immunofluorescent consecutive section of a) is comprised of an intermingling network of Nkx2.5 positive cardiomyocytes (j) and periostin positive fibroblasts (k). **RV** indicates right ventricle; **RA**, right atrium; **LA**, left atrium; **LV**, left ventricle; Scale bars: (a), (g) = 300µm; (b-f) = 30µm; (h-l) = 60µm.

DISCUSSION

AVRT is a relatively common tachyarrhythmia in fetuses and neonates that appears to resolve in the majority of cases during the first year of life.[1,2] It has been suggested that APs involved in these tachycardias are remnants of the primary AV canal myocardium, which disappear during development and maturation of the annulus fibrosus before and after birth.[12,18] Although presence of APs has been demonstrated during normal cardiac development in human fetuses and neonates, their etiology and conducting properties as well as their causative role in AVRT are largely unrevealed.[17-20] It is known that APs can be associated with congenital heart disease specifically with abnormal tricuspid valve development like in Morbus Ebstein.[21] In a minority of cases genetic mutations are involved,[22,23] like *PRKAG2* in familial Wolff-Parkinson-White pre-excitation syndrome[24] or in *Alk3* which results in a disrupted annulus fibrosus with Cx43 positive APs in mouse.[5]

AP location in relation to arrhythmias

The conducting properties of the primitive AV canal myocardium has recently been demonstrated in mouse embryos.[15] Here we show that annulus fibrosus development occurs near the Cx43 negative AV canal myocardium.[25] Furthermore, the presence of antegrade conducting Cx43 negative APs were demonstrated, which significantly decreased in number and size along normal mouse heart development, but sometimes remained present at late post-septated stages (Figure 5).

Recently, similar APs were demonstrated during normal quail heart development, where most APs were found at the postero-septal aspect of the tricuspid valve orifice.[12] In contrast, we demonstrated the majority of APs at the antero-lateral aspect of mitral orifice in mouse. In quail the preferential location of right postero-septal APs might be explained by the physiological delay of right ventricular inflow tract formation with prolonged isolation of this part of the annulus fibrosus.[16] This might also shed light on the observation that occasionally right sided APs directly penetrate through the annulus fibrosus, whereas left sided APs rather more frequently skirt the annulus and have a more epicardial position as observed in autopsy studies of human Wolff-Parkinson-White syndrome.[26] It seems tempting to postulate that APs, which directly penetrate the isolating annulus, as observed in the current study, are related to normal AV junction isolation and disappear along fetal and early postnatal life.

Interestingly, the left antero-lateral APs observed in late post-septated embryonic mouse hearts have been reported in studies on cardiac conduction system (CCS) development by means of CCS-*lacZ* expression. Bundles of *lacZ* expressing cardiomyocytes were observed at the same left antero-lateral position at the developing AV junction, which did not form part of the developing CCS. In some hearts these bundles could be traced until postnatal stages and have been related to Wolff-Parkison-White syndrome.[14]

Differences with respect to morpho-histology and electrophysiology were noticed between the mitral and tricuspid valve orifice. In early post-septated hearts a significant majority of APs were observed around the mitral valve orifice, and also the largest total AP-width was found in this area both in early and late post-septated hearts. These histological findings seem to correlate with the electrophysiological recordings showing that in the majority of base-to-apex activated post-septated hearts, the LVB (and not the RVB) is activated prior or concurrent to the LVA. However, a coincidental relationship can not be expelled, since a direct relation between morphologically observed APs and their individual ability to conduct could not be made.[12] Especially at early post-septated stages multiple APs are present of which some might act as innocent bystanders i.e. not able to conduct.

Recently, we demonstrated the presence of APs during human heart development, which also decreased along embryonic and fetal life.[18] It remains to be determined whether these physiological APs in human are functional and can form the substrates for AVRT. Interestingly, APs involved in AVRT are more often located around the mitral valve orifice,[27]

which seems to correspond to the high frequency of conducting left sided APs as observed in the current study.

Periostin expression in relation to annulus fibrosus formation and persistent APs

Periostin is expressed in the developing annulus fibrosus,[12,18] specifically at locations where separation of atrial and ventricular myocardium is needed. At these regions periostin might induce formation of isolating fibrous tissue, since it directly regulates collagen-I fibrillogenesis.[8]

The broad Cx43 negative antero-lateral APs around the mitral orifice, which most probably have an imperative role in the large group of early LVB and concurrent activated hearts, were predominantly periostin negative at early post-septated stages. This seems to indicate that only APs negative for periostin are able to conduct, which correspond to recent findings of electrophysiological studies in neonatal mouse hearts.[5] At later stages, periostin expression increases near the left antero-lateral APs suggesting an active process of isolation in that particular region. Interestingly, annulus fibrosus formation is not strictly limited to the prenatal stages, since contemporary studies demonstrated that formation of the fibrous structures of the heart extends into early postnatal development.[28,29] Therefore, we postulate that periostin has an important role in AV junction isolation by stimulation of fibrous tissue formation, thereby separating atrial and ventricular myocardium, which subsequently will lead to regression of conducting APs pre- and postnatally.

The regulation of periostin and the exact way it contributes in annulus fibrosus formation remains to be elucidated. However, it has been demonstrated that several growth factors including BMPs,[30] TGF-β[7] and PDGFs[31] are involved, which are highly expressed in the developing AV region. In addition, state-of-art studies performed in avian hearts indicated that epicardium derived cells play a key role in periostin regulation involved in annulus fibrosus development. Inhibition of early epicardial outgrowth, resulted in a disturbed annulus fibrosus development coinciding with a high frequency of periostin negative antegrade conducting APs.[10,11]

CONCLUSION

The current study demonstrates that antegrade conducting APs, which are remnants of Cx43 negative primitive AV canal myocardium, remain present until late fetal stages of normal mouse heart development. These conducting APs can act as substrate for AVRT. Ongoing formation and maturation of the annulus fibrosus in which periostin appears to have an important role, may explain spontaneous resolution of these arrhythmias in fetuses and neonates.

REFERENCES

1. Bauersfeld U, Pfammatter JP, Jaeggi E. Treatment of supraventricular tachycardias in the new millennium-drugs or radiofrequency catheter ablation? *Eur J Pediatr*. 2001;160:1-9.

2. Ko JK, Deal BJ, Strasburger JF, Benson DW, Jr. Supraventricular tachycardia mechanisms and their age distribution in pediatric patients. *Am J Cardiol*. 1992;69:1028-1032.

3. Naheed ZJ, Strasburger JF, Deal BJ, Benson DW, Jr., Gidding SS. Fetal tachycardia: mechanisms and predictors of hydrops fetalis. *J Am Coll Cardiol*. 1996;27:1736-1740.

4. Wessels A, Markman MW, Vermeulen JL, Anderson RH, Moorman AF, Lamers WH. The development of the atrioventricular junction in the human heart. *Circ Res*. 1996;78:110-117.

5. Gaussin V, Morley GE, Cox L, Zwijsen A, Vance KM, Emile L, Tian Y, Liu J, Hong C, Myers D, Conway SJ, Depre C, Mishina Y, Behringer RR, Hanks MC, Schneider MD, Huylebroeck D, Fishman GI, Burch JB, Vatner SF. Alk3/Bmpr1a receptor is required for development of the atrioventricular canal into valves and annulus fibrosus. *Circ Res*. 2005;97:219-226.

6. Okagawa H, Markwald RR, Sugi Y. Functional BMP receptor in endocardial cells is required in atrioventricular cushion mesenchymal cell formation in chick. *Dev Biol*. 2007;306:179-192.

7. Horiuchi K, Amizuka N, Takeshita S, Takamatsu H, Katsuura M, Ozawa H, Toyama Y, Bonewald LF, Kudo A. Identification and characterization of a novel protein, periostin, with restricted expression to periosteum and periodontal ligament and increased expression by transforming growth factor beta. *J Bone Miner Res*. 1999;14:1239-1249.

8. Norris RA, Damon B, Mironov V, Kasyanov V, Ramamurthi A, Moreno-Rodriguez R, Trusk T, Potts JD, Goodwin RL, Davis J, Hoffman S, Wen X, Sugi Y, Kern CB, Mjaatvedt CH, Turner DK, Oka T, Conway SJ, Molkentin JD, Forgacs G, Markwald RR. Periostin regulates collagen fibrillogenesis and the biomechanical properties of connective tissues. *J Cell Biochem*. 2007;101:695-711.

9. Kruzynska-Frejtag A, Machnicki M, Rogers R, Markwald RR, Conway SJ. Periostin (an osteoblast-specific factor) is expressed within the embryonic mouse heart during valve formation. *Mech Dev*. 2001;103:183-188.

10. Kolditz DP, Wijffels MC, Blom NA, van der Laarse A, Hahurij ND, Lie-Venema H, Markwald RR, Poelmann RE, Schalij MJ, Gittenberger-de Groot AC. Epicardium-derived cells in development of annulus fibrosus and persistence of accessory pathways. *Circulation*. 2008;117:1508-1517.

11. Lie-Venema H, Eralp I, Markwald RR, Van Den Akker NM, Wijffels MC, Kolditz DP, van der Laarse A, Schalij MJ, Poelmann RE, Bogers AJ, Gittenberger-de Groot AC. Periostin expression by epicardium-derived cells is involved in the development of the atrioventricular valves and fibrous heart skeleton. *Differentiation*. 2008;76:809-819.

12. Kolditz DP, Wijffels MC, Blom NA, van der Laarse A, Markwald RR, Schalij MJ, Gittenberger-de Groot AC. Persistence of functional atrioventricular accessory pathways in postseptated embryonic avian hearts: implications for morphogenesis and functional maturation of the cardiac conduction system. *Circulation*. 2007;115:17-26.

13. Chuck ET, Freeman DM, Watanabe M, Rosenbaum DS. Changing activation sequence in the embryonic chick heart. Implications for the development of the His-Purkinje system. *Circ Res*. 1997;81:470-476.

14. Rentschler S, Vaidya DM, Tamaddon H, Degenhardt K, Sassoon D, Morley GE, Jalife J, Fishman GI. Visualization and functional characterization of the developing murine cardiac conduction system. *Development*. 2001;128:1785-1792.

15. Valderrabano M, Chen F, Dave AS, Lamp ST, Klitzner TS, Weiss JN. Atrioventricular ring reentry in embryonic mouse hearts. *Circulation*. 2006;114:543-549.

16. Jongbloed MR, Wijffels MC, Schalij MJ, Blom NA, Poelmann RE, van der Laarse A, Mentink MM, Wang Z, Fishman GI, Gittenberger-de Groot AC. Development of the right ventricular inflow tract and moderator band: a possible morphological and functional explanation for Mahaim tachycardia. *Circ Res*. 2005;96:776-783.

17. Robb JS, Kaylor CT, Turman W.G. A study of specialized heart tissue at various stages of development of the human fetal heart. *Am J Med*. 1948;5:324-336.

18. Hahurij ND, Gittenberger-de Groot AC, Kolditz DP, Bokenkamp R, Schalij MJ, Poelmann RE, Blom NA. Accessory atrioventricular myocardial connections in the developing human heart: relevance for perinatal supraventricular tachycardias. *Circulation*. 2008;117:2850-2858.

19. James TN. Normal and abnormal consequences of apoptosis in the human heart. From postnatal morphogenesis to paroxysmal arrhythmias. *Circulation*. 1994;90:556-573.

20. Truex RC, Bishof JK, Hoffman EL. Accessory atrioventricular muscle bundles of the developing human heart. *Anat Rec*. 1958;131:45-59.

21. Smith WM, Gallagher JJ, Kerr CR, Sealy WC, Kasell JH, Benson DW, Jr., Reiter MJ, Sterba R, Grant AO. The electrophysiologic basis and management of symptomatic recurrent tachycardia in patients with Ebstein's anomaly of the tricuspid valve. *Am J Cardiol*. 1982;49:1223-1234.

22. Vidaillet HJ, Jr., Pressley JC, Henke E, Harrell FE, Jr., German LD. Familial occurrence of accessory atrioventricular pathways (preexcitation syndrome). *N Engl J Med*. 1987;317:65-69.

23. Roberts R. Genomics and cardiac arrhythmias. *J Am Coll Cardiol*. 2006;47:9-21.

24. Gollob MH, Green MS, Tang AS, Gollob T, Karibe A, Ali Hassan AS, Ahmad F, Lozado R, Shah G, Fananapazir L, Bachinski LL, Roberts R. Identification of a gene responsible for familial Wolff-Parkinson-White syndrome. *N Engl J Med*. 2001;344:1823-1831.

25. Delorme B, Dahl E, Jarry-Guichard T, Briand JP, Willecke K, Gros D, Theveniau-Ruissy M. Expression pattern of connexin gene products at the early developmental stages of the mouse cardiovascular system. *Circ Res*. 1997;81:423-437.

26. Becker AE, Anderson RH, Durrer D, Wellens HJ. The anatomical substrates of wolff-parkinson-white syndrome. A clinicopathologic correlation in seven patients. *Circulation*. 1978;57:870-879.

27. Strasburger JF, Cheulkar B, Wichman HJ. Perinatal arrhythmias: diagnosis and management. *Clin Perinatol*. 2007;34:627-652.

28. Visconti RP, Markwald RR. Recruitment of new cells into the postnatal heart: potential modification of phenotype by periostin. *Ann N Y Acad Sci*. 2006;1080:19-33.

29. Kruithof BP, Krawitz SA, Gaussin V. Atrioventricular valve development during late embryonic and postnatal stages involves condensation and extracellular matrix remodeling. *Dev Biol*. 2007;302:208-217.

30. Inai K, Norris RA, Hoffman S, Markwald RR, Sugi Y. BMP-2 induces cell migration and periostin expression during atrioventricular valvulogenesis. *Dev Biol*. 2007;315:383-396.

31. Lindner V, Wang Q, Conley BA, Friesel RE, Vary CP. Vascular injury induces expression of periostin: implications for vascular cell differentiation and migration. *Arterioscler Thromb Vasc Biol*. 2005;25:77-83.

Nathan D. Hahurij[1, 2]
Adriana C. Gittenberger-de Groot[2]
Denise P. Kolditz[2, 3]
Regina Bökenkamp[1]
Martin J. Schalij[3]
Robert E. Poelmann[2]
Nico A. Blom[1]

[1] Department of Pediatric Cardiology, Leiden University Medical Center, Leiden, The Netherlands.
[2] Department of Anatomy & Embryology, Leiden University Medical Center, Leiden, The Netherlands.
[3] Department of Cardiology, Leiden University Medical Center, Leiden, The Netherlands.

7

Accessory atrioventricular myocardial connections in the developing human heart, relevance for perinatal supraventricular tachycardias

ABSTRACT

Background.
Fetal and neonatal atrioventricular reentrant tachycardias (AVRTs) can be life threatening but resolve in most cases during the first year of life. Transient presence of accessory atrioventricular (AV) myocardial connections during annulus fibrosus development may explain this phenomenon.

Methods and Results
45 human embryonic, fetal and neonatal sectioned hearts (4 to 36 weeks of development) were studied immunohistochemically. Accessory myocardial AV connections were quantified and categorized according to their specific location and 3D AMIRA reconstructions were made. Between 4 and 6 weeks of development: atrial and ventricular myocardium was continuous at the primitive AV canal. At 6-10 weeks: numerous accessory myocardial AV connections were identified at the left (45%), right (35%) and septal (20%) region of the AV junction. Most right sided accessory connections comprised distinct myocardial strands, left sided connections consisted of larger myocardial continuities. At 10-20 weeks: all accessory AV connections comprised discrete myocardial strands and gradually decreased in number. The majority of accessory connections were located at the right AV junction (67%), predominantly at the lateral aspect (45%). At the left AV junction 17% and at the septal region 16% of the accessory connections were observed. 3D reconstructions of the developing AV nodal area at these stages demonstrated multiple AV nodal related accessory connections. From 20 weeks until birth and in neonatal hearts no more accessory myocardial AV connections were observed.

Conclusions
Isolation of the AV junction is a gradual and ongoing process and particularly right lateral accessory myocardial AV connections are commonly found at later stages of normal human cardiac development. These transitory accessory connections may act as substrate for AVRTs in fetuses or neonates.

INTRODUCTION

Atrioventricular reentrant tachycardia (AVRT) requiring the presence of an accessory atrioventricular (AV) myocardial pathway (AP) is the most common type of supraventricular tachycardia (SVT) in both the fetus and newborn.[1,2] AVRT is a potentially life threatening problem in this young age group and these tachycardias are sometimes difficult to control with antiarrhythmic drug therapy.[3,4,5] However, most tachycardias spontaneously resolve within the

first months of life and more than 60% of patients require no antiarrhythmic drug therapy and remain free of symptoms after the age of one year.[2,4] This self-limiting character of most perinatal AVRTs suggests that the majority of the accessory AV pathways involved eventually disappear after birth. It is unknown whether APs involved in perinatal AVRT have a different etiology as compared to APs involved in AVRT presenting later in life. We hypothesize that self-limiting perinatal AVRT can be explained by the transitory presence of accessory myocardial connections during the normal process of isolation of the AV junction in cardiac development.

Shortly after the formation of the primary heart tube, the heart is subjected to extensive remodelling processes.[6] Previous studies have shown that around the seventh week of human development, the separation process of the atrial and ventricular myocardium at the primitive AV canal has started. As from the twelfth week of development atrial and ventricular myocardium are separated by a layer of fibrous tissue, the annulus fibrosus, in which the AV conduction axis comprises the only myocardial continuity.[7] Recently, electrophysiological studies in avian[8] and mouse models[9,10] have shown that up to late stages of cardiac development multiple accessory AV myocardial connections were present. These accessory connections demonstrated retrograde[10] and antegrade AV conduction and gradually decreased in number at subsequent developmental stages.[8] In addition, an electrophysiological study in mice demonstrated the onset of AVRT at early stages of development.[10]

In this study we investigated the presence and the specific locations of accessory AV myocardial pathways in relation to the process of formation of the annulus fibrosus during the different stages of normal heart development in humans.

MATERIAL AND METHODS

Hearts

The human embryonic, fetal and neonatal hearts (n=45) were obtained from the collection of the Department of Anatomy and Embryology of the Leiden University Medical Center, The Netherlands. The study was approved by the local Medical Ethical Committee. All hearts were already sectioned either in transverse, frontal or sagittal plain and immunohistochemically stained with different myocardial (HHF-35, DAKO, Glostrup, Denmark; Myosin, α-MHC and β-MHC kindly supplied by A.F.M. Moorman) and fibrous tissue (Fibronectin, A245, DAKO, Glostrup, Denmark ; CollagenVI, Southern Biotechnology, Birmingham, AL ; Laminin, PU078, BioGenex, San Remon, USA) markers. Furthermore, histological stained sections were used: Haematoxylin eosin (HE), Resorcin-fuchsin-iron haematoxylin-picric acid-thiazin red (modified Verhoeff-Van Gieson stain) and Azan. A detailed description of staining protocols can be found in previous publications.[11,12]

According to pregnancy duration and Crown-Rump-Length (CRL) all embryos, fetuses and neonates were separated into 4 groups of subsequent gestational stages of development: Group 1: 4 weeks / CRL5mm - 6 weeks / CRL11mm (n=2); Group 2: 6 weeks / CRL11mm - 10 weeks / CRL 40 mm (n=7); Group 3: 10 weeks / CRL 40mm - 20 weeks / CRL164-170mm (n=27); Group 4: 20 weeks / CRL164-170 -birth- neonates (n=9).

The hearts were carefully studied section by section for the presence of accessory AV myocardial connections at the left, right and septal area of the AV junction using an Olympus BH-2 light microscope. An accessory myocardial AV connection was defined as an uninterrupted strand of myocardium, which crosses the annulus fibrosus in addition to the AV conduction axis in post-septated hearts.

All accessory myocardial AV connections in the embryonic or fetal hearts were categorized based on their specific location in the AV junction. The accessory myocardial connections related to the developing atrioventricular node (AVN) were described separately.

Immunohistochemistry

Additional immunohistochemical experiments were performed using MLC-2a and periostin specific antibodies as additional myocardium and fibrous tissue markers respectively. All embryonic hearts were fixed in 4% paraformaldehyde (PFA), after dehydration they were embedded in paraffin. The embedded hearts were 5 μm sectioned and mounted 1 to 6 onto protein / glycerin coated slides, so 6 different staining procedures could be performed on one embryo. After dehydration of the slides, inhibition of the endogenous peroxidase was performed for MLC-2a with a solution of 0.3% H_2O_2 in PBS for 20 min. For periostin antigen retrieval was performed in 0.01M Citric buffer of Ph 6.0 at 97°C for 12 minutes, followed by inhibition of the endogenous peroxidase in a solution of 0.3% H_2O_2 in PBS for 20 min. Overnight incubation with the primary antibody was performed with the following antibodies: 1/2000 anti-atrial myosin light chain 2 (MLC-2a, gift from S.W. Kubalak) and 1/1000 anti-periostin (gift from R.R. Markwald). The primary antibodies were dissolved in PBS-Tween-20 with 1% Bovine Serum Albumin (BSA, Sigma Aldrich, USA). The slides were rinsed between subsequent incubation steps: PBS (2x) and PBS-Tween-20 (1x). For both MLC-2a and periostin, a 40 min incubation with the secondary antibodies was performed using 1/200 goat-anti-rabbit-biotin (Vector Laboratories, USA, BA-100) and 1/66 goat serum (Vector Laboratories, USA, S1000) in PBS-Tween-20. Thereafter a 40 minute incubation with ABC-reagent (Vector-Laboratories, USA, PK 6100) was performed. For visualisation, all slides were incubated with 400 μg/ml 3-3'di-aminobenzidin tetrahydrochloride (DAB, Sigma-Aldrich Chemie, USA, D5637) dissolved in Tris-maleate buffer pH7.6 to which 20 μl H_2O_2 was added for 10 min. 0.1% Haematoxylin (Merck, Darmstad, Germany) was used to counter stain the slides: MLC-2a 10 sec and periostin 5 sec, followed by rinsing with tap water for 10 minutes. Finally, the slides were dehydrated and mounted with Entellan (Merck, Darmstadt, Germany).

AMIRA reconstruction

3D reconstructions were made of the developing AVN region, as described earlier[9], using the AMIRA software package (Template Graphics Software, San Diego, USA).

The authors had full access to and take responsibility for the integrity of the data. All authors have read and agree to the manuscript as written.

RESULTS

4 weeks / CRL 5 mm – 6 weeks / CRL 11 mm (n=2)

At 4 weeks (CRL 5 mm) of development the heart tube had looped and the common atrium was completely positioned above the primitive left ventricle. Large endocardial cushions were observed in the region of the common outflow tract and at the anterosuperior and posteroinferior luminal side of the primitive AV canal. At this stage, the atrial and ventricular myocardium was continuous at the region of the primitive AV junction. At 5 weeks (CRL 7 mm) the formation of the right ventricle had started and the future left and right ventricle were clearly discernible. In the AV canal region the myocardium of the primitive atria and the ventricles was continuous (data not shown).

6 weeks / CRL 11 mm – 10 weeks / CRL 40 mm (n=7)

Between 6-7 weeks, the AV cushions had fused and the future tricuspid and mitral valve orifice of the AV junction became visible. Almost all atrial and ventricular myocardium was still continuous at the AV junction. Around the seventh week of development ventricular septation was nearly completed, thereby separating the left and right blood streams. The separation of atrial and ventricular myocardium had clearly commenced at the right dorsal aspect of the embryonic heart and to a lesser extent at the left dorsal side. At 7 to 8 weeks, ventricular septation was completed and formation of the partially AV cushion derived tricuspid valves at the right and mitral valve at the left AV junction had started. At the end of the ninth week AV cushion tissue was no longer observed, and well shaped mitral and tricuspid valves were present at the AV junction. At this stage, the atrial and ventricular myocardium was almost completely separated by the fibrous tissue of the developing annulus fibrosus. At the dorsal side of the fetal heart a distinct AV myocardial continuity was observed which corresponded to the developing AV conduction axis, comprising the developing AVN and the bundle of His. Between 6 and 10 weeks of development, many parts of the AV junction showed an incomplete isolation at the annulus fibrosus (Figure 1a-c). Accessory AV myocardial connections were found both at the left (45%), right (35%) and septal (20%) region of the AV junction (Figure 1d). Most of the accessory myocardial connections were identified as broad accessory AV

myocardial continuities. At the dorsal aspect of the right AV junction accessory connections consisted of small single myocardial strands.

At the right AV junction, the so-called right atrioventricular ring (RAVR) bundle could easily be distinguished from the atrial myocardium as a separate structure. The RAVR bundle, considered to be part of the embryonic AV conduction system, formed a ring of myocardium around the tricuspid annulus at the atrial side (Figure 2a).[13]

Interestingly, the majority of the right sided accessory myocardial AV connections (65%) were located subendocardially and made contact with the RAVR bundle. In all examined hearts the isolating tissue between the RAVR bundle and the ventricular myocardium was not as extensive
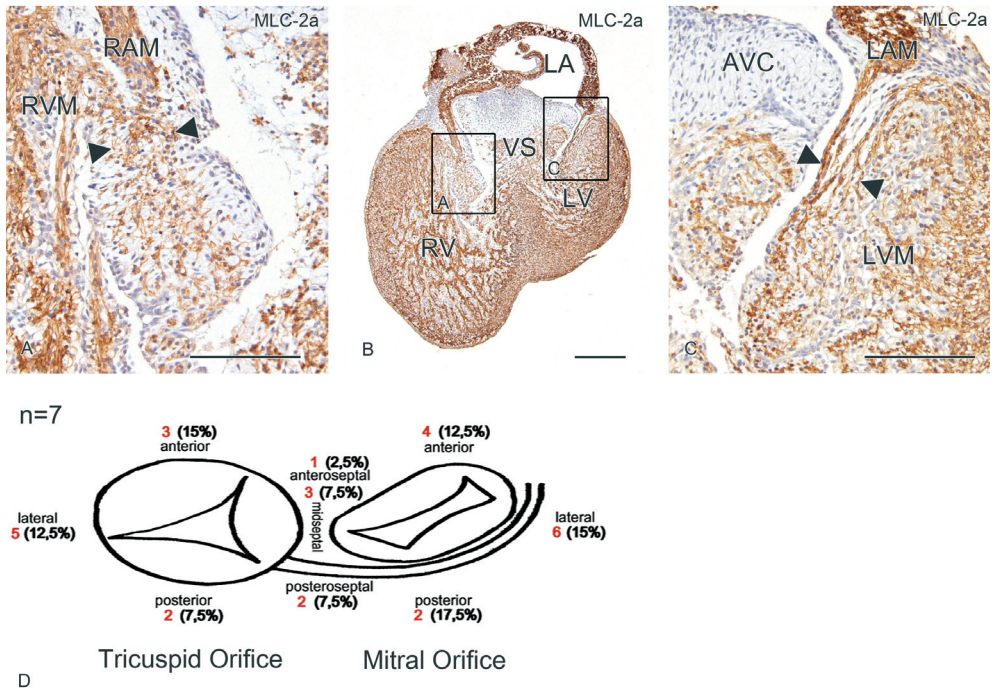

Figure 1. Separation of atrial and ventricular myocardium at 6 to 10 weeks of development. In early post-septated hearts large myocardial continuities between atrial and ventricular myocardium were observed at the right AV junction (a, magnification of boxed area in b) and left AV junction (c magnification of boxed area in b), as shown in these frontal sections of an MLC-2a stained embryonic heart of 7 weeks of development (b). The region between the **arrowheads** in (a) and (c) show the myocardial continuity at the left and right lateral AV junction. (d) Between 6 and 10 weeks of development 7 hearts were studied, the **red numbers** indicate the total number of hearts in which accessory myocardial AV continuities were observed at a specific location at the tricuspid and mitral orifice of the developing AV junction. The **percentages** represent the total amount of accessory myocardial AV continuities at a specific location, compared to the total number of accessory myocardial AV continuities at the entire AV junction. **VS** indicates ventricular septum; **LA**, left atrium; **LV**, left ventricle; **LAM**, left atrial myocardium; **LVM**, left ventricular myocardium; **RV**, right ventricle; **RAM**, right atrial myocardium; **RVM**, right ventricular myocardium. Scale bars: (a), (c) = 150μm; (b) = 300μm.

as at other locations at the AV junction. Frequently, only a single layer of fibrous tissue was observed between the RAVR bundle and the ventricular myocardium.

10 weeks / CRL 40 mm - 20 weeks / CRL 164-170 mm (n=27)

Between 10 (CRL 40 mm) and 20 weeks (CRL 164-170 mm) of development the annulus fibrosus and valve formation had progressed further and cardiac development was mainly dominated by growth. At the left AV junction, the annulus fibrosus had become a firm structure with a thick layer of fibrous tissue isolating the left atrial and ventricular myocardium (Figure 2d-f).

The developing AVN was positioned in the right posteroseptal region and was continuous with the bundle of His traversing the annulus fibrosus behind the aorta. At the right AV junction the annulus fibrosus was more fragile and accessory myocardial AV connections were
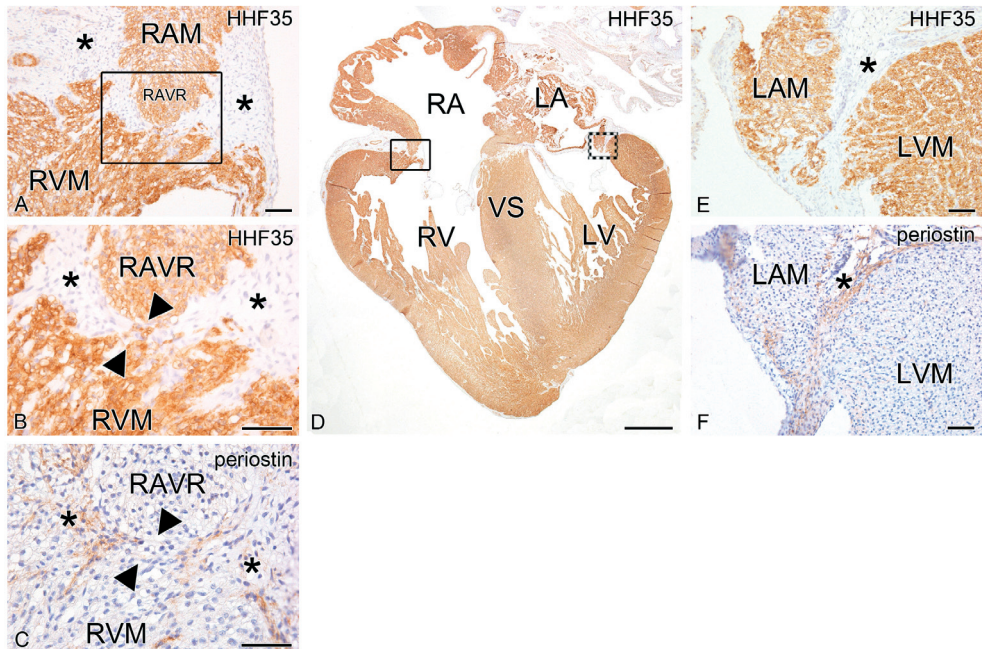

Figure 2. Separation of atrial and ventricular myocardium at eleven weeks of development. The right AV junction (a, magnification of boxed area in d) of an eleven week old fetal heart frontally sectioned (d). Atrial and ventricular myocardium is separated by a layer of periostin positive fibrous annulus fibrosus tissue (**asterisk** in a, b and c). HHF-35 positive accessory AV myocardial connections (region between **arrowheads** in b, magnification of boxed area in a), negative for periostin (c adjacent section of b), were present between the right atrioventricular ring (**RAVR**) bundle and the right ventricular myocardium (**RVM**). (e) Magnification of dotted box in (d) shows that the left atrial myocardium (**LAM**) and left ventricular myocardium (**LVM**) are separated by a thick layer of periostin positive (f adjacent section of e) fibrous annulus fibrosus tissue (asterisk in e and f). **RA** indicates right atrium; **RV**, right ventricle; **LA**, left atrium; **LV**, left ventricle; **VS**, ventricular septum. Scale bars: (d) = 1mm; all others = 60μm.

159

frequently found especially adjacent to the RAVR bundle (Figure 2a-d), which could still be observed in most hearts up to 20 weeks.

Between 10 and 20 weeks broad accessory AV myocardial continuities as seen at earlier embryonic stages, could no longer be detected. However, up to 20 weeks of development numerous accessory myocardial AV connections were identified (Figure 3a-e). At these stages, all accessory myocardial AV connections only consisted of single strands of myocardium crossing the annulus fibrosus (Figure 3c-e). As expected, the majority of accessory myocardial AV connections were now located at the right AV junction (67%) and only 17% were located at the left AV junction. Furthermore, 16% of accessory myocardial AV connections were observed at the midseptal and anteroseptal region of the AV junction (Figure 3f). Right sided connections (45%) were located subendocardially at the lateral aspect of the right AV junction, mostly related to the RAVR bundle (Figure 3c, e).

20 weeks / CRL 164-170 mm – birth - neonatal stages (n=9)

The annulus fibrosus of 5 fetal and 4 neonatal hearts was examined completely. In both fetal and neonatal hearts no accessory myocardial AV connections were observed at the left, right and septal area of the AV junction (data not shown).

Accessory connections related to the developing AVN

The developing AVN and bundle of His were examined during different stages of fetal heart development. The cardiomyocytes of the AVN were large pale and rounded cells and could be well distinguished from the adjacent atrial working myocardium (data not shown). From 10 weeks onward the developing AVN remained positioned anterior to the coronary sinus ostium to the mid-atrial septum, immediately adjacent to the tricuspid annulus (Figure 4a). Shortly after completion of ventricular septation, the bundle of His was a prominent structure crossing the annulus fibrosus in the midseptal region continuing at the ventricular side divided into a left and right bundle branch. Along fetal heart development the bundle of His was better isolated and could be easily identified from the surrounding structures. During subsequent stages of development until birth, numerous small strands of cardiomyocytes originating from the AVN region, penetrated the annulus fibrosus. These accessory AV nodal extensions of large pale rounded cardiomyocytes connected to the ventricular septal myocardium but had no relationship with the penetrating bundle of His (Figure 4a, b). Sections and a three dimensional reconstruction of the AVN region and AV nodal accessory connections of a 14,2 week fetal heart are shown in Figure 4.
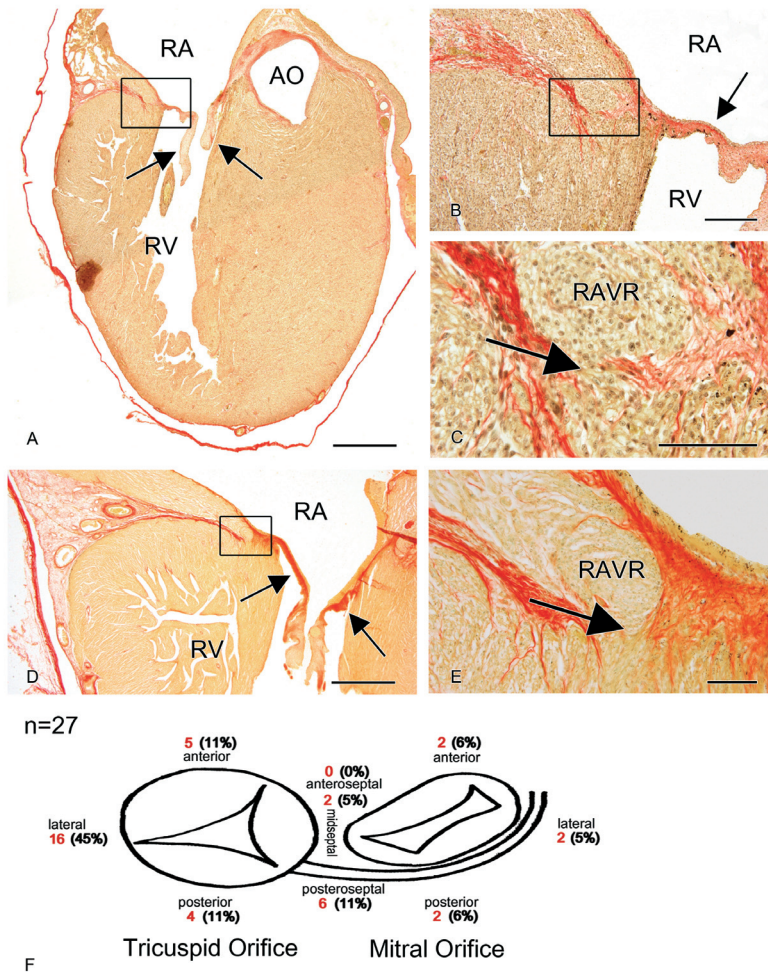
Figure 3. Separation of atrial and ventricular myocardium at 10 to 20 weeks of development. Between 10 and 20 weeks of development several accessory myocardial AV connections bypassing the AV conduction axis were present. (a) Modified Verhoeff-Van Gieson stain stained frontal section of a 15,3 week fetal heart in which myocardium is stained yellow-brown and fibrous tissue is stained red. (b) Represents the boxed area in (a) showing a detail of the annulus fibrosus of the right AV junction which is in continuity with the base of the tricuspid valve (**arrows** in a and b). (c) Detail of the boxed area in (b), showing the right atrioventricular ring (**RAVR**) bundle which is in continuity with the ventricular myocardium, thereby creating an accessory myocardial AV connection (**arrow** in c). (d) Shows a frontal section of the right AV junction of a fetal heart of 19,6 weeks of development. The **arrows** indicate the tricuspid valve in continuity with the fibrous tissue of the annulus fibrosus (**red**). (e) Represents the magnification of the boxed area in (d) showing an accessory myocardial AV connection in contact with the RAVR bundle (**arrow** in e). Between 10 and 20 weeks of development 27 fetal hearts were investigated for the presence of accessory myocardial AV connections at the developing AV junction (f). The **red numbers** indicate the total number of hearts in which accessory myocardial AV connections were present at a specific location at the AV junction. The **percentages** represent the amount of accessory myocardial AV connections at a specific location at the AV junction compared to the total number of accessory myocardial AV connections at the entire AV junction. **RA** indicates right atrium; **RV**, right ventricle; **AO**, aorta. Scale bars: (a), (d) = 1mm; (b) = 200μm; (c), (e) = 100μm.
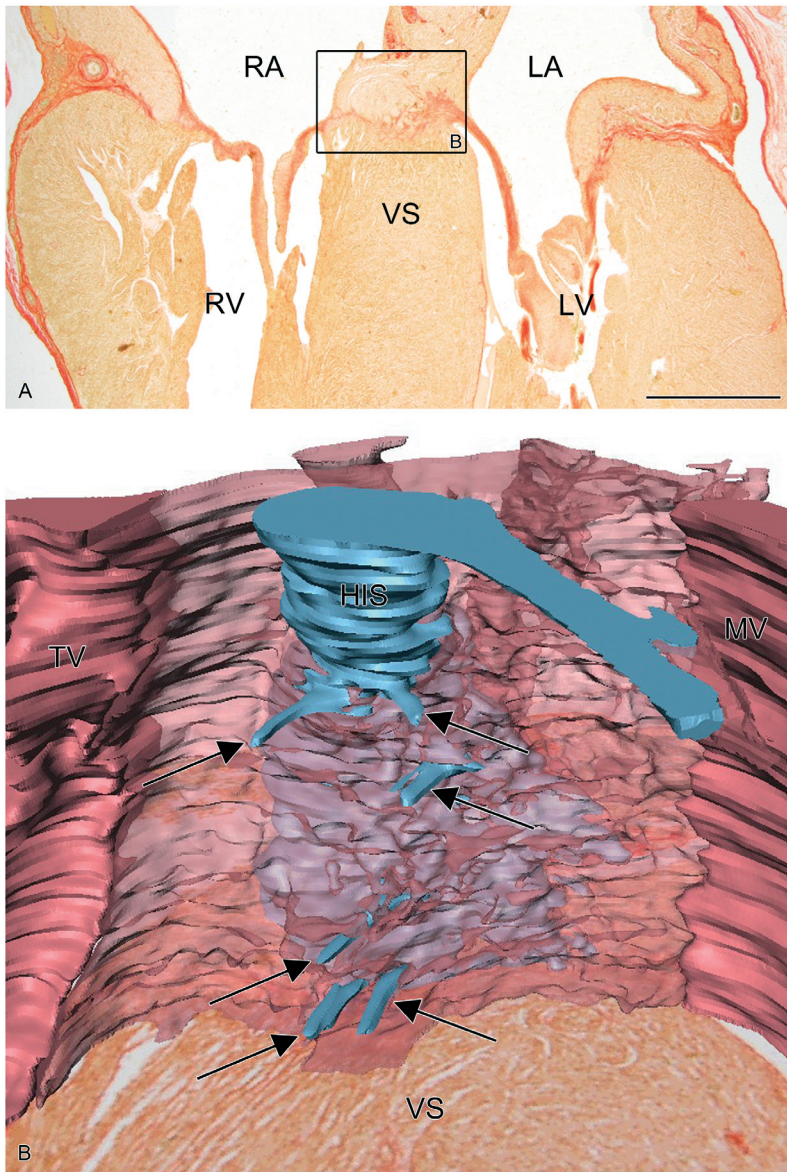
Figure 4. Accessory atrioventricular connections related to the developing atrioventricular node (AVN). (a) Shows a modified Verhoeff-Van Gieson stain stained transverse section of a 14,2 week fetal heart. The boxed area in (a) shows the AVN region of which a 3D reconstruction is shown in (b). During subsequent stages of development until birth multiple accessory myocardial connections related to the AVN were observed. (b) The 3D reconstruction visualizes a frontal view of these so-called nodoventricular connections (**arrows** in b) penetrating the annulus fibrosus (**red transparent**) and connecting the AVN with the ventricular septal (**VS**) myocardium. For display purpose the extensions have been elongated. **RA** indicates right atrium; **LA**, left atrium; **RV**, right ventricle; **LV**, left ventricle. In the 3D reconstruction, **red** indicates base of mitral valve (**MV**) and tricuspid valve (**TV**); **blue**, myocardium of the atrioventricular conduction axis, including the bundle of His (**HIS**). Scale bar: a = 1mm.

DISCUSSION

SVTs affect about 0.1% of fetuses and newborns. In most cases the substrate for arrhythmia is an abnormal electrical conduction through an accessory AV myocardial pathway causing a circus movement between atria and ventricles.[1] However, the majority of children presenting with AVRT in the fetal or neonatal period has no recurrences after the age of one year and show disappearance of ventricular preexcitation and non-inducibility of AVRT by transesophageal electrophysiological studies in approximately one third of the patients.[14,15] This self-limiting character of most AVRTs in fetuses and newborns is an intriguing clinical phenomenon, but the mechanism has not yet been elucidated. AVRT in this age group has been speculated to originate from the transient presence of conducting APs during the normal process of maturation of the annulus fibrosus.[8,16] The development of this isolating structure involves several processes in which the endocardial cushions lining the luminal side of the primitive AV canal together with the inward migration of the epicardially located AV sulcus tissue have an important role.[17-19] Recently, it has been shown in more detail that a combination of bone-morphogenetic-protein (BMP) signalling,[20,21] periostin an osteoblast–specific factor[22] and epicardial derived cells, which enter the heart at the AV sulcus play a key role in this process.[23,24]

The etiology of APs has not been elucidated. The majority of APs conduct antegradely as seen in patients with Wolff-Parkinson-White (WPW) syndrome (OMIM #194200; incidence in general population 1,5 per 1000 persons),[25] the prevalence of WPW syndrome in children under 13 years of age is lower (0.07%).[26] In adults, twenty-five percent of APs involved in AVRT are concealed indicating that they only have retrograde conducting properties.[27] In infants, the percentage of concealed APs is higher, approximately 60%.[28] In the majority of cases of WPW syndrome there is no familial involvement. However, significant minority of cases are inherited as a single gene disorder or occur as part of a syndrome with a strong genetic basis.[25,29,30] Recently *PRKAG2* gene missense mutations have been identified to be involved in familial WPW syndrome often associated with cardiac hypertrophy.[30] Animal studies have shown that mutations in the *Alk3* gene result in a disrupt formation of the annulus fibrosus causing ventricular preexcitation via posterior paraseptal bypass tracts.[20] The differences in location and specific electrophysiological properties of APs as well as their association with structural heart disease like hypertrophic cardiomyopathy and congenital heart disease indicate that not all APs share the same etiological pathway.

Previous studies have demonstrated the presence of accessory myocardial AV connections between atrial and ventricular myocardium during normal embryological and fetal heart development in humans[16,31,32] and other mammals.[9,10] However, the present study for the first time systematically describes the presence and the specific locations of gradually disappearing accessory AV myocardial connections crossing the developing annulus fibrosus in human

embryonic, fetal and neonatal hearts. We demonstrate that atrial and ventricular myocardium was continuous at the primitive AV canal at early stages of development. First separation of atrial and ventricular myocardium by the developing annulus fibrosus was observed at the right dorsal AV junction around 7 weeks of development and myocardial continuity persisted longer near the left junction. Total separation of atrial and ventricular myocardium was completed around ten to eleven weeks, which corresponds to other studies regarding the formation of the annulus fibrosus in developing human hearts.[7] However, numerous accessory AV myocardial connections can be identified up to the end of the second trimester of pregnancy. Comparable to other studies[16] these accessory AV myocardial connections were observed at the subendocardial aspect of both the right and left lateral AV junction of the heart. In the second and third trimester the left AV ring becomes firmly isolated by a thick layer of fibrous tissue followed by isolation of the right AV ring.

Especially the isolation of the right AV ring is weak and frequently consists only of very thin layers of fibrous tissue. Up to 20 weeks of gestation small AV myocardial strands remain present near the lateral side of the tricuspid valve that are mainly located subendocardially. The high frequency of these right sided accessory myocardial AV connections and the weak isolation of especially this part of the AV junction might be associated with the normal developmental process of the right ventricular inflow tract. In early stages of heart development, as observed in the current study, the common atrium is completely positioned above the left ventricle. Formation of the right ventricular inflow tract starts with a groove, which is embedded in the myocardium of the primary fold. As a result of the expansion and outgrowth of this myocardial groove the right ventricular inflow tract will be formed, which eventually establishes the right part of the AV junction.[9] Therefore, the formation of the right ventricular inflow tract might result in a weaker isolation and a high frequency of accessory myocardial AV connections, since this part of the AV junction develops subsequent to the already existent left AV junction.

The right sided AV myocardial connections frequently are located in close relationship with the RAVR bundle.[13] This semicircular structure forms part of the temporary embryological specialized AV conduction system and is continuous with the AVN posteriorly. In the fetus it can be identified as a ring of node-like cells in the right atrium just above the tricuspid valve that obliterates later on.[13,33,34] These accessory myocardial AV connections seem to correspond to the presumed multiple AV nodes and pathways as originally reported by Kent and reviewed by Anderson (1996).[35] The relationship of right sided accessory myocardial AV connections with the RAVR bundle could explain the decremental properties as seen in some of the right sided APs.[36]

Within the developing AVN small myocardial extensions can be identified that cross the annulus fibrosus and connect the developing AVN with the ventricular septal myocardium. These AV nodal extensions remain present until birth. The presence of the so-called

nodoventricular connections in fetal and neonatal hearts has been reported earlier and this phenomenon has been described as fetal dispersion of the AVN.[37] In the first months after birth extensive remodelling of the fibrous heart skeleton including the AVN area takes place,[31,38] in which the AVN becomes a more solid structure.[39] AV nodal extensions appear to be a common finding in neonatal hearts, although it has been associated with sudden infant death syndrome in the past.[40] In theory, nodoventricular pathways could provide the substrate for SVT, but to our knowledge this rare form of reentrant tachycardia has not been documented in the perinatal period.

Recently, the temporary presence of functional accessory myocardial AV connections has been demonstrated by electrophysiological studies in avian hearts up to late stages of fetal development. These connections appeared to have antegrade conducting properties, which was demonstrated by unipolar electrogram recordings showing premature left and right ventricular base activation in post-septated hearts.[8] Furthermore, studies performed in mammals[9,10] showed that in normal mouse embryos conducting accessory AV pathways are present during cardiac development that can actually create the substrate for reentrant tachycardias. Some of these pathways even appeared to have decremental properties as observed in the Mahaim preexcitation syndrome.[9] In normal human fetuses the conducting properties of transient accessory AV connections, depending on factors such as intercellular coupling remain to be elucidated as well as their capability to establish a pathway for AVRT. However, these accessory myocardial AV connections in human fetuses and their specific locations show strong similarities with the conducting accessory myocardial AV connections as demonstrated in avians and mice.[8-10]

APs in adult patients with AVRT are mostly found around the mitral valve orifice and approximately 60% are located in the left ventricular free wall.[27] In the pediatric age group the incidence of APs around the tricuspid annulus appears to be higher.[41] APs around the tricuspid valve are usually located at the subendocardial aspect of the heart, whereas left sided APs can also have a more epicardial course in the AV sulcus. This implicates that the persistence of subendocardially located accessory myocardial AV connections as demonstrated in normal fetuses could only partly explain the pathogenesis of APs in patients with AVRT. However the delayed disappearance of fetal APs as reported in the current study offers a good explanation for the onset and disappearance of fetal and neonatal AVRT. One-third of the fetuses and neonates with AVRT have WPW syndrome showing ventricular pre-excitation on the postnatal electrocardiogram, the others have concealed APs with only retrograde conduction.[42] Although late recurrences of tachycardia after 8 to 10 years have been reported in neonates with WPW syndrome, the majority of these children remains free of symptoms during life.[43] Recently it has been reported that the group of neonates with concealed APs has an even better prognosis and more than 80% remain asymptomatic after the first year, without recurrences later in life.[42]

In the present study we have demonstrated that accessory myocardial AV connections remain present up to late stages of fetal heart development, which indicates that the process of isolation of the AV junction is a continuous process not finished by the time of birth. The temporary presence of these accessory myocardial AV connections could serve as substrate for perinatal AVRT.

FUNDING SOURCES

REFERENCES

1. Bauersfeld U, Pfammatter JP, Jaeggi E. Treatment of supraventricular tachycardias in the new millennium--drugs or radiofrequency catheter ablation? *Eur J Pediatr*. 2001;160:1-9.
2. Ko JK, Deal BJ, Strasburger JF, Benson DW, Jr. Supraventricular tachycardia mechanisms and their age distribution in pediatric patients. *Am J Cardiol*. 1992;69:1028-1032.
3. Simpson JM, Sharland GK. Fetal tachycardias: management and outcome of 127 consecutive cases. *Heart*. 1998;79:576-581.
4. Naheed ZJ, Strasburger JF, Deal BJ, Benson DW, Jr., Gidding SS. Fetal tachycardia: mechanisms and predictors of hydrops fetalis. *J Am Coll Cardiol*. 1996;27:1736-1740.
5. Weindling SN, Saul JP, Walsh EP. Efficacy and risks of medical therapy for supraventricular tachycardia in neonates and infants. *Am Heart J*. 1996;131:66-72.
6. Gittenberger-de Groot AC, Bartelings MM, Deruiter MC, Poelmann RE. Basics of cardiac development for the understanding of congenital heart malformations. *Pediatr Res*. 2005;57:169-176.
7. Wessels A, Markman MW, Vermeulen JL, Anderson RH, Moorman AF, Lamers WH. The development of the atrioventricular junction in the human heart. *Circ Res*. 1996;78:110-117.
8. Kolditz DP, Wijffels MC, Blom NA, van der Laarse A, Markwald RR, Schalij MJ, Gittenberger-de Groot AC. Persistence of functional atrioventricular accessory pathways in postseptated embryonic avian hearts: implications for morphogenesis and functional maturation of the cardiac conduction system. *Circulation*. 2007;115:17-26.
9. Jongbloed MR, Wijffels MC, Schalij MJ, Blom NA, Poelmann RE, van der Laarse A, Mentink MM, Wang Z, Fishman GI, Gittenberger-de Groot AC. Development of the right ventricular inflow tract and moderator band: a possible morphological and functional explanation for Mahaim tachycardia. *Circ Res*. 2005;96:776-783.
10. Valderrabano M, Chen F, Dave AS, Lamp ST, Klitzner TS, Weiss JN. Atrioventricular ring reentry in embryonic mouse hearts. *Circulation*. 2006;114:543-549.
11. Oosthoek PW, Wenink AC, Vrolijk BC, Wisse LJ, Deruiter MC, Poelmann RE, Gittenberger-de Groot AC. Development of the atrioventricular valve tension apparatus in the human heart. *Anat Embryol (Berl)*. 1998;198:317-329.
12. Gittenberger-de Groot AC, Bartram U, Oosthoek PW, Bartelings MM, Hogers B, Poelmann RE, Jongewaard IN, Klewer SE. Collagen type VI expression during cardiac development and in human fetuses with trisomy 21. *Anat Rec A Discov Mol Cell Evol Biol*. 2003;275:1109-1116.

13. Blom NA, Gittenberger-de Groot AC, Deruiter MC, Poelmann RE, Mentink MM, Ottenkamp J. Development of the cardiac conduction tissue in human embryos using HNK-1 antigen expression: possible relevance for understanding of abnormal atrial automaticity. *Circulation*. 1999;99:800-806.

14. Deal BJ, Keane JF, Gillette PC, Garson A, Jr. Wolff-Parkinson-White syndrome and supraventricular tachycardia during infancy: management and follow-up. *J Am Coll Cardiol*. 1985;5:130-135.

15. Benson DW, Jr., Dunnigan A, Benditt DG. Follow-up evaluation of infant paroxysmal atrial tachycardia: transesophageal study. *Circulation*. 1987;75:542-549.

16. Truex RC, Bishof JK, Hoffman EL. Accessory atrioventricular muscle bundles of the developing human heart. *Anat Rec*. 1958;131:45-59.

17. Wenink AC, Gittenberger-de Groot AC. The role of atrioventricular endocardial cushions in the septation of the heart. *Int J Cardiol*. 1985;8:25-44.

18. Wenink AC, Gittenberger-de Groot AC. Embryology of the mitral valve. *Int J Cardiol*. 1986;11:75-84.

19. Rothenberg F, Efimov IR, Watanabe M. Functional imaging of the embryonic pacemaking and cardiac conduction system over the past 150 years: technologies to overcome the challenges. *Anat Rec A Discov Mol Cell Evol Biol*. 2004;280:980-989.

20. Gaussin V, Morley GE, Cox L, Zwijsen A, Vance KM, Emile L, Tian Y, Liu J, Hong C, Myers D, Conway SJ, Depre C, Mishina Y, Behringer RR, Hanks MC, Schneider MD, Huylebroeck D, Fishman GI, Burch JB, Vatner SF. Alk3/Bmpr1a receptor is required for development of the atrioventricular canal into valves and annulus fibrosus. *Circ Res*. 2005;97:219-226.

21. Okagawa H, Markwald RR, Sugi Y. Functional BMP receptor in endocardial cells is required in atrioventricular cushion mesenchymal cell formation in chick. *Dev Biol*. 2007;306:179-192.

22. Kruzynska-Frejtag A, Machnicki M, Rogers R, Markwald RR, Conway SJ. Periostin (an osteoblast-specific factor) is expressed within the embryonic mouse heart during valve formation. *Mech Dev*. 2001;103:183-188.

23. Eralp I, Lie-Venema H, Bax NA, Wijffels MC, van der Laarse A, Deruiter MC, Bogers AJ, Van Den Akker NM, Gourdie RG, Schalij MJ, Poelmann RE, Gittenberger-de Groot AC. Epicardium-derived cells are important for correct development of the Purkinje fibers in the avian heart. *Anat Rec A Discov Mol Cell Evol Biol*. 2006;288:1272-1280.

24. Gittenberger-de Groot AC, Vrancken Peeters MP, Mentink MM, Gourdie RG, Poelmann RE. Epicardium-derived cells contribute a novel population to the myocardial wall and the atrioventricular cushions. *Circ Res*. 1998;82:1043-1052.

25. Vidaillet HJ, Jr., Pressley JC, Henke E, Harrell FE, Jr., German LD. Familial occurrence of accessory atrioventricular pathways (preexcitation syndrome). *N Engl J Med*. 1987;317:65-69.

26. Sano S, Komori S, Amano T, Kohno I, Ishihara T, Sawanobori T, Ijiri H, Tamura K. Prevalence of ventricular preexcitation in Japanese schoolchildren. *Heart*. 1998;79:374-378.

27. Kuck KH, Schluter M. Junctional tachycardia and the role of catheter ablation. *Lancet*. 1993;341:1386-1391.

28. Benson DW, Jr., Dunnigan A, Benditt DG, Pritzker MR, Thompson TR. Transesophageal study of infant supraventricular tachycardia: electrophysiologic characteristics. *Am J Cardiol*. 1983;52:1002-1006.

29. Roberts R. Genomics and cardiac arrhythmias. *J Am Coll Cardiol*. 2006;47:9-21.

30. Gollob MH, Green MS, Tang AS, Gollob T, Karibe A, Ali Hassan AS, Ahmad F, Lozado R, Shah G, Fananapazir L, Bachinski LL, Roberts R. Identification of a gene responsible for familial Wolff-Parkinson-White syndrome. *N Engl J Med*. 2001;344:1823-1831.

31. James TN. Normal and abnormal consequences of apoptosis in the human heart. From postnatal morphogenesis to paroxysmal arrhythmias. *Circulation*. 1994;90:556-573.

32. Robb JS, Kaylor CT, Turman W.G. A study of specialized heart tissue at various stages of development of the human fetal heart. *Am J Med*. 1948;5:324-336.

33. Viragh S, Challice CE. The development of the conduction system in the mouse embryo heart. I. The first embryonic A-V conduction pathway. *Dev Biol*. 1977;56:382-396.

7

34. Wessels A, Vermeulen JL, Viragh S, Kalman F, Lamers WH, Moorman AF. Spatial distribution of "tissue-specific" antigens in the developing human heart and skeletal muscle. II. An immunohistochemical analysis of myosin heavy chain isoform expression patterns in the embryonic heart. *Anat Rec*. 1991;229:355-368.

35. Anderson RH, Ho SY, Gillette PC, Becker AE. Mahaim, Kent and abnormal atrioventricular conduction. *Cardiovasc Res*. 1996;31:480-491.

36. Haissaguerre M, Cauchemez B, Marcus F, Le Metayer P, Lauribe P, Poquet F, Gencel L, Clementy J. Characteristics of the ventricular insertion sites of accessory pathways with anterograde decremental conduction properties. *Circulation*. 1995;91:1077-1085.

37. James TN, Marshall TK. XVIII. Persistent fetal dispersion of the atrioventricular node and His bundle within the central fibrous body. *Circulation*. 1976;53:1026-1034.

38. Visconti RP, Markwald RR. Recruitment of new cells into the postnatal heart: potential modification of phenotype by periostin. *Ann N Y Acad Sci*. 2006;1080:19-33.

39. James TN. Cardiac conduction system: fetal and postnatal development. *Am J Cardiol*. 1970;25:213-226.

40. James TN. Sudden death in babies: new observations in the heart. *Am J Cardiol*. 1968;22:479-506.

41. Morady F. Catheter ablation of supraventricular arrhythmias: state of the art. *J Cardiovasc Electrophysiol*. 2004;15:124-139.

42. Tortoriello TA, Snyder CS, Smith EO, Fenrich AL, Jr., Friedman RA, Kertesz NJ. Frequency of recurrence among infants with supraventricular tachycardia and comparison of recurrence rates among those with and without preexcitation and among those with and without response to digoxin and/or propranolol therapy. *Am J Cardiol*. 2003;92:1045-1049.

43. Perry JC, Garson A, Jr. Supraventricular tachycardia due to Wolff-Parkinson-White syndrome in children: early disappearance and late recurrence. *J Am Coll Cardiol*. 1990;16:1215-1220.

CLINICAL PERSPECTIVE

Atrioventricular reentrant tachycardias presenting in fetal or neonatal life can be life threatening but also tend to resolve in the majority of patients in the first year of life. The etiology of accessory pathway mediated tachycardias in the perinatal period has not been elucidated. In early embryonic development the atrial and ventricular myocardium are continuous in the primitive atrioventricular canal. The atrioventricular conduction axis will then develop, which coincides with separation of the atrial and ventricular myocardium by formation of the annulus fibrosus. Annulus fibrosus development involves several processes in which the endocardial atrioventricular cushions lining the luminal side of the primitive atrioventricular canal together with the inward migration of the epicardially located atrioventricular sulcus tissue have an important role. In post-septated human hearts we demonstrated the presence of numerous accessory atrioventricular myocardial connections around both the mitral and tricuspid annulus during normal cardiac development. At the end of the second trimester the connections gradually decreased in number and size, and were located mostly around the tricuspid annulus. The persistence of fetal atrioventricular connections may serve as substrate for atrioventricular reentrant tachycardia in the fetus and newborn. The self-limiting character of most of these tachycardias could be explained by loss of the substrate due to the ongoing development of the annulus fibrosus, a process not completely finished by the time of birth.

7

Nathan D. Hahurij[1]
Nico A. Blom[1]
Enrico Lopriore[2]
Mohammad I. Aziz[3]
Helene T.C. Nagel[4]
Lieke Rozendaal[1]
Frank P.H.A. Vandenbussche[3]

[1] Department of Pediatric Cardiology, Leiden University Medical Center, Leiden, The Netherlands.
[2] Division of Neonatology, Department of Pediatrics, Leiden University Medical Center, Leiden, The Netherlands.
[3] Division of Fetal Medicine, Department of Obstetrics, Leiden University Medical Center, Leiden,
   The Netherlands.
[4] Department of Obstetrics and Gynecology, Bronovo Hospital, The Hague, The Netherlands.

8

Perinatal management and long-term cardiac outcome in fetal arrhythmia

ABSTRACT

Background

Cardiac arrhythmias are commonly observed in the fetus, however, may have major consequences for fetal development and post natal life.

Aims

To evaluate the perinatal management and cardiac outcome of fetuses with tachy- or bradyarrhythmia.

Study design

Perinatal management, outcome and long-term cardiac follow-up were evaluated retrospectively in consecutive fetuses with cardiac arrhythmias.

Results

Forty-four fetuses were diagnosed: supraventricular tachycardia (SVT, n=28), atrial flutter (AF, n=7) and atrioventricular block (AVB, n=9). The overall incidence of cardiac anomalies was 18% mainly in the AVB group; hydrops was present in 34%. Direct or trans-placental fetal anti-arrhythmic medication was given in 76%. Mortality was 6% in SVT / AF and 78% in the AVB group, respectively. AF resolved in all patients. In the SVT group, Wolff-Parkinson-White (WPW) syndrome was present in 21%, diagnosed at birth or later in life. After the age of one year about 90% of patients in the SVT group remained asymptomatic and free of drugs (median follow-up 76 months).

Conclusions

Mortality rate is low in patients with fetal SVT and AF but high in patients with AVB. Related morbidity includes WPW syndrome and congenital cardiac anomalies. Electrocardiographic screening is recommended in all fetal SVT cases before adolescence since WPW syndrome may occur later in life.

INTRODUCTION

Fetal arrhythmias are common in clinical practice with a frequency ranging from 1% to 3% of all pregnancies. Most of these arrhythmias reflect transient, isolated atrial ectopic beats. However, sustained episodes of tachy- or bradyarrhythmia do occur and can lead to congestive heart failure, hydrops, fetal or neonatal demise, or severe neurologic morbidity in survivors.[1-7]

The most common forms of fetal tachycardias are supraventricular tachycardia (SVT) and atrial flutter (AF). The majority of fetal SVTs are atrioventricular reentry tachycardias (AVRT) caused by the presence of an accessory atrioventricular myocardial pathway.[8] If indicated, anti-arrhythmic drugs can be given transplacentally or directly to the fetus. In SVT and AF, various anti-arrhythmic drugs are used, including digoxin, flecainide, sotalol and amiodarone.[9]

More than three quarters of fetal bradycardia cases are caused by complete atrioventricular block (AVB). AVB in the absence of structural heart disease is mostly auto-immune mediated by maternal anti-Ro (SS-A) or anti-La (SS-B) antibodies.[10] In AVB, transplacental steroid treatment may reduce the effects of inflammation and fibrosus of the conduction system caused by maternal antibodies.[11] Complete AVB in the presence of complex congenital heart disease (CHD) has a poor prognosis.[12,13]

Elective delivery by cesarean section can be performed in the third trimester of pregnancy to start direct neonatal therapy (anti-arrhythmic drugs, radiofrequency catheter ablation or pacemaker therapy). The goal of pre- and postnatal treatment of tachycardia is to achieve sinus rhythm or to reduce the fetal heart rate in order to prevent heart failure or death. In most cases of fetal tachycardia, medication can be stopped within the first year after delivery. However, in cases of fetal and neonatal SVT recurrences can be expected in approximately 30% of patients later in life.[14] The aim of this study was to evaluate the perinatal management and long-term cardiologic outcome of fetuses with tachy- or bradyarrhythmia diagnosed at our center.

MATERIAL AND METHODS

Patients

We searched both our antenatal and neonatal databases for infants with in-utero cardiac arrhythmia, diagnosed between January 1990 and December 2005 at the Leiden University Medical Center, which is a tertiary fetal referral center. Arrhythmias included both tachy- and bradyarrhythmias. Sinus tachycardias, transient sinus bradycardias, premature atrial or ventricular contractions and ventricular tachycardias were excluded. In this time period the management protocol included complete work up with ultrasound examination and consultation of the pediatric cardiologist. Fetal ultrasound included detailed anatomic imaging of the fetal heart to diagnose or exclude cardiac defects. Routine karyotype was obtained in fetuses with suspected structural heart disease.

Fetal Diagnosis and Therapy

SVT as a result of AVRT was diagnosed if there was a 1:1 atrioventricular conduction observed at a rate of 200-400 beats / min. AF was diagnosed when the atrial rate was

300-450 beats / min. Ventricular rates in AF depended on the degree of atrioventricular conduction block, usually 200-250 beats / min. The highest (peak) fetal heart rate was noted to give an indication of the severity of the tachycardia. AVB was classified as second degree or complete AVB based on M-mode evaluation and Doppler-flow measurements. Fetal hydrops was defined as a fluid collection visible on ultrasound in two or more cavities of the fetal body.[15] Maternal serum antibody titers (anti-cardiolipin antibodies, anti-Ro (SS-A) and anti-La (SS-B) were obtained in case of a heart block.

Anti-arrhythmic therapy was started when arrhythmias were sustained or associated with hemodynamic compromise prior to 34 weeks' gestation. After 34 weeks' gestation, such cases were delivered. A baseline electrocardiography (ECG) of the mother was obtained before the treatment started and maternal cardiac monitoring was conducted during the loading period to detect early signs of toxicity. During the study period, the following drugs were used: digoxin, sotalol, flecainide, amiodarone and adenosine. Digoxin was administered to the mother in adjusted oral doses to maintain a maternal serum therapeutic level of 1-2 ng/mL (loading dose 2x0.75 mg, maintenance 0.25-0.5 mg, maximum 0.75 mg/daily). Flecainide (oral dose 200-400 mg daily) and sotalol (oral dose 2x80-160 mg daily) were used as secondary agents. Amiodarone was administered by combined direct fetal intravenous and maternal oral and intravenous route. Direct fetal amiodarone therapy consisted of amiodarone on the basis of estimated fetal weight (10 mg/kg). In some cases adenosine was given intravenously (0.1 mg/kg) as direct fetal therapy just before amiodarone therapy. Drugs to treat AVB were given to the mother included ritodrine (intravenously 9 mg / hour), dexamethasone (4 mg daily) and fenoterol (intravenously 150 µgram/hour).

After birth, if tachycardia or AVB was present, ECGs were made to confirm antenatal diagnosis. In all SVT and AF cases, ECGs were made during sinus rhythm to detect ventricular preexcitation (deltawave) caused by anterograde conduction through an accessory pathway (WPW syndrome).

Long-term cardiac follow-up

With approval of the protocol by the institutional review board of the Leiden University Medical Center, family physicians were contacted by letter to explain the aims and nature of the study. After consultation with the family physician, parents were sent an explanatory letter asking their permission to review all medical records and their cooperation for testing the children. All cases were evaluated by a pediatric cardiologist and included medical history, physical examination and ECG. Additional studies, i.e. 24 hour-Holter monitoring, exercise-test and ECG were performed if children were symptomatic. Long-term neurodevelopmental outcome was also assessed and has been reported separately.[16]

RESULTS

Study population characteristics

During the 16-year study period, 44 pregnancies were referred to our center because of sustained fetal tachy- or bradyarrhythmia. Figure 1 shows the overall outcome of the 44 fetuses with arrhythmia. Perinatal characteristics of the study population are presented in Table 1.

The mechanism of SVT was AVRT in all cases. One infant in the SVT group with cardiomyopathy and encephalopathy due to hydroxyglutaric aciduria died at the age of 5 months. The AVB cases consisted of complete AVB (n=7) and second degree AVB (n=2). Two of 9 cases had auto-immune associated AVB, 5 had complex congenital heart malformations and 2 had a severe form of long QT syndrome (LQT8 or Timothy syndrome). In the AVB group were 3 fetal deaths and 4 postnatal deaths (Table 2). One case of infant death in the AVB group (LQT8) occurred after follow-up.
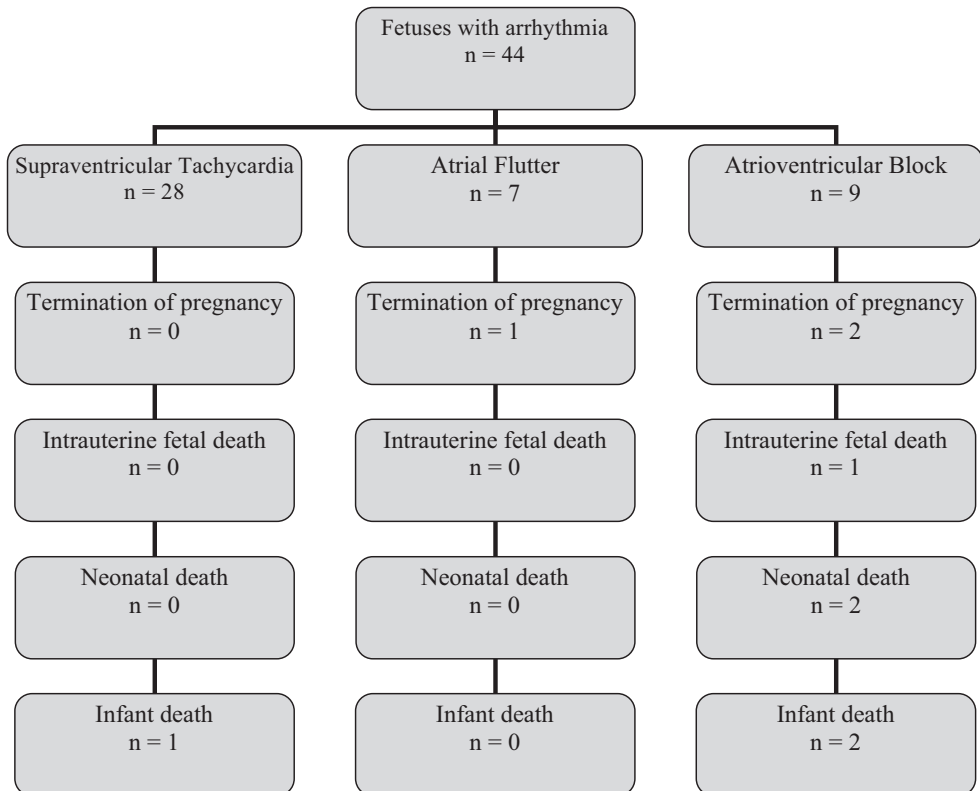

Figure 1. Flowchart showing the outcome of the 44 studied fetuses with tachy- or bradyarrhythmias.

Prenatal drug therapy

Clinical data and details in all 19 cases of tachyarrhythmia treated prenatally with anti-arrhythmic medication are presented in Table 3. During anti-arrhythmic therapy, sinus rhythm was achieved in 77% (7/9) non-hydropic and in 75% (6/8) hydropic tachycardia fetuses. There was a trend towards multidrug therapy in the more recent years. Clinical data and details in the 3 cases of prenatally treated bradyarrhythmia are presented in Table 4.

Short-term follow-up

Neonatal management and outcome in live-born infants is presented in Table 5. The overall incidence of cardiac anomalies in the study population was 18% (8/44). In the SVT group 1 infant had a ventricular septal defect and 1 infant had cardiomyopathy, polyvalvular disease and pulmonary stenosis. In the AF group, 1 infant was found to have coarctation of the aorta. In the AVB group, 5 of 9 infants had complex CHD (congenitally corrected transposition of the great arteries (cc-TGA), n=2; left atrial isomerism, n=1; ventricular septal defect, pulmonary stenosis, cardiomyopathy, n=1; endocardial fibroelastosis, n=1). Postnatally, AVB block remained present in all survivors (n=6) and 5 patients received pacemaker therapy immediately after birth.

In 67% of AF-fetuses and 78% of SVT-fetuses episodes of tachycardia or incessant tachycardia remained present after birth. Nineteen of the 28 children in the SVT group were treated with medication after birth. SVT was self-limiting in 74% (14/19), and treatment could be stopped within the first year of life. Five of 28 fetal SVT (AVRT) cases had WPW syndrome, as

Table 1. Characteristics of the study population by type of arrhythmia.

Type of arrhythmia	Supraventricular Tachycardia (n = 28)	Atrial Flutter (n = 7)	Atrioventricular Block (n = 9)
Maternal age – years[a]	28 (20 – 39)	31 (24 – 39)	32 (28 – 36)
Male fetus – % (n)	61 (17)	43 (3)	44 (4)
Gestational age at diagnosis of arrhythmia – weeks[a]	29 (18 – 40)	30 (24 – 38)	23 (12 -37)
Peak/slowest fetal heart rate – beats/min[a]	247 (200 – 400)	237 (200 – 250)	55 (45 – 70)
Fetal hydrops – % (n)	39 (11)	-	44 (4)
Antenatal therapy – % (n)	57 (16)	43 (3)	33 (3)
Duration of antenatal therapy – days[a]	56 (12 – 95)	49 (43 – 96)	33 (12 – 93)
Gestational age at birth – weeks[a]	38 (30 – 42)	37 (36 – 38)	36 (30 – 40)
Birth weight – grams[a]	2993 (1547 – 3965)	3282 (2530 – 4726)	2704 (2300 – 3470)

[a]Value given as median (range).

demonstrated by the presence of ventricular preexcitation on the ECG at birth. In 2 cases, radiofrequency catheter ablation of an accessory pathway was performed in the first months of life due to drug-refractory tachycardias. AF was treated with anti-arrhythmic therapy (n=4) or cardioversion (n=2). After initial conversion to sinus rhythm, AF did not recur in all 6 cases. Interestingly, in two AF cases the presence of an accessory pathway was demonstrated. One AF case showed WPW syndrome on ECG after cardioversion, another AF case developed recurrent AVRT requiring anti-arrhythmic therapy.

Long-term cardiac follow-up

Long-term follow-up was obtained from 28 infants of the 36 survivors. Eight of the 36 surviving infants could not be followed due to declined consent or lack of contact address. At the time of cardiac assessment the median age of the children was 76 months ranging from 6 months to 15 years of age.

Twenty-three children were examined in the SVT-group. No cases still required drug therapy, and no cases were treated with catheter ablation after the first year of life. Twenty-two of 23 patients were still asymptomatic and only one child (six year old) with self-limiting SVTs after birth complained of short episodes of palpitations. Three of 5 cases of postnatal WPW syndrome showed normalization of ECG on follow-up with disappearance of ventricular preexcitation. Interestingly, a new case of asymptomatic WPW syndrome was found in a 9 year old child who had a normal ECG and self-limiting SVTs at birth. In cases of WPW syndrome follow-up ECGs were recommended and instructions were given on how to act when symptoms occur.

Table 2. Details on cases of tachy- or bradyarrhythmias leading to fetal or infant death.

Arrhythmia	Complementary Diagnosis	Outcome
SVT	D2 – hydroxyglutaric aciduria induced cardiomyopathy	Died at age of 5 months
AF	Trisomy – 21	Termination of pregnancy
AVB	-	Termination of pregnancy
AVB	Left isomerism	Termination of pregnancy
AVB	Corrected transposition of the great arteries, pulmonal stenosis	Intrauterine fetal death
AVB	Maternal Sjögren syndrome	Pacemaker, died at age of 20 months
AVB	Endocardial fibroelastosis	Pacemaker, died at age of 2 days
AVB	Long QT – syndrome	Pacemaker, died at age of 29 days
AVB	Long QT – syndrome	Pacemaker, implantable cardioverter defibrilator, surgery, died at the age of 2 years

SVT = Supraventricular Tachycardia; AF = Atrial Flutter; AVB = Atrioventricular Block

Table 3. Clinical data on cases of tachyarrhythmia treated with prenatal maternal and direct fetal medication.

Year	Type of arrhythmia	Continuous or intermittent	Fetal hydrops	Maternal and direct fetal drug therapy	Conversion (after number of days of therapy)
1992	SVT	continuous	yes	D → F → D → cs	no
1994	SVT	continuous	yes	D + K	unknown
1994	SVT	intermittent	no	D	yes (66)
1996	SVT	intermittent	yes	S	yes (7)
1997	SVT	intermittent	no	D	unknown
1997	AF	intermittent	no	S	no
1997	SVT	intermittent	no	S	yes (19)
1998	AF	intermittent	no	D → D + S	yes (14)
1998	SVT	continuous	yes	S → S + D → D + F	yes (5)
1998	SVT	continuous	yes	S → D + F → F	yes (5)
1999	SVT	intermittent	yes	F → F + D	yes (5)
2000	SVT	intermittent	no	D → D + F → F	yes (4)
2001	SVT	continuous	no	D	yes (4)
2002	SVT	intermittent	no	D	yes (16)
2002	SVT	continuous	yes	F → F + D → Ad(cc) + Am(cc) + Ad(cc) + Am(iv/o) → Am(iv) D(iv)	yes (19)
2003	SVT	intermittent	yes	D + F → D + S → Am(cc/iv/o) → Am(cc/iv/o) → cs	no
2004	SVT	intermittent	no	F	yes (1)
2004	AF	continuous	no	F → F + D → cs	no
2004	SVT	intermittent	yes	D + F → Ad(cc) + Am(cc/iv/o)	yes (12)

SVT = Supraventricular Tachycardia; AF = Atrial Flutter; cs = elective preterm delivery by Cesarean Section; iv = intravenous; cc = cordocentesis; o = oral; D = Digoxin; F = Flecainide; K = Kinidine sulphate; S = Sotalol; Ad = Adenosine; Am = Amiodarone.

In the AF group, 5 of 6 cases remained free of arrhythmia symptoms. Four of 6 underwent neurological and cardiac examination. The ECG was normal in 3 of 4. One 2 year old AF case with postnatal WPW syndrome had remained asymptomatic but the ECG still showed ventricular preexcitation. A 9 year old AF case had developed drug refractory AVRT after birth and underwent successful catheter ablation at the age of 4 years. One 4-year old child with AF had coarctation of the aorta and self-limiting AF. The patient underwent coarctectomy and remained asymptomatic after surgery.

Morbidity and mortality rate in the AVB group was extremely high. One infant with cc-TGA received a DDD pacemaker at the age of 6 years and was in good clinical condition at the age of 9 years. Echocardiographic follow-up showed good function of the systemic right ventricle. One autoimmune mediated AVB case developed cardiomyopathy and died unexpectedly during a period with fever and pneumonia at 1.5 years of age. Another AVB case with fetal hydrops received a pacemaker immediately after birth but died on day 2 after birth. Postmortem analysis showed extensive endocardial fibroelastosis. There were two cases of functional 2:1 AV block associated with a severe form of long QT-syndrome, LQTS 8 or Timothy-syndrome. In one case a pacemaker was placed, but the infant died 29 days after birth because of uncontrollable ventricular arrhythmias. The other case also received a pacemaker followed by implantation of an implantable cardioverter defibrillator (ICD) at the age of three months. The ECG showed extreme QT-prolongation and T-wave alternans. He had recurrent ICD shocks for torsade des pointes and died at the age of 2 years of ventricular arrhythmia and cardiomyopathy after stellectomy of the left ganglion stellatum (Table 2).

Table 4. Clinical data on 3 AVB cases in which drug therapy was applied.

Year	Fetal heart rate	Fetal hydrops	Maternal and direct fetal drug therapy	Outcome
1996	45 beats/minute (3°- block)	no	DXM $\rightarrow$ DXM + R $\rightarrow$ cs at 37 weeks	Died at 1.5 years of age
2001	48 beats/minute (3°- block)	yes	R $\rightarrow$ cs at 30 weeks	Died 2 days after birth
2005	45 beats/minute (2°- block)	yes	F $\rightarrow$ cs at 34 weeks	Cardiomyopathy, pacemaker, severe developmental delay

DXM = Dexamethason; R = Ritodrine; F = Fenoterol; cs = elective delivery by Cesarean Section.

Table 5. Management and neonatal outcome in live-born infants (n=40).

Management or Outcome	Supraventricular Tachycardia (n = 28)	Atrial Flutter (n = 6)	Atrioventricular Block (n = 6)
Neonatal arrhythmia – % (n)	78 (22)	67 (4)	100 (6)
Neonatal ward admision – % (n)	89 (25)	100 (6)	100 (6)
Admission duration – days[a]	6 (1 – 61)	6 (4 – 21)	22 (2 – 42)
Mechanical Ventilation at birth – % (n)	14 (4)	33 (2)	83 (5)
Neonatal anti-arrhythmic therapy – % (n)	86 (19)	67 (4)	100 (6)
Anti-arrhythmic medication – % (n)	61 (17)	17 (1)	-
+ electric cardioversion – % (n)	-	33 (2)	-
+ accessory pathway ablation – % (n)	7 (2)	17 (1)	-
+ pacemaker implantation – % (n)	-	-	83 (5)
+ implantable cardioverter – defibrillator – % (n)	-	-	17 (1)

[a]Value given as median (range).

DISCUSSION

We studied perinatal management and long-term cardiac outcome of a consecutive cohort of fetuses with tachy- and bradyarrhythmias.

In the SVT and AF group mortality was remarkably low (6%) and limited to one postnatal death due to severe metabolic disease and one case of termination of pregnancy due to trisomy 21. In contrast to other studies,[2,5] there was no tachycardia-related mortality despite presence of fetal hydrops, young gestational age and the need for maternal or direct fetal drug therapy in a significant number of cases. There is a broad experience in management of fetal SVT and AF, although studies in literature remain limited to retrospective case series.[17,18] In general, maternal drug therapy is opted if tachycardia is intermittent or incessant before 32 to 35 weeks of gestation. Digoxin is often used for SVT and AF in non-hydropic fetuses, although many centers nowadays prefer sotalol or flecainide as drug of choice. Sotalol appears to be more effective than digoxin for treatment of AF.[19,20] In the presence of fetal hydrops, flecainide or amiodarone has become the therapy of choice for SVT.[5]

In 2006, Cuneo *et al*. reviewed literature with regard to the outcome of fetal tachyarrhythmias. They report conversion rates in SVT cases in the range from 23-62% with standard transplacental therapy with relative low mortality in this group. If second-line agents were indicated, mortality rates of 19% with flecainide and 25-30% with sotalol were reported. The combined mortality rate for hydropic and non-hydropic fetuses with AF was 8%.[21] There was no tachycardia-related mortality in the present series, which may be explained by relatively

aggressive treatment strategies with timely switch to alternative transplacental therapies or direct fetal drug therapy after failure of first or second line therapy especially in young and hydropic fetuses.

Thus far, there are very limited data on long-term postnatal outcome of fetal tachycardias.[1] Similar to other studies, AF resolved spontaneously or after cardioversion in all fetal AF cases. Interestingly, we found the presence of an accessory pathway in 2/6 fetal AF cases, which has been reported previously.[22] In the present study the majority of SVT cases remained symptomatic and required drug therapy after birth and two neonates even underwent radiofrequency catheter ablation in the first months of life. Twenty-one percent of SVT cases had WPW syndrome, which corresponds to the incidence of WPW syndrome in neonates with SVTs.[14] In the present series none of the SVT group required medication at median age of 72 months and only one child had mild symptoms. These findings indicate that around 90% of the fetal SVT group, including those with WPW syndrome, becomes asymptomatic without medication after the age of one year. These findings slightly differ with series on AVRT in neonates showing a low recurrence rate in AVRT cases without WPW syndrome but a high recurrence rate in AVRT cases with WPW syndrome.[14]

In this cohort, ventricular preexcitation (WPW syndrome) disappeared in 3 of 5 patients but also newly appeared in one patient on follow-up. There is a risk of sudden cardiac death in approximately 1% of patients with WPW syndrome, caused by atrial fibrillation and a fast ventricular response through the accessory pathway.[23] Therefore, we advocate to perform ECGs at around 8-12 years of life in all children with fetal AVRT to identify possible cases of WPW syndrome. Curative treatment by catheter ablation has become first line therapy in older symptomatic children and adults with WPW syndrome and should be considered in older asymptomatic children after episodes of fetal AVRT.[24]

In the present series the outcome of the group of fetal AVB was disappointing and 7/9 AVB cases died, including one of the two cases with auto-immune mediated AVB due to cardiomyopathy. The poor clinical outcome of this small series can be explained because the majority of AVB cases had either severe CHD (n=5) or LQTS8 (n=2), a severe type of LQTS with poor postnatal prognosis due to lethal ventricular arrhythmias. Previous reports have shown that fetal AVB has relatively poor prognosis and mortality rates are high during the first 12 months of life.[25] Jaeggi *et al.* described clinical outcome in large series of AVB cases. In cases of autoimmune mediated AVB the rates of live birth and 1-year survival were 88% and 75% respectively as compared to rates of only 56% and 19% in cases associated with major structural CHD (*P*<0.0001). They conclude, like in earlier reports, that AVB associated with major structural heart disease other than cc-TGA has an extremely poor outcome.[26] In fetuses with AVB and left atrial isomerism survival rates between 0 and 22% have been reported.[21] The use of dexamethasone as therapy for auto-immune-mediated AVB remains controversial. Several studies have reported improved survival rate after introduction of

dexamethasone treatment for fetal auto-immune AVB.[11] In contrast, a recent study by Lopes *et al*. described the clinical outcome of 116 fetuses with autoimmune-mediated AVB (49%) and CHD related AVB (51%), mainly left atrial isomerism. They showed high survival rate (>90%) in untreated fetuses with autoimmune-mediated AVB, questioning the rationale for steroid therapy in this group. This study further confirmed that poor outcome is highly associated with CHD, fetal hydrops and a slow ventricular rate (<55 bpm).[27]

In conclusion, fetal SVT and AF has low mortality and excellent long-term prognosis, although in some cases aggressive treatment strategies, including direct fetal therapy and radiofrequency catheter ablation in the first year of life, are required. Furthermore, we recommend ECG screening before adolescence to detect WPW syndrome in this patient population. Fetal AVB in the presence of CHD or long QT-syndrome has a dismal prognosis with high pre- and postnatal mortality.

ACKNOWLEDGMENTS

REFERENCES

1. Boldt T, Eronen M, Andersson S. Long-term outcome in fetuses with cardiac arrhythmias. *Obstet Gynecol*. 2003;102:1372-1379.
2. Simpson JM, Sharland GK. Fetal tachycardias: management and outcome of 127 consecutive cases. *Heart*. 1998;79:576-581.
3. Eronen M, Heikkila P, Teramo K. Congenital complete heart block in the fetus: hemodynamic features, antenatal treatment, and outcome in six cases. *Pediatr Cardiol*. 2001;22:385-392.
4. Vlagsma R, Hallensleben E, Meijboom EJ. Supraventricular tachycardia and premature atrial contractions in fetus. *Ned Tijdschr Geneeskd*. 2001;145:295-299.
5. van Engelen AD, Weijtens O, Brenner JI, Kleinman CS, Copel JA, Stoutenbeek P, Meijboom EJ. Management outcome and follow-up of fetal tachycardia. *J Am Coll Cardiol*. 1994;24:1371-1375.
6. Schade RP, Stoutenbeek P, de Vries LS, Meijboom EJ. Neurological morbidity after fetal supraventricular tachyarrhythmia. *Ultrasound Obstet Gynecol*. 1999;13:43-47.
7. Sonesson SE, Winberg P, Lidegran M, Westgren M. Foetal supraventricular tachycardia and cerebral complications. *Acta Paediatr*. 1996;85:1249-1252.
8. Kleinman CS, Nehgme RA. Cardiac arrhythmias in the human fetus. *Pediatr Cardiol*. 2004;25:234-251.
9. Oudijk MA, Ruskamp JM, Ambachtsheer BE, Ververs TF, Stoutenbeek P, Visser GH, Meijboom EJ. Drug treatment of fetal tachycardias. *Paediatr Drugs*. 2002;4:49-63.
10. Ho SY, Esscher E, Anderson RH, Michaelsson M. Anatomy of congenital complete heart block and relation to maternal anti-Ro antibodies. *Am J Cardiol*. 1986;58:291-294.
11. Jaeggi ET, Friedberg MK. Diagnosis and management of fetal bradyarrhythmias. *Pacing Clin Electrophysiol*. 2008;31 Suppl 1:S50-S53.

12. Baschat AA, Gembruch U, Knopfle G, Hansmann M. First-trimester fetal heart block: a marker for cardiac anomaly. *Ultrasound Obstet Gynecol*. 1999;14:311-314.

13. Jaeggi ET, Hamilton RM, Silverman ED, Zamora SA, Hornberger LK. Outcome of children with fetal, neonatal or childhood diagnosis of isolated congenital atrioventricular block. A single institution's experience of 30 years. *J Am Coll Cardiol*. 2002;39:130-137.

14. Tortoriello TA, Snyder CS, Smith EO, Fenrich AL, Jr., Friedman RA, Kertesz NJ. Frequency of recurrence among infants with supraventricular tachycardia and comparison of recurrence rates among those with and without preexcitation and among those with and without response to digoxin and/or propranolol therapy. *Am J Cardiol*. 2003;92:1045-1049.

15. Phibbs RH. Hydrops fetalis and other causes of neonatal edema and ascitis. In: *Fetal and neonatal physiology*. Philadelphia, PA: Saunders; 1992. p1319-1325

16. Lopriore E, Aziz MI, Nagel HT, Blom NA, Rozendaal L, Kanhai HH, Vandenbussche FP. Long-term neurodevelopmental outcome after fetal arrhythmia. *Am J Obstet Gynecol*. 2009;201:46-51.

17. Frohn-Mulder IM, Stewart PA, Witsenburg M, Den Hollander NS, Wladimiroff JW, Hess J. The efficacy of flecainide versus digoxin in the management of fetal supraventricular tachycardia. *Prenat Diagn*. 1995;15:1297-1302.

18. Krapp M, Baschat AA, Gembruch U, Geipel A, Germer U. Flecainide in the intrauterine treatment of fetal supraventricular tachycardia. *Ultrasound Obstet Gynecol*. 2002;19:158-164.

19. Jaeggi E, Fouron JC, Drblik SP. Fetal atrial flutter: diagnosis, clinical features, treatment, and outcome. *J Pediatr*. 1998;132:335-339.

20. Oudijk MA, Michon MM, Kleinman CS, Kapusta L, Stoutenbeek P, Visser GH, Meijboom EJ. Sotalol in the treatment of fetal dysrhythmias. *Circulation*. 2000;101:2721-2726.

21. Cuneo BF. Outcome of fetal cardiac defects. *Curr Opin Pediatr*. 2006;18:490-496.

22. Lisowski LA, Verheijen PM, Benatar AA, Soyeur DJ, Stoutenbeek P, Brenner JI, Kleinman CS, Meijboom EJ. Atrial flutter in the perinatal age group: diagnosis, management and outcome. *J Am Coll Cardiol*. 2000;35:771-777.

23. Mazur A, Meisel S, Shotan A, Strasberg B. The mechanism of sudden death in the Wolff-Parkinson-White syndrome. *J Cardiovasc Electrophysiol*. 2005;16:1393.

24. Joung B, Lee M, Sung JH, Kim JY, Ahn S, Kim S. Pediatric radiofrequency catheter ablation: sedation methods and success, complication and recurrence rates. *Circ J*. 2006;70:278-284.

25. Eronen M, Siren MK, Ekblad H, Tikanoja T, Julkunen H, Paavilainen T. Short- and long-term outcome of children with congenital complete heart block diagnosed in utero or as a newborn. *Pediatrics*. 2000;106:86-91.

26. Jaeggi ET, Hornberger LK, Smallhorn JF, Fouron JC. Prenatal diagnosis of complete atrioventricular block associated with structural heart disease: combined experience of two tertiary care centers and review of the literature. *Ultrasound Obstet Gynecol*. 2005;26:16-21.

27. Lopes LM, Tavares GM, Damiano AP, Lopes MA, Aiello VD, Schultz R, Zugaib M. Perinatal outcome of fetal atrioventricular block: one-hundred-sixteen cases from a single institution. *Circulation*. 2008;118:1268-1275.

8

9

General Discussion

For several decades researchers all over the world, driven by curiosity and in their way to discover new treatment modalities for cardiovascular disease, tried to unravel unexplored processes within cardiovascular development. Although knowledge significantly increased on certain mechanisms underlying this complicated developmental process other questions automatically occurred, creating the basis for future (ongoing) research.

In this thesis we focused on normal and abnormal cardiac development in relation to congenital heart disease and supraventricular arrhythmias. In **Part I** of this thesis we described the development of the posterior heart field (PHF) derived venous pole of the heart specifically in correlation to the role of *Shox2* (**Chapter 2 and 3**)[1] and *podoplanin* (**Chapter 4 and 5**)[2,3] in that particular area. Furthermore, the developmental processes in this region seem to have an important role in the anlage of the cardiac conduction system (CCS) and epicardial lineage development of the heart. In the second part (**Part II**) the aetiology of a specific subtype of supraventricular tachycardias (SVTs) i.e. atrioventricular (AV) re-entry tachycardias (AVRTs) are related to normal heart development in mammals (**Chapter 6 and 7**).[4] Finally, **Chapter 8** demonstrates the late outcome of fetal brady- and tachyarrhythmias.[5]

PART I   THE POSTERIOR HEART FIELD

9.1 CARDIAC DEVELOPMENT AND THE HEART FORMING FIELDS

In the early tri-laminar embryonic body the up-regulation of specific genes i.e. *GATA-4*[6] and *Nkx2.5*[7,8] in the splanchnic mesoderm already demarcates the heart forming regions. At the present time it is well accepted that the cardiomyocytes forming to the heart derive from two progenitor areas, the so-called first and second heart fields (or lineages).[9-11] As mentioned in **Chapter 1**, it is still unclear whether the contribution of these progenitor areas / fields occurs in a strictly separate manner or that it may be regarded as a continuum during cardiogenesis. The first heart field gives rise to the primary heart tube by fusion of the two laterally located cardiac mesodermal primordia. This primary heart tube mainly encompasses the AV canal and the future left ventricle, which is connected to the inflow and outflow tract. Lineage tracing and immunohistochemical expression studies indicated that these first heart field derived cardiomyocytes of the primary heart tube express Nkx2.5 and become negative for Isl1 after differentiation.[9,12] Subsequently, at the venous as well as the arterial pole second heart field (SHF) derived cardiomyocytes are added to this primary heart tube.[9,10,13-16] At the arterial pole the contribution of the SHF has been divided into two sub-lineages i.e. the anterior[16,17] and secondary heart fields[15] contributing *Isl1* positive cardiomyocytes to the proximal and distal outflow tract, respectively. Although the cardiac outflow tract, with respect to its formation

and maturation is a highly complicated and an appealing cardiac structure, it lays outside the scope of the current thesis. Here, we specifically studied the contribution of the SHF to the venous pole of the heart i.e. the PHF due to the conserved expression of *Shox2* (**Chapter 2 and 3**)[1] and *podoplanin* (**Chapter 4 and 5**)[2,3] in that particular area.

In contrast to the Nkx2.5 positive myocardium from the first heart field, we observed an addition of Nkx2.5 negative cells that were positive for *Shox2* and *podoplanin* as well as the myocardial marker MLC-2a at the venous pole of the heart.[1,2] This population of cardiomyocytes is considered to be derived from the PHF and highly resembles the SHF derived Isl1 positive cardiomyocytes that are added to both poles of the primary heart tube.[9,13] Moreover, *Isl1* mutant mouse embryos fail to extend their primary heart tube at the arterial as well as venous pole.[9] Similar developmental abnormalities were also observed at the venous pole of *Shox2* and *podoplanin* mutants where there is hypoplasia of the Nkx2.5 negative / MLC-2a positive myocardium, which can be studied in **Chapter 2, 3** and **5**.

9.2 THE PHF IN CARDIO-MORPHOGENESIS WITH RESPECT TO THE ROLE OF *SHOX2* AND *PODOPLANIN*

The contribution of the PHF to the venous pole of the heart is suggested to start around 8.5 days post conception (dpc) of mouse heart development shortly after looping of the heart tube has started. In chick however, addition of PHF derived cardiomyocytes occurs already in the tubular heart stage, since in avian the configuration of a tubular straight heart remains present longer as compared to mammals. The signaling pathways and specific genes involved in the development of the PHF partially do have overlap with the SHF derived cardiomyocytes at the outflow tract of the heart: *Isl1*,[9] *Id2*,[18] *Mesp-1*,[19] *Pitx2*,[20,21] *SP3*,[22] T-box genes 2 and 3 (*Tbx2*, *Tbx3*)[23,24] and the bone morphogenetic genes 2 and 4 (*Bmp2, Bmp4*).[15,25] Furthermore, a subset of transcription factors has been identified to be solely responsible for PHF anlage i.e. Tbx18,[12,26] Tbx5[27] as well as the genes described in this thesis: *Shox2* (**Chapter 2 and 3**)[1,28] and *podoplanin* (**Chapter 4 and 5**).[2,3]

In **Chapter 4 and 5** we demonstrate a common gene expression pattern within the PHF derived cardiomyocytes in the *podoplanin* mouse model. In early mouse heart development the expression of *podoplanin* in the cuboidal-shaped epithelium of the coelomic cavity and the adjacent MLC-2a positive sinus venosus myocardium stimulates the possibility that the dorsal coelomic cavity encompasses the area where the PHF derived cardiomyocytes originate from.[2,3] A cuboidal-shape of the epithelium is related to an active Epithelial-to-Mesenchymal Transformation (EMT) process, which can also be observed in other areas during cardiogenesis, like the developing AV cushions[29,30] and the epicardium.[31,32] Interestingly, for *podoplanin* a role in cell migration and invasion in EMT has been established in several cancer types.[33]

In this thesis we were able to demonstrate that during cardiogenesis a similar *podoplanin* mediated EMT processes in the coelomic epithelium occurs via interactions with E-cadherin and Rho-A (**Chapter 5**).[3] For *Shox2* a functional link with regard to the EMT process has not yet been demonstrated. Moreover, it is not expressed in the cuboidal-shaped coelomic epithelium so that a contributory role in EMT remains to be investigated.

The first impression of the important role of the PHF in heart development became obvious by studying the expression patterns of *podoplanin* and *Shox2* in the developing heart. Both genes showed to have a highly restricted spatio-temporal expression pattern that largely overlaps at the developing venous pole of the heart. These areas include the myocardium in which the sinus horns are embedded, the pulmonary veins, the venous valves and parts of the developing CCS including the sinoatrial node (SAN), AV node (AVN) region, common bundle (CB) and primitive bundle branches.[1,2] Moreover at the venous pole expression of *podoplanin* and *Shox2* was also observed in the pro-epicardial organ (PEO) from which the epicardium derives (**Chapter 9.2.1** ***"PHF and epicardial development"***).[1,2,34] The abrogated development of the sinus venosus myocardium and epicardial lineage in *Shox2* as well as *podoplanin* knockout mouse embryos confirmed the important role of the PHF in cardiogenesis. Interestingly, mutations in several other genes that have a critical role in PHF anlage show a comparable abnormal cardiac phenotype including: hypoplasia of the sinus venosus myocardium leading to a diminished incorporation of the sinus horns in the developing heart; hypoplasia of the venous valves, the atrial myocardium, the atrial septum and abnormal development of the dorsal mesenchymal protrusion as was demonstrated recently in the *Pdgfr-α* knockout mouse.[35] Furthermore, abnormal pulmonary vein development has been described in *podoplanin* mutants.[36]

Shox2 not only has a role in the anlage of the sinus venosus but also in differentiation of the PHF derived cardiomyocytes.[1,28,37] The PHF derived sinus venosus myocardium is characterized by expression of MLC-2a and the pacemaker channel HCN4 and absence of Nkx2.5, Cx40, Cx43[1] and Nppa at early stages of development.[28] At later stages (>14.5 dpc) except for the SAN, the sinus venosus myocardium attains an "atrial differentiation program" becoming positive for Nkx2.5, Cx40, Cx43 and Nppa and loosing expression of HCN4.[38] As from that moment expression of *Shox2* becomes limited to the SAN region. Therefore, *Shox2* is postulated to have an essential role in differentiation of PHF derived myocardium. This is further substantiated by the fact that the hypoplastic SAN and sinus venosus myocardium in *Shox2* mutants shows an aberrant expression pattern resembling to that seen in normal atrial working myocardium.[1,28] The exact signaling pathways via which *Shox2*, most likely in combination with other genes, regulates differentiation of the sinus venosus myocardium remain to be elucidated. However, some strong candidates are *Tbx3*,[39] *Tbx5*,[37] *Pdgfr-α*[35] and *Pitx2c*,[40] which all show a specific spatio-temporal expression pattern in the PHF derived sinus venosus myocardium during cardiogenesis.

9.2.1 PHF and epicardial development

The epicardium covering the outer layer of the heart derives from the PEO, a cauli-flower like structure located near the sinus venosus area of the developing heart. From the PEO, epicardial cells start to migrate to cover the complete surface of the heart.[41] The epicardium, covering the outflow tract of the heart derives from a separate region.[42] After spreading of the epicardium subsequent EMT of these cells leads to formation of the EPDCs, which enter the heart to fulfill several roles within cardiac development.[41] The significant role of the epicardium in cardiogenesis is largely demonstrated in avian hearts with mechanical / chemical inhibition of the epicardial outgrow from the PEO, leading to several cardiac malformations, including: myocardial non-compaction, abnormal development of the coronary arteries,[43] AV valves,[44] Purkinje fibers[45] and a disturbed anlage of the annulus fibrosus resulting in accessory pathways (APs) causing ventricular pre-excitation.[44,46] Furthermore, abrogated epicardial lineage development may also result in an aberrant cardiac looping process as observed in *Sp3* mutant mouse embryos.[22]

Several genes including, *Shox2* (**Chapter 3**), *podoplanin*,[34] *Pdgfr-α*,[35] *Tbx5*[27,47] and *Tbx18*[48] involved in sinus venosus / PHF anlage also seem to have an imperative role in epicardial lineage development. A postulated common pool of progenitor cells from which both the PHF and the PEO derive may explain why abnormal PHF and epicardial lineage development frequently coincide. Interestingly, recent studies demonstrated a specific region in the dorsal mesocardium characterized by *Tbx18* positive and *Nkx2.5* negative cells, which contributes to both the sinus venosus and PEO in developing hearts.[12,49] Although in these studies this specific area located in the dorsal mesocardium was not referred to as the PHF-region, we truly consider that with respect to the role of this specific area in heart development, it perfectly matches with the definition of the PHF.

In **Chapter 3** the disturbed epicardial lineage development in *Shox2* mutants was demonstrated. The spreading and migration of the epicardium in these mice seemed not to be as abnormal as observed in *podoplanin* and *Pdgfr-α* knockout mouse embryos, which also showed severe epicardial blebbing and multiple myocardial perforations in the ventricles.[34,35] These phenotypic differences may be related to the observation that unlike *Shox2*, *podoplanin* and *Pdgfr-α* are expressed in the complete epicardium covering the heart where both are suggested to be involved in local EMT processes. Moreover, *Pdgfr-α* has recently been demonstrated to be involved in regulation of *Wt1*,[35] which has a major role in regulation of snail and E-cadherin, representing two key factors in the EMT process.[50] Similarly, *podoplanin* (as was demonstrated in **Chapter 5**)[3] also contributes in the regulation of EMT mediators. Consequently, we postulate that especially the local involvement of factors like *podoplanin* and *Pdgfr-α* in EMT leads to a more severely abrogated epicardial lineage development as compared to those who are only expressed in the PEO during cardiogenesis, like *Shox2* (**Chapter 3**).

9

9.2.2 The PHF in relation to development of the CCS

Two theories have been put forward regarding the development and origin of the cardiomyocytes contributing to the CCS (**Chapter 1.4.1** *"The origin and development of the CCS"*). In short, the *"specification and ballooning theory"* state that the CCS derives from pre-specified cardiomyocytes in the primary heart tube. During cardiogenesis, these cardiomyocytes will retain their primitive phenotype by expression of specific genes / transcription factors that will prevent these cardiomyocytes to attain a working myocardium phenotype.[51-53] The second theory, the "*recruitment theory*" states that the CCS derives from a pool of multi-potent undifferentiated cardiomyogenic cells.[54-56]

As discussed in **Chapter 4**,[2] the second theory is more in line with the contribution of the PHF to the formation of the CCS, since it does not exclude other cell lineages to be involved i.e. the NCCs[57,58] and the PHF (including the epicardium). Moreover, with respect to our observations in the *Shox2* (**Chapter 2 and 3**)[1] as well as *podoplanin* (**Chapter 5**)[3] mouse model, we conclude that the CCS is not a completely primary heart tube derived structure, which argues to the first theory. However, in our opinion the concept of the heart fields including the PHF, demonstrated that overlap exists between the two main theories. Recently, Christoffels and Moorman[59] also did an attempt to link both theories. They suggested that cardiomyocytes that are recruited according to the "*recruitment theory*" can be considered as the precursor cells, which via the "*specification and ballooning theory*" will contribute to the definitive structures of the CCS.[59] Unfortunately, the place of second heart field derived structures was not specifically included in these considerations.

Our data indicated that newly added PHF derived cardiomyocytes to the venous pole, which can be recognized by their unique expression pattern (i.e. positive for MLC-2a, HCN4 and negative for Nkx2.5, Cx40 and Cx43), contribute to major parts of the CCS (**Chapter 2, 3 and 5**).[1,3] In the embryonic heart areas similar in expression pattern and location have also been described in the "*specification and ballooning theory*" that contribute to the mature CCS and are referred to as primitive myocardium.[51-53] Interestingly, as mentioned in **Chapter 1.4.1** *"The origin and development of the CCS"*, the areas of primitive myocardium also show overlap with the transitional zones i.e. the sinu-atrial transition, AV transition, primary ring and ventriculo-arterial transition (**Chapter 1 - Figure 5c**).[60] These transitional zones can be discriminated based on the expression patterns of several markers involved in CCS development.[61-64] Therefore, we may speculate that the primitive myocardium at the venous pole, which largely resembles to the sinu-atrial transitional zone, is PHF derived. The spatio-temporal expression of specific transcription factors / genes like: *Tbx2*, *Tbx5*[59] and *Shox2* (**Chapter 2 and 3**)[1] may regulate the differentiation of the PHF derived primitive myocardium so that it partially forms the CCS, whereas others parts will attain a working myocardial differentiation program. Most likely, comparable differentiation processes occur at other embryonic regions harboring the primitive myocardium, which corresponds to other transitional

zones. Finally, with respect to the role of the heart fields in CCS development, it can not be excluded that some parts of CCS might have a contribution from the first (i.e. primary heart tube) as well as the second heart field.

In this thesis we mainly focused on development of the SAN a structure that can easily be discriminated in early stages of mouse heart development.[65] In *Shox2* and *podoplanin* knockout embryos the SAN is severely hypoplastic. Although it is now well established that the SAN, like the complete sinus venosus myocardium, is a PHF derived structure the exact signaling pathways involved in differentiation of this highly complex region remains largely unknown. Moreover, contemporary studies demonstrated that different regions within the SAN i.e. solid head (or node) and tail along the terminal crest, show distinct expression patterns of genes,[39] which has been related to the even more complex SAN electrophysiological properties.[66]

However, we were able to unravel a small part of this complicated issue, by showing aberrant differentiation of SAN (and sinus venosus) cardiomyocytes in *Shox2* mutants.[1,28] In the SAN an up-regulation of Nkx2.5, Cx40, Cx43 and Nppa that normally encode for an atrial differentiation program was observed. This of course suggests an abnormal pacemaking function in *Shox2* mutant hearts. Most strikingly, the *Shox2* morpholino injections in Zebra fish embryos in **Chapter 2** as well as the electrophysiological recordings in embryonic *Shox2* mutant mouse hearts in **Chapter 3**, indeed confirmed a decreased / bradycardic heart rate.[1] The lowered heart rate in *Shox2* mutants has been related to a decreased expression or absence of the pacemaker channel HCN4 due to up-regulation of Nkx2.5.[28] This of course seems to be a reasonable explanation since bradycardia has been reported in patients with mutations in the *HCN4* gene.[67] Remarkably, in our studies we did not find absence of HCN4 in *Shox2* mutant embryos. Moreover, the intensity of HCN4 expression in the hypoplastic SAN was comparable to that observed in embryonic wildtype hearts. So, what then could be the underlying mechanism of the lowered heart rate in mutants?

In our opinion the hypoplasia of the SAN itself might explain its deteriorated function, since electrophysiological mapping studies in human[68] and animal[69-71] largely demonstrated that pacemaking occurs in a widely distributed area in the SAN creating a pacemaking complex. Under physiological circumstances, as cycle length decreases, the leading pacemaker area shifts towards the upper region in the SAN (head / solid node).[71] On the other hand, an increase in cycle length leads to an inferior shift of the leading pacemaker area. In line with that, it seems reasonable to speculate that in case of hampered SAN anlage the physiological shift of the leading pacemaker-site through the pacemaking complex fails. Consequently, this might underlie the observed bradycardic heart rate in *Shox2* mutant embryos.

Besides the important role of the PHF in development of the SAN, the contribution of the PHF to others parts of the CCS was not studied in detail in this thesis. However, in embryonic hearts the expression of *Shox2*[1] and *podoplanin*[2] highly overlap with other components of the developing CCS i.e. AVN, CB and primitive left and right bundle branches. Furthermore,

9

191

expression was observed in the myocardium of the atria that comprise the location of the internodal pathways. Notably, Espinoza-Lewis *et al*. did not find *Shox2* expression in the CB and primitive bundle branches, so that the exact role of *Shox2* in that particular part of the heart remains doubtful.[28] Nevertheless, a more extensive role of the PHF in CCS development is strengthened by the observation that expression patterns of *Shox2* and *podoplanin* highly resembles to that of other markers, which have been used to study CCS development like: CCS-*LacZ*,[62] *MinK-LacZ*,[64] *Hnk-1*,[61,72] *Leu7*[73,74] and *PSA-NCAM*.[75] In the near future lineage tracing studies most probably will have an essential role in unraveling the exact contribution of the PHF in development of the more peripheral regions of the CCS.

9.2.3 The PHF in congenital heart malformations and clinical implications

In **Part I** of this thesis, we demonstrated that the PHF has a major role in heart development, as indirectly can also be appreciated by the high mortalities rates of *Shox2* (**Chapter 2 and 3**)[1] and *podoplanin* (**Chapter 5**)[3] mutant mouse embryos. Similar mortality rates have been reported in other mouse models for PHF development.[35]

The PHF is involved in formation and differentiation of the sinus venosus myocardium but also has an important role in CCS and epicardial lineage development. Consequently, abnormal PHF anlage may encompasses a broad variety of cardiac malformations ranging from structural heart defects to certain types of cardiac arrhythmias, or combination of events like: the association between SAN dysfunction and atrial septal defects (ASD) in patients with mutations in the *Tbx5* gene causing Holt-Oram syndrome;[76] or mutations in *Nkx2.5* that leads to disturbed AV conduction and ASD and / or ventricular septal defects (VSD).[77,78]

With respect to cardiac arrhythmias related to abnormal PHF development, we postulate that they may either occur secondarily to the structural cardiac malformations, or be due to abnormal myocardial differentiation of the PHF derived myocardium i.e. by the maintenance or re-expression of the characteristic expression pattern (positive for MLC-2a, HCN4 and negative for Nkx2.5, Cx40 and Cx43) pre- or postnatally. Therefore, it seems tempting to speculate that the preferential location of arrhythmias like atrial ectopic tachycardia (AET) that are occasionally observed at fetal stages of development, is rendered by areas of abnormal differentiated PHF derived myocardium. However, to our knowledge a clear link has not yet been demonstrated.

Table 1 summarizes the cardiac abnormalities, which are postulated to be related to abnormal PHF anlage.

Abnormal Posterior Heart Field development

epicardial lineage

sinus venosus / atrium

Structural abnormalities

* Ventricular septal defects[22, 34]
* Myocardial abnormalities[this thesis, 22, 34, 35]
    - fenestrations
    - non-compaction
* Abnormal cardiac looping[22]
* Disturbed annulus fibrosis formation[44, 46]
    - accessory AV pathways (APs)
* Mitral / Tricuspid valve malformation[22, 44]
    - Ebstein abnormality
* Abnormal Purkinje fiber network[45]
* Coronary artery defects[34, 43]
* Outflow tract abnormalities[22, 34]

Arrhythmia

* Supraventricular tachycardia [44, 46]
    - AVRT (including WPW)

Structural abnormalities

* CCS malformations[this thesis, 1, 3, 34, 35]
    - hypoplasia sinoatrial node
* Atrial septal defects[this thesis, 35, 36]
* Myocardial abnormalities[this thesis, 1, 3, 34 - 36]
    - hypoplasia SV myocardium
    - thin atrial myocardium
* Venous valve abnormalities[this thesis, 1, 35]
* Abnormal SV incorporation[this thesis, 3, 36]

Arrhythmia

* Sinoatrial node dysfunction [this thesis]
    - sick sinus syndrome
* Supraventricular tachycardia[this thesis]
    - atrial ectopic tachycardia
    - atrial fibrillation
* AV conduction axis abnormalities
    - AVNRT, AVB

Table 1. Schematic representation of congenital heart defects that can be related to abnormal development of the Posterior Heart Field (PHF) derived myocardium. The PHF contributes cells to the sinus venosus / atrium and pro-epicardial organ from which the epicardial lineage develops, the congenital heart defects are separated in two columns correspondingly. Whether the PHF also contributes to the atrioventricular (**AV**) conduction axis remains uncertain, therefore this text is indicated in grey. The numbers in this table refer to the individual references that can be obtained from the reference list of this chapter. **AVB** indicates AV block; **AVRT**, AV reentry tachycardia; **AVNRT**, AV nodal reentry tachycardia; **CCS**, cardiac conduction system; **SV**, sinus venosus; **WPW**, Wolff-Parkinson-White.

9

PART II NORMAL HEART DEVELOPMENT IN RELATION TO AVRT

The development of the mature impulse propagation through the heart not only involves formation of the CCS, proper isolation of specific areas within the heart is extremely important as well. "Leakage" of the cardiac impulse might occur via so-called accessory AV myocardial pathways (APs) at locations where the isolating layer between the atria and ventricles, the annulus fibrosus, is absent. APs are involved in AVRTs, a sub-group of SVTs, which represent the largest group of tachy-arrhythmias within the pediatric age group.[79] Strikingly, almost two-thirds of fetuses diagnosed with SVT based on AP-pathology remains free of arrhythmia before the age of one year without further medical treatment.[80,81]

In **Part II** of this thesis we have related the process of normal heart development, including that of the CCS, AV junction and annulus fibrosus, to spontaneous disappearance of AVRTs at fetal and neonatal stages of development.

9.3 DEVELOPMENT OF THE AV JUNCTION IN RELATION TO TEMPORARY PRESENCE OF APs

9.3.1 Development of the AV junction - Morphology

The AV junction is a complex region in the heart that harbors several important cardiac structures. Imagine that you are facing towards a mature heart from a superior view, from which the atria are cut-off in a transverse plane at the level of the AV junction. Then, two separate orifices including their valvular-apparatus can be discriminated; The mitral valve orifice at the left and at the tricuspid valve orifice at the right side. The fibrous tissue of the mitral and tricuspid valves is in continuity with the annulus fibrosus, surrounding both orifices (**Chapter 1- Figure 7**). In the septal region a single myocardial continuity i.e. the AV conduction axis can be discriminated that penetrates through the annulus fibrosus, to interconnect the atrial with the ventricular (septal) myocardium. This part of the CCS connects superiorly (atrial level) to the AVN and inferiorly (ventricular level) to the bundle branches.

It is noteworthy, with respect to the developmental process underlying the AV junction, that at the very early embryonic stages the heart only consists of a single heart tube. This primary heart tube solely comprises the myocardium contributing to the future left ventricle and AV canal (first heart field derived) and directly connects to the cardiac in- and outflow tract. So, at these stages there is neither presence of an AV junction with two separate AV orifices nor a specialized AV conduction axis.[82] Due to the addition of SHF-derived cardiomyocytes (**Part I**) and complex remodeling processes of the heart, including cardiac looping and septation, the mitral and the tricuspid valve orifice will appear. The formation of the two

independent AV orifices has been demonstrated by our group in a study on the development of the right ventricular inflow tract in CCS-*LacZ* transgenic mice.[83] Shortly after looping of the heart tube, the contours of the primitive left and right ventricles can be discriminated, which are interconnected via the primary interventricular foramen. At these stages (mouse 10.5 dpc; human ≈ E28), the atrial part of the heart still connects to the ventricular part via a single orifice, the primitive AV canal, which by then is mainly positioned above the future left ventricle (**Chapter 1 - Figure 5**). Subsequently, due to outgrowth of the right ventricle, a remodeling of the primary fold will occur, that will eventually form the right ventricular inflow tract.[83] Eventually, by completion of ventricular septation and remodeling of the endocardial located AV cushions, which mainly contribute to formation of the mitral and tricuspid valves, the two individual AV orifices including their valvular apparatuses will appear.

More or less subsequent to formation of the mitral and tricuspid valve orifice, the separation of the AV myocardial continuity in the AV canal is initiated. This process of annulus fibrosus formation, as was already mentioned in **Chapter 1.5.1** *"Annulus fibrosus: The isolating system"*, involves interaction between epicardially located AV sulcus tissue and endocardial located AV cushion tissue.[84-88] In **Chapter 6** and **7**,[4] we demonstrated that formation of the annulus fibrosus in mouse as well as in human already starts at pre-septation stages of development, by formation of fibrous tissue near the primitive AV canal. Around the twelfth week of human development, as was also demonstrated by others,[84] the complete atrial and ventricular myocardium are separated by the annulus fibrosus through which the AV conduction axis forms the only myocardial continuity between the atria and ventricles.

In this thesis we mainly focused on the role of periostin, primarily known as osteoblast-specific factor 2,[89] in the formation of the annulus fibrosus. Periostin was postulated to have an important role within this particular process because of its proven ability to directly regulate collagen-I fibrillogenesis.[90] In human (**Chapter 7**),[4] mouse (**Chapter 6**) and quail[44,46,91] hearts we did observe high expression of periostin in the developing annulus fibrosus especially at locations where isolation is mandatory, all the way through cardiac development. Intriguingly, state-of-the-art stem cell studies demonstrated that cardiomyocytes-like cells can be newly generated by reprogramming fibroblasts.[92] With respect to that, it is thrilling to speculate whether a sort of natural differentiation mechanism occurs in an opposite direction near the AV junction so that cardiomyocytes become isolating fibroblasts that contribute to the annulus fibrosus. In this thesis, we did however not find a link that substantiates that hypothesis. Our periostin expression data in mouse showed that in the developing AV junction periostin is never co-expressed in cardiomyocytes (**Chapter 6**). For now we may only put forward that periostin is in someway involved in fibrous tissue formation given its proven role in collagen-I fibrillogenesis.[90] Whether periostin is the key factor in AV isolation remains doubtful, since recent studies in *periostin*

mutant mice showed that *periostin* null mutants are largely normal and do not show an abnormal cardiac phenotype.[93]

Other known factors involved in formation of the annulus fibrosus are bone-morphogenetic proteins (BMP) signaling[94,95] and epicardial cells.[44,46,96] The contributory role of BMPs and the epicardium is substantiated by the fact that disturbed BMP signaling in *Alk3* knockout mice[94] as well as hampered epicardial outgrowth in quail[44,46] leads to defects in annulus fibrosus formation with multiple abnormal myocardial AV connections (i.e. APs) between the atria and ventricles that are electrophysiological functional.[44,46] The role of the epicardium / EPDCs in annulus fibrosus formation is substantiated by the observation that *in vitro* cell cultures of human and quail EPDCs express periostin so that they subsequently may have an important role in collagen-I fibrillogenesis.[44] The contribution of especially the epicardium insinuates that the PHF (**Part I**) also has a role in annulus fibrosus development (**Table 1**).

Nevertheless, there are still numerous unidentified signaling pathways involved in the anlage of the annulus fibrosus. Furthermore, it remains highly fascinating why formation of AV isolation especially does not occur in the AV conduction axis leading to complete AV block (AVB).

9.3.2 Development of the AV junction - Electrophysiology

The main purpose of annulus fibrosus development is to prevent "leakage" of the cardiac impulse from the atria to the ventricles (or the other way around) via APs that bypass the AV conduction axis including the AVN and His-Purkinje-system (HPS). Consequently, APs can only be identified once the AV conduction axis has become functional at a specific moment in cardiac development. Before the presence of this axis, the complete primitive AV canal myocardium itself renders the area for normal AV conduction. Fascinatingly, in a looped heart tube the primitive AV canal myocardium was already demonstrated to have slow conducting properties in chick.[97] These conducting properties might be explained by a restricted expression pattern of certain gap junction proteins in that specific area.[98,99] We for instance demonstrated that during development Cx43, involved in rapid impulse conduction through the atria and ventricles, is never expressed in the primitive AV canal / AV junction.[99] (**Chapter 6**) In someway, these slow conducting properties of the primitive AV canal myocardium at the early stages of development resemble the decremental properties of the mature AVN that will reside in this specific area. Therefore, it is tempting to postulate that the AVN, at least partially, derives from this slow conducting primitive AV canal myocardium.

During cardiac development the transition of the ventricular activation pattern from base-to-apex into the mature apex-to-base activation coincides with a functional AV conduction axis mainly with respect to maturation of the HPS. Furthermore, studies in chick and quail hearts demonstrated that this process highly correlates with completion of ventricular septation.[91,100,101](**Chapter 1.4.2 *"Action potential generation and propagation in the***

developing heart"). However, as demonstrated in **Chapter 6**, the majority of normal developing embryonic mouse hearts already show a mature apex-to-base activation pattern far before completion of ventricular septation. This observation is substantiated by several optical mapping studies performed in pre-septated embryonic mouse hearts, which also demonstrated a functional AV conduction axis at these stages of development.[63,102] These observations might indicate that: (1) the transition to a mature apex-to-base ventricular activation patterns in mouse hearts is not related to completion of ventricular septation as is suggested to be the case in avian hearts; (2) pre-septated embryonic mouse hearts may already have a functional and / or preferential pathways for fast AV impulse propagation, which primarily activates the apex before the base in the developing ventricles.

9.3.3 APs during normal heart development

The incidental presence of APs during normal heart development has already been reported in human,[103-105] mouse[83] and chick.[106] Our group was the first that studied the presence and course of APs during subsequent stages of normal heart development. The initial studies performed in quail demonstrated the presence of electrophysiological functional APs, which appeared to be remnants of the early embryonic primitive AV canal myocardium. These APs were located around both the developing mitral and tricuspid valve orifice and decreased in number and size at subsequent stages of development.[91] This thesis for the first time describes the presence and course of APs during normal mammalian heart development. In both mouse (**Chapter 6**) and human (**Chapter 7**)[4] APs, more or less similar to those observed in quail, could be observed until late stages of fetal life, which gradually decreased in number and size.

Between species, some differences were observed in the preferential location of APs at the annulus fibrosus. At late stages of human heart development most APs were observed sub-endocardially at the lateral aspect of the tricuspid valve orifice.[4] Fetal quail hearts also demonstrated the majority of APs around that orifice, however in quail the APs were positioned to a more septal position in the AV junction.[91] On the other hand, in fetal mouse hearts most APs were located at an antero-lateral position near the mitral valve orifice (**Chapter 6**).

The persistence of especially right sided APs at later stages of development, as observed in human and quail, might be related to the process that is involved in the formation of the right ventricular inflow tract. In contrast to the left ventricular inflow tract, the right inflow tract is a newly formed orifice which originates from a groove in the primary fold.[83] In addition, the concept of the *"transitional zones"* (**Chapter 1.4.1. *"The origin and development of the CCS"***), which describes the presence of four transitional zones in the looped embryonic heart tube based on the expression of CCS developmental markers, contributes to this idea. Especially the dorsal side of the right AV junction may be formed by a myocardium of three transitional zones: the sinu-atrial transition, the AV transition and the primary fold, as can also be

appreciated in **Figure 5d** in **Chapter 1**.[60] The left AV junction however, only receives a contribution from the sinu-atrial transition and the AV transition. Consequently, we postulate that both the physiological delay and a far more complicated developmental process of the right AV junction explains the higher incidence of persistent right sided APs at late fetal stages of development. Furthermore, we may comment that the preferential location of persistent APs (in human) is not related to the location where annulus fibrosus formation initiates during heart development, since **Chapter 7** describes that formation of this isolating structure starts near the right AV junction / future tricuspid valve orifice.[4,84]

As was demonstrated in **Chapter 6**, the majority of APs during fetal stages of mouse heart development are located near the mitral valve orifice. The mean AP-width also appeared larger at the left AV junction. Remarkably, unlike in avian and human,[4,91] in all fetal mouse hearts a broad AP could be observed at an antero-lateral position near the mitral valve orifice. The presence of more or less identical pathways at this specific location in the developing AV junction has been reported before. Rentschler *et al*. demonstrated in their study on CCS development by means of *LacZ* expression several APs that interconnected the left atrium and ventricle along the free wall. These *LacZ* expressing APs, which were not part of the mature CCS, were observed at subsequent stages of development including neonatal mouse hearts and have been related to WPW-syndrome.[63] Thus far, it remains unclear what exactly causes the high incidence of especially left sided APs in mouse fetuses, at least an interspecies differences can not be excluded.

9.3.4 APs - specialized tissue or ordinary working myocardium?

The APs studied in normal heart development in human (**Chapter 7**),[4] mouse (**Chapter 6**) and avian[91] are all supposed to be remnants of the early primitive AV canal myocardium. However, from electrophysiological studies we do know that not all APs share similar electrophysiological characteristics. In Mahaim tachycardia the APs have decremental properties resembling that of the AVN,[107] which might indicate that some APs are composed of specialized conducting tissue. Furthermore, it is well known that APs involved in Mahaim tachycardia have a morphological-relation with the specialized CCS and interconnect the AVN or His bundle to the fascicles or ventricular muscle.[108] Nevertheless, the question remains whether the presence of APs with decremental properties can also be related to the normal process of cardiac development.

Contemporary studies by Jongbloed *et al*. related right ventricular inflow tract development to be one of the underlying mechanisms for atrio-fasciculair tracts. In that study functional APs were observed at the right AV junction, which connected to the right bundle branch via the moderator band.[83] Interestingly, in **Chapter 7** we demonstrated multiple APs between the developing AVN and the ventricular septal myocardium in human fetal hearts. These APs appeared to have a similar cellular morphology as compared to that of AVN cells, which might

indicate that they have specialized conducting properties. Furthermore, we observed that the majority of APs at the tricuspid valve orifice are related to the right AV ring bundle (RAVRB). This ring of specialized cells located around the developing tricuspid valve orifice is believed to be a remnant of the more extensive embryonic CCS that deteriorates during fetal life. The RAVRB can be detected by expression of various markers for the developing CCS, like: *HNK-1*,[61,109] *Leu7*,[73] CCS-*LacZ*.[62,83] In several species a similar structure can also be recognized around the developing mitral valve orifice, which has been referred to as the left AV ring bundle (LAVRB).[2,110,111] In young animals these ring bundles have also been found and tend to express a specific subset of markers, which also demarcate the CCS.[110] The fact that these ring bundles make contact with the AVN via the AV nodal extensions might suggest a role in normal AV conduction, however at present there are no electrophysiological studies which support to this idea.[110]

It seems tempting to postulate that APs with decremental properties (i.e. in Mahaim tachycardia) are those that are related to the embryonic CCS i.e. RAVRB or LAVRB located at the AV junction. The exact mechanism by which these ring bundles deteriorate remains unknown. However, we may speculate that ongoing myocardial differentiation as observed in other parts of the developing CCS has an important role so that these ring bundles (and if present the related APs) loose their specialized (decremental) properties and become ordinary working myocardium.

9.4 AVRT IN THE FETUS AND THE YOUNG – CLINICAL IMPLICATIONS

The AVRTs represent the largest group of tachy-arrhythmias pre- and postnatally and can be potentially life-threatening.[80,81] From fetal life up to adolescence, the APs underlying AVRT can present at the tricuspid as well as mitral valve orifice. The incidence of APs tends to be higher at the left / mitral valve orifice.[112-114] The etiology of the APs underlying this specific type of arrhythmia is largely unknown. In a minority of cases genetic mutations are involved, like *PRKAG-2* (in familiar WPW-syndrome)[115,116] and *ALK3* (in mice).[94] Furthermore, high numbers of APs are found in combination with other forms of congenital heart disease i.e. Ebstein anomaly[117,118] and congenital corrected Transposition of the Great Arteries (ccTGA).[119] In rare cases, an intra-cardiac tumor has been reported to serve as substrate for AVRT.[120,121] Intriguingly, the majority of otherwise healthy fetuses and neonates that initially suffer from AVRT remain free of symptoms before the age of one year without additional anti-arrhythmic therapy (**Chapter 8**).[5,79,81] A prolonged cardiac maturation during the first year of life might cause APs to spontaneously disappear, so that AVRT automatically resolves. This is supported by the observation that especially the development of the fibrous structures of the heart that includes the annulus fibrosus, extends into post-natal life.[122,123]

This thesis fully supports the theory that APs are remnants of the early primitive AV canal and that prolonged cardiac maturation leads to disappearance of AVRT during the first year of life. This theory is best substantiated by the observation that: (1) Functional accessory AV myocardial connections are present during normal mouse heart development that might serve as APs (**Chapter 6**);[4] (2) These APs, which can be found around the tricuspid as well as mitral valve orifice, decrease in number and size at subsequent stage of heart development and accordingly might explain the self limiting character of AVRT (**Chapter 6 and 7**);[4] (3) In human hearts many APs were related to the RAVRB that encompasses a part of the embryonic CCS that deteriorates later on, which might explain why some APs have specialized properties (**Chapter 7**).

The ongoing maturation of the annulus fibrosus offers a good explanation for spontaneous AVRT disappearance. However, it remains uncertain why approximately one-third of patients have a recurrent episode of AVRT later in life.[124] In line with that, it is still unknown why the incidence of certain forms of tachy-arrhythmia like AVNRT increases with age.[81,125] At the moment there are no studies giving answers to those specific questions. It seems however interesting to state in general that cardiac development is not a process that is completed at the time of birth. Especially, for cardiac arrhythmias in the paediatric age group it might be speculated that postnatal cardio-morphogenesis has an important role.

REFERENCES

1. Blaschke RJ, Hahurij ND, Kuijper S, Just S, Wisse LJ, Deissler K, Maxelon T, Anastassiadis K, Spitzer J, Hardt SE, Scholer H, Feitsma H, Rottbauer W, Blum M, Meijlink F, Rappold G, Gittenberger-de Groot AC. Targeted mutation reveals essential functions of the homeodomain transcription factor Shox2 in sinoatrial and pacemaking development. *Circulation*. 2007;115:1830-1838.
2. Gittenberger-de Groot AC, Mahtab EA, Hahurij ND, Wisse LJ, Deruiter MC, Wijffels MC, Poelmann RE. Nkx2.5-negative myocardium of the posterior heart field and its correlation with podoplanin expression in cells from the developing cardiac pacemaking and conduction system. *Anat Rec (Hoboken)*. 2007;290:115-122.
3. Mahtab EA, Vicente-Steijn R, Hahurij ND, Jongbloed MR, Wisse LJ, Deruiter MC, Uhrin P, Zaujec J, Binder BR, Schalij MJ, Poelmann RE, Gittenberger-de Groot AC. Podoplanin deficient mice show a rhoa-related hypoplasia of the sinus venosus myocardium including the sinoatrial node. *Dev Dyn*. 2009;238:183-193.
4. Hahurij ND, Gittenberger-de Groot AC, Kolditz DP, Bokenkamp R, Schalij MJ, Poelmann RE, Blom NA. Accessory atrioventricular myocardial connections in the developing human heart: relevance for perinatal supraventricular tachycardias. *Circulation*. 2008;117:2850-2858.
5. Hahurij ND, Blom NA, Lopriore E, Aziz MI, Nagel HT, Rozendaal L, Vandenbussche FPHA. Perinatal management and long-term cardiac outcome in fetal arrhythmia. *Early Hum Dev*. 2010;87:83-87.
6. Laverriere AC, MacNeill C, Mueller C, Poelmann RE, Burch JB, Evans T. GATA-4/5/6, a subfamily of three transcription factors transcribed in developing heart and gut. *J Biol Chem*. 1994;269:23177-23184.
7. Frasch M. Intersecting signalling and transcriptional pathways in Drosophila heart specification. *Semin Cell Dev Biol*. 1999;10:61-71.
8. Schultheiss TM, Xydas S, Lassar AB. Induction of avian cardiac myogenesis by anterior endoderm. *Development*. 1995;121:4203-4214.

9. Cai CL, Liang X, Shi Y, Chu PH, Pfaff SL, Chen J, Evans S. Isl1 identifies a cardiac progenitor population that proliferates prior to differentiation and contributes a majority of cells to the heart. *Dev Cell*. 2003;5:877-889.

10. Vincent SD, Buckingham ME. How to make a heart: the origin and regulation of cardiac progenitor cells. *Curr Top Dev Biol*. 2010;90:1-41.

11. Watanabe Y, Buckingham M. The formation of the embryonic mouse heart: heart fields and myocardial cell lineages. *Ann N Y Acad Sci*. 2010;1188:15-24.

12. Mommersteeg MT, Dominguez JN, Wiese C, Norden J, de Gier-de Vries C, Burch JB, Kispert A, Brown NA, Moorman AF, Christoffels VM. The sinus venosus progenitors separate and diversify from the first and second heart fields early in development. *Cardiovasc Res*. 2010;87:92-101.

13. Kelly RG. Molecular inroads into the anterior heart field. Trends *Cardiovasc Med*. 2005;15:51-56.

14. de la Cruz MV, Sanchez GC, Arteaga MM, Arguello C. Experimental study of the development of the truncus and the conus in the chick embryo. *J Anat*. 1977;123:661-686.

15. Waldo KL, Kumiski DH, Wallis KT, Stadt HA, Hutson MR, Platt DH, Kirby ML. Conotruncal myocardium arises from a secondary heart field. *Development*. 2001;128:3179-3188.

16. Mjaatvedt CH, Nakaoka T, Moreno-Rodriguez R, Norris RA, Kern MJ, Eisenberg CA, Turner D, Markwald RR. The outflow tract of the heart is recruited from a novel heart-forming field. *Dev Biol*. 2001;238:97-109.

17. Kelly RG, Brown NA, Buckingham ME. The arterial pole of the mouse heart forms from Fgf10-expressing cells in pharyngeal mesoderm. *Dev Cell*. 2001;1:435-440.

18. Martinsen BJ, Frasier AJ, Baker CV, Lohr JL. Cardiac neural crest ablation alters Id2 gene expression in the developing heart. *Dev Biol*. 2004;272:176-190.

19. Saga Y, Miyagawa-Tomita S, Takagi A, Kitajima S, Miyazaki J, Inoue T. MesP1 is expressed in the heart precursor cells and required for the formation of a single heart tube. *Development*. 1999;126:3437-3447.

20. Poelmann RE, Jongbloed MR, Gittenberger-de Groot AC. Pitx2: a challenging teenager. *Circ Res*. 2008;102:749-751.

21. Liu C, Liu W, Palie J, Lu MF, Brown NA, Martin JF. Pitx2c patterns anterior myocardium and aortic arch vessels and is required for local cell movement into atrioventricular cushions. *Development*. 2002;129:5081-5091.

22. van Loo PF, Mahtab EA, Wisse LJ, Hou J, Grosveld F, Suske G, Philipsen S, Gittenberger-de Groot AC. Transcription factor Sp3 knockout mice display serious cardiac malformations. *Mol Cell Biol*. 2007;27:8571-8582.

23. Christoffels VM, Hoogaars WM, Tessari A, Clout DE, Moorman AF, Campione M. T-box transcription factor Tbx2 represses differentiation and formation of the cardiac chambers. *Dev Dyn*. 2004;229:763-770.

24. Hoogaars WM, Tessari A, Moorman AF, de Boer PA, Hagoort J, Soufan AT, Campione M, Christoffels VM. The transcriptional repressor Tbx3 delineates the developing central conduction system of the heart. *Cardiovasc Res*. 2004;62:489-499.

25. Stottmann RW, Choi M, Mishina Y, Meyers EN, Klingensmith J. BMP receptor IA is required in mammalian neural crest cells for development of the cardiac outflow tract and ventricular myocardium. *Development*. 2004;131:2205-2218.

26. Christoffels VM, Mommersteeg MT, Trowe MO, Prall OW, Gier-de Vries C, Soufan AT, Bussen M, Schuster-Gossler K, Harvey RP, Moorman AF, Kispert A. Formation of the Venous Pole of the Heart From an Nkx2-5-Negative Precursor Population Requires Tbx18. *Circ Res*. 2006;98:1555-1563.

27. Bruneau BG, Nemer G, Schmitt JP, Charron F, Robitaille L, Caron S, Conner DA, Gessler M, Nemer M, Seidman CE, Seidman JG. A murine model of Holt-Oram syndrome defines roles of the T-box transcription factor Tbx5 in cardiogenesis and disease. *Cell*. 2001;106:709-721.

28. Espinoza-Lewis RA, Yu L, He F, Liu H, Tang R, Shi J, Sun X, Martin JF, Wang D, Yang J, Chen Y. Shox2 is essential for the differentiation of cardiac pacemaker cells by repressing Nkx2-5. *Dev Biol*. 2009;327:376-385.

29. Markwald R, Eisenberg C, Eisenberg L, Trusk T, Sugi Y. Epithelial-mesenchymal transformations in early avian heart development. *Acta Anat (Basel)*. 1996;156:173-186.

9

30. Potts JD, Runyan RB. Epithelial-mesenchymal cell transformation in the embryonic heart can be mediated, in part, by transforming growth factor beta. *Dev Biol*. 1989;134:392-401.

31. Vrancken Peeters MP, Gittenberger-de Groot AC, Mentink MM, Poelmann RE. Smooth muscle cells and fibroblasts of the coronary arteries derive from epithelial-mesenchymal transformation of the epicardium. *Anat Embryol (Berl)*. 1999;199:367-378.

32. Lie-Venema H, Gittenberger-de Groot AC, van Empel LJ, Boot MJ, Kerkdijk H, de Kant E, Deruiter MC. Ets-1 and Ets-2 transcription factors are essential for normal coronary and myocardial development in chicken embryos. *Circ Res*. 2003;92:749-756.

33. Martin-Villar E, Scholl FG, Gamallo C, Yurrita MM, Munoz-Guerra M, Cruces J, Quintanilla M. Characterization of human PA2.26 antigen (T1alpha-2, podoplanin), a small membrane mucin induced in oral squamous cell carcinomas. *Int J Cancer*. 2005;113:899-910.

34. Mahtab EA, Wijffels MC, Van Den Akker NM, Hahurij ND, Lie-Venema H, Wisse LJ, Deruiter MC, Uhrin P, Zaujec J, Binder BR, Schalij MJ, Poelmann RE, Gittenberger-de Groot AC. Cardiac malformations and myocardial abnormalities in podoplanin knockout mouse embryos: Correlation with abnormal epicardial development. *Dev Dyn*. 2008;237:847-857.

35. Bax NA, Bleyl SB, Gallini R, Wisse LJ, Hunter J, Van Oorschot AA, Mahtab EA, Lie-Venema H, Goumans MJ, Betsholtz C, Gittenberger-de Groot AC. Cardiac malformations in Pdgfralpha mutant embryos are associated with increased expression of WT1 and Nkx2.5 in the second heart field. *Dev Dyn*. 2010;239:2307-2317.

36. Douglas YL, Mahtab EA, Jongbloed MR, Uhrin P, Zaujec J, Binder BR, Schalij MJ, Poelmann RE, Deruiter MC, Gittenberger-de Groot AC. Pulmonary vein, dorsal atrial wall and atrial septum abnormalities in podoplanin knockout mice with disturbed posterior heart field contribution. *Pediatr Res*. 2009;65:27-32.

37. Puskaric S, Schmitteckert S, Mori AD, Glaser A, Schneider KU, Bruneau BG, Blaschke RJ, Steinbeisser H, Rappold G. Shox2 mediates Tbx5 activity by regulating Bmp4 in the pacemaker region of the developing heart. *Hum Mol Genet*. 2010;19:4625-4633.

38. Mommersteeg MT, Hoogaars WM, Prall OW, de Gier-de Vries C, Wiese C, Clout DE, Papaioannou VE, Brown NA, Harvey RP, Moorman AF, Christoffels VM. Molecular pathway for the localized formation of the sinoatrial node. *Circ Res*. 2007;100:354-362.

39. Wiese C, Grieskamp T, Airik R, Mommersteeg MT, Gardiwal A, de Gier-de Vries C, Schuster-Gossler K, Moorman AF, Kispert A, Christoffels VM. Formation of the sinus node head and differentiation of sinus node myocardium are independently regulated by Tbx18 and Tbx3. *Circ Res*. 2009;104:388-397.

40. Franco D, Campione M. The role of Pitx2 during cardiac development. Linking left-right signaling and congenital heart diseases. *Trends Cardiovasc Med*. 2003;13:157-163.

41. Lie-Venema H, Van Den Akker NM, Bax NA, Winter EM, Maas S, Kekarainen T, Hoeben RC, Deruiter MC, Poelmann RE, Gittenberger-de Groot AC. Origin, fate, and function of epicardium-derived cells (EPDCs) in normal and abnormal cardiac development. *ScientificWorldJournal*. 2007;7:1777-1798.

42. Perez-Pomares JM, Phelps A, Sedmerova M, Wessels A. Epicardial-like cells on the distal arterial end of the cardiac outflow tract do not derive from the proepicardium but are derivatives of the cephalic pericardium. *Dev Dyn*. 2003;227:56-68.

43. Eralp I, Lie-Venema H, Deruiter MC, Van Den Akker NM, Bogers AJ, Mentink MM, Poelmann RE, Gittenberger-de Groot AC. Coronary artery and orifice development is associated with proper timing of epicardial outgrowth and correlated Fas-ligand-associated apoptosis patterns. *Circ Res*. 2005;96:526-534.

44. Lie-Venema H, Eralp I, Markwald RR, Van Den Akker NM, Wijffels MC, Kolditz DP, van der Laarse A, Schalij MJ, Poelmann RE, Bogers AJ, Gittenberger-de Groot AC. Periostin expression by epicardium-derived cells is involved in the development of the atrioventricular valves and fibrous heart skeleton. *Differentiation*. 2008;76:809-819.

45. Eralp I, Lie-Venema H, Bax NA, Wijffels MC, van der Laarse A, Deruiter MC, Bogers AJ, Van Den Akker NM, Gourdie RG, Schalij MJ, Poelmann RE, Gittenberger-de Groot AC. Epicardium-derived cells are important for correct development of the Purkinje fibers in the avian heart. *Anat Rec A Discov Mol Cell Evol Biol*. 2006;288:1272-1280.

46. Kolditz DP, Wijffels MC, Blom NA, van der Laarse A, Hahurij ND, Lie-Venema H, Markwald RR, Poelmann RE, Schalij MJ, Gittenberger-de Groot AC. Epicardium-derived cells in development of annulus fibrosus and persistence of accessory pathways. *Circulation*. 2008;117:1508-1517.

47. Hatcher CJ, Diman NY, Kim MS, Pennisi D, Song Y, Goldstein MM, Mikawa T, Basson CT. A role for Tbx5 in proepicardial cell migration during cardiogenesis. *Physiol Genomics*. 2004;18:129-140.

48. Kraus F, Haenig B, Kispert A. Cloning and expression analysis of the mouse T-box gene Tbx18. *Mech Dev*. 2001;100:83-86.

49. van Wijk B, van den Berg G, Abu-Issa R, Barnett P, van der Velden S, Schmidt M, Ruijter JM, Kirby ML, Moorman AF, Van Den Hoff MJ. Epicardium and myocardium separate from a common precursor pool by crosstalk between bone morphogenetic protein- and fibroblast growth factor-signaling pathways. *Circ Res*. 2009;105:431-441.

50. Martinez-Estrada OM, Lettice LA, Essafi A, Guadix JA, Slight J, Velecela V, Hall E, Reichmann J, Devenney PS, Hohenstein P, Hosen N, Hill RE, Munoz-Chapuli R, Hastie ND. Wt1 is required for cardiovascular progenitor cell formation through transcriptional control of Snail and E-cadherin. *Nat Genet*. 2010;42:89-93.

51. Moorman AF, de Jong F, Denyn MM, Lamers WH. Development of the cardiac conduction system. *Circ Res*. 1998;82:629-644.

52. Christoffels VM, Burch JB, Moorman AF. Architectural plan for the heart: early patterning and delineation of the chambers and the nodes. *Trends Cardiovasc Med*. 2004;14:301-307.

53. Christoffels VM, Habets PE, Franco D, Campione M, de Jong F, Lamers WH, Bao ZZ, Palmer S, Biben C, Harvey RP, Moorman AF. Chamber formation and morphogenesis in the developing mammalian heart. *Dev Biol*. 2000;223:266-278.

54. Pennisi DJ, Rentschler S, Gourdie RG, Fishman GI, Mikawa T. Induction and patterning of the cardiac conduction system. *Int J Dev Biol*. 2002;46:765-775.

55. Gourdie RG, Harris BS, Bond J, Justus C, Hewett KW, O'Brien TX, Thompson RP, Sedmera D. Development of the cardiac pacemaking and conduction system. *Birth Defects Res C Embryo Today*. 2003;69:46-57.

56. Cheng G, Litchenberg WH, Cole GJ, Mikawa T, Thompson RP, Gourdie RG. Development of the cardiac conduction system involves recruitment within a multipotent cardiomyogenic lineage. *Development*. 1999;126:5041-5049.

57. Poelmann RE, Gittenberger-de Groot AC. A subpopulation of apoptosis-prone cardiac neural crest cells targets to the venous pole: multiple functions in heart development? *Dev Biol*. 1999;207:271-286.

58. Poelmann RE, Jongbloed MR, Molin DG, Fekkes ML, Wang Z, Fishman GI, Doetschman T, Azhar M, Gittenberger-de Groot AC. The neural crest is contiguous with the cardiac conduction system in the mouse embryo: a role in induction? *Anat Embryol (Berl)*. 2004;208:389-393.

59. Christoffels VM, Moorman AF. Development of the cardiac conduction system: why are some regions of the heart more arrhythmogenic than others? *Circ Arrhythm Electrophysiol*. 2009;2:195-207.

60. Gittenberger-de Groot AC, Jongbloed MR, Poelmann RE. Normal and Abnormal Cardiac development. In: Moller JH, Hoffman JIE (eds). *Pediatric Cardiovascular Medicine*. New York, USA: Churchill Livingstone; 2010: in press.

61. Blom NA, Gittenberger-de Groot AC, Deruiter MC, Poelmann RE, Mentink MM, Ottenkamp J. Development of the cardiac conduction tissue in human embryos using HNK-1 antigen expression: possible relevance for understanding of abnormal atrial automaticity. *Circulation*. 1999;99:800-806.

62. Jongbloed MR, Schalij MJ, Poelmann RE, Blom NA, Fekkes ML, Wang Z, Fishman GI, Gittenberger-de Groot AC. Embryonic conduction tissue: a spatial correlation with adult arrhythmogenic areas. *J Cardiovasc Electrophysiol*. 2004;15:349-355.

63. Rentschler S, Vaidya DM, Tamaddon H, Degenhardt K, Sassoon D, Morley GE, Jalife J, Fishman GI. Visualization and functional characterization of the developing murine cardiac conduction system. *Development*. 2001;128:1785-1792.

64. Kondo RP, Anderson RH, Kupershmidt S, Roden DM, Evans SM. Development of the cardiac conduction system as delineated by minK-lacZ. *J Cardiovasc Electrophysiol*. 2003;14:383-391.

9

65. Viragh S, Challice CE. The development of the conduction system in the mouse embryo heart. *Dev Biol*. 1980;80:28-45.

66. Boyett MR, Honjo H, Kodama I. The sinoatrial node, a heterogeneous pacemaker structure. *Cardiovasc Res*. 2000;47:658-687.

67. Nof E, Luria D, Brass D, Marek D, Lahat H, Reznik-Wolf H, Pras E, Dascal N, Eldar M, Glikson M. Point mutation in the HCN4 cardiac ion channel pore affecting synthesis, trafficking, and functional expression is associated with familial asymptomatic sinus bradycardia. *Circulation*. 2007;116:463-470.

68. Boineau JP, Canavan TE, Schuessler RB, Cain ME, Corr PB, Cox JL. Demonstration of a widely distributed atrial pacemaker complex in the human heart. *Circulation*. 1988;77:1221-1237.

69. Boineau JP, Schuessler RB, Roeske WR, Autry LJ, Miller CB, Wylds AC. Quantitative relation between sites of atrial impulse origin and cycle length. *Am J Physiol*. 1983;245:781-789.

70. Liu J, Dobrzynski H, Yanni J, Boyett MR, Lei M. Organisation of the mouse sinoatrial node: structure and expression of HCN channels. *Cardiovasc Res*. 2007;73:729-738.

71. Schuessler RB, Boineau JP, Bromberg BI. Origin of the sinus impulse. *J Cardiovasc Electrophysiol*. 1996;7:263-274.

72. Wenink AC, Symersky P, Ikeda T, Deruiter MC, Poelmann RE, Gittenberger-de Groot AC. HNK-1 expression patterns in the embryonic rat heart distinguish between sinuatrial tissues and atrial myocardium. *Anat Embryol* (Berl). 2000;201:39-50.

73. Aoyama N, Tamaki H, Kikawada R, Yamashina S. Development of the conduction system in the rat heart as determined by Leu-7 (HNK-1) immunohistochemistry and computer graphics reconstruction. *Lab Invest*. 1995;72:355-366.

74. Ikeda T, Iwasaki K, Shimokawa I, Sakai H, Ito H, Matsuo T. Leu-7 immunoreactivity in human and rat embryonic hearts, with special reference to the development of the conduction tissue. *Anat Embryol (Berl)*. 1990;182:553-562.

75. Watanabe M, Timm M, Fallah-Najmabadi H. Cardiac expression of polysialylated NCAM in the chicken embryo: correlation with the ventricular conduction system. *Dev Dyn*. 1992;194:128-141.

76. Basson CT, Bachinsky DR, Lin RC, Levi T, Elkins JA, Soults J, Grayzel D, Kroumpouzou E, Traill TA, Leblanc-Straceski J, Renault B, Kucherlapati R, Seidman JG, Seidman CE. Mutations in human TBX5 [corrected] cause limb and cardiac malformation in Holt-Oram syndrome. *Nat Genet*. 1997;15:30-35.

77. Schott JJ, Benson DW, Basson CT, Pease W, Silberbach GM, Moak JP, Maron BJ, Seidman CE, Seidman JG. Congenital heart disease caused by mutations in the transcription factor NKX2-5. *Science*. 1998;281:108-111.

78. Benson DW, Silberbach GM, Kavanaugh-McHugh A, Cottrill C, Zhang Y, Riggs S, Smalls O, Johnson MC, Watson MS, Seidman JG, Seidman CE, Plowden J, Kugler JD. Mutations in the cardiac transcription factor NKX2.5 affect diverse cardiac developmental pathways. *J Clin Invest*. 1999;104:1567-1573.

79. Naheed ZJ, Strasburger JF, Deal BJ, Benson DW, Jr., Gidding SS. Fetal tachycardia: mechanisms and predictors of hydrops fetalis. *J Am Coll Cardiol*. 1996;27:1736-1740.

80. Bauersfeld U, Pfammatter JP, Jaeggi E. Treatment of supraventricular tachycardias in the new millennium--drugs or radiofrequency catheter ablation? *Eur J Pediatr*. 2001;160:1-9.

81. Ko JK, Deal BJ, Strasburger JF, Benson DW, Jr. Supraventricular tachycardia mechanisms and their age distribution in pediatric patients. *Am J Cardiol*. 1992;69:1028-1032.

82. Gittenberger-de Groot AC, Bartelings MM, Deruiter MC, Poelmann RE. Basics of cardiac development for the understanding of congenital heart malformations. *Pediatr Res*. 2005;57:169-176.

83. Jongbloed MR, Wijffels MC, Schalij MJ, Blom NA, Poelmann RE, van der Laarse A, Mentink MM, Wang Z, Fishman GI, Gittenberger-de Groot AC. Development of the right ventricular inflow tract and moderator band: a possible morphological and functional explanation for Mahaim tachycardia. *Circ Res*. 2005;96:776-783.

84. Wessels A, Markman MW, Vermeulen JL, Anderson RH, Moorman AF, Lamers WH. The development of the atrioventricular junction in the human heart. *Circ Res*. 1996;78:110-117.

85. Van Mierop LH, Alley RD, Kausel HW, Stranahan A. The anatomy and embryology of endocardial cushion defects. *J Thorac Cardiovasc Surg*. 1962;43:71-83.

86. Odgers PN. The development of the atrio-ventricular valves in man. *J Anat*. 1939;73:643-657.

87. Wenink AC, Gittenberger-de Groot AC. The role of atrioventricular endocardial cushions in the septation of the heart. *Int J Cardiol*. 1985;8:25-44.

88. Wenink AC, Gittenberger-de Groot AC. Embryology of the mitral valve. *Int J Cardiol*. 1986;11:75-84.

89. Horiuchi K, Amizuka N, Takeshita S, Takamatsu H, Katsuura M, Ozawa H, Toyama Y, Bonewald LF, Kudo A. Identification and characterization of a novel protein, periostin, with restricted expression to periosteum and periodontal ligament and increased expression by transforming growth factor beta. *J Bone Miner Res*. 1999;14:1239-1249.

90. Norris RA, Damon B, Mironov V, Kasyanov V, Ramamurthi A, Moreno-Rodriguez R, Trusk T, Potts JD, Goodwin RL, Davis J, Hoffman S, Wen X, Sugi Y, Kern CB, Mjaatvedt CH, Turner DK, Oka T, Conway SJ, Molkentin JD, Forgacs G, Markwald RR. Periostin regulates collagen fibrillogenesis and the biomechanical properties of connective tissues. *J Cell Biochem*. 2007;101:695-711.

91. Kolditz DP, Wijffels MC, Blom NA, van der Laarse A, Markwald RR, Schalij MJ, Gittenberger-de Groot AC. Persistence of functional atrioventricular accessory pathways in postseptated embryonic avian hearts: implications for morphogenesis and functional maturation of the cardiac conduction system. *Circulation*. 2007;115:17-26.

92. Ieda M, Fu JD, Delgado-Olguin P, Vedantham V, Hayashi Y, Bruneau BG, Srivastava D. Direct reprogramming of fibroblasts into functional cardiomyocytes by defined factors. *Cell*. 2010;142:375-386.

93. Rios H, Koushik SV, Wang H, Wang J, Zhou HM, Lindsley A, Rogers R, Chen Z, Maeda M, Kruzynska-Frejtag A, Feng JQ, Conway SJ. periostin null mice exhibit dwarfism, incisor enamel defects, and an early-onset periodontal disease-like phenotype. *Mol Cell Biol*. 2005;25:11131-11144.

94. Gaussin V, Morley GE, Cox L, Zwijsen A, Vance KM, Emile L, Tian Y, Liu J, Hong C, Myers D, Conway SJ, Depre C, Mishina Y, Behringer RR, Hanks MC, Schneider MD, Huylebroeck D, Fishman GI, Burch JB, Vatner SF. Alk3/Bmpr1a receptor is required for development of the atrioventricular canal into valves and annulus fibrosus. *Circ Res*. 2005;97:219-226.

95. Okagawa H, Markwald RR, Sugi Y. Functional BMP receptor in endocardial cells is required in atrioventricular cushion mesenchymal cell formation in chick. *Dev Biol*. 2007;306:179-192.

96. Gittenberger-de Groot AC, Vrancken Peeters MP, Mentink MM, Gourdie RG, Poelmann RE. Epicardium-derived cells contribute a novel population to the myocardial wall and the atrioventricular cushions. *Circ Res*. 1998;82:1043-1052.

97. de Jong F, Opthof T, Wilde AA, Janse MJ, Charles R, Lamers WH, Moorman AF. Persisting zones of slow impulse conduction in developing chicken hearts. *Circ Res*. 1992;71:240-250.

98. van Kempen MJ, Fromaget C, Gros D, Moorman AF, Lamers WH. Spatial distribution of connexin43, the major cardiac gap junction protein, in the developing and adult rat heart. *Circ Res*. 1991;68:1638-1651.

99. Delorme B, Dahl E, Jarry-Guichard T, Briand JP, Willecke K, Gros D, Theveniau-Ruissy M. Expression pattern of connexin gene products at the early developmental stages of the mouse cardiovascular system. *Circ Res*. 1997;81:423-437.

100. Chuck ET, Freeman DM, Watanabe M, Rosenbaum DS. Changing activation sequence in the embryonic chick heart. Implications for the development of the His-Purkinje system. *Circ Res*. 1997;81:470-476.

101. Rothenberg F, Watanabe M, Eloff B, Rosenbaum D. Emerging patterns of cardiac conduction in the chick embryo: waveform analysis with photodiode array-based optical imaging. *Dev Dyn*. 2005;233:456-465.

102. Valderrabano M, Chen F, Dave AS, Lamp ST, Klitzner TS, Weiss JN. Atrioventricular ring reentry in embryonic mouse hearts. *Circulation*. 2006;114:543-549.

103. Truex RC, Bishof JK, Hoffman EL. Accessory atrioventricular muscle bundles of the developing human heart. *Anat Rec*. 1958;131:45-59.

104. Robb JS, Kaylor CT, Turman W.G. A study of specialized heart tissue at various stages of development of the human fetal heart. *Am J Med*. 1948;5:324-336.

105. James TN. Normal and abnormal consequences of apoptosis in the human heart. From postnatal morphogenesis to paroxysmal arrhythmias. *Circulation*. 1994;90:556-573.

106. Lieberman M, Paes de CA. The Electrophysiological Organization of the Embryonic Chick Heart. *J Gen Physiol*. 1965;49:351-363.

9

107. Bohora S, Dora SK, Namboodiri N, Valaparambil A, Tharakan J. Electrophysiology study and radiofrequency catheter ablation of atriofascicular tracts with decremental properties (Mahaim fibre) at the tricuspid annulus. *Europace*. 2008;10:1428-1433.

108. Scheinman MM. History of Wolff-Parkinson-White syndrome. *Pacing Clin Electrophysiol*. 2005;28:152-156.

109. Nakagawa M, Thompson RP, Terracio L, Borg TK. Developmental anatomy of HNK-1 immunoreactivity in the embryonic rat heart: co-distribution with early conduction tissue. *Anat Embryol (Berl)*. 1993;187:445-460.

110. Yanni J, Boyett MR, Anderson RH, Dobrzynski H. The extent of the specialized atrioventricular ring tissues. *Heart Rhythm*. 2009;6:672-680.

111. Bakker ML, Boukens BJ, Mommersteeg MT, Brons JF, Wakker V, Moorman AF, Christoffels VM. Transcription factor Tbx3 is required for the specification of the atrioventricular conduction system. *Circ Res*. 2008;102:1340-1349.

112. Kugler JD, Danford DA, Deal BJ, Gillette PC, Perry JC, Silka MJ, Van Hare GF, Walsh EP. Radiofrequency catheter ablation for tachyarrhythmias in children and adolescents. The Pediatric Electrophysiology Society. *N Engl J Med*. 1994;330:1481-1487.

113. Kannankeril PJ, Gotteiner NL, Deal BJ, Johnsrude CL, Strasburger JF. Location of accessory connection in infants presenting with supraventricular tachycardia in utero: clinical correlations. *Am J Perinatol*. 2003;20:115-119.

114. Goldstein M, Dunnigan A, Milstein S, Benson DW, Jr. Bundle branch block during orthodromic reciprocating tachycardia onset in infants. *Am J Cardiol*. 1989;63:301-306.

115. Gollob MH, Green MS, Tang AS, Gollob T, Karibe A, Ali Hassan AS, Ahmad F, Lozado R, Shah G, Fananapazir L, Bachinski LL, Roberts R. Identification of a gene responsible for familial Wolff-Parkinson-White syndrome. *N Engl J Med*. 2001;344:1823-1831.

116. Gollob MH, Seger JJ, Gollob TN, Tapscott T, Gonzales O, Bachinski L, Roberts R. Novel PRKAG2 mutation responsible for the genetic syndrome of ventricular preexcitation and conduction system disease with childhood onset and absence of cardiac hypertrophy. *Circulation*. 2001;104:3030-3033.

117. Oh JK, Holmes DR, Jr., Hayes DL, Porter CB, Danielson GK. Cardiac arrhythmias in patients with surgical repair of Ebstein's anomaly. *J Am Coll Cardiol*. 1985;6:1351-1357.

118. Kiernan TJ, Fahy G. Multiple accessory pathways, dual AV nodal physiology, non-compacted myocardium and patent foramen ovale in a patient with Ebstein's anomaly: report of a case. *Int J Cardiol*. 2007;114:412-413.

119. Hornung TS, Calder L. Congenitally corrected transposition of the great arteries. *Heart*. 2010;96:1154-1161.

120. Van Hare GF, Phoon CK, Munkenbeck F, Patel CR, Fink DL, Silverman NH. Electrophysiologic study and radiofrequency ablation in patients with intracardiac tumors and accessory pathways: is the tumor the pathway? *J Cardiovasc Electrophysiol*. 1996;7:1204-1210.

121. Emmel M, Brockmeier K, Sreeram N. Rhabdomyoma as accessory pathway: electrophysiologic and morphologic confirmation. *Heart*. 2004;90:43.

122. Visconti RP, Markwald RR. Recruitment of new cells into the postnatal heart: potential modification of phenotype by periostin. *Ann N Y Acad Sci*. 2006;1080:19-33.

123. Kruithof BP, Krawitz SA, Gaussin V. Atrioventricular valve development during late embryonic and postnatal stages involves condensation and extracellular matrix remodeling. *Dev Biol*. 2007;302:208-217.

124. Perry JC, Garson A, Jr. Supraventricular tachycardia due to Wolff-Parkinson-White syndrome in children: early disappearance and late recurrence. *J Am Coll Cardiol*. 1990;16:1215-1220.

125. Weindling SN, Saul JP, Walsh EP. Efficacy and risks of medical therapy for supraventricular tachycardia in neonates and infants. *Am Heart J*. 1996;131:66-72.

Summary

Samenvatting

SUMMARY

This thesis consists of two parts: **Part I** (**Chapter 2 - 5**) illustrates the role of the posterior heart field (PHF) in cardiac development, mainly with respect to formation of the venous pole and parts of the cardiac conduction system (CCS). Furthermore, abnormal PHF development is related to congenital heart disease including conduction disturbances.

Part II (**Chapter 6 - 8**) correlates the process of heart development with the etiology of atrioventricular reentry tachycardias (AVRTs) that are frequently observed during perinatal stages of development.

Chapter 1 – The first chapter provides an extensive overview concerning the processes involved in heart development, which are studied and referred to in **Part I** and **Part II** of this thesis. In general it can be stated that the heart develops from two independent lineages of cardiomyocytes, the first (i.e. primary) and second heart field (SHF) respectively. The first heart field gives rise to the primary heart tube. Subsequently, newly generated SHF derived cardiomyocytes are added at the outflow as well as the inflow tract of the developing heart. The contribution of the SHF to the outflow tract is distinguished in an anterior and secondary heart field. At the venous pole we refer the contribution of the SHF as the PHF. The first chapter also describes the important contribution of the epicardium and cardiac neural crest cells in heart development. During cardiogenesis the cardiac conduction system is formed. The theories explaining the development of this highly specialized system, the individual components and the emerging impulse propagation are discussed. Furthermore, an introduction is provided on the formation of the isolating layer between the atria and ventricles: the annulus fibrosus. This structure has an imperative role in the strictly regulated impulse propagation through the heart. Defects in the annulus fibrosus lead to accessory atrioventricular (AV) myocardial pathways (APs) between the atria and ventricles, which may result in abnormal impulse propagation and AVRTs. This chapter concludes by discussing the different types of brady- and tachyarrhythmias including the current treatment modalities in fetuses and neonates.

PART I

Chapter 2 – The important role of the Short stature homeobox gene 2 (*Shox2*) is demonstrated in heart development. *Shox2* is crucial for the anlage of the PHF derived myocardium at the venous pole of the heart including the sinus venosus myocardium, the sinoatrial node (SAN) and the venous valves as was shown by severe hypoplasia of these structures in *Shox2* mutant mice. *Shox2* null mutants furthermore, demonstrated marked atrial dilation and embryonic lethality between 12.5 and 13.5 dpc. A functional link between *Shox2* and the early myocardial

marker Nkx2.5 was established. Absence of *Shox2* leads also to aberrant differentiation of the PHF derived myocardium including up-regulation of Nkx2.5, Cx43 and Cx40 in the SAN, which suggests a disturbed pacemaking function. *Shox2* antisense morpholino injections in Zebrafish embryos indeed confirmed presence of SAN dysfunction.

Chapter 3 – In addition to the previous chapter, here electrophysiological experiments were performed in *Shox2* mutant embryonic mouse hearts. Compared to wildtype, *Shox2* mutants showed a decreased heart rate despite the presence of the pacemaker channel HCN4 in the hypoplastic SAN. Furthermore, a role for *Shox2* in epicardial lineage development was demonstrated. *Shox2* mutants have a smaller size of the pro-epicardial organ (PEO), normal epicardial spreading and decreased numbers of epicardium derived cells (EPDCs) at locations of a thin ventricular myocardial wall. Furthermore, abnormal ventricular morphology and trabecularization were observed, both possibly related to abnormal epicardial lineage development. These data substantiate the hypothesis that the sinus vensosus myocardium and the epicardium derive from a common pool of progenitor cells (i.e. the PHF). Both abnormal pacemaker and epicardial lineage development may contribute to the early embryonic death of *Shox2* mutant mice.

Chapter 4 – In this chapter the derivatives of the PHF were studied further by the expression of transmembrane protein podoplanin, a novel marker in heart development. Podoplanin not only stains the characteristic MLC-2a positive and Nkx2.5 negative PHF derived sinus venosus myocardium, but also the adjacent cuboidal-shaped coelomic epithelium near the sinus venosus. It was speculated that this podoplanin positive cuboidal-shaped coelomic epithelium represents the area from which the PHF derived cells originate via a process called epithelial-to-mesenchymal transformation (EMT). Furthermore, podoplanin expression was present in the wall of the developing pulmonary vein and CCS including the SAN and the AV conduction axis. These data support the hypothesis that major parts of the CCS share PHF characteristics.

Chapter 5 – By using *podoplanin* mutant and wildtype mouse embryos, the role and possible mechanism of *podoplanin* in PHF development was further evaluated. *Podoplanin* null embryos demonstrated hypoplasia of the PHF myocardium including the SAN, the primary atrial septum, dorsal atrial wall and the myocardium lining the cardinal and pulmonary veins. An abnormal differentiation by up-regulation of Nkx2.5 and Cx43 in the hypoplastic SAN as demonstrated in *Shox2* mutants (**Chapter 2** and **3**), was not observed. **Chapter 5** confirms that the coelomic epithelium near the sinus venosus contributes to the PHF derived myocardium. In *podoplanin* mutants the epithelium lining the coelomic cavity showed an aberrant expression of E-cadherin and Rho-A, which are normally controlled by *podoplanin*. Therefore, it might

be concluded that *podoplanin* mutant mice suffer from a disturbed EMT process since both E-cadherin and Rho-A are key factors in EMT.

PART II

Chapter 6 – This chapter describes the presence and course of functional APs at subsequent stages of normal mouse heart development. Electrophysiological unipolar electrode recordings in embryonic and fetal mouse hearts demonstrated the presence of multiple antegrade (atrium-to-ventricle) conducting APs up till late stages of fetal life. Morphological analysis of these hearts clearly demonstrated and confirmed the presence of multiple APs crossing the isolating annulus fibrosus directly connecting the atrial and ventricular myocardium. These APs were all composed of primitive, Cx43 negative AV canal myocardium and could be observed around the developing mitral as well as tricuspid valve orifice. At subsequent developmental stages these APs significantly decreased in number and size around both AV orifices. The transient persistence of these APs could explain the high incidence of AVRTs in the perinatal period of human development.

Chapter 7 – In this chapter the developing annulus fibrosus was studied in human embryonic fetal and neonatal hearts, to investigate whether APs are also present in normal human heart development as is the case in mouse (**Chapter 6**). Approximately up till six weeks of development the myocardium in the AV canal is continuous between atrium and ventricle. In the period thereafter the formation of the annulus fibrosus starts at the AV junctional area. APs were detected around the developing mitral as well as tricuspid valve orifice. Initially, these APs consisted of broad myocardial continuities crossing the annulus fibrosus. At later stages the APs only comprised single myocardial strands. Most APs around the tricuspid valve orifice were related to the right AV ring bundle (RAVRB), which is a remnant of the more extensive embryonic CCS. APs could be detected up till 20 weeks of pregnancy. From that moment and in neonatal hearts no APs were detected anymore. Reconstructions of the AV node area demonstrated multiple APs that directly interconnect the AV node with the myocardium at the top of the ventricular septum. These APs related to the AV node could be observed until birth.

Chapter 8 – This chapter evaluates the perinatal management and cardiac outcome of fetuses that suffer from severe tachy- or bradyarrhythmia. A retrospective data analysis demonstrated a low mortality rate in fetuses with supraventricular tachycardia (including AVRT) and atrial flutter, although in some cases aggressive treatment strategies, including direct fetal therapy and radiofrequency catheter ablation in the first year of life, were mandatory. Furthermore, for detection of Wolff-Parkinson-White (WPW) syndrome, ECG screening before adolescence is recommended in children that have suffered from SVT in fetal life. Fetal bradyarrhythmia

based on an AV block (AVB) coincides with high mortality rates especially in the presence of congenital cardiac anomalies and long QT-syndrome.

Chapter 9 – The final chapter encompasses the general discussion of this thesis and discusses the contents of **Part I** and **Part II**. **Part I** describes the important role of the PHF in cardiac development including the sinus venosus myocardium, the epicardial lineage and parts of the CCS. We specifically shed new light on the anlage of the SAN. Although our data also insinuates a role for the PHF in formation of the more peripheral part of the CCS (i.e the AV node, bundle of His and bundle branches), lineage tracing studies are still mandatory to unravel the true contribution of the PHF to those parts of the CCS. Furthermore, abnormal PHF anlage is related to congenital heart malformations, including supraventricular arrhythmias. **Part II** discusses the normal development of the annulus fibrosus at the AV junction in relation to the persistence of myocardial continuities between the atria and ventricles, which might serve as an AP for abnormal AV conduction. Our data illustrates that the temporary persistence of these APs during heart development, might explain the presence and spontaneously disappearance of AVRTs in fetuses and neonates. However, question remains why some patients have a recurrent (or a de novo) episode of AVRT later in life, morphological as well as electrophysiological changes postnatally might be involved but ought to be studied in more detail in the future.

S

SAMENVATTING

Dit proefschrift bestaat uit twee delen. **Deel I** (**Hoofdstuk 2 – 5**) beschrijft de rol van het "posterior heart field" (PHF) in de ontwikkeling van het hart, daarbij ligt de focus voornamelijk op de aanleg van de veneuze pool en delen van het cardiale impuls geleidingssysteem. Tevens wordt een gestoorde aanleg van het PHF gerelateerd aan congenitale hartafwijkingen inclusief hartritmestoornissen. In **deel II** (**Hoofdstuk 6 – 8**) wordt het proces van hartontwikkeling gerelateerd aan de oorzaak van atrioventriculaire (AV) reentry tachycardieën (AVRTs) die vaak rond de geboorte voorkomen.

Hoofdstuk 1 – Het eerste hoofdstuk omvat een uitgebreid overzicht van de verschillende processen die betrokken zijn bij de aanleg en ontwikkeling van het hart. In **deel I** en **deel II** van dit proefschrift zal naar deze processen worden gerefereerd, daarnaast zullen sommige van deze processen ook ten dele verder worden bestudeerd. Globaal kan worden aangenomen dat het hart is opgebouwd uit twee afzonderlijke hartspiercel vormende gebieden, te weten het "first heart field" en het "second heart field" (SHF). De hartspiercellen die het primaire hartbuisje vormen zijn afkomstig van het "first heart field." Zowel aan de in- als de uitstroom van dit primaire hartbuisje worden nieuwe hartspiercellen toegevoegd, deze zijn afkomstig van het SHF. De bijdrage van het SHF aan de uitstroom van het hart kan worden onderscheiden in een "anterior heart field" en een "secondary heart field." De toevoeging van de SHF afkomstige hartspiercellen aan de instroom van het hart hebben wij het PHF genoemd. Het eerste hoofdstuk laat ook de belangrijke bijdrage van het epicard en de cardiale neurale lijst cellen zien in de ontwikkeling van het hart. Tijdens het hartontwikkelingsproces vindt de aanleg van het cardiale impuls geleidingssysteem plaats. De hedendaagse theorieën betreffende de ontwikkeling van dit gespecialiseerde systeem, de afzonderlijke componenten van dit systeem, en de geleiding van de cardiale impuls door het ontwikkelende hart komen aanbod. Ook wordt een inleiding gegeven over de aanleg van de laag isolatie tussen de atria en de ventrikels: de annulus fibrosus. Deze isolerende structuur heeft een belangrijke rol in een gecoördineerde impulsgeleiding door het hart. Een defect in de annulus fibrosus leidt tot extra hartspiervezelverbindingen tussen atria en ventrikels, de zogenaamde "accessory pathways" (APs). De aanwezigheid van deze APs kan leiden tot een abnormale cardiale impulsgeleiding en het ontstaan van AVRTs. Tot slot wordt in het laatste deel van dit hoofdstuk ingegaan op de verschillende vormen van brady- en tachyaritmieën, inclusief de huidige behandelstrategieën bij foetussen en neonaten.

DEEL I
Hoofdstuk 2 – Dit hoofdstuk beschrijft de rol van het Short stature homeobox gen 2 (*Shox2*) in de aanleg en ontwikkeling van het hart. *Shox2* heeft een essentiële rol in de aanleg van de

PHF afkomstige hartspiercellen aan de veneuze pool van het hart, inclusief de sinoatriale knoop (pacemaker) en de veneuze kleppen. Het belang van *Shox2* in de aanleg van deze structuren wordt bevestigd door ernstige onderontwikkeling (hypoplasie) van deze structuren in muizen embryo's met mutaties in het *Shox2* gen. Daarnaast vertonen *Shox2* gemuteerde embryo's een ernstige vergroting (dilatatie) van de atria en gaan dood tussen dag 12.5 en 13.5 van de ontwikkeling. Ook wordt in dit hoofdstuk een functionele link gelegd tussen *Shox2* en de vroege hartspiercel marker Nkx2.5. De afwezigheid van *Shox2* leidt tot een abnormale differentiatie van de PHF afkomstige hartspiercellen, onder andere resulterend in een verhoogde expressie van Nkx2.5, Cx43 and Cx40 in de sinoatriale knoop van het hart. Deze abnormale differentiatie van de sinoatriale knoop impliceert een gestoorde functie welke middels *Shox2* antisense morpholino injecties in Zebravis embryo's wordt bevestigd. In de geïnjecteerde Zebravis embryo's wordt een abnormale pacemakerfunctie waargenomen.

Hoofdstuk 3 – In navolging van het voorgaande hoofdstuk worden hier de resultaten besproken van de elektrofysiologische experimenten in harten van *Shox2* gemuteerde muizen embryo's. Ondanks de aanwezigheid van HCN4, het belangrijkste pacemaker kanaal, in de hypoplastische sinoatriale knoop van de *Shox2* gemuteerde embryo's vertonen deze harten tragere hartfrequenties vergeleken met de hartfrequenties van normale embryonale harten. In dit hoofdstuk wordt ook de rol van *Shox2* in de ontwikkeling van het epicard beschreven. *Shox2* mutanten hebben een kleiner pro-epicard orgaan (PEO), laten normale epicardiale verspreiding zien, en hebben minder epicardium derived cells (EPDCs) met name op de plaatsen waar de wanden van de hartkamers dun zijn. Tevens wordt in *Shox2* gemuteerde harten een abnormale morfologie van de ventrikels en het trabekelsysteem waargenomen, beide afwijkingen zijn mogelijke gerelateerd aan een abnormale aanleg en signalering van het epicard. Het feit dat *Shox2* mutanten zowel epicardiale afwijkingen als een gestoorde aanleg van de hartspiercellen van de veneuze pool laten zien, draagt bij aan de hypothese dat beiden vanuit dezelfde hartvormende regio ontstaan, het PHF. De abnormale epicardiale ontwikkeling en de gestoorde pacemaker functie in *Shox2* mutanten dragen mogelijk beiden bij aan de embryonale letaliteit.

Hoofdstuk 4 – In dit hoofdstuk worden de structuren van het hart die afkomstig zijn van het PHF verder bestudeerd aan de hand van de expressie van het transmembraan eiwit podoplanine, een nieuwe marker binnen het hartontwikkelingsonderzoek. Podoplanine kleurt niet alleen de karakteristieke MLC-2a positieve en Nkx2.5 negatieve sinus venosus hartspiercellen aan die allen afkomstig zijn van het PHF, maar ook het aanliggende kubische epitheel van de coeloom holte dat direct naast de sinus venosus hartspiercellen gelegen is. Gepostuleerd wordt dat dit kubische podoplanine positieve coeloomholte epitheel de regio representeert van waar de PHF hartspiercellen ontstaan door een proces genaamd: "Epithelial-to-Mesenchymal Transformation"

(EMT). Expressie van podoplanine wordt ook waargenomen in de wand van de ontwikkelende pulmonaal venen en in het ontwikkelende cardiale impuls geleidingssysteem, onder andere in de sinoatriale knoop en de atrioventriculaire geleidingsas. Deze data draagt bij aan de hypothese dat belangrijke delen van het cardiale impuls geleidingssysteem en het PHF overeenkomstige eigenschappen vertonen.

Hoofdstuk 5 – Met behulp van normale muizen embryo's en muizen embryo's met een mutatie in het *podoplanine* gen, wordt in dit hoofdstuk de rol van *podoplanine* in de ontwikkeling van het PHF verder onderzocht. *Podoplanine* gemuteerde embryo's laten een onderontwikkeling (hypoplasie) zien van de PHF afkomstige onderdelen van het hart, te weten: de sinoatriale knoop, het primaire atrium septum en de hartspiercellen gelegen rond de ontwikkelende cardinaal en pulmonaal venen. In deze embryo's wordt echter geen abnormale differentiatie van hartspiercellen gezien zoals in *Shox2* gemuteerde embryo's met een verhoogde expressie van Nkx2.5 en Cx43 (**Hoofdstuk 2** en **3**). In **hoofdstuk 5** wordt bevestigd dat het epitheel van de coeloomholte grenzend aan de sinus venosus bijdraagt aan de PHF afkomstige hartspiercellen. In *podoplanine* gemuteerde embryo's wordt in het epitheel van de coeloomholte een abnormale expressie van E-cadherin en Rho-A gezien, welke normaliter beiden door *podoplanine* worden gereguleerd. Gezien E-cadherin en Rho-A belangrijke factoren in het EMT proces zijn mag geconcludeerd worden dat dit proces in *podoplanine* mutanten verstoord is.

DEEL II

Hoofdstuk 6 – Dit hoofdstuk beschrijft de aanwezigheid en het beloop van APs in opeenvolgende stadia in normale muizen hartontwikkeling. Elektrofysiologische experimenten middels unipolaire elektrode opnames in embryonale en foetale harten, tonen de aanwezigheid van vele in antegrade richting (van atrium naar ventrikel) geleidende APs tot op late foetale stadia van de ontwikkeling. Morfologische analyse van deze harten bevestigen de aanwezigheid van multipele APs die direct door de isolerende annulus fibrosus heen de hartspiercellen van de atria met de die van de ventrikels verbinden. Al deze extra verbindingen rond zowel de ontwikkelende mitralis als de tricuspidalis hartklep openingen bestaan uit hartspiercellen van het primitieve AV kanaal gekenmerkt door de afwezigheid van Cx43 expressie. Tijdens opeenvolgende stadia van de ontwikkeling vindt een significante afname van zowel het aantal als de omvang van de APs rond beide AV hartklep openingen plaats. Het tijdelijk persisteren van deze APs kan een verklaring zijn voor de hoge incidentie van AVRTs in de perinatale stadia van de ontwikkeling bij de mens.

Hoofdstuk 7 – In dit hoofdstuk wordt de ontwikkeling van de annulus fibrosus bestudeerd tijdens embryonale, foetale en neonatale stadia van de ontwikkeling in de mens. Daarbij wordt

specifiek gelet op de aanwezigheid van APs zoals aangetoond tijdens normale muizen hartontwikkeling (**Hoofdstuk 6**). Tot ongeveer 6 weken van de ontwikkeling vormen de hartspiercellen van de atria en ventrikels een continuïteit via het primitieve AV kanaal. In de opeenvolgende periode start de formatie van de annulus fibrosus in het AV overgangsgebied. APs worden dan zowel rond de ontwikkelende mitralis als tricuspidalis hartklep opening waargenomen. Initieel omvatten deze APs brede AV continuïteiten van hartspiercellen, op latere stadia bestaan de APs slechts uit individuele bundels van hartspiercellen die door de annulus fibrosus direct de atria met de ventrikels verbinden. De meeste APs gelegen rond de tricuspidalis hartklep opening zijn gerelateerd aan de rechter AV ring bundel (RAVRB), een overblijfsel van het meer uitgebreidere embryonale cardiale impuls geleidingsysteem. APs werden tot 20 weken van de zwangerschap waargenomen, vanaf dat moment en in de neonatale harten konden geen APs meer worden geïdentificeerd. De reconstructies van het AV knoop gebied laten multiple APs zien die direct de AV knoop met de top van het ventrikel septum verbinden, deze APs werden tot aan de geboorte waargenomen.

Hoofdstuk 8 – Dit hoofdstuk evalueert de behandelstrategieën en de klinische uitkomsten van foetussen die in-utero gediagnosticeerd zijn met ernstige vormen van tachy- en bradyritmieën. Middels retrospectieve data analyse wordt aangetoond dat foetale supraventriculaire tachycardieën (inclusief AVRTs) en atriumflutter gepaard gaan met een lage mortaliteit. Desondanks waren bij sommige patiënten wel agressieve behandelstrategieën noodzakelijk, zoals directe foetale therapie en radiofrequency katheter ablatie in het eerste levensjaar. Tevens wordt aangeraden om bij kinderen die een foetale supraventriculaire tachycardie hebben doorgemaakt nog voor de adolescentie een ECG screening te verrichten voor het Wolff-Parkinson-White syndrom, ook in die gevallen waarbij geen ventriculaire pre-excitatie aanwezig was op het postnatale ECG. De foetale bradyritmieën die veroorzaakt worden door een atrioventriculair blok (AVB) hebben een hoge mortaliteit, specifiek wanneer deze gepaard gaan met andere congenitale hartafwijkingen of het lange QT-syndroom.

Hoofdstuk 9 – Het laatste hoofdstuk omvat de algemene discussie van dit proefschrift, waarin afzonderlijk de inhoud van **Deel I** en **Deel II** wordt bediscussieerd. **Deel I** beschrijft de belangrijke rol van het PHF in hartontwikkeling inclusief de sinus venosus hartspiercellen, het epicard en delen van het cardiale impuls geleidingssysteem. Specifiek worden nieuwe inzichten getoond met betrekking tot de aanleg van de sinoatriale knoop. Ondanks het feit dat de resultaten beschreven in dit proefschrift ook een rol voor het PHF in de aanleg van de perifere delen van het cardiale impuls geleidingssyteem (AV knoop, bundel van His en bundeltakken) suggereren, zijn in de toekomst lineage tracing studies vereist om de ware bijdrage van het PHF aan die delen van het cardiale impuls geleidingssysteem te bevestigen. Tot slot wordt in **Deel I** een abnormale aanleg van het PHF gerelateerd aan congenitale

hartafwijkingen inclusief supraventriculaire hartritmestoornissen. **Deel II** bediscussieert de normale ontwikkeling van de annulus fibrosus in het AV overganggebied in relatie tot het persisteren van hartspiervezel continuïteiten tussen atria en ventrikels die kunnen fungeren als APs voor abnormale AV geleiding. Onze data illustreert dat het tijdelijk persisteren van APs tijdens de hartontwikkeling een verklaring kan zijn voor het optreden en het spontaan verdwijnen van AVRTs in foetussen en neonaten. Het blijft echter tot op heden onduidelijk waarom sommige patiënten een herhaalde (of een eerste episode) van AVRT doormaken op een later stadium van het leven. Mogelijk liggen postnatale elektrofysiologische en morfologische veranderingen in het hart hieraan ten grondslag, dit dient in ieder geval nog nader onderzocht te worden.

Abbreviations

α-MHC	alpha myosin heavy chain
β-MHC	beta myosin heavy chain

A

A	atrium
Ad	Adenosine
AET	atrial ectopic tachycardia
AF	atrial flutter
ALK-3	activin receptor-like kinase-3
Am	Amiodarone
ANOVA	analysis of variance
ANT	anterior
Ao	aorta
AP(s)	accessory pathway(s)
AS	atrial septum
AV	atrioventricular
AVB	atrioventricular block
AVC	atrioventricular canal
AVc	atrioventricular cushion
AVN	atrioventricular node
AVNRT	atrioventricular nodal reentry tachycardia
AVR	atrioventricular ring
AVRT(s)	atrioventricular reentry tachycardia(s)

B

BMP	bone morphogenetic protein
bpm	beats per minute

C

CA	common atrium
CB	common bundle
cc	cordocentesis
cc-TGA	congenital corrected transposition of the great arteries
CCS	cardiac conduction system

CE	coelomic epithelium
CHD	congenital heart disease
CRL	crown rump length
CS	coronary sinus (ostium)
cs	cesarean section
CV	cardinal vein
Cx	connexin

D

D	Digoxin
DAP	3-3'diaminobenzidine tetrahydrochloride
DAW	dorsal atrial wall
DDD	dual pacing, dual sensing and dual mode pacemaker
DL	dextral looping
DMP	dorsal mesenchymal protrusion
DNA	deoxyribonucleic acid
DOT	distal outflow tract
dpc	days post conception
DXM	Dexamethason

E

E	embryonic day
ECG	electrocardiogram
EMT	epithelial-to-mesenchymal transformation
EP	electrophysiological
Ep	epicardium
EPDC(s)	epicardium derived cell(s)
ES	embryonic stem cells

F

F	Fenoterol
Fb	fibroblast
Fl	Flecanaide
FGF	fibroblast growth factor
FITC	fluorescein isothiocyanate

G

GATA	globulin transcription factor
ggl	cardiac ganglia

H

HCN4	hyperpolarization-activated cyclic nucleatide-gated cation channel-4
HH	Hamburger and Hamilton stage
HHF35	human heart fibroblast 35 / muscle actin
HIS	bundle of His
HNK-1	human natural killer-1
HPS	His Purkinje system

I

IAS	inter atrial septum
Id2	inhibitor of differentiation 2
ICD	implantable cardioverter defibrillator
ICV	inferior caval vein
IFT	inflow tract
Isl1	islet-1
iv	intravenous

K

K	Kinidine sulphate
KO	knockout

L

LA	left atrium
LAM	left atrial myocardium
LAMP2	lysosomal-associated membrane protein-2
LAVR(B)	left atrioventricular ring (bundle)
LacZ	beta-galactosidase
LBB	left bundle branch
LCV	left cardinal vein

Leu-7	leukaemia-associated protein 7
LQTS	long QT-syndrome
LV	left ventricle
LVA	left ventricular apex
LVB	left ventricular base
LVM	left ventricular myocardium
LVV	left venous valve

M

MCG	magnetocardiography
MD	medical doctor
MEF2c	myocyte-specific enhancer factor 2c
Mink	misshappen/nik-related kinase
MLC-2a	myosin light chain-2 atrium
MV	mitral valve

N

NCC	neural crest cell
Nkx2.5	NK2 transcription factor related locus 5
ns	not significant

O

o	oral
OFc	outflow tract cushion
O(F)T	outflow tract

P

PA	pulmonary artery
PAA	pharyngeal arch arteries
PBS	phosphate-buffered saline
PCR	polymerase chain reaction
Pdgf(r-α)	platelet derived growth factor (receptor-alpha)
PEO	pro-epicardial organ
PF	primary fold
PFA	paraformaldehyde

A

PHF	posterior heart field
PJRT	permanent junctional reciprocating tachycardia
PLV	primitive left ventricle
Podo	podoplanin
POT	proximal outflow tract
POST	posterior
PPC	pericardio-peripleural cavity
PRKAG2	protein kinase, AMP-activated, noncatalytic, gamma-2
PRV	primitive right ventricle
PV	pulmonary vein

R

R	Ritodrine
RA	right atrium
RAM	right atrial myocardium
RAoRB	retro aortic root branch
RAVR(B)	right atrioventricular ring (bundle)
RBB	right bundle branch
RCV	right cardinal vein
RFA	radiofrequency ablation
Rho-A	Ras homolog gene-A
RNA	ribonucleic acid
RT-PCR	reverse transcriptase-polymerase chain reaction
RV	right ventricle
RVB	right ventricular base
RVM	right ventricular myocardium
RVV	right venous valve

S

S	Sotalol
SAN	sinoatrial node
SAR	sinu-atrial ring
SCV	superior caval vein
SD	standard deviation

SEM	standard error of means
SHOX	short stature homeobox
SHOX2	short stature homeobox 2
SMC	smooth muscle cell
SP3	specificity protein-3
SPSS	statistical package for the social sciences
SS	septum spurium
SV	sinus venosus
SVT	supraventricular tachycardia

T

Tbx	T-box
TGA	transposition of the great arteries
TGF(-β)	transforming growth factor (-beta)
TRITC	tetramethyl rhodamine iso-thiocyanate
TV	tricuspid valve

V

V	ventricle
VAR	ventriculo-arterial ring
VP	venous pole
VS	ventricular septum
VV	venous valve

W

WPW	Wolff-Parkinson-White
WT	wildtype
Wt1	wilms'tumor

A

Curriculum Vitae

CURRICULUM VITAE

Nathan D. Hahurij was born on November 9th 1981 in Nieuw-Roden, The Netherlands and graduated school from the Alfa-college (VWO, Groningen, The Netherlands) in 2001. That same year he continued his education by enrolling to study Medicine at the University of Leiden. As part of his Bachelor study he started a scientific research internship focusing on the role of *Shox2* in cardiac development, under the supervision of Prof. Dr. A.C. Gittenberger-de Groot in the department of Anatomy & Embryology of the Leiden University Medical Center (LUMC). Upon completion of this project he was awarded a Bachelors degree (doctoraal bul) in December 2005. He was accepted as Ph.D. candidate in a partnership between the Departments of Pediatric Cardiology and Anatomy & Embryology (LUMC) in January 2006. Here he could further pursue his scientific interest in cardiac development under the supervision of Prof. Dr. N.A. Blom and Prof. Dr. A.C. Gittenberger-de Groot. His Ph.D-research focused on the etiology of atrioventricular reentry tachycardias in fetuses and the young as well as the role of the posterior heart field in cardiogenesis. In February 2008 he started his medical internships in order to complete his education as medical doctor. The succeeding two years were filled with both internship training and Ph.D research. He also submitted a research proposal to the Dutch Heart Foundation outlining a two-year project focusing on the role of hemodynamics in the development of congenital heart disease, and was consequently awarded a Dr. E. Dekker grant (No 2009T070). In February 2010, drs Hahurij received his medical degree and became a resident (ANIOS) in the Department of Pediatrics (headed by Prof. Dr. H.S.A. Heymans) of the Academic Medical Center, Amsterdam, The Netherlands. In August 2010 he returned to the LUMC to complete his Ph.D study and to initiate the "post-doctoral project" granted by the Dutch Heart Foundation, which is carried out in the Department of Pediatric Cardiology (Prof. Dr. N.A. Blom, supervisor) in collaboration with the Anatomy & Embryology department (Prof. Dr. A.C. Gittenberger-de Groot) of the LUMC. In order to acquire embryonic and fetal echocardiography skills, he was temporarily employed (January – March 2011) as research fellow at the Mouse Imaging Centre of the Hospital for Sick Children in Toronto, Canada under the supervision of Dr. Y.Q. Zhou and Prof. Dr. M. Henkelman. For the future, he plans to further pursue his interests in cardiac development and congenital heart disease at both clinical and scientific aspects.

Acknowledgements

ACKNOWLEDGEMENTS

List of Publications

LIST OF PUBLICATIONS

PAPERS

Blaschke RJ, Hahurij ND, Kuijper S*, Just S*, Wisse LJ, Deissler K, Maxelon T, Anastassiadis K, Spitzer J, Hardt SE, Schöler H, Feitsma H, Rottbauer W, Blum M, Meijlink F, Rappold G[#], Gittenberger-de Groot AC[#]. Targeted mutation reveals essential functions of the homeodomain transcription factor *Shox2* in sinoatrial and pacemaking development.
Circulation. 2007;115:1830-1838

Gittenberger-de Groot AC, Mahtab EA, Hahurij ND, Wisse LJ, DeRuiter MC, Wijffels MCEF, Poelmann RE. Nkx2.5-negative myocardium of the posterior heart field and its correlation with podoplanin expression in cells from the developing cardiac pacemaking and conduction system.
Anat Rec (Hoboken). 2007;290:115-122

Mahtab EA, Wijffels MCEF, Van Den Akker NM, Hahurij ND, Lie-Venema H, Wisse LJ, DeRuiter MC, Uhrin P, Zaujec J, Binder BR, Schalij MJ, Poelmann RE, Gittenberger-de Groot AC. Cardiac malformations and myocardial abnormalities in *podoplanin* knockout mouse embryos: Correlation with abnormal epicardial development.
Dev Dyn. 2008;237:847-857

Kolditz DP, Wijffels MCEF, Blom NA, Van Der Laarse A, Hahurij ND, Lie-Venema H, Markwald RR, Poelmann RE, Schalij MJ, Gittenberger-de Groot AC. Epicardium-derived cells in development of the annulus fibrosus and persistence of accessory pathways.
Circulation. 2008;117:1508-1517

Hahurij ND, Gittenberger-de Groot AC, Kolditz DP, Bökenkamp R, Schalij MJ, Poelmann RE, Blom NA. Accessory atrioventricular myocardial connections in the developing human heart: relevance for perinatal supraventricular tachycardias.
Circulation. 2008;117:2850-2858

Mahtab EA, Hahurij ND*, Vicente-Steijn R*, Jongbloed MR, Wisse LJ, DeRuiter MC, Uhrin P, Zaujec J, Binder BR, Schalij MJ, Poelmann RE, Gittenberger-de Groot AC. *Podoplanin* deficient mice show a RhoA-related hypoplasia of the sinus venosus myocardium including the sinoatrial node.
Dev Dyn. 2009;238:183-193

Hahurij ND, Blom NA, Lopriore E, Aziz MI, Nagel HT, Rozendaal L, Vandenbussche FPHA. Perinatal management and long-term cardiac outcome in fetal arrhythmia.
Early Hum Dev. 2011;87:83-87

Hahurij ND, Kolditz DP, Bökenkamp R, Markwald RR, Schalij MJ, Poelmann RE, Gittenberger-de Groot AC, Blom NA. Accessory atrioventricular myocardial pathways in mouse heart development; substrate for supraventricular tachycardia.
Pediatr Res. 2011 (in press)

Hahurij ND, Blom NA, Meijlink F, Mahtab EA, Wisse LJ, Bökenkamp R, Kolditz DP, Schalij MJ, Poelmann RE, Jongbloed MRM, Gittenberger-de Groot AC. *Shox2* in pacemaker and epicardial development; functional implications.
Submitted for publication

PEER REVIEWED ABSTRACTS

Gittenberger-de Groot AC, Hahurij ND, Mahtab EA, Wisse LJ, DeRuiter MC, Wijffels MCEF, Poelmann RE. The posterior heart field contributes novel myocardium to the sinus venosus, sinoatrial and atrioventricular nodes as demonstrated by MLC2-a, Nkx2.5 and podoplanin staining.
Bi-Annual meeting of the European Society of Cardiology working group on cardiovascular development and pathology, Malaga, Spain, March 2006

Blaschke RJ, Hahurij ND, Kuijper S, Wisse LJ, Rottbauer W, Meijlink F, Rappold G, Gittenberger-de Groot AC. Targeted mutation reveals essential functions of *Shox2* in sinus venosus and sinoatrial development.
13th Annual Weinstein Cardiovascular development conference, Saint Petersburg, Florida, USA, May 2006

Gittenberger-de Groot AC, Mahtab EA, Hahurij ND, Wisse LJ, DeRuiter MC, Wijffels MCEF, Poelmann RE. The posterior heart field contributes novel myocardium to the sinus venosus, sinoatrial and atrioventricular nodes as demonstrated by Nkx2.5 and Podoplanin staining.
13th Annual Weinstein Cardiovascular development conference, Saint Petersburg, Florida, USA, May 2006

Hahurij ND. Persistence of functional accessory atrioventricular pathways in normal embryonic and fetal hearts relevance for clinical arrhythmias.
Annual meeting Paediatric Cardiology 2006, Nijmegen, The Netherlands, May 2006

Blaschke RJ, Hahurij ND, Kuijper S, Wisse LJ, Rottbauer W, Meijlink F, Rappold G, Gittenberger-de Groot AC. Targeted mutation reveals essential functions of *Shox2* in sinus venosus and sinoatrial development.
Annual meeting "Nederlandse Anatomen Vereniging (NAV)", Lunteren, The Netherlands, January 2007

Gittenberger-de Groot AC, Mahtab EA, Hahurij ND, Wisse LJ, DeRuiter MC, Wijffels MCEF, Poelmann RE. The posterior heart field contributes novel myocardium to the sinus venosus, sinoatrial and atrioventricular nodes as demonstrated by Nkx2.5 and podoplanin staining. Annual meeting
Annual meeting "Nederlandse Anatomen Vereniging (NAV)", Lunteren, The Netherlands, January 2007

Hahurij ND, Blaschke RJ, Kuijper S, Wisse LJ, Rottbauer W, Meijlink F, Rappold G, Gittenberger-de Groot AC. Targeted mutation reveals essential functions of *Shox2* in sinus venosus and sinoatrial development.
Leiden International Medical Students Congress 2007, Leiden, The Netherlands, March 2007

Hahurij ND, Blom NA, Kolditz DP, Wijffels MCEF, Bökenkamp R, Markwald RR, Schalij MJ, Poelmann RE, Gittenberger-de Groot AC. Accessory atrioventricular myocardial connections in the developing human heart, relevance for perinatal supraventricular tachycardias.
28th Annual Scientific Sessions Heart Rhythm Society (HRS), Denver, Colorado, USA, May 2007. Published in: Heart Rhythm. 2007;4(5):S44

Hahurij ND, Blom NA, Kolditz DP, Wijffels MCEF, Bökenkamp R, Markwald RR, Schalij MJ, Poelmann RE, Gittenberger-de Groot AC. Presence of accessory pathways in the developing human heart, possible explanation for fetal and neonatal atrioventricular reentrant tachycardias.
42nd Annual Meeting of the Association for European Paediatric Cardiology (AEPC), Warsaw, Poland, May 2007. Published in: Cardiology in the Young 2007;17(1):26

Hahurij ND, Blom NA, Kolditz DP, Wijffels MCEF, Bökenkamp R, Markwald RR, Schalij MJ, Poelmann RE, Gittenberger-de Groot AC. Presence of accessory pathways in the developing human heart, possible explanation for fetal and neonatal atrioventricular reentrant tachycardias.
European Society of Cardiology (ESC) congress, Vienna, Austria, September 2007. Published in: European Heart Journal. 2007;28:102

Hahurij ND, Kolditz DP, Bökenkamp R, Markwald RR, Schalij MJ, Poelmann RE, Gittenberger-de Groot AC, Blom NA. Functional accessory atrioventricular myocardial pathways in mouse heart development "Basis for transient perinatal supraventricular tachycardias".
29th Annual Scientific Sessions Heart Rhythm Society (HRS), San Fransisco, California, USA, May 2008. Published in: Heart Rhythm. 2008;5:S40

Kolditz DP, Vicente-Steijn R, Hahurij ND, Pijnappels DP, Blom NA, Jongbloed MRM, Poelmann RE, Gittenberger-de Groot AC. Embryonic development of the atrioventricular node from triple AV-nodal primordial in relation to AV-reentrant tachycardia etiology.
29th Annual Scientific Sessions Heart Rhythm Society (HRS), San Fransisco, California, USA, May 2008. Published in: Heart Rhythm. 2008;5:S7

Hahurij ND, Kolditz DP, Bökenkamp R, Markwald RR, Schalij MJ, Poelmann RE, Gittenberger-de Groot AC, Blom NA. Functional accessory atrioventricular myocardial pathways in mouse heart development "Basis for transient perinatal supraventricular tachycardias".
43rd Annual Meeting of the Association for European Paediatric Cardiology (AEPC), Venice, Italy, May 2008. Published in: Cardiology in the Young. 2008;18:1-106

Kolditz DP, Pijnappels DA, Blom NA, Hahurij ND, Gittenberger-de Groot AC, Schalij MJ. Embryonic development of the Atrio-Ventricular Node from Triple AV Nodal Primordia in Relation to Arrhythmia Etiology.
43rd Annual Meeting of the Association for European Paediatric Cardiology (AEPC), Venice, Italy, May 2008. Published in: Cardiology in the Young. 2008;18:1-106

Vicente-Steijn R, Mahtab EA, Hahurij ND, Jongbloed MRM, DeRuiter MC, Uhrin P, Binder BR, Schalij MJ, Poelmann RE, Gittenberger-de Groot AC. Mice lacking *Podoplanin* show hypoplasia of the sinus venosus myocardium and the sinoatrial node.
15th Annual Weinstein Cardiovascular development conference, Houston, Texas, USA, May 2008

Hahurij ND, Kolditz DP, Bökenkamp R, Markwald RR, Schalij MJ, Poelmann RE, Gittenberger-de Groot AC, Blom NA. Functional accessory atrioventricular myocardial pathways in mouse heart development "Basis for transient perinatal supraventricular tachycardias".
European Society of Cardiology (ESC) congress, Munich, Germany, September 2008. Published in: European Heart Journal. 2008;29:652

Vicente-Steijn R, Mahtab EA, Hahurij ND, Jongbloed MRM, DeRuiter MC, Uhrin P, Binder BR, Schalij MJ, Poelmann RE, Gittenberger-de Groot AC. Mice lacking Podoplanin show a RhoA related hypoplasia of the sinoatrial node and the sinus venosus myocardium.
7th Dutch-German Joint Meeting of the Molecular Cardiology Groups, Hamburg, Germany, January 2009

Hahurij ND, Blom NA, Meijlink F, Mahtab EA, Wisse LJ, Bökenkamp R, Kolditz DP, Schalij MJ, Poelmann RE, Jongbloed MRM, Gittenberger-de Groot AC. *Shox2* in pacemaker and epicardial development.
1st annual Rembrandt Institute Meeting for Cardiovascular Science (RICS), Leiden, The Netherlands, December 2010

Hahurij ND, Blom NA, Meijlink F, Mahtab EA, Wisse LJ, Bökenkamp R, Kolditz DP, Schalij MJ, Poelmann RE, Jongbloed MRM, Gittenberger-de Groot AC. *Shox2* in pacemaker and epicardial development.
45th Annual Meeting of the Association for European Paediatric Cardiology (AEPC), Granada, Spain, May 2011